Emission control by sulphur addition

PSO-2005 FU-5206 final report

Ahrenfeldt, Jesper; Andersen, Jimmy; Bruno, Emiliano; Glarborg, Peter; Henriksen, Ulrik Birk; Lin, Weigang; Marshall, Paul; Rasmussen, Christian Lund

Publication date:
2007

Document Version
Publisher's PDF, also known as Version of record

PSO-2005 FU-5206 final report

Emission control by sulphur addition

Jesper Ahrenfeldt
Jimmy Andersen
Emiliano Bruno
Peter Glarborg
Ulrik Birk Henriksen
Weigang Lin
Paul Marshall
Christian Lund Rasmussen

Institut for Mekanik Energi og Konstruktion /
Institut for Kemiteknik
Danmarks Tekniske Universitet
2800 Kgs. Lyngby

CHEC Report No. 0706
September 2007/Januar 2008

Contents

Summary and conclusions

This project aims to evaluate the potential of sulfur addition for emission control in natural gas combustion in swirl-stabilized diffusion flames and in engines. The impact of addition of small amounts of sulfur on the fuel oxidation rate is investigated and the mechanisms of interaction are analyzed. The project is divided into 3 tasks, which are described briefly below. The project is a collaboration between Department of Mechanical Engineering (The Biomass Gasification Group) and Department of Chemical Engineering (CHEC) at DTU.

Task 1: Addition of SO_2 to swirl-burner experiments with natural gas.

A number of experiments on the effect of SO_2 addition on the emission of CO, unburned hydrocarbons (UHC) and NO in combustion of natural gas in a swirl-stabilized burner under slightly fuel-rich conditions have been conducted. The results show that addition of small amounts of sulfur to the natural gas stream results in a considerable reduction of the emission of CO and UHC. If the sulfur is added to the secondary or tertiary combustion air, either no effect or a slight increase in the CO emission are observed.

Task 2: Addition of SO_2 to tests with a natural gas fired engine.

This task involves an experimental study of SO_2 addition's influence on emissions from a natural gas spark-ignition engine. A blend of 5% SO_2 in nitrogen is added to the air-fuel mixture in a natural gas SI engine. The tests are repeated at different values of equivalence ratio and SO_2 addition, at the same boundary conditions. The concentrations of CO, UHC and NO in the exhaust gas are measured. In rich conditions, CO and UHC emissions show a slight increase with SO_2 addition, whilst NO emissions decrease. In lean conditions, CO and UHC emissions slightly decrease and NO emissions increase with injection of additive. The effect on NO is proportional to an opposite effect on CO. It seems that NO emission has a lower dependence on the equivalence ratio when SO_2 is added. These effects are very weak and the uncertainties due to the fluctuations of the emissions are relevant. The effect of SO_2 addition on the instability of the emissions is investigated, but no relevant result is found.
SO_2 addition has not relevant effects on the emissions from a natural gas spark-ignition engine. The experimental set-up and the methods used during the tests are explained.

Task 3: Investigation of the mechanisms for the interaction of sulfur with fuel oxidation.

The oxidation chemistry for CO/H_2 is analyzed with and without addition of sulfur. Based on the work on this chemistry in the PSO-project FU2207, supplemented with a number of theoretically derived rate constants for important elementary reactions, a chemical kinetic model has been established. This model is able to describe most of the experimental results from work at DTU and in literature satisfactory. However, the promoting effect of small amounts of SO_2 cannot at this point be explained. The interaction of sulfur with other pollutant species (NO, chlorine, soot) has also been discussed.

Resumé

Formålet med dette projekt har været dels at vurdere potentialet for svovltilsætning mhp emissionkontrol ved naturgasfyring i swirl-stabiliserede diffusionsflammer og i motorer, dels om muligt at afklare mekanismerne for effekten af små mængder svovl på oxidationhastigheden af brændslet. Projektet er et samarbejde mellem Institut for Kemiteknik (CHEC) og Mekanik, Energi og Konstruktion (Forgasningsgruppen) på DTU.

Delprojekt 1: Tilsætning af SO_2 til swirl-brænderforsøg med naturgas.

Der er udført en række forsøg med indflydelse af SO_2 tilsætning på emissionen af CO, uforbrændte kulbrinter (UHC) og NO ved forbrænding af naturgas i en swirl-stabiliseret brænder ved svagt understøkiometriske betingelser. Resultaterne viser, at tilsætning af små mængder svovl til naturgas-strømmen medfører en betydelig reduktion af emissionen af CO og UHC. Tilsættes svovl til sekundær eller tertiærluft ses enten ingen effekt eller en svag stigning i CO emissionen.

Delprojekt 2: Tilsætning af SO_2 til forsøg med naturgas-drevet motor.

Der er udført en række forsøg med indflydelse af SO_2 tilsætning på emissionen af CO, uforbrændte kulbrinter (UHC) og NO ved forbrænding af naturgas i en motor under varierende støkiometriske betingelser ($0.8 < \lambda < 1.6$). Resultaterne viser, at tilsætning af små mængder svovl til naturgas/luft-strømmen ikke medfører betydelige ændringer i emissionen af CO, UHC eller NO.

Delprojekt 3: Afklaring af mekanismer for interaktion mellem svovl og oxidation af CO/H_2.

I dette delprojekt oxidationskinetikken for CO/H_2 med og uden svovltilsætning blevet undersøgt. På basis af arbejdet med denne kinetik i PSO-projekt FU2207, suppleret med en række teoretisk udledte hastighedskonstanter for vigtige elementarreaktioner, er der opstillet en kemisk kinetisk model, som er i stand til at beskrive hovedparten af de eksperimentelle observationer, der er til rådighed fra laboratorieforsøg på KT og i litteraturen, tilfredsstillende. Modellen kan ikke forklare hvorledes tilsætning af små mængder svovl kan katalysere oxidationen af CO under svagt brændselsrige betingelser, som observeret i diffusionsflammer. Interaktionen af svovl med andre miljøskadelige komponenter (NO, klor, sod) er ligeledes blevet undersøgt.

Praktiske anvendelser og forslag til videre arbejde

Nærværende projekt har bidraget til at afklare effekten af tilsætning af små mængder SO_2 til forbrænding af naturgas i hhv. en 35 kW swirlbrænder og en dieselmotor. Resultaterne viser, at SO_2 tilsætning kan medføre en betragtelig reduktion af emissionen af CO og uforbrændt ved støkiometrisk forbrænding i swirlbrænderen, mens effekten ifm. en naturgasfyret motor er negligibel. Udfra resultaterne i nærværende projekt vurderes det, at effekten på emissionen fra en motor drevet på forgasningsgas også vil være beskeden.

Som beskrevet af Knut Berge i et internt notat omkring dette projekt (PSO 6540) og nævnt i bilag 1 af nærværende rapport, er der i Sverige gennemført en udvidet undersøgelse af effekter af tilsætning af svovlholdige additiver ved forbrænding af biomasse i forskellige kedeltyper: Boblende fluid bed, cirkulerende fluid bed, ristefyring og støvfyring. Resultaterne af disse undersøg fremgår af Värmeforsk (VF) rapport nr. 908: "Decreased emissions of CO and NOx by injection of ammonium sulphate into the combustion chamber", dateret februar 2005. Foruden at beskrive de udførte forsøg med injektion af ammoniumsulfat, beskriver rapporten også en række andre erfaringer i Sverige med anvendelse af svovladditiver, bl.a. i forbindelse med såvel ristefyring som støvfyring.

Knut Berge opsummerer resultaterne fra VF rapporten i følgende punkter:

- Tilsætning af svovladditiver ved forbrænding af biobrændsler anvendes driftsmæssigt på en række svenske anlæg. Baggrunden herfor er, at den specifikke CO emission kan reduceres ved fastholdt luftoverskud, hvilket indebærer, at der ved fastholdt CO emission kan køres med lavere luftoverskud. Dette medfører i sin tur, at NO_x emissionen reduceres. Da der i Sverige betales afgift pr. kg. NO_x emitteret, er der store besparelser hermed. I tillæg opnås en bedre kedelvirkningsgrad ved at røgtabet reduceres som følge af det lavere luftoverskud.
- Ved træstøvfyring har tilsætning af meget små svovlmængder en kraftig effekt i form af reduceret CO, helt op til 90 %. Forsøg med svovltilsætning ved støvfyring af kornafrens gav ingen væsentlig effekt, hvilket tilskrives, at svovlindholdet i kornafrens er væsentligt højere end i træ.
- Erfaringer med tilsætning af svovl ved ristefyring viser lignende effekter som for støvfyring. Ved anvendelse af lavsvovlige brændsler som træflis og bark er der opnået CO reduktioner på 70 - 90 % ved fastholdt luftoverskud.
- Det fastslås, at der er et stort behov for yderligere forskning for at forklare de grundlæggende mekanismer bagved svovls evne til at reducere CO udslippet.

Nærværende projekt har desværre ikke kunne give en forklaring på svovls evne til, i små koncentrationer, at reducere problemer med CO og uforbrændt drastisk, både i mindre swirlbrændere (dette projekt) og i en række fuldskalaforsøg i Sverige. Vores vurdering er, at der ligger forskellige mekanismer til grund for effekten i den naturgasfyrede swirlbrænder og i fuldskalaforsøgene med forbrænding af træ. I swirlbrænderen ser fænomenet ud til at skyldes interaktioner i den brændselsrige kerne af diffusionsflammen; her har tilsætning af SO_2 ifm. sekundærluften eller i udbrændingszonen enten ingen eller endda en negativ indflydelse på CO emissionen. At SO_2 tilsætning under udbrændingsbetingelser normalt vil øge problemer med CO oxidation er i overensstemmelse med en række laboratorieforsøg omkring oxidation af CO og CO/H2 (se appendiks 4 i nærværende rapport). I de svenske forsøg rapporteres en derimod en markant reduktion af CO ved SO_2 tilsætning i udbrændingszonen.

Som påpeget af Knut Berge er dette et vigtigt område og der er fortsat behov for arbejde med henblik på, at anvendelsesmuligheder i Danmark afdækkes. Det ville derfor være nærliggende at arbejde videre med denne problemstilling. I et evt. fortsættelsesprojekt skulle der fokuseres på den eller de reaktionsmekanisner, der er ansvarlig for effekten i de svenske forsøg, dvs. ved træforbrænding og med fokus på udbrændingszonen. De væsentlige forskelle ift. nærværende projekt er tilstedeværelsen af gasformig klor og alkalimetaller, samt partikler (både kokspartikler, aerosoler og flyveaske). Både klor og alkalimetaller vides at reagere med svovl i gasfasen (se appendiks 3) og det er også muligt at reaktioner kan katalyseres på partikeloverflader. For at afklare mekanismerne, vil det være en fordel at udføre forsøg under kontrollerede forhold i laboratoriereaktorer; her kan der opnås reaktionsbetingelser, der svarer til dem man ser ved træforbrænding i fuld skala, blot uden komplikationerne ved de meget komplekse strømningsforhold. Når mekanismerne er afklaret, kan en vurdering af anvendelsesmuligheder foretages.

0. Personnel and cooperation

0.1 Personnel

Project responsible:	Peter Glarborg
Principal researchers:	Emiliano Bruni (MEK), Jimmy Andersen (KT), Jesper Ahrenfeldt (MEK), Ulrik Henriksen (MEK), Weigang Lin (KT), Christian Lund Rasmussen (KT), Peter Glarborg (KT)
Technicians:	Jørn Hansen (KT) Thomas Wolfe (KT) Lillian Holgersen (KT)

0.2. Cooperation

International collaboration	Paul Marshall (University of North Texas, USA)

1. Project background, objectives and tasks

Background:

Experiences from Swedish full-scale tests on wood combustion on grates and in fluidized beds, as well as from preliminary experiments conducted in CHEC in a bench-scale swirl-stabilized burner fired with natural gas and with a mixture of natural gas and wood, show that addition od sulfur compounds in small amounts may lead to a dramatic change in fuel conversion, showing as a considerable reduction in the CO emission. For wood-fired systems the Swedish experiences show furthermore that S-addition serves to reduce problems with deposits and corrosion. Apart from the results from Sweden, the considerable impact of sulfur additives in small concentrations is not described in the literature, and the mechanism is unknown. The purpose of this project is partly to understand the mechanism(s) responsible for these effects and partly to assess the potential for sulfur addition as a means for emission control in wood-fired systems (CO emissions) and in engines combusted with natural gas (UHC, aldehyde emissions) or gasification gas (CO emissions). Sulfur can be added directly or as co-combustion with a sulfur-containing secondary fuel – for instance addition of strawto wood combustion. The project involves laboratory experiments, bench-scale experiments (swirl burner) and engine tests. The results are interpreted in terms of detailed reaction mechanisms and the implications for the relevant practical combustion systems are outlined.

Project:

The project is divided into 3 tasks, which are described briefly below. The project is a collaboration between Department of Mechanical Engineering (The Biomass Gasification Group) and Department of Chemical Engineering (CHEC) at DTU.

Task 1: Addition of SO_2 to swirl-burner experiments with natural gas.

A number of experiments on the effect of SO_2 addition on the emission of CO, unburned hydrocarbons (UHC) and NO in combustion of natural gas in a swirl-stabilized burner under slightly fuel-rich conditions have been conducted. The results show that addition of small amounts of sulfur to the natural gas stream results in a considerable reduction of the emission of CO and UHC. If the sulfur is added to the secondary or tertiary combustion air, either no effect or a slight increase in the CO emission are observed.

Task 2: Addition of SO_2 to tests with a natural gas fired engine.

A number of tests have been conducted, investigating the influence of addition of SO_2 on the emission of CO, unburned hydrocarbons (UHC) and NO in the combustion of natural gas in an engine under varying stoichiometric conditions ($0.8 < \lambda < 1.6$). The resultats show that addition of small amounts of sulfur to the natural gas stream has no significant effect on the emissions of CO, UHC or NO.

Task 3: Investigation of the mechanisms for the interaction of sulfur with fuel oxidation.

The oxidation chemistry for CO/H_2 is analyzed with and without addition of sulfur. Based on

the work on this chemistry on the PSO-project FU2207, supplemented with a number of theoretically derived rate constants for important elementary reactions, a chemical kinetic model has been established. This model is able to describe most of the experimental results from work at DTU and in literature satisfactory. However, the promoting effect of small amounts of SO_2 cannot at this point be explained. The interaction of sulfur with other pollutant species (NO, chlorine, soot) has also been discussed.

2. Summary of results

Task 1: Addition of SO_2 to swirl-burner experiments with natural gas.

This task is reported in detail in Appendix 1 and the reader is referred to this section. Experiments conducted in a 35 kW bench scale swirl burner confirms the full scale observations, in that up to 90% reduction (1000 ppm) in CO emission is obtained by adding 60 ppm of SO_2 to a slightly fuel rich natural gas combustion. Reduction of the amount of unburned hydrocarbons was also observed. However addition of SO_2 to the tertiary combustion air instead of the natural gas caused an increase in CO emission. This result indicates that, unlike the full-scale experiments, the combustion promoting effect of SO_2 is occurring in the fuel rich flame zone. Experiments of adding SO_2 to different gas flows point to this conclusion and changing the sampling position to just below the flame confirm that the effect of SO_2 is present in top region of the reaction chamber. These results also seem to exclude surface reactions on reactor walls as a pathway to combustion promotion by SO_2, mainly because of the necessity of adding the SO_2 to the natural gas in order to see an effect. The experiment where SO_2 is sampled just below the flame, and the 26 kW fuel rich experiment shows that at very rich conditions, as in the diffusion flame, SO_2 is not likely to be the dominant sulfur species – and other sulfur species (maybe S or SH radicals) are likely to play the dominant combustion promoting effect. Quantitatively the effect seems to increase with increasing natural gas flows, even though this results in lower sulfur concentrations. But higher natural gas flows also result in increased flame lengths and it is possible that this increased sulfur presence in reducing zone area stimulates the combustion promoting effect of SO_2. The effect of adding SO_2 is quantitatively quite similar to that of adding O_2 to the flame, and this observation adds to the suspicion of SO_2 being able to contribute to/ be converted to radical chain carriers.

It remains an open question how it is possible for sulfur to contribute to the combustion process, and especially how it is possible to promote the combustion in a more than molar equivalent fashion (60 ppm SO_2 results in a 1000 ppm CO decrease). Recirculation zones in the top region of the reaction chamber can maybe account for an increased residence time for the sulfur species, making it possible for them to be reused in multiple reaction series.

It has not been possible to find a catalytic CO oxidation reaction mechanism by kinetic modeling of gas phase reactions with addition of small amounts of sulfur. Only the radical recombining effect of SO_2 at low temperatures was observed to cause increasing CO emissions as expected from the literature.

Increased soot formation is mentioned as a likely explanation for the CO decrease and references in the literature is found, where sulfur is known to increase soot formation during diesel engine combustion. Sulfur was also found incorporated in soot remnants from clean burning natural gas combustion indicating a connection between sulfur and soot formation.

This theory also correlates the observed trends of increased O_2 concentrations with increasing SO_2 addition.

Task 2: Addition of SO_2 to tests with a natural gas fired engine.

This task is reported in detail in Appendix 2 and the reader is referred to this section. The purpose of the project was to investigate the possibilities of reducing the emissions of CO, UHC and NO from natural gas fired spark ignition engines by injection of SO_2 to the air-fuel mixture. Previous work carried out on biomass fired boilers and on swirl-stabilized natural gas flames shows that addition of sulphur compounds helps to decrease the emissions of CO (20-60%) and has an effect on NO_X emissions.

The present experiments have been carried out at the Biomass Gasification Group, Technical University of Denmark, as a collaboration between the Department of Mechanical Engineering and the Department of Chemical Engineering. The engine used for the tests was a 3,1 litre MWM spark ignition gas engine, rated to produce 20 kW power. SO_2 has been added in different amounts to the air-fuel mixture at different values of equivalence ratio.

The tests showed that in rich conditions a small increase of the CO emission is observed. In lean conditions the CO emission seems to decrease when SO_2 is being added. These effects are very small and the uncertainties due to the variance of the results are relevant. Small effects on UHC emission are observed when adding SO_2 in lean conditions. The NO emission is slightly affected by SO_2 addition. When SO_2 is added in stoichiometric conditions, the NO emission is lower compared to the baseline (no addition). When SO_2 is added in lean conditions, the NO emission increases. Thus, in presence of SO_2 addition, NO emission has a lower dependence on the equivalence ratio with respect to the baseline case. Since the NO emission from SI engines is due mainly to the thermal mechanism, a lower dependency on the equivalence ratio could allow a decrease in the excess of air without increasing significantly the NO level. The effects observed for NO are coupled to the effects observed for CO. Fluctuations of the emissions due to the instability of the engine are observed and investigated. Relevant results related to SO_2 addition are not found. The output power of the engine is not affected by SO_2 addition. All the effects observed during the tests are very weak.

The results of the experiments carried out at the Biomass Gasification Group show that the injection of SO_2 has not any significant effect on CO, UHC and NO emissions from a natural gas fired spark ignition engine. It is anticipated that the effect on emissions from an engine run on gasification gas will also be negligible, but more work is required to confirm this.

Task 3: Investigation of the mechanisms for the interaction of sulfur with fuel oxidation.

This task is reported in details in Appendices 3 and 4, and the reader is referred to these sections. The oxidation chemistry for CO/H_2 is analyzed with and without addition of sulfur. Based on the work on this chemistry on the PSO-project FU2207, supplemented with a number of theoretically derived rate constants for important elementary reactions, a chemical kinetic model has been established.

It is well established from experiments in premixed, laminar flames, jet-stirred reactors, flow

reactors, and batch reactors that SO_2 acts to catalyze hydrogen atom removal at stoichiometric and reducing conditions. However, the commonly accepted mechanism for radical removal, SO_2+H(+M) = HOSO(+M), HOSO+H/OH = SO_2+H_2/H2O, has been challenged by recent theoretical and experimental results. Based on ab initio calculations for key reactions, the kinetic model for this chemistry was updated and the mechanism of fuel/SO_2 interactions was re-examined. It was found that the interaction of SO_2 with the radical pool is more complex than previously assumed, involving HOSO and SO, as well as, at high temperatures also HSO, SH and S. The revised mechanism with a high rate constant for H+SO_2 recombination and with SO+H_2O, rather than SO_2+H_2, as major products of the HOSO+H reaction is in agreement with a range of experimental results from batch and flow reactors, as well as laminar flames.

Even though the effect of SO_2 on oxidation of H_2 and moist CO can be predicted quite well over a wide range of conditions, the interaction of sulfur with the fuel oxidation is not completely understood. Recent results from natural gas combustion in turbulent diffusion flames (task 1 above) and from wood combustion on a grate and in FBC (Swedish reports) indicate that for low-sulfur fuels addition of sulfur in small amounts may enhance the CO burnout. Small amounts of SO_2 are seen to cause a dramatic decrease in the CO emission. These results are not consistent with the model predictions discussed above. The sensitizing mechanism apparently occurs on the fuel side of the flame sheet and may involve sulfur/soot interactions, but it is not known at this point. The results from wood combustion obtained under excess air burnout conditions seem to involve another sensitizing mechanism, which is also yet to be explained. It has been reported that sulfur, present in petroleum-derived fuels, promotes engine knock and decreases the antiknock effectiveness of lead alkyls. The influence of sulfur compounds depends markedly on the nature of the hydrocarbon fuel and in particular its pre-flame reactions. The mechanism is not known in detail, but it may involve attack of sulfur-containing radicals on the hydrocarbon fuel (see Appendix 3).

The interaction of sulfur with other pollutant species (NO, chlorine, soot) has also been discussed, as can be found in Appendix 3.

The Influence of Sulfur on Natural Gas Combustion

APPENDIX 1

1. March 2006

By: s001378 Jimmy Andersen

Supervisors: Peter Glarborg, Weigang Lin,
Jesper Ahrenfeldt and Ulrik Henriksen

Summary

Recent full-scale observations have shown that addition of small amounts of sulfur to combustion processes may significantly decrease CO emissions. [1]

Experiments conducted in a bench scale swirl burner confirms the full scale observations, up to 90% reduction (1000 ppm) in CO emission is obtained by adding 60 ppm of SO_2 to a slightly fuel rich natural gas combustion. Reduction of the amount of unburned hydrocarbons was also observed. However addition of SO_2 to the tertiary combustion air instead of the natural gas caused an increase in CO emission. This result indicated that the presence of sulfur in the flame region is needed in order to obtain a reduction in CO emission.

It has not been possible to find a catalytic CO oxidating reaction mechanism by kinetic modeling of gas phase reactions with addition of small amounts of sulfur. Only the radical recombining effect of SO_2 at low temperatures was observed to cause increasing CO emissions as expected from the literature. [7,11-15]

Increased soot formation is mentioned as a likely explanation for the CO decrease and references in the literature is found, where sulfur is known to increase soot formation during diesel engine combustion. [45] Sulfur was also found incorporated in soot remnants from clean burning natural gas combustion [46] indicating a connection between sulfur and soot formation. This theory also correlates the observed trends of increased O_2 concentrations with increasing SO_2 addition.

Summary (in Danish)

Erfaringer fra fuldskalaforsøg har tidligere vist, at tilsætning af små mængder svovl kan reducere CO emissioner betydeligt.[1] Formålet med dette projekt var at bekræfte og forklare denne effekt.

Forsøg udført på en bench scale forsøgsopstilling, som operer med en swirl stabiliseret naturgasflamme bekræfter denne CO reducerende effekt. Idet op til 90 % reduktion i CO emissionen (1000 ppm reduktion) er observeret ved tilsætning af 60 ppm SO_2 ved marginalt understøkiometriske forbrændingsforhold. Der blev også observeret en moderat reduktion i emissionen af uforbrændte kulbrinter. Tilsætning af SO_2 til den tertiære forbrændingsluft i stedet for til naturgasstrømmen forårsagede derimod en stigning i CO emissionen. Denne observation indikerer, at tilstedeværelsen af svovl i flammen er nødvendig for at opnå en CO reducerende effekt.

Det har ikke været mulig at forklare denne CO reducerende effekt af SO_2 ud fra kinetisk modellering af gas fase reaktioner. Den veldokumenterede radikal rekombinerende effekt af SO_2 [7,11-15] kunne kun forklare en øget CO emission ved lave temperaturer (<1300 K).

Øget soddannelse bliver foreslået som en sandsynlig forklaring på den svovlforårsagede CO reduktion. Studier af diesel forbrænding i en motor har tidligere beskrevet øget soddannelse på grund af øget svovlindhold i brændslet. [45] Desuden er svovl også blevet observeret inkorporeret i sodrester fra tilsyneladende ”ikke sodende” naturgasflammer [46], hvilket indikerer en sammenhæng mellem soddannelse og svovlindhold. Denne teori passer også med observerede tendenser til øget iltindhold i røggassen, ved øget SO_2 tilsætning til en swirl stabiliseret naturgasflamme.

Table of content

1. Introduction

In combustion systems the presence of sulfur is a problem, since the emission of SO_2 leads to acid rain, furthermore sulfur is known to participate in corrosion mechanisms on boiler walls and superheaters. Because of the acid rain issue current legislation forces coal combustion facilities to desulfurize the flue gas.

In some wood fuels the sulfur content is very low, and recent full-scale experiments have shown that adding sulfur to different wood-fuels can cause a significant decrease in the CO outlet. [1] Bench scale experiments conducted at CHEC have verified the trend observed in the Swedish full-scale experiments, that adding tiny amounts of sulfur can significantly decrease CO emissions.[2] However the mechanism responsible for this sulfur-induced CO decrease is so far unknown.

The objective of this project is to reveal the reaction mechanism responsible for this CO decrease by sulfur interactions, the nature of this alleged CO promoting effect has only recently been observed and so far not explained in known literature.

Being able to increase the combustion rate by adding sulfur can especially have significance for gas engine and wood combustion where CO (and unburned hydrocarbon) emissions can be a problem.

This report contains three major parts; the first part is a literature study describing the influence of sulfur chemistry in combustion. The second part is an experimental section containing description and results from two experimental setups; a bench scale swirl burner and a 22 kW natural gas fired engine. And the final part is a modeling section where a CFD analysis of the swirl burner and appliance of different kinetic sulfur sub models have been performed in order to analyze the experimental results.

2. Combustion in general

Several different techniques are used when turning fuels into energy, these techniques are used in different types of combustion facilities, for instance fixed bed and fluid bed combustion boilers. The phenomenon described in the introduction, where sulfur promotes CO oxidation is observed in both fixed bed and fluid bed facilities and in different lab/bench scale reactors. [1, 2]

2.1. The combustion process

One of the combustion types used in the Swedish full scale experiments [1], in where CO decrease when adding sulfur is observed, is grate fired combustion. During combustion of wood in a grate fired (fixed bed type) plant, the fuel will enter the boiler and undergo different reaction processes on the grate [4]:

1. Heating and drying
2. Pyrolysis
3. Combustion of pyrolysis gases
4. Char combustion and gasification

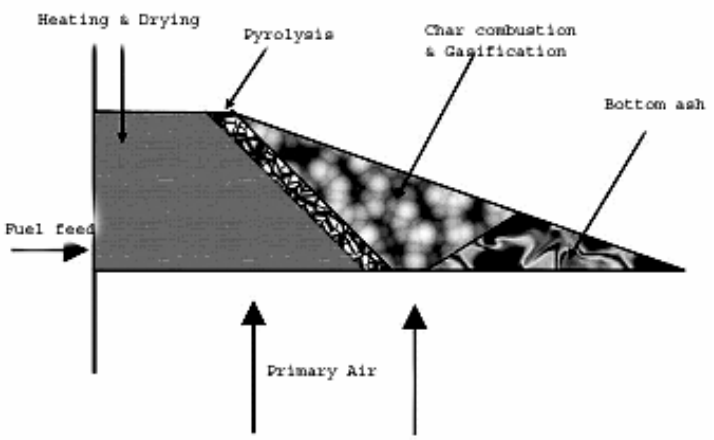

Figure 2.1: *Typical combustion front in a grate fired plant [3].*

Figure 2.1 displays how fuel on a grate undergoes the different reaction processes. The heating and drying phase results in evaporation of water from the fuel.

Pyrolysis is a thermal process taking place at temperatures from 400-800˚C for wood fuels, fuel components with low boiling point will melt and evaporate. Furthermore a thermal degradation of the major fuel molecules will begin, and minor molecules will gasify at the present temperature

conditions. This results in the release of gases and tars from the bed leaving a char residue on the grate. [4]

The gases released during the pyrolysis will self ignite in the gas phase above the fuel, due to the contact with primary and secondary air creating a more oxidative environment.

In the char combustion and gasification zone two different sets of reactions occur; oxygen from the primary air causes a direct heterogeneous combustion of the fuel gives products as CO, CO_2 and H_2O. Products from the direct combustion can participate in gasification processes in the fuel [4]:

(2.1) $Fuel(C_xH_yO_z)\ (s) + (x\text{-}z)\ H_2O\ (g) \rightarrow x\ CO\ (g) + (x\text{-}z+½y)\ H_2\ (g)$

(2.2) $Fuel(C_xH_yO_z)\ (s) + (x\text{-}z)\ CO_2\ (g) \rightarrow (2x\text{-}z)\ CO\ (g) + ½y\ H_2\ (g)$

In fuel rich condition, the shift equilibrium ensures that CO_2 is present as a gasification reactant:

(2.3) $CO\ (g) + H_2O\ (g) \rightarrow CO_2\ (g) + H_2\ (g)$

The oxidative gasification gases will continue through the reactor freeboard, where they also take part in homogenous gas phase oxidation reactions with the secondary air.

Later on in the reactor tertiary air is added to ensure oxidation of the remaining oxidative gases, which mostly is CO, this is done to obtain a maximum energy conversion of the fuel. [4]

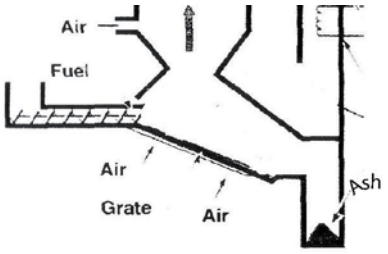

Figure 2.2: *Typical sketch of the lower part of the boiler room. [3]*

Figure 2.2 shows a sketch of a typical grate fired combustion facility, where the main parameters to control the combustion are the degree of grinding of the fuel and the air inlet [4].

In a fluid bed facility conditions will be significantly different because a much better mixing of the fuel with air is obtained, however locally the fuel will still undergo some of the same processes as described above.

2.2. Fuel types

The fuel type has a large influence on which chemical processes that occur during combustion. Table 1 shows some fuel characteristics for coal, which is the most commonly used fuel for energy production in Denmark, but also for the biofuels wood and straw. Growing interest in using CO_2 neutral fuels makes combustion of biofuels attractive.

Table 1: *Fuel data for coal, straw and wood [4]*

	Coal	Straw	Wood chips	Basis
Heating value – MJ/kg	**32,8** (28-39)	**18,6** (18,0-19,2)	**19,5** (18,4-20,4)	dry and ash free
Water content	**10,0 %** (6%-26%)	**14 %** (8%-23%)	**45 %** (20%-60%)	as received
Volatile content	(20%-35%)	**78 %** (75%-81%)	**81%** (79%-84%)	Dry basis
Ash	**12,1 %** (1%-23%)	**4,5 %** (2%-8%)	**1,0 %** (0,3%-4%)	
Hydrogen – H	**4,4 %** (3%-6%)	**5,9 %** (5,4%-6,4%)	**5,8 %** (5,0%-6,4%)	
Carbon – C	**72,5 %** (66%-83%)	**47,5 %** (45%-49%)	**50,0 %** (49%-52%)	
Nitrogen – N	**1,6 %** (1%-2%)	**0,7 %** (0,3%-1,5%)	**0,3 %** (0,1%-0,6%)	
Sulfur – S	**1,2 %** **(0%-4%)**	**0,15 %** **(0,1%-0,2%)**	**0,05%** **(<0,1%)**	
Chlorine – Cl	**0,1 %** (0%-0,36%)	**0,4 %** (0,1%-1,1%)	**0,02 %** (<0,1%)	
Silicon – Si	**3,2 %** (0%-7%)	**0,8 %** (0,1%-2,0%)	**0,1 %** (<0,8%)	
Iron – Fe	**0,7 %** (0%-1,7%)	**0,01 %** (<0,03%)	**0,02 %** (0,1%-0,6%)	
Calcium – Ca	**0,3 %** (0%-1,3%)	**0,4 %** (0,2%-0,5%)	**0,2 %** (0,1%-0,6%)	
Sodium – Na	**0,1 %** (0%-0,4%)	**0,07 %** (0,04%-0,13%)	**0,04 %** (<0,1%)	
Potassium – K	**0,1 %** (0%-4%)	**1,0 %** (0,2%-2,6%)	**0,1 %** (0,05%-0,2%)	

Table 1 shows a significant difference in heating value between coal and biomass, furthermore wood contains a great amount of water, which in reality decreases the heating value further. But what is really interesting regarding this project is the sulfur content. It is only when using fuels with very low sulfur content, such as wood or natural gas (sulfur content of a ~5 ppm [5]), that a combustion promoting effect of adding sulfur has been seen. [1, 2]

2.3. Sulfur in solid fuels

Sulfur in solid fuels can be present as either organic or inorganic sulfur. The inorganic sulfur is present either as sulphates or pyrite (FeS_2). The organic sulfur is bound in aliphatic functional groups (R-SH), in aromatic rings or as sulphides (R-S-R')[7,9]. The composition of organic and inorganic sulfur in wood can be seen in table 2.

Table 2: *Distribution of organic and inorganic sulfur in wood and coal*

	Coal [7]	**Wood (fibreboard) [9]**
Organic	**41-73 %**	**~ 55 %**
Pyritic	**22-50 %**	
Sulphate	**1-27 %**	**~45%**

Table 2 indicates that sulfur is bound in significant amounts both organically and inorganically in both wood and coal. In natural gas sulfur is almost entirely present as H_2S, but other species such as CS_2 and COS may be present also [5,7].

3. Sulfur chemistry in combustion

Sulfur has so far been thought of as a problematic compound during combustion. Almost all sulfur will leave a reactor as SO_2 [6,7], which is an unwanted emission gas since it can be oxidized in the atmosphere and return as sulfuric acid in acid rain. Therefore current Danish legislation only permits emission of 200 mg SO_2/Nm^3 (3 % O_2 flue gas) from biomass fired boilers [8], this corresponds to 70 ppm of sulfur in the flue gas or an initial sulfur content in the fuel of ~0,9 % S. Comparing these emission limits with the sulfur content in wood from table 1 shows that it in most cases is possible to add some sulfur to wood combustion without having to desulfurize the flue gas.

3.1. Sulfur during the pyrolysis process

van Lith et al. [9] found that at pyrolysis temperatures (~500˚C) practically all of the organic sulfur is released when combusting wood due to decomposition of the organic matrix, but also pyritic sulfur is expected to be released at low temperatures, or to convert to pyrrhotite and be released at higher temperatures [7]. van Lith et al. found practically no sulfur release between 500 and 850˚C,[9] which means that for wood combustion, the remaining sulfur is expected to be released from the char combustion zone.

During pyrolysis the main gaseous compound released is H_2S, but also CS_2 and COS are present in a reducing gaseous environment. [6, 10]

3.2. Sulfur in char combustion

When the fuel temperature increases due to exothermic combustion reactions the less volatile inorganic sulfur species will eventually be released to the gas phase. The sulfur release is expected to be complete at a temperature of 1150˚C [9]. Above 1000˚C alkali sulphates will start evaporating, but at lower temperatures reactions between sulphates and ash constituents can provoke SO_2 release. [9]

Evaporated alkali sulphates can form aerosols in the gas phase, these small particles can condensate on superheaters causing corrosion; alkali chlorides do however show even more pronounced corrosion ability. [3] Minimizing corrosion by adding sulfur and preventing highly corrosive alkali chlorides to form (instead alkali sulphates are produced) is therefore a very positive effect of sulfur addition. [30]

4. Heterogeneous sulfur reactions

Gas-phase sulfur reactions are treated in Appendices 3 and 4 of this report, but also heterogeneous sulfur reactions may be of importance. Sulfur oxides is known as a catalyst poison in many catalysis applications, most well-known is probably the poison of automobile exhaust catalyst which remove CO and NO. [23] Boiler and superheater parts in combustion reactors are assumed to be made of some kind of steel alloy components consisting of the transition metals iron (Fe), Chromium (Cr) and Nickel (Ni). In most combustion systems there will therefore be potential for heterogeneous reaction between gas phase sulfur and the surface metals.

4.1. Sulfur – Nickel interactions

SO_2 is expected to decompose on most transition metal surfaces [23].

Sellers and Shustorovich [24] reports from their theoretical study of sulfur oxides on transition metals that only full dissociation of SO_2 is possible:

(4.1) $SO_2(g) \rightarrow S(ads) + O(ads) + O(ads)$

Since the partial dissociation yielding adsorbed SO as a product is energetically unfavorable compared to the full dissociation. This full dissociation is especially feasible on Ni. [24]

Of particular interest to this project is the reaction:

(4.2) $SO_2 + CO \rightarrow S + O + CO_2$

Reaction 4.2 is described by Sellers and Shustorovich, the reaction is reported as being exothermic on Ni (ΔH=-39 kcal/mol), and the authors assume the reaction to proceed without activation energy barriers. [24]

It is however not certain that pure Ni sites are available at the surface. In an oxygen containing environment metal oxides tend to form at the surface.

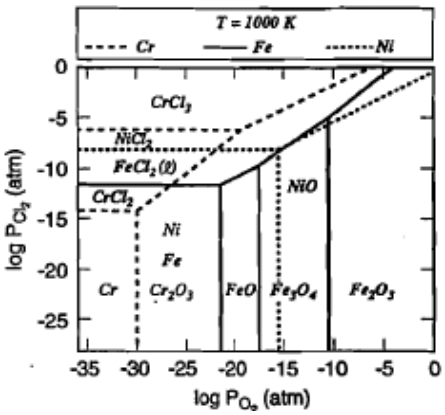

Figure 4.1: *Stability diagram for a Fe-Cr-Ni-O-Cl system at 1000 K [28]*

Figure 4.1 shows that in an environment of 3% O_2 ($\log(p_{O2})$=-1,5 at atmospheric pressure) NiO will be the preferred Ni specie, this may change as the temperature changes within the reactor.
NiO is however not an unreactive surface, SO_2 is found to be able to dissociate on NiO as well, especially on defective NiO sites. [26] Also oxidation of SO_2 can occur on NiO sites at elevated temperatures (500-1100°C) forming SO_3 this heterogeneously catalyzed oxidation peaks in the temperature window from 650-800°C. [27] This opens up for the possibility that SO_3 in comparatively large amounts can be formed at the wall surfaces, where the temperature is lower, since SO_3 is thermodynamically favored at lower temperatures (below 1220°C) [25] and NiO provides a reaction path to overcome the slow kinetics.

This literature search on Ni – sulfur interactions definitely shows a reactive trend and it could be that gas solid interactions between S and Ni can lead to combustion promotion.

4.2. Sulfur – Cr/Fe interactions

According to figure 4.1 both Fe and Cr is also expected to be in some kind of oxide state in the combustion reactor. Many investigations regarding reactions between sulfur species and Fe / Cr surfaces have been conducted with the aim of revealing corrosion mechanisms.
In alkali metal deposits Fe_2O_3 is reported to catalyze the oxidation of SO_2 to SO_3, which within the deposit can cause further corrosion. [7,28] Dunn et al. found that different binary and tertiary catalyst (oxides of V, Fe, Re, Cr, Nb, Mo and W) all have the ability to undergo redox cycles and oxidize SO_2 to SO_3. The SO_3 production rate shows no dependence on the SO_2 surface coverage. [29]
This could imply that a little SO_2 in the flue gas is enough to cause a maximum oxidation to SO_3 by surface reactions. If not taking part in corrosion reactions this SO_3 could maybe take part in CO oxidation in the gas phase.

5. Sulfur and soot formation.

This chapter is now covered by Appendix 3 of the current report.

6. Combustion promotion results by sulfur addition

The chemical nature of sulfur in combustion systems was previously thought as being inhibitive [7,11-15], however three recent independent observations has shown the opposite effect:

1. Flow reactor experiments conducted by Alzueta et al. published in 2001. [14]
2. Swedish full scale combustion experiments supplemented by lab experiments (Varmeforsk project 908 published February 2005). [1]
3. Swirl combustion experiments from CHEC research center conducted in 2005. [2]

This chapter contains a brief summary of the results and reaction conditions during these, for this project, very relevant experiments.

6.1. Flow reactor experiments by Alzueta et al. [14]

This section is now covered by Appendices 3 and 4 of the current report.

6.2. Varmeforsk project 908 [1]

In Swedish combustion facilities Idbäcken KVV (Bubbling Fluidized Bed) and Brista KVV (Circulating Fluidized Bed) ammonium sulphate was continuously added to the flue gas downstream of the combustion zone. This was done in order to minimize corrosion and deposit formation. The addition occurs just after the combustion zone, where the content of unburned hydrocarbons in the flue gas is low. Injection of ammoniumsulphate at this position has been patented. [30]

Until the harvest 2003 no CO decreasing effect of adding ammonium sulphate to the flue gas was observed, in Idbäcken this was thought to be because the sulfur content in the co-fired combustion fuel was sufficiently high and in Brista the CO levels are generally very low. However during the harvest in 2003 Brista observed higher CO levels when the sulphat dosing accidentally was turned off.

Also in 2003 Lindau and Skog [31] conducted experiments adding elementary sulfur to a BFB plant in Falun. The general observations was that the SO_2 and HCl emissions increased slightly, but the CO and UHC (Unburned HydroCarbon) concentrations in the flue gas and the amount of unburned C in the fuel decreased about 50%. Lindau and Skog proposed a mechanism where K_2SO_4 catalytically increases CO oxidation. The amount of S added was 20 mg/ MJ fuel (~ 400 mg/kg dry wood chips using the table 1 content ~ 0,04 % ~ 32 ppm SO_2 increase in flue gas) [31].

After these observations sulfur addition was tried in several combustion systems, both BFB CFB and grate fired boilers and even in a powder burner at Drefviken. Not all of these sulfur addition experiments resulted in a CO decrease, but since an analysis of the fuels used are not enclosed in the report it is difficult to estimate if the fuel itself in some cases could have contained a sufficient amount of sulfur so that adding more would have no effect.

Table 4 contains an overview of the plants where sulfur was added.

Table 4: *Summary of Swedish full scale sulfur addition experiments*

Facility	Combustion technique	Fuel	S addition type	Result
Falun	30 MW BFB	GROT*, bark, chips and Saw dust	Elementary S to the fuel	CO decrease ~50 %
Idbäckverket	100 MW BFB	RT-chips**, wood, coal	Sulphate-S	No effect observed (See text)
Eskilstuna	110 MW BFB	50% GROT*, 25% bark and 25% saw dust	Sulphate-S	CO decrease 20-60% (see text)
Nässjö	35 MW CFB	GROT*	Elmnt. S / sulphate-S	Less SO_2 (see text)
Växjö	110 MW CFB	Wood fuel	Elmnt. S / sulphate-S	Less SO_2 (see text)
Brista	120 MW CFB	Wood chips, bark and saw dust	Sulphate-S	CO decrease (see text)
Skinnskatteberg	10 MW Grate	Moist bark	Elmnt. S	CO decrease
Lövholmen	12 MW Grate	Sawmill by-products	Sulphate-S	CO decrease
Malmö(SYSAV)	30 MW Grate	Waste	Elmnt. S	No effect observed
Karskär	60 MW Grate	Bark	Elmnt. S / sulphate-S	CO decrease
Södertälje	80 MW Grate	Waste	Elmnt. S (granulates)	No effect observed
Händelö	117 MW Grate	Wood+RT-chips**	Elmnt. S	
Drefviken	80 MW Powderburner	Wood dust	Elmnt. S / fuel S	CO decrease 90 %

*Wood branches and treetops, ** Waste wood chips

Table 4 do however show some general trends, the combustion technique and the S addition type does not seem to be important, but the fuel needs to be S lean, waste and coal fired plants do not show an effect, wood fired facilities do. The powder burner in Drefsviken showed significant CO decrease already by adding 2 mg S/MJ (~40 mg/kg ~0,004 % S in fuel ~3 ppm SO_2 increase in flue gas).

At Nässjö and Växjö experiments show that sulphate addition to the cyclone causes less SO_2 emission and less bottom ash sulphate than addition of elementary sulfur to the fuel.

Pilot scale experiments were also conducted in a 5-10 kW ceramic isolated FB combustor. Temperatures in the pilot plant were between 850 and 880°C when firing wood pellets and 970-1025°C when firing gasol (propane and butane gas mixture). The additives were injected in 3 different positions; 0,7; 0,85 or 1,25m above the fuel "boat", the 0,7 m position is just above the flame from the secondary air burnout (secondary air injected at 0,5m).

The pilot scale experiments show that almost every sulfur species added can decrease the CO level, the only exception is K_2SO_4 which causes a slight increase. These results clearly reject the proposed

mechanism by Lindau and Skog. The amount of added S has an effect on the CO level up to ~15 mg S/MJ (~1200 mg/kg dry wood chips using the table 1 content ~ 0,12 % ~ 100 ppm SO_2 increase in flue gas) beyond this S addition level the CO emission seems to stagnate.
The pilot scale experiments definitely indicate that S causes a CO decrease, and the experiments with gasol point to the fact that the CO oxidations occurs without interactions with ash components. The authors also conclude a general trend of optimized CO decrease when S is added together with N species (ammonium). The CO removal process seems to occur at least down to 800°C.

Full scale experiments where conducted at Eskilstuna power plant. Ammonium sulphate was added at four different positions; with the fuel, with the secondary air, with the tertiary air and in the SNCR zone (The zone where urea or ammonia can be injected to reduce NO to N_2). The temperature in the SNCR zone is expected to be 900-950°C.

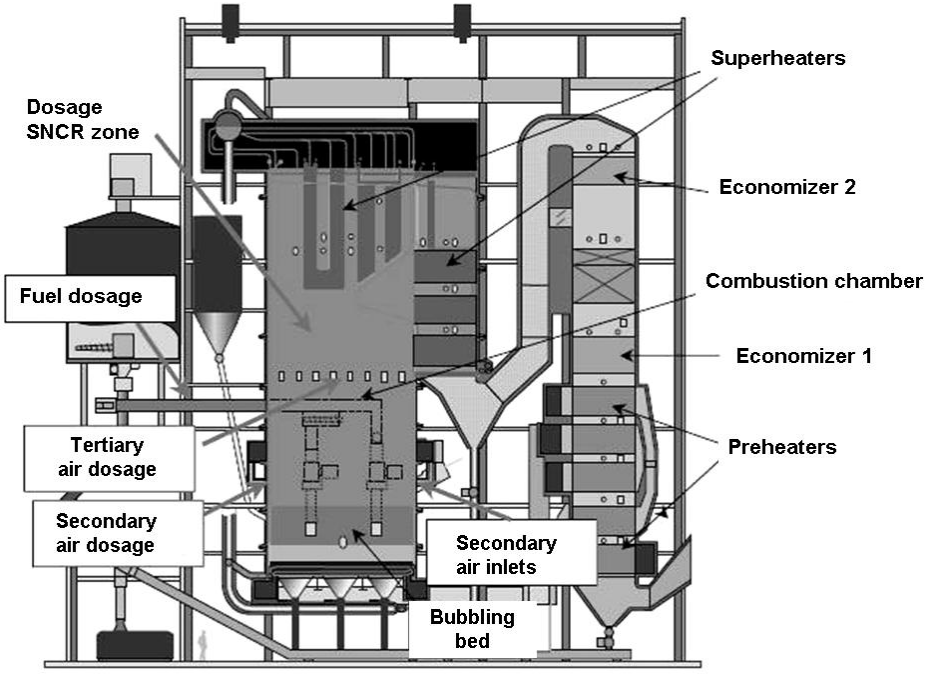

Figure 5.3: *Sketch of Eskilstuna power plant (Bubbling Fluidized Bed). [1]*

Experiments where conducted at low and high effect (respectively 55 and 70 MW) and with different O_2 concentrations in the flue gas (3,3%;2,5% or 1,5% O_2).
Results show 20-60% reduction of the CO level, largest decrease for the highest CO levels (low O_2 concentrations). The results also indicate a slightly higher CO decrease when adding S to the

tertiary air (~ 45% CO decrease), but the effect was also significant when adding in the SNCR zone (~20-40% CO decrease). It was also reported that further S addition beyond 23 mg S/MJ (~ 460 mg/kg dry wood chips using the table 1 content ~ 0,05 % ~ 40 ppm SO_2 increase in flue gas) did not cause a significant decrease in CO emission.

The NO levels have throughout the project been a bit more inconsistent, adding ammonium sulphate can in some cases reduce NO, but also more reactive N is added, it is also remarkable that less NH_3 is emitted when adding ammonium sulphate.

The authors imply a gas phase mechanism with reactions between S and the complex radical system, where S must enter in some kind of catalytic fashion in order to oxidize more than 100 times as much CO.

Finally an analysis of the particles caught in the bag filter shows an increase in particle size when adding ammonium sulphate. This increase was concluded to be due to an increased conversion of KCl to K_2SO_4.

6.3. Preliminary swirl combustion experiments at CHEC [2]

A thorough explanation of the bench scale swirl burner will follow in chapter 9. Preliminary combustion experiments where carried out with a 15 kW reactor efficiency. At first natural gas was fired, which gave the results seen in figure 6.4.

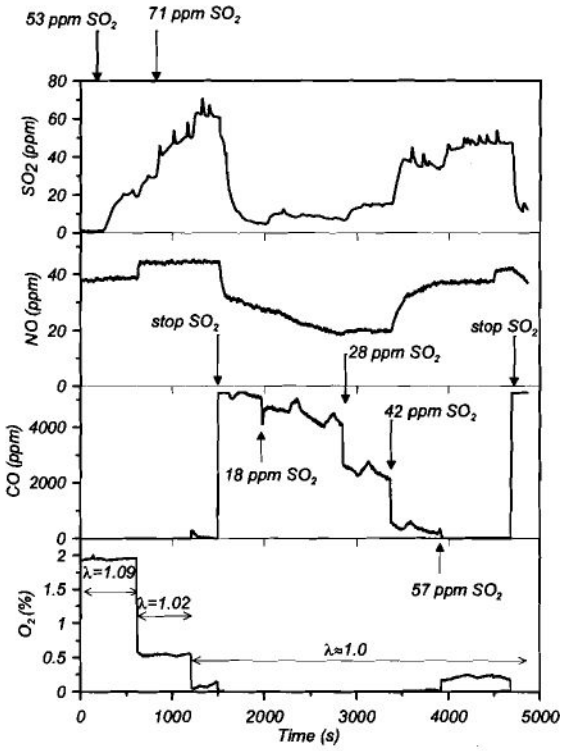

Figure 6.4*: Swirl burner results from natural gas combustion experiments in swirl burner. [2]*

Figure 6.4 shows a clear effect of SO_2 addition on CO level at stoichiometric conditions (fuel lean conditions resulted in a complete combustion so an eventual effect on CO can not be observed).
When co-firing natural gas and wood powder (see results figure 6.5) a generally higher level of CO is observed, and a large fluctuation of O_2 and CO emission is observed probably because of fluctuations in the solid feed.

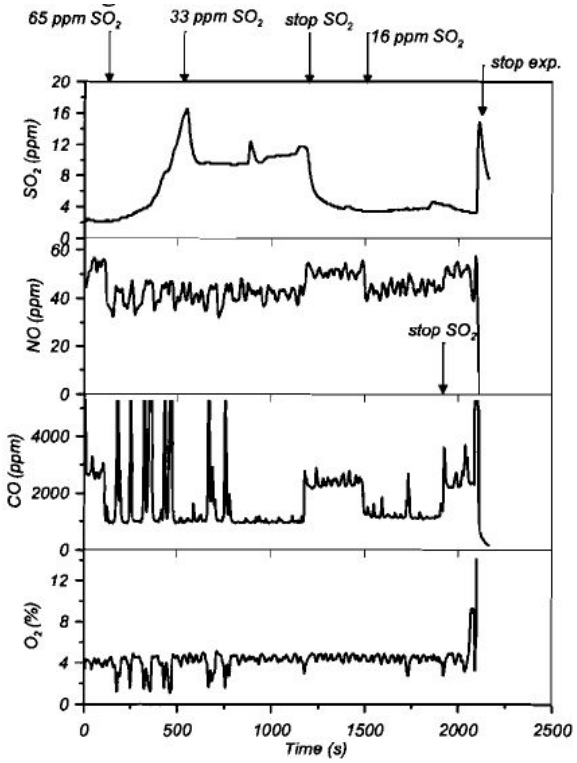

Figure 6.5: *Emissions from swirl burner when co-firing natural gas and wood powder. [2]*

Even though fluctuations disturb the emissions, an oxidizing effect is observed when adding SO_2. The CO decrease is observed to be almost identical when adding 33 and 16 ppm SO_2.

After the co-firing experiment yet another natural gas experiment was conducted, the results from this experiment surprisingly showed a very strange behavior, where initially no effect of SO_2 addition is observed and eventually a CO increase is observed, the totally opposite effect compared to the first experiment. However a strange behavior of the SO_2 emission is not in compliance with the amount let in, which could be explained by deposit formation and destruction.

The influence of SO_2 addition at different oxygen levels were investigated in a co-firing experiment.

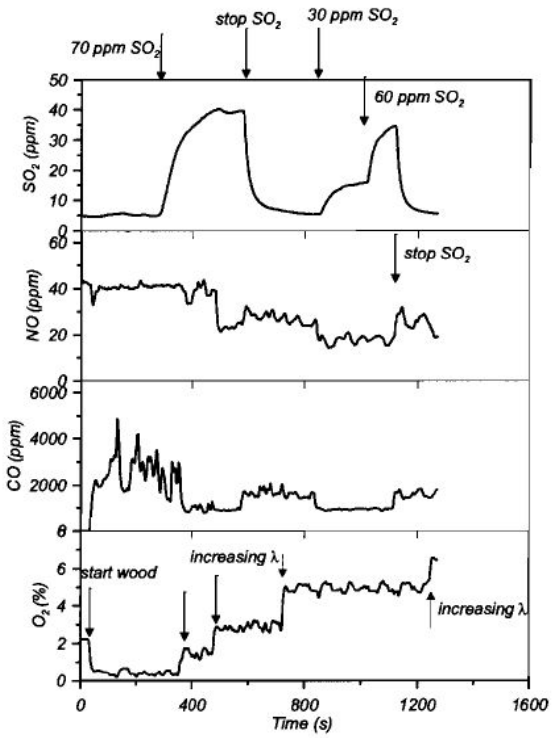

Figure 6.6: *SO_2 addition at different air excess levels.[2]*

Again in figure 6.6 an CO levels decrease when SO_2 is added. Surprisingly the O_2 level does not seem to have as much effect on the CO outlet concentration when increased beyond 1,75 %. It is also noticed that increasing the SO_2 level from 30 to 60 ppm did not change CO emissions.

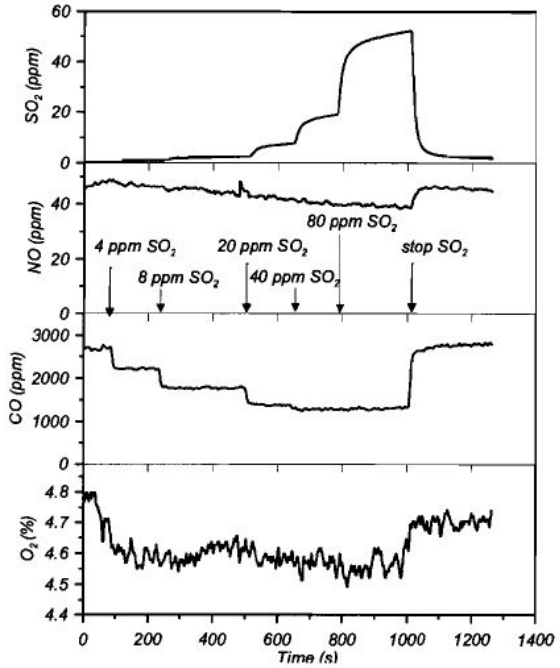

Figure 6.7: *SO_2 addition at high O_2 concentration during co-firing wood and natural gas. [2]*

In figure 6.7 the pronounced effect is again seen for co-firing this time at a relatively high O_2 level ~4,6 %. What is especially interesting in figure 6.7 is the observation that the effect of SO_2 addition drastically decreases going from 8 to 20 ppm, and no effect is observed when increasing to 80 ppm. The behavior of O_2 level is (although fluctuating) in accordance with CO levels, which reassuringly points to a CO oxidation when SO_2 is added (and not increased hydrocarbon emission).

Throughout the experiments the amount of SO_2 added does not seem to equal the observed emissions, so either a significant amount of S leaves the reactor as other gas species (SO_3, SO or H_2S), or an accumulation (deposit formation) occurs in the reactor.

7. Discussion and mechanism theories

The results featured in the previous chapter show that sulfur species can promote CO combustion. The effect does not occur because of reactions with the ash components, and the fact that sulfur addition in the SNCR zone also can cause a CO decrease suggests that a promotion caused by S – species occur late in the reactor and most probably with sulfur in an oxidized state (presumably SO_2 or SO_3), the effect is presumably taking place at temperatures from 1000˚C and below. This also hints that the effect primarily is an oxidation of CO and not an increased rate of combustion of hydrocarbons earlier in the combustion process.

The amount of sulfur needed to reach the maximum CO decrease capacity seems to vary from reactor to reactor. This is without a doubt due to different initial sulfur contents in the fuel, but also the alkali content can play a role, since the S species are to form alkali sulphates, probably before sulfur can take part in CO oxidation mechanism. There do however seem to be a saturation point regarding the effect of added S - increasing the sulfur concentration beyond this point have little or no promoting effect.

The following section contains a list of theories that could explain the mechanism responsible for the CO oxidation:

- A local increased oxidation of SO_2 to SO_3 taking place on deposits or reactor walls (maybe caused by Fe_2O_3 as implied in [7,28] or NiO [27] could give increased SO_3 content which then could react as part of the reaction sequence stated by Dagaut et al.[13]:

  $SO_3 + HO_2 \rightleftharpoons HOSO_2 + O_2$

  $HOSO_2 + M \rightleftharpoons SO_2 + OH + M$

  This would overall lead to a conversion of the less reactive HO_2 to OH, which is the main CO oxidizing radical.

- The catalysis by Ni metal or NiO becomes dominant in a small temperature window or maybe even at local fluctuating temperatures causing the fully dissociated SO_2 to react with CO at low temperatures and causing desorbtion of S species (S or SO) at elevated temperatures leaving an active site open for yet another SO_2 to dissociate:

  $SO_2 \rightarrow S\ (ads) + 2\ O\ (ads)$

  $O\ (ads) + CO\ (g/ads) \rightarrow CO_2\ (g)$

  $S\ (ads) + O\ (ads) \rightleftharpoons SO\ (g)$ (at higher temperatures)

Another similar mechanism could be that the O atoms from the dissociated SO_2 oxidize two CO molecules on the metal surface and desorbs as CO_2. Afterwards O_2 from the flue gas reacts with the S atom leaving a new dissociated SO_2 molecule.

The fact that there seems to be a maximum SO_2 concentration where after more SO_2 in the flue gas has no further promoting effect indicate a 0^{th} order rate constant (or a competing inhibiting cycle) typical for heterogeneous catalysis where the number of active sites defines the rate of reaction. However both the pilot scale experiments [1] and flow reactor experiments [14] in ceramically isolated reactors have shown the promoting effect of sulfur.

- A homogeneous gas phase reaction mechanism, where a major sulfur specie promotes oxidation of CO through radical chain branching reaction mechanisms.

  Some promoting reaction cycles suggested in the literature could be [14]:

  $SO_2 + H \rightleftharpoons SO + OH$

  $SO + O_2 \rightleftharpoons SO_2 + O$

  It maybe that the decomposition of HOSO to OH and SO is underrated in current kinetic models as indicated by Murakami et al. [18] But also the rate constant for the reaction between HO_2 and SO_2 studied by Wang and Hou [16] could be an interesting parameter to vary in current kinetic models and a combination of reaction from [14,16 and 18] could lead to a dramatically promoting sequence:

  $HO_2 + SO_2 \rightleftharpoons HOSO + O_2$

  $HOSO \rightleftharpoons SO + OH$

  $SO + O_2 \rightleftharpoons SO_2 + O$

In total $HO_2 \rightleftharpoons OH + O$

The kinetic modeling by Cerru et al. [12] accomplishes to model the work by Alzueta et al. nicely and the same model is still able to predict systems where S seems inhibiting, this work supports that a pure gas phase reaction mechanism could be responsible for the sulfur promotion.

- Sulfur species could inhibit the soot formation in the combustion flame resulting in fewer hydrocarbons escaping the flame zone and competing with CO for the reaction with oxidating radicals. This would overall result in lower CO emissions.

The literature study on soot behavior supports that S species can inhibit soot formation and the work by Puri et al. indicates soot formation can influence the overall combustion efficiency. [39]

- Sulfur species increases soot formation, which changes the gas phase stoichiometry so that less carbon and therefore less CO is present.

The studies on sulfur influencing diesel soot formation [45] and the presence of sulfur in soot from natural gas flames [46] could indicate that sulfur species plays an active role in soot formation.

8. Conclusion on literature study

The extend of the Swedish full scale experiments [1] is so comprehensive, that this promoting effect of sulfur on CO oxidation cannot be ignored as experimental uncertainties. Conclusions from these experiments are that the sulfur promoting effect occurs in the latter part of the combustion zone, and at temperatures from 1000˚C and lower.

A search in the literature with focus on gas phase reaction mechanisms with sulfur that could explain a promoting mechanism has given no clear answer. It seems that rate and thermodynamic data on key reactions are attached with some uncertainties, so a pure gas phase reaction mechanism is indeed possible even though sulfur so far has been thought of as being a combustion inhibitor in the literature.

Heterogeneous reactions between gaseous sulfur components and transition metals from a steel alloy, which most combustion boilers are made of, could have a decisive catalytic impact that could be responsible for the promoting effect of sulfur on combustion.

The literature study has confirmed that reactions between sulfur species and metal surfaces do take place, and two reaction mechanisms has been suggested; a direct oxidation of CO by adsorbed O atoms from dissociated SO_2 molecules and a mechanism where metal surfaces oxidize SO_2 to SO_3, which is then reduced in the gas phase resulting in an overall increase of combustion reactive radicals.

An inhibiting effect of sulfur species on soot formation could also transmit to the downstream regions of the combustion system resulting in an increased CO combustion and thereby lower emissions.

Or sulfur could increase soot formation thereby increasing the amount of carbon in the solid state, resulting in emission of less CO.

In order to get an idea about the reaction mechanism responsible for this combustion promotion, extensive experiments needs to be carried out varying both sulfur content and combustion conditions, but also increasing the surface area of specific metals could be interesting in order to get an idea of the potential of heterogeneous catalysis in the reactor.

9. Experimental setups

This chapter contains a description of the experimental setups used during the project. For reference to the engine setup, see appendix 2.

9.1. The swirl burner

A swirl burner has been used to investigate the process of combusting natural gas with addition of small amounts of SO_2.

The reactor consists of three different parts; a swirl burner, a reactor chamber and a post reactor system which all will be described in the following sections. The burner is capable of firing natural gas as well as solid fuels (which was not used in this project).

The reactor is 1,9 m long with an inner diameter of 315 mm, the combustion occurs from the top and down. The recommended thermal capacity of the burner is 20 kW. [47]

9.1.1. Gas feeding system

Before the gases reach the burner it runs through a rather complicated monitoring system and operating panel. The operating panel, displayed schematically and virtually in figure 9.1, controls the gas supply to the burner. Natural gas is delivered from a central grid at an overpressure of 22 mbar (<PI 3> displays the natural gas overpressure). Valve <BV 2> is used to regulate the natural gas flow to the burner. The natural gas also passes a digital flow meter <FI 2> that measures the flow at the current atmospheric conditions. Then the gas passes a filter and a pressure regulator <PREG 20> that reduces the pressure. After the pressure regulator the gas passes through a pressure switch <PC 4> and to magnetic valves <MV 15> and <MV 16>, which can be closed by the burner control box.

It is also possible to add ammonia to the natural gas line, the valve <MV 14> which also can be switched manually (or automatically in case of a burner shut down) to purge N_2 through instead of ammonia. The feed rate of NH_3 is controlled at the needle valve <NV 11> and indicated on the flow meter <FI 13>.

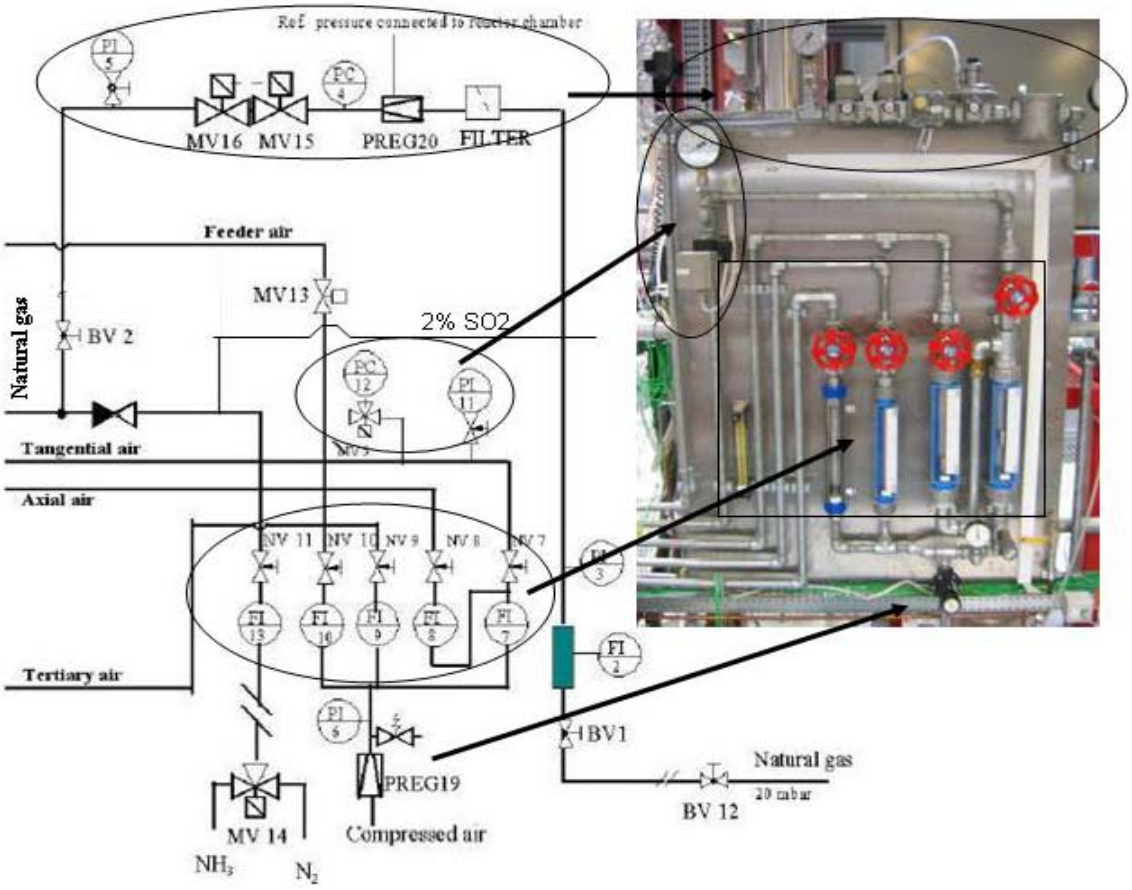

Figure 9.1: *PI diagram and picture of the gas operating panel [47]*

The combustion air is supplied from the centralized compressed air system. It is reduced to 2 bar by a reducing valve <PREG 19> and the pressure after the valve is indicated by <PI 6>. The compressed air is divided into four passages indicating the different air burner inlets; tangential air, axial air, tertiary air and feeder air (which has not been used during this project). The needle valves <NV 7>, <NV 8> and <NV 9> are used to control the different airflows, which are monitored on the rotameters <FI 7>, <FI 8> and <FI 9>. The scale unit for the rotameters is Nl/min and they are calibrated for conditions 2 bar and 20°C. The tangential air passes a pressure indicator <PI 11> and a pressure switch <PC 12>, which is connected to the burner control box. If the tangential air pressure drops below 0,3 bar the set up will shut down. [48]

A 50 liter 2 % SO_2 in N_2 bottle is positioned in a gas central in an adjacent building. The gas pressure from the bottle is held at a pressure of 5 bar. The gas is lead through teflon pipes to the upper deck, where a first a ball valve and then a Bronkhorst (1 Nl N_2/min) mass flow controller makes it possible to control the desired amount of SO_2 gas lead in to the reactor. The addition of SO_2 gas is most often done to the NH_3/N_2 line before entering the natural gas flow as illustrated in

figure 9.1, experiments have been done where SO_2 was added to the air flows (both tertiary, tangential and axial).

9.1.2. The swirl burner

A schematic drawing of the actual swirl burner device, which ensures the swirling nature of the flame, is shown in figure 9.2.

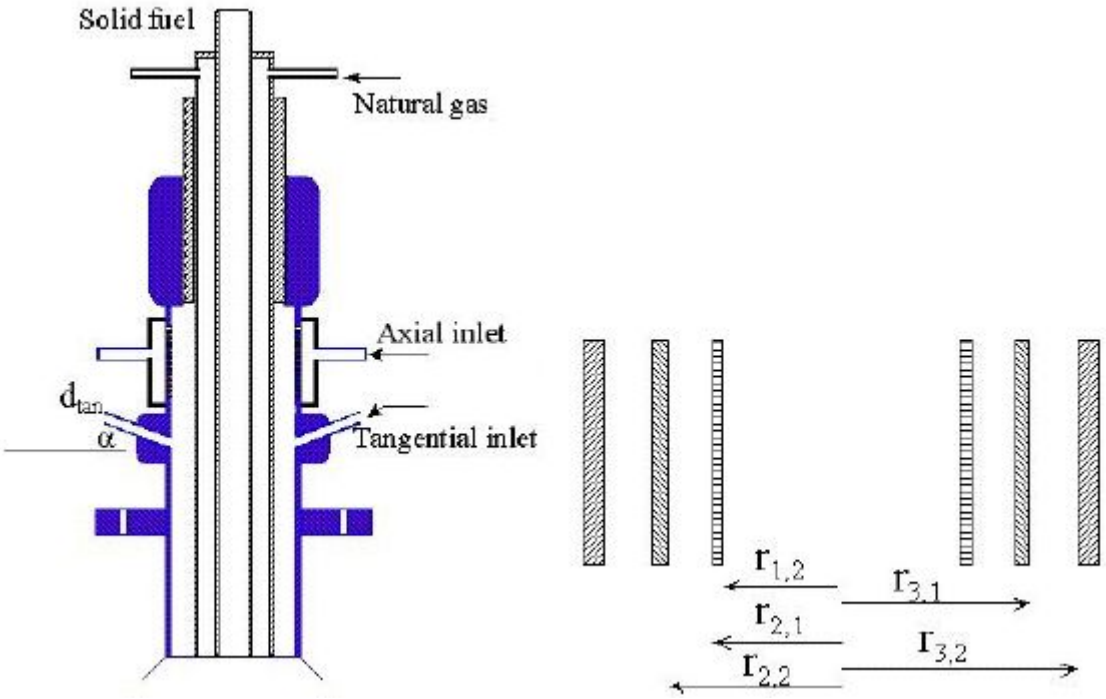

Figure 9.2: *Right: Schematic drawing of the swirl burner. [47]*

The natural gas runs from the gas feeding system to the burner in the inner annular of the pipe, and a swirling combustion air runs on the outer annular side meeting the fuel at the reactor chamber. So it is obvious that the flame that emerges is a non-premixed (diffusion flame). Diffusion flames are characterized by having oxidizer and fuel separated when they enter the burner mouth, the chemical reactions will take place at the interface of the flame, and mixing of the fuel and oxidizer will occur through diffusion. [49]

9.1.3. General description of swirling flows

The degree of swirling of the combustion air can be controlled by the ratio of axial to tangential air, this degree of swirl is usually described by the swirl number, S, which is a dimensionless number defined as the ratio of axial flux of angular momentum to the flux of axial momentum divided by the radius of the burner:

(9.1) $$S = \frac{G_\varphi}{G_x \, r_b}$$

Where the momentum fluxes can be found as:

(9.2) $$G_\varphi = \int_{r_1}^{r_2} 2\pi \, \rho u \, w r^2 \, dr$$

(9.3) $$G_x = \int_{r_1}^{r_2} 2\pi \, r(p + \rho u^2) \, dr$$

Where ρ is the gas density, u and w are respectively the axial and tangential velocity components at radius r, p is the static gauge pressure and r_1 and r_2 are the radial limits of the burner. Assuming that the gas velocities at the burner exit are evenly distributed, the gauge pressure in equation 9.3 can be neglected and the flux of axial momentum can be expressed as:

(9.4) $$G_x = A \, \rho \, u^2$$

A being the burner cross section. In appendix B an example on how to calculate the swirl number is shown. [48]

This degree of swirling affects the flame size and shape, stability and flow dynamics within the reaction chamber. Internal and external reaction zones (IRZ and ERZ) occur due to shear and mixing with surrounding fluids giving rise to pressure fields in order to stabilize the centrifugal force. [50] The formation of IRZ should start at S ~0,6. [48]

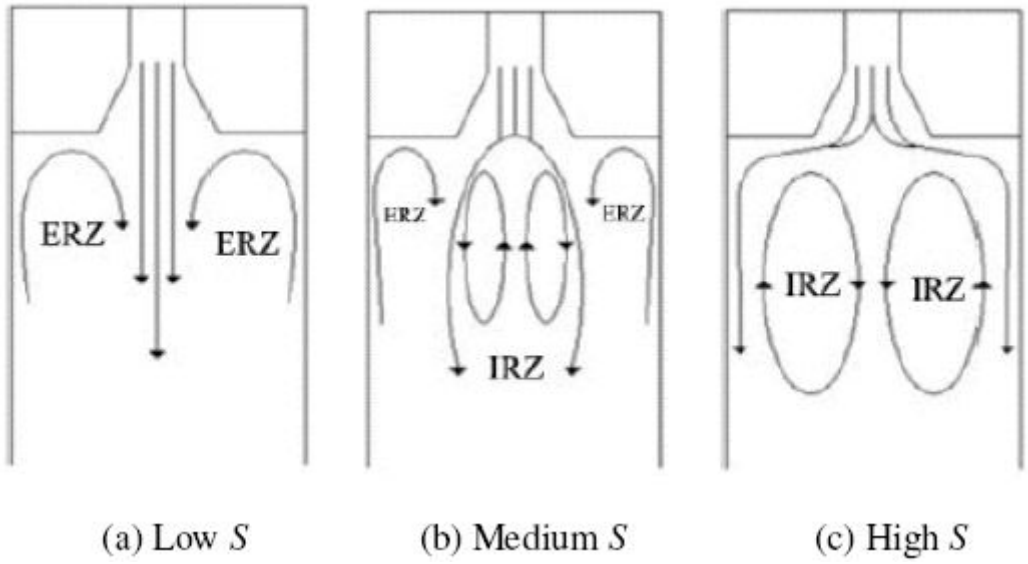

Figure 9.3: *The influence of swirl number on fluid dynamics. [48]*

The reaction chamber and specific burner design do however also influence the flow fields, for the specific burner configuration used in this project natural gas will enter the reaction chamber from an inner tube meeting an IRZ as shown in figure 9.3.

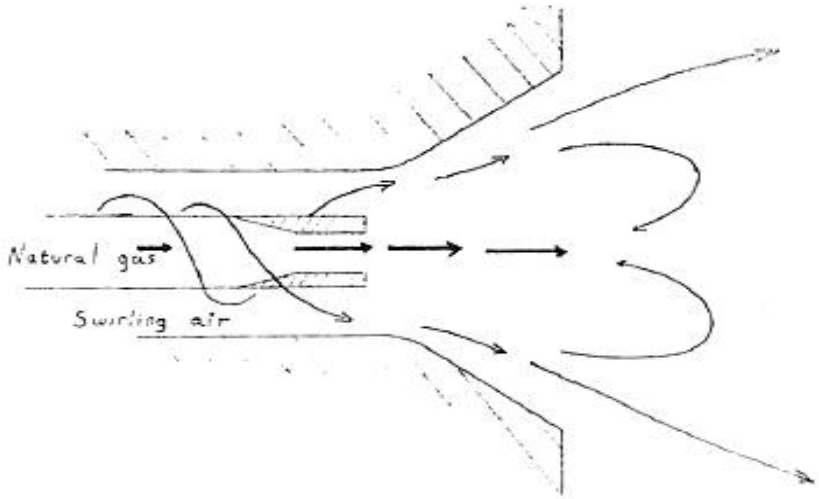

Figure 9.4 : *Illustration of flow path lines. [48]*

Figure 9.4 also illustrates how the swirling nature of the annular flow causes recirculation zones.
In order to describe the flow and mixing patterns in this specific burner accurately a CFD approach has been taken, this is described in chapter 11.

9.1.4. The reaction chamber and post reactor system

The combustion chamber is a 1,9 m long cylinder with an inner diameter of 315 mm. The cylinder walls are made of high density refractory cement (The experiments conducted by Weigang Lin described in chapter 6 where made with steel walls). When operating the burner a flame stands out from the swirl burner, the flame is observable through the two windows and the flue gas leaves the reactor at the bottom as indicated in figure 9.5.

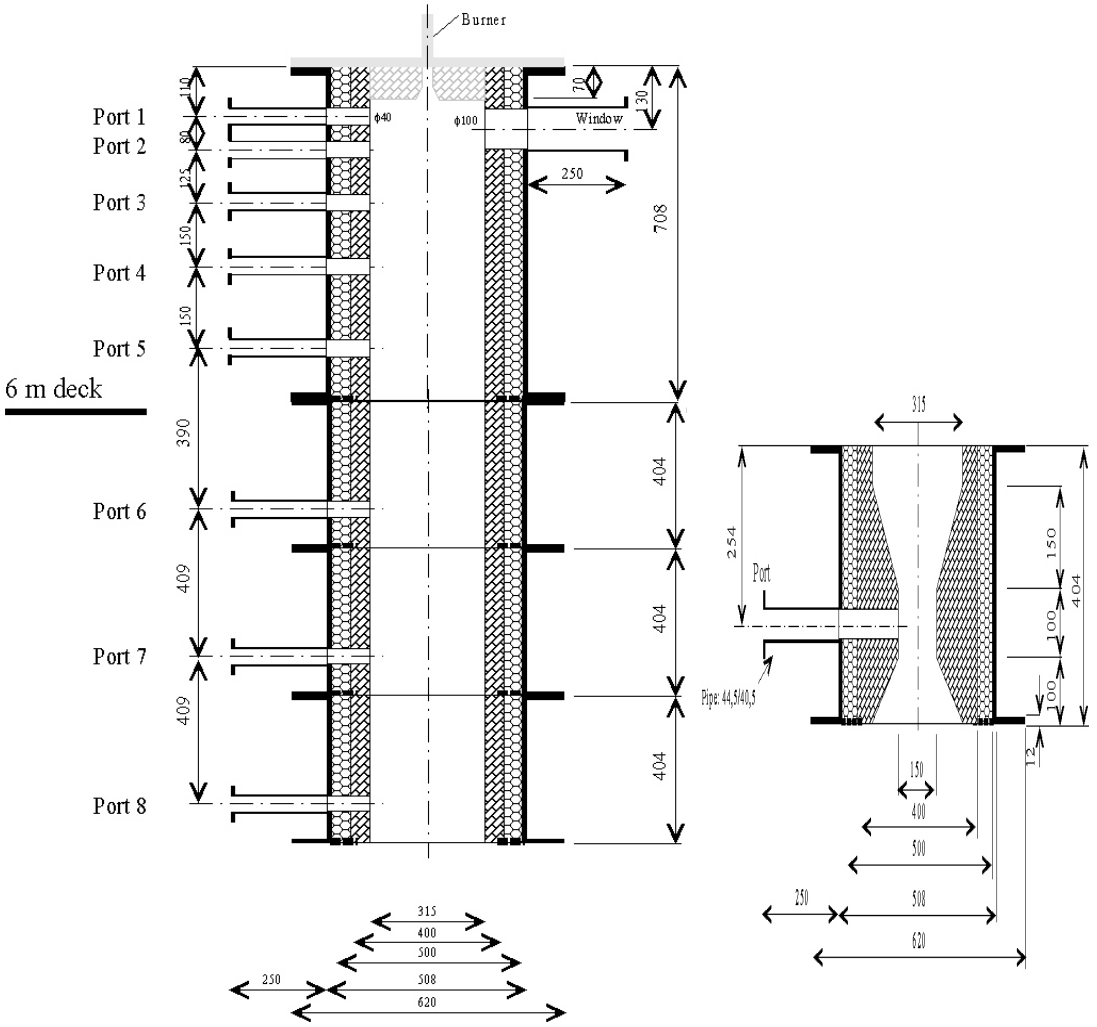

Figure 9.5: *A schematic drawing of the reactor chamber, during the experiments a neck has been inserted in the 2nd part of the reactor (the part with port 6) reducing the diameter from 31,5 cm to 15,1 cm.*

Tertiary air has throughout the experiments been added via a probe through port 6, so that the air came out at the center of the pipe. Temperature measurements were conducted using thermocouples placed in the center of the reaction chamber from port 2, 6 and 7. The gas sampling has been conducted from port 8 or from port 4.

The post reactor system consists of a reactor bottom, a particle separator and a heat exchanger. The particle separator is only necessary when firing with solid fuels, which has not been done during this project. The heat exchanger ensures cooling of the flue gas to 25-40°C (depending on the fuel load) before the flue gas is sucked through a fan on the service roof and merged with flue gas pipes from other setups into the main stack.

The outer surface of the reactor is enclosed by an air screen and by insulation material so the surface is not hot apart from at the reactor top and bottom. Furthermore the reactor is operated at sub pressure conditions (4 mbar sub pressure) to avoid harmful emission gases (mainly CO) to reach the surrounding work area in case of a leak. [47] Because of the screening and the sub pressure conditions it is quite easy to work on the reactor while it is running – for instance by changing gas sampling position or replacing thermocouples without having to shut down the entire system.

9.1.5. Gas sampling and analysis

The gas sample line (from port 4 or 8) is traced at 130°C. The gas is filtered at 150°C before it is cooled to 3°C to remove the water. From here the sample gas is pumped to a central gas analyzer station. [47]

Four gas analyzers have been used; a 3000HM THC analyzer, which works by using a FID (Flame Ion Detector) technique for measuring the amount of unburned hydrocarbons in the flue gas. A Eco Physics CLD 700 EL NO/NO_x analyzer that analyzes first the NO by oxidizing it with O_3 and observing the radiation emissions, afterwards any NO_x is reduced to NO and the same O_3 procedure is used for observing the newly converted NO. Two Fischer-Rosemount NGA 2000 analyzers were used one able to measure CO, CO2 and O_2 concentrations the other measures SO_2 and NO. A NDIR (Non Dispersive Infra Red) technique is used for measuring CO and CO_2, while O_2 is measured by a paramagnetic method.

These analyzers are calibrated daily in order to ensure accurate gas analysis. A data acquisition program (Labview) converts both the analogue signals from the analyzers and thermocouples to digital signals, these data are continuously stored.

9.1.6. Operation of the swirl burner

The burner system is started by setting natural gas and airflows to a desired (close to stoichiometric) level, then igniting the flame is done by switching the on/off button on the controller box. If the tangential air pressure is sufficiently high (above 0,3 bar) removal of any gases in the system is done for 30 seconds. Subsequently a purge of the natural gas is lead in to the reactor by opening the magnetic valves <MV 1> and <MV 2> (see figure 9.1) and an igniter provides a spark to ignite the flame. If the flame is successfully ignited the flame detector will (eventually) receive a stable flame signal at 5 V. If the flame is not successfully ignited the flame detector will shut the natural gas supply and the procedure will have to be done again. [48]

A number of safety precautions has been taken to ensure that the swirl burner can run safely even when left unattended. The flame extinguishes, if the pressure is less than 2 mbar below atmospheric pressure or if the cooling water temperature exceeds 60°C the burner will shut down. [47]

After the flame has been ignited the natural gas flow is set at the desired level and then the burner needs to reach a stable temperature state, this can take up to 15 hours if the burner was completely cold before start up.
The purpose of the experiments conducted within this project was to estimate the effect of SO_2 on CO emissions. However the reactor provides a pretty good and almost total combustion of natural gas, so even at 1 % O_2 in the flue gas no CO is detected. Therefore when having a hot reactor with the desired natural gas loading, the air flow is lowered to just below stoichiometric level where a CO level in the ppm range is obtainable. Thereafter SO_2 can be added and effects on CO can be investigated.
It can however be very difficult to get a stable CO emission since the CO oxidation can be very sensitive to temperature fluctuations, but also leaking into the reactor can significantly affect CO levels at this sensitive stoichiometric state.

For a more detailed description of how to operate the burner see the work by Dabkowski and the original setup description [47, 48].

10. Results and discussion

This chapter contains the most important results obtained through the experimental work on the set ups described in the previous chapter. For results of the engine experiments, see App. 2 of the present report.

10.1. Discussion of results from swirl burner experiments

It was clear from the beginning that the burner has a pretty good combustion efficiency and it was therefore necessary to lower the air - fuel ratio slightly under stoichiometric conditions (λ~0,95) in order to get any CO emissions. At these conditions the emission levels are very sensitive to even small changes in the air flow, so sometimes it has been difficult to obtain steady CO levels – leaking of air into the reactor and unsteady reactor temperatures are probably some of the explanations for unstable CO emissions even several hours after setting the flow specifications.

So every experiment has been conducted after setting the desired fuel and air flows and then waiting a while for CO emissions to stabilize. Hereafter 2 % SO_2 was injected with stepwise increase of the flow up to a maximum flow of 1 Nl/min, while allowing SO_2 emissions to stabilize before any new increase. Finally the SO_2 was turned off and this sudden decrease in SO_2 addition often resulted in drastic CO jumps as the results in the following sections will show.

Several very different experiments were conducted on the swirl burner setup.

Initially a series of experiments were done to investigate the effect of SO_2 on CO at different burner loads. At each burner load experiments of adding SO_2 was done at 4 different air flow settings:

1. An experiment where the swirl number is high
2. An experiment with a lower swirl number
3. An experiment where some of the combustion air (axial or tangential air) is replaced with tertiary air
4. A fuel rich experiment where hydrocarbon emissions are monitored.

The results from this experimental series are presented in appendix C and the most important results are discussed in section 10.1.1.

Another set of experiments were done, where the position for sampling the gas to the analysers was changed from the reactor bottom to a position just below the flame, the result from these experiments can be found in appendix D and a discussion follows in section 10.1.2.

The way the SO_2 was injected into the reactor was also varied; from adding it to the natural gas flow, injections were performed into the tangential, axial and tertiary airflows as well. The results from this can be found in appendix E and a discussion is in section 10.1.3.

Ammonia was added to the flame in combination with SO_2 to induce NO formation in order to investigate any interactions between NO and SO_2 and what impact they might have on the CO levels. The results from these experiments can be found in appendix F and a discussion will follow in section 10.1.4.

Finally O_2 in similar amounts as SO_2 was added to the flame to compare if the oxidative nature of SO_2 in itself can account for the effect on CO emissions or a more detailed chemical mechanism is responsible. The results from these experiments will follow in appendix G and a discussion of the results is found in section 10.1.5.
Appendix H contains a small discussion of the reproducibility of the results.

10.1.1. First experimental series

In the very first experiment an obvious effect was seen on the CO emissions when adding SO_2. Figure 10.1 shows the emission of CO and SO_2 during this experiment.

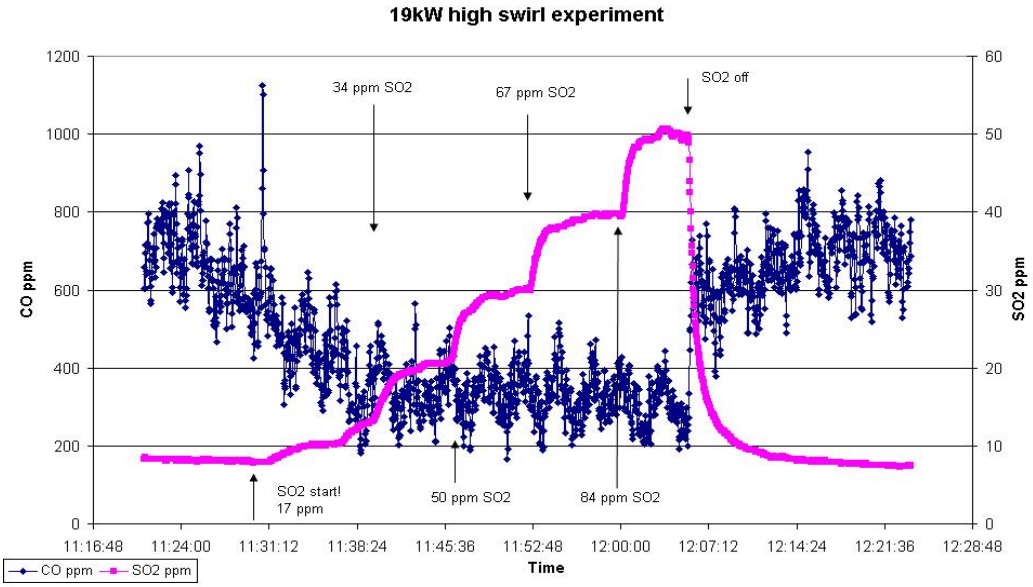

Figure 10.1: *CO and SO_2 emissions from a 19 kW high swirl number experiment.*

Many of the trends noticeable in figure 10.1 was typical for these experiments, for instance the CO levels are very fluctuating but also the relationship between the calculated SO_2 emissions and the

observed emissions does not add up – approximately one third to half of the SO_2 seems to be missing, which could be because sulfur leaves the reactor as another sulfur specie than SO_2, even though SO_2 is expected to be the thermodynamically favoured sulfur component [7]. Other reasons could be that sulfur participates in deposit formation so that it is accumulated in the reactor or the sulfur could be incorporated in soot, which is filtered out before the gas analysers. The most important result from figure 10.1 is however that the CO emission seems to decrease as SO_2 is lead to the system – this effect is especially pronounced when the SO_2 is turned off, this often leads to immediate increase in CO emission. When the SO_2 flow is opened a fluctuation is observed in the CO emission this is also a typical observation probably due to the flow disturbance – the CO level quickly return to the initial level. Any dilution effects from adding the SO_2 is assumed to be negligible, since the overall gas flow is about 250 times higher.

Figure 10.2 show the emissions of total hydrocarbons (THC), CO and SO_2 from a 19 kW fuel rich experiment.

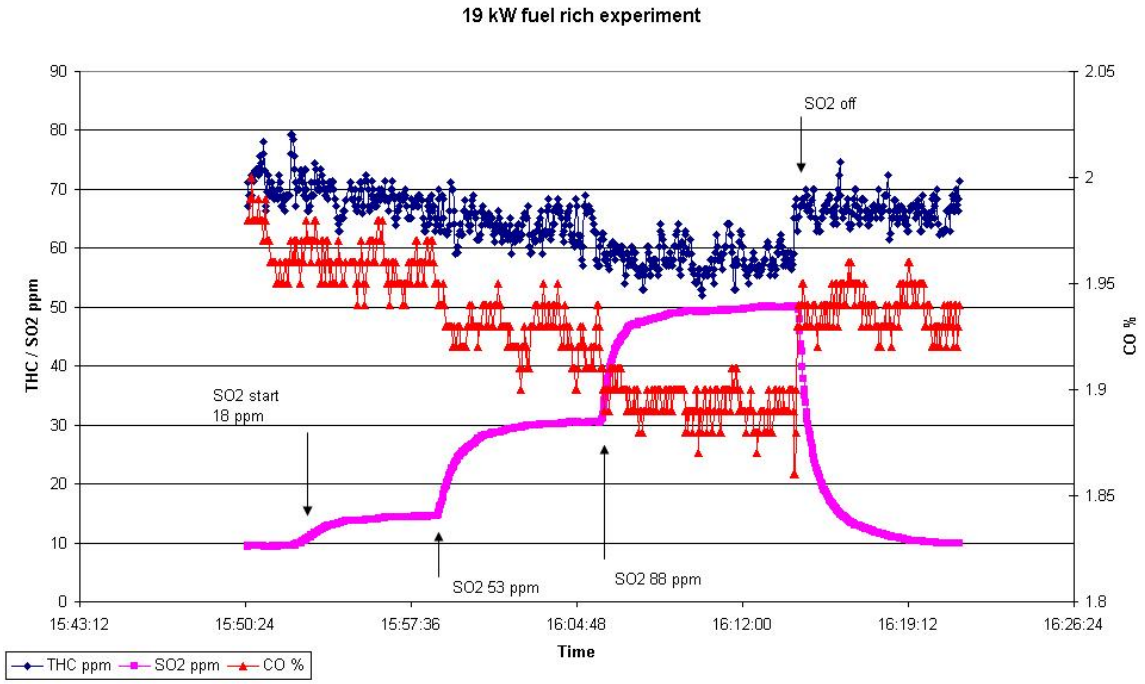

Figure 10.2: *THC, CO and SO_2 emissions from a 19 kW fuel rich experiment.*

It appears from figure 10.2 that the effect of SO_2 affects both THC and CO emissions, this result leads to the conclusion that the effect of sulfur is a general combustion promoting effect probably due to an increase in chain carrying radicals and not an effect specifically on CO oxidation.

Table 5 summarizes the main results from this experimental series. The effect on emissions given in the right columns is based on the observed emission change when SO_2 is turned off.

Table 5: *Summary of experimental results*

Burner effect / kW	Experiment type	Reactor temperature °C Port 2 / Port 6 / Port 7	CO reduction ppm / %	THC reduction ppm / %
8	High swirl	970 / 600 / 425	No	-
8	Low swirl	970 / 600 / 425	No	-
8	Fuel rich	915 / 590 / 398	No	50ppm ~ 10%
13	High swirl	1140 / 835 / 615	No	-
13	Low swirl	1158 / 835 / 620	No	-
13	Tertiary air	1040 / 935 / 690	150ppm ~ 15%	-
13	Fuel rich	1090 / 815 / 615	Observable	50ppm ~10%
19	High swirl	1200 / 870 / 650	400ppm ~ 50 %	-
19	Low swirl	1170 / 910 / 710	450ppm ~ 40 %	-
19	Tertiary air	1210 / 955 / 720	500ppm ~ 25 %	-
19	Fuel rich	1260 / 930 / 700	Observable	15ppm ~ 30 %
23*	*Tertiary air*	1347 / 1050 / 820	500ppm ~ 35 %	-
23**	*Tertiary air*	1340 / 1050 / 830	500ppm ~ 25 %	-
26	High swirl	1410 / 1050 / 875	1000ppm ~ 90 %	-
26	Low swirl	1325 / 1010 / 870	600ppm ~ 75 %	-
26	Tertiary air	1300 / 1150 / 890	800ppm ~ 35 %	-
26	Fuel rich	1325 / 1050 / 835	Observable	30ppm ~ 10 %

* *Result is from an experiment described in appendix D*

** *Result is from an experiment described in appendix E*

The main conclusions from the results presented in table 5 are that at higher burner efficiencies the effect of SO_2 on combustion emissions seems to increase – figure 10.3 gives a better illustration of this correlation between burner effects i.e. reactor temperatures and CO reduction.

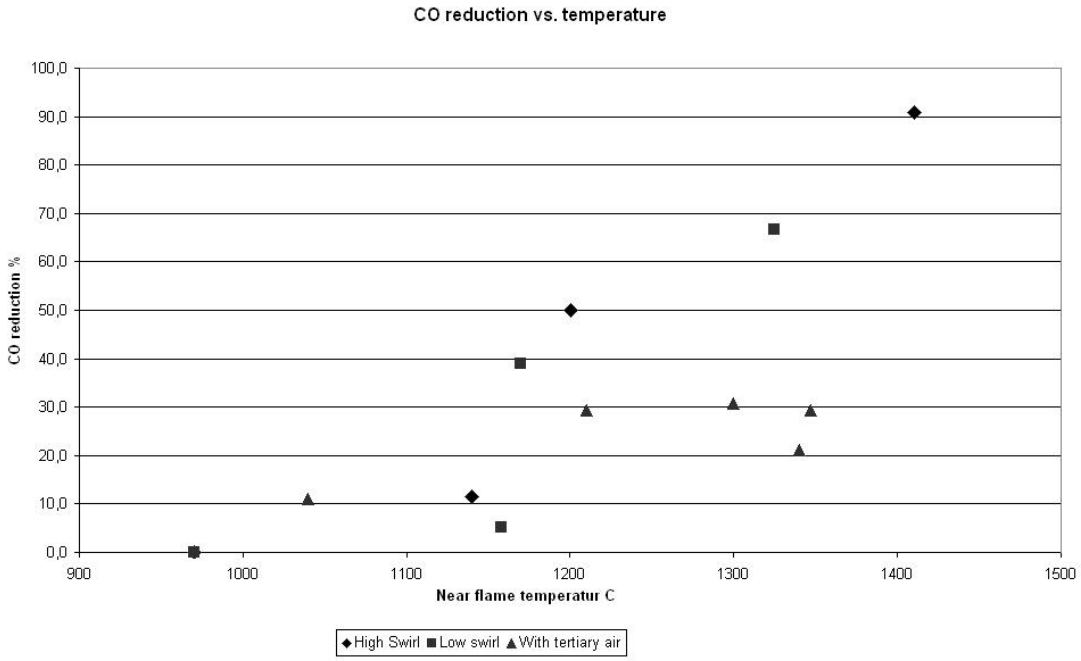

Figure 10.3: *Correlation between CO reduction and near flame temperatures.*

Figure 10.3 show an almost linear increase in CO reduction starting with near flame temperatures around 1000°C.

A parameter that could prevent any combustion promotion by SO_2 is the available oxygen in the flue gas – since these experiments are conducted at slightly fuel rich conditions the remaining oxidizer in the flue gas is limited, which is also seen on the O_2 emissions which at all experiments (except for the 8 kW experiments) are practically 0 %, so the availability of oxidizer also influences the emission reductions.

It is difficult to see differences in emission reductions between the high and low swirl experiment but in general the reduction (in percentage) is a bit lower for the tertiary air experiments – this could be because the effect of SO_2 is taking place in the top flame region of the burner, and for the tertiary air experiments even less oxygen is available in this region.

Since the burner is so effective that no CO is observed at fuel lean conditions it is difficult, based on these experiments, to predict what would happen in an actual power producing combustion system, where flue gas oxygen concentrations are much higher.

As table 5 and figure 10.3 shows a 90 % reduction in CO emission was obtained in a 26 kW experiment.

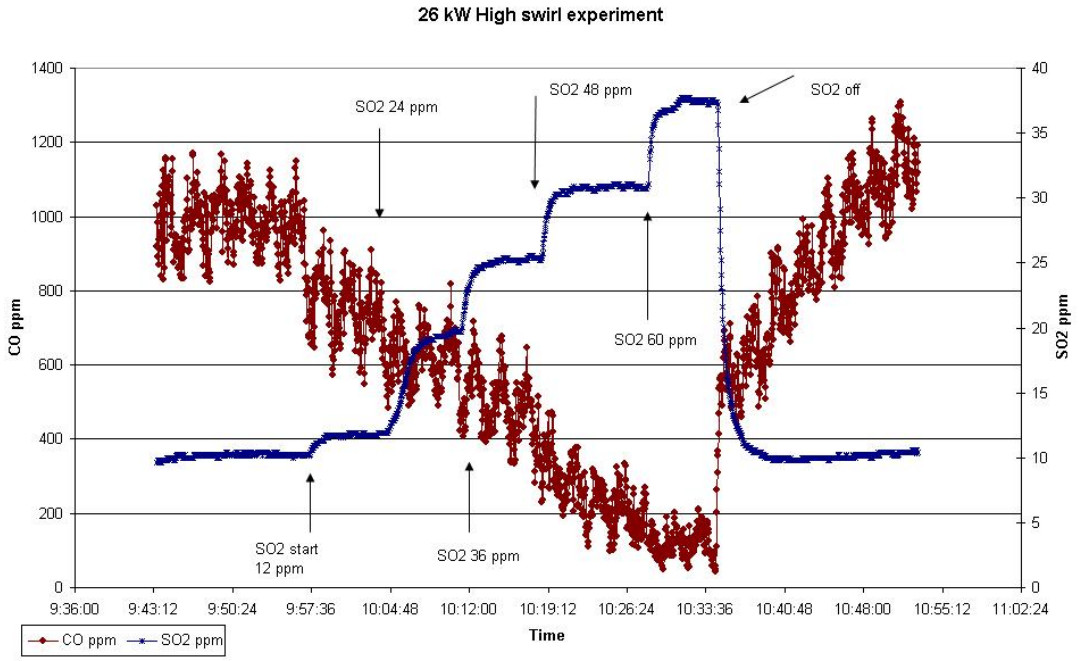

Figure 10.4: *CO and SO_2 emissions from a 26 kW high swirl experiment.*

Figure 10.4 shows the CO and SO_2 emissions from the experiment where the maximum CO reduction was observed. It is clear from figure 10.4 that the CO emission decreases stepwise as SO_2 is added, and when SO_2 is turned off an increase in CO levels from ~100 to ~1100 ppm is observed. The temperature in the flame region was measured to 1400°C. Since only 60 ppm of SO_2 is added to the combustion process it is clear that the effect of SO_2 on CO emission is more extensive than can be accounted for by the stoichiometric amount of S and O added.

10.1.2. Sample positions

The graph in figure 10.5 illustrates emissions from a 23 kW experiment, where the gas sampling occurred from the bottom.

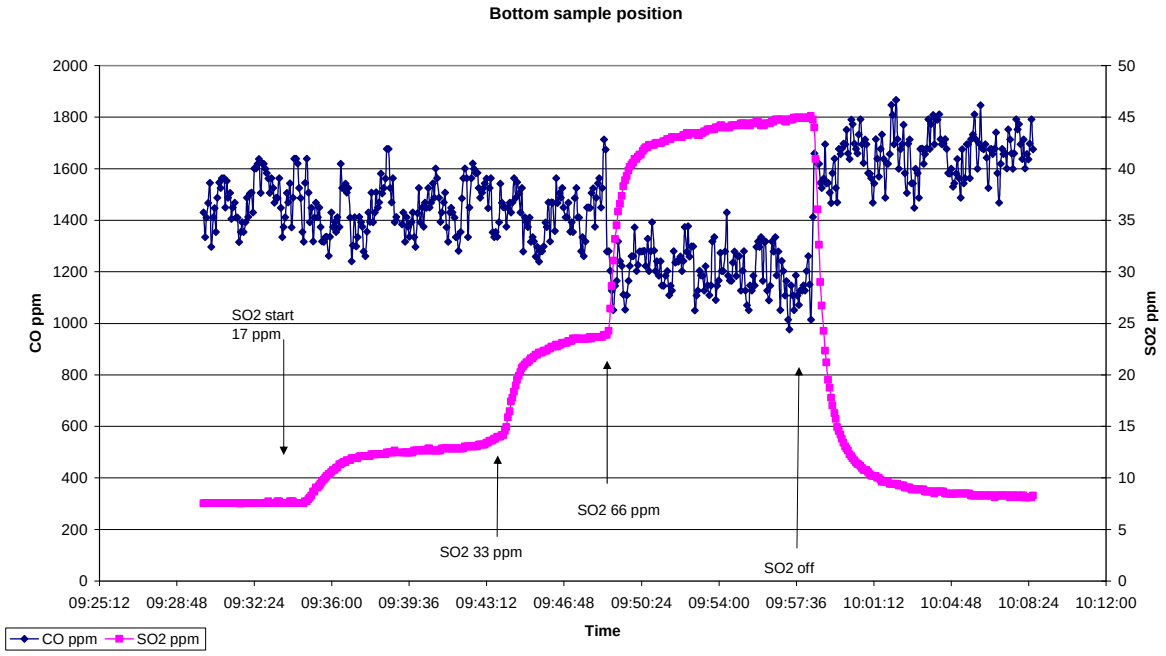

Figure 10.5: *CO and SO_2 emissions from a 23 kW tertiary air experiment- sampled from port 8 (the bottom sampling position where all other samples also has been collected).*

It is this experiment that is included in table 5. Figure 10.5 shows the characteristic jump in CO emission when SO_2 is turned off.

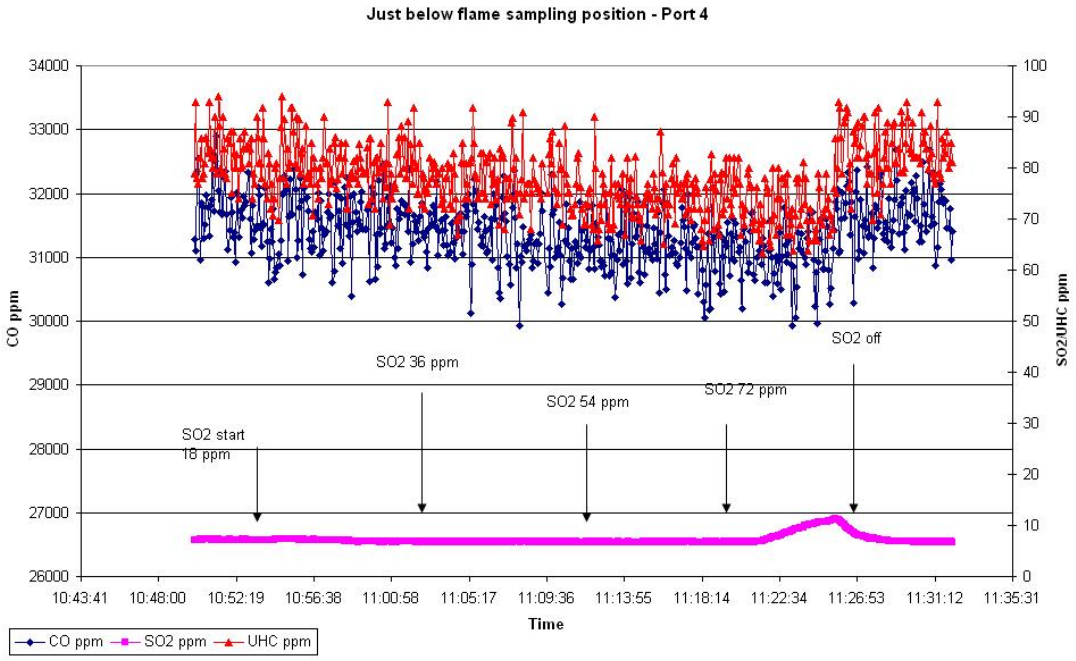

Figure 10.6: *UHC, CO and SO_2 emissions from a 23 kW tertiary air experiment- sampled from port 4.*

Figure 10.6 show an identical experiment as 10.5 the only difference is that the flue gas is sampled from the centre of the reactor just below the flame. What is interesting is that SO_2 is not emitted until late in the experiment most likely because sulfur appears as another gas compound probably H_2S – a similar observation were done for the 23 kW fuel rich experiment. Another explanation could be that the SO_2 was adsorbing on the sampling probe. Changing the sampling position verifies the suspicion from the first experimental series, that the promoting effect of SO_2 take place in the near flame region – it is unclear from these experiments whether the effect only takes place in the flame region or it continuously promotes oxidation in the post flame region as well.

10.1.3. Adding SO_2 in different flow streams.

A set of experiments were made, where the SO_2 was added to different flow streams – in all previous experiments the SO_2 has been added to the natural gas (as displayed on figure 9.1) but it was of interest to establish if the promoting effect of SO_2 only was occurring in the flame region, or if addition of SO_2 further downstream could have an effect.

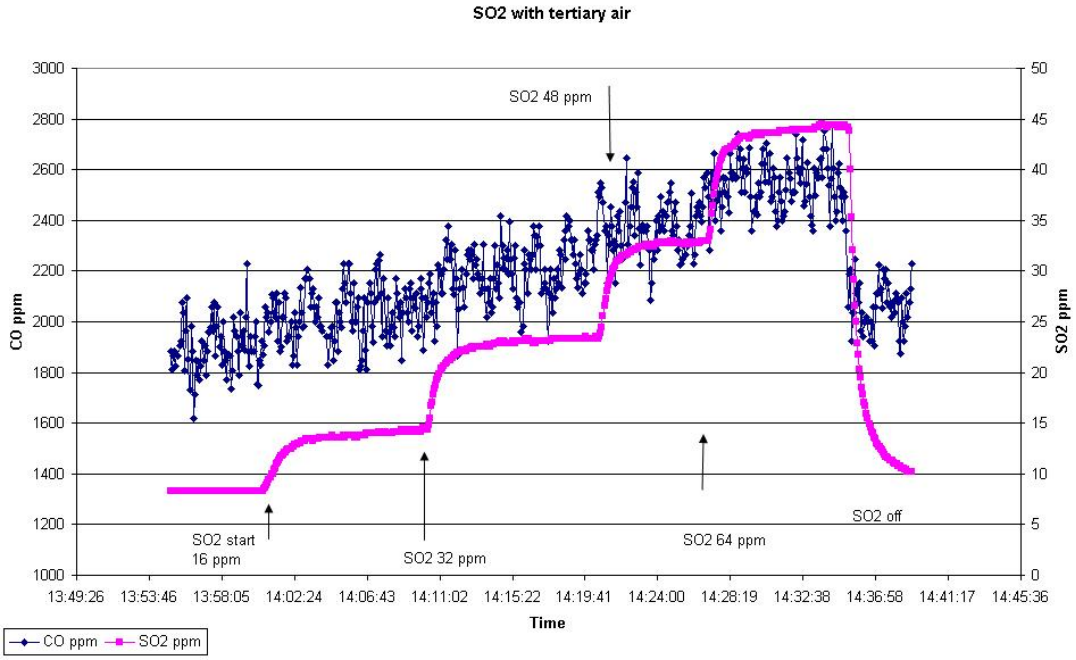

Figure 10.7: *CO and SO_2 emissions from a 23 kW experiment*
SO_2 is added with the tertiary air flow.

It is very surprising to see from figure 10.7 that addition of SO_2 to the tertiary air causes an obvious increase in CO emissions. This is probably due to the radical recombining effect of SO_2 described in the literature study (chapter 3).

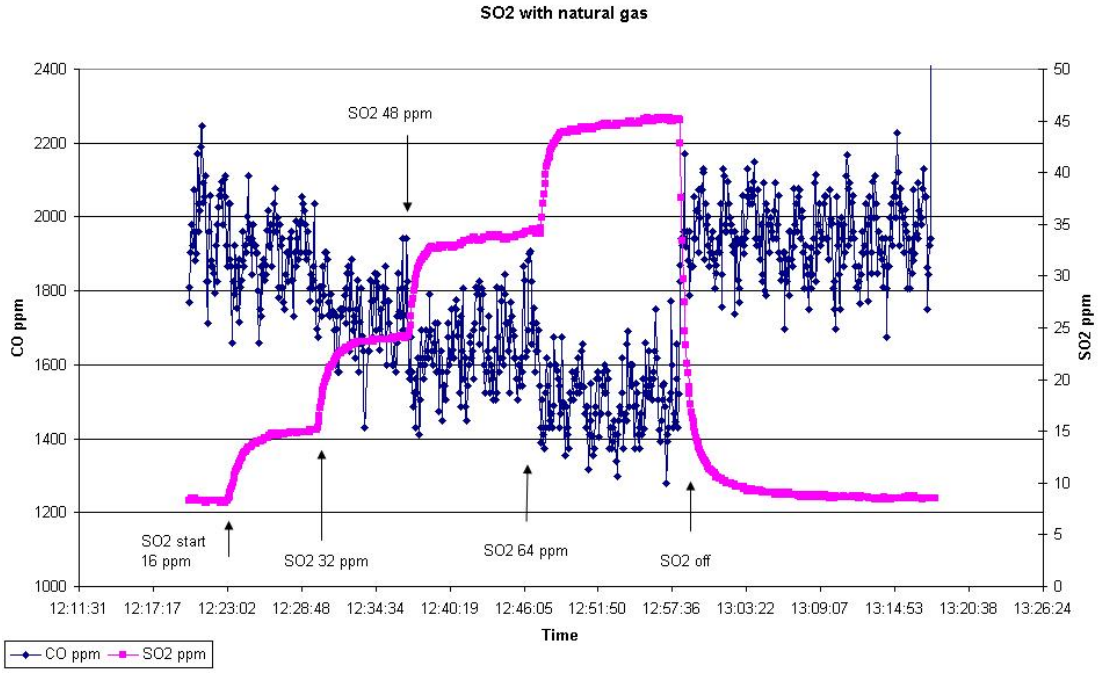

Figure 10.8: *CO and SO_2 emissions from a 23 kW experiment*
SO_2 is added with the natural gas flow.

Comparing figure 10.8 and 10.7 shows a rather surprising result; injection with natural gas promotes combustion, injection with tertiary air inhibits combustion.

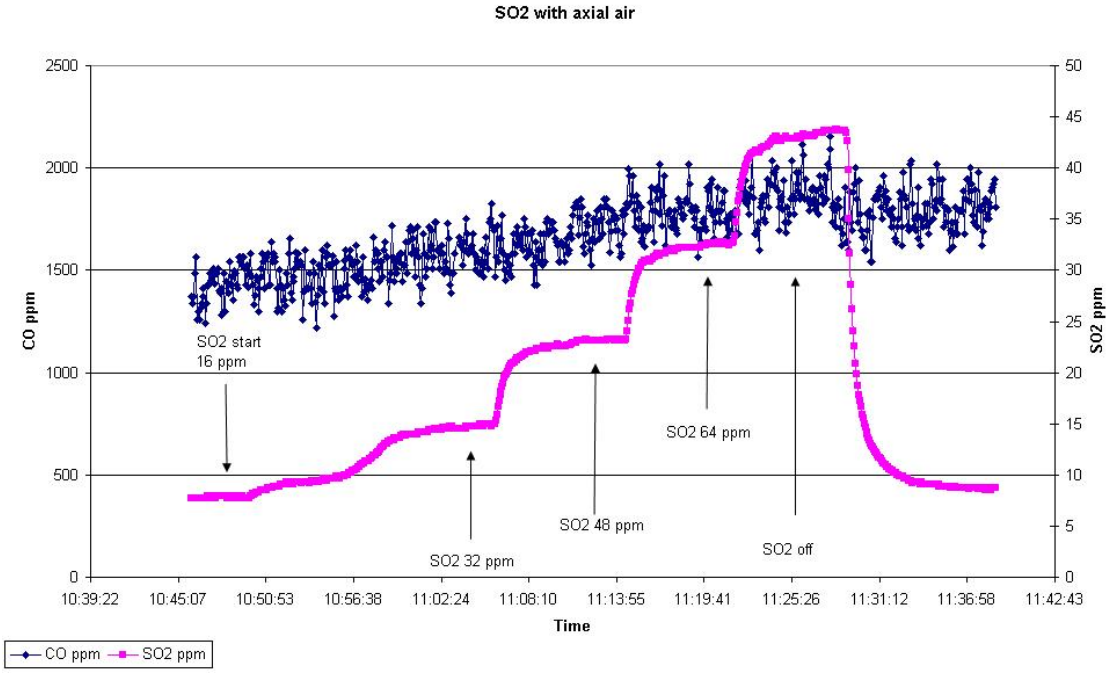

Figure 10.9: *CO and SO_2 emissions from a 23 kW experiment*
SO_2 is added with the axial airflow.

Figure 10.9 shows the effect of SO_2 on CO emissions when SO_2 is added to the axial airflow. In this case it appears that the CO emissions are a bit unstable, but not much seems to happen when the SO_2 flow is turned off (maybe a small decrease in CO emissions). This could imply that a promoting effect of SO_2 is occurring in the top region of the burner – most dominant in the flame region. In the second combustion stage the effect is however inhibiting – as seen when adding SO_2 to the tertiary air. For the experiment shown in figure 10.9 an explanation for the lack of effect could be that these two regionally decided effects; promotion in the top and inhibition in the bottom balances out.

10.1.4. Simultaneous addition of ammonia and SO_2

In order to investigate the effect of NO on the combustion promoting effect of SO_2 experiments were made, where both SO_2 and NH_3 was added to the natural gas flow. NH_3 was added to provoke NO formation in the flame – addition of NO gas would have been preferred, but there was no available NO gas in the right amount and setup already had the possibility to add NH_3.

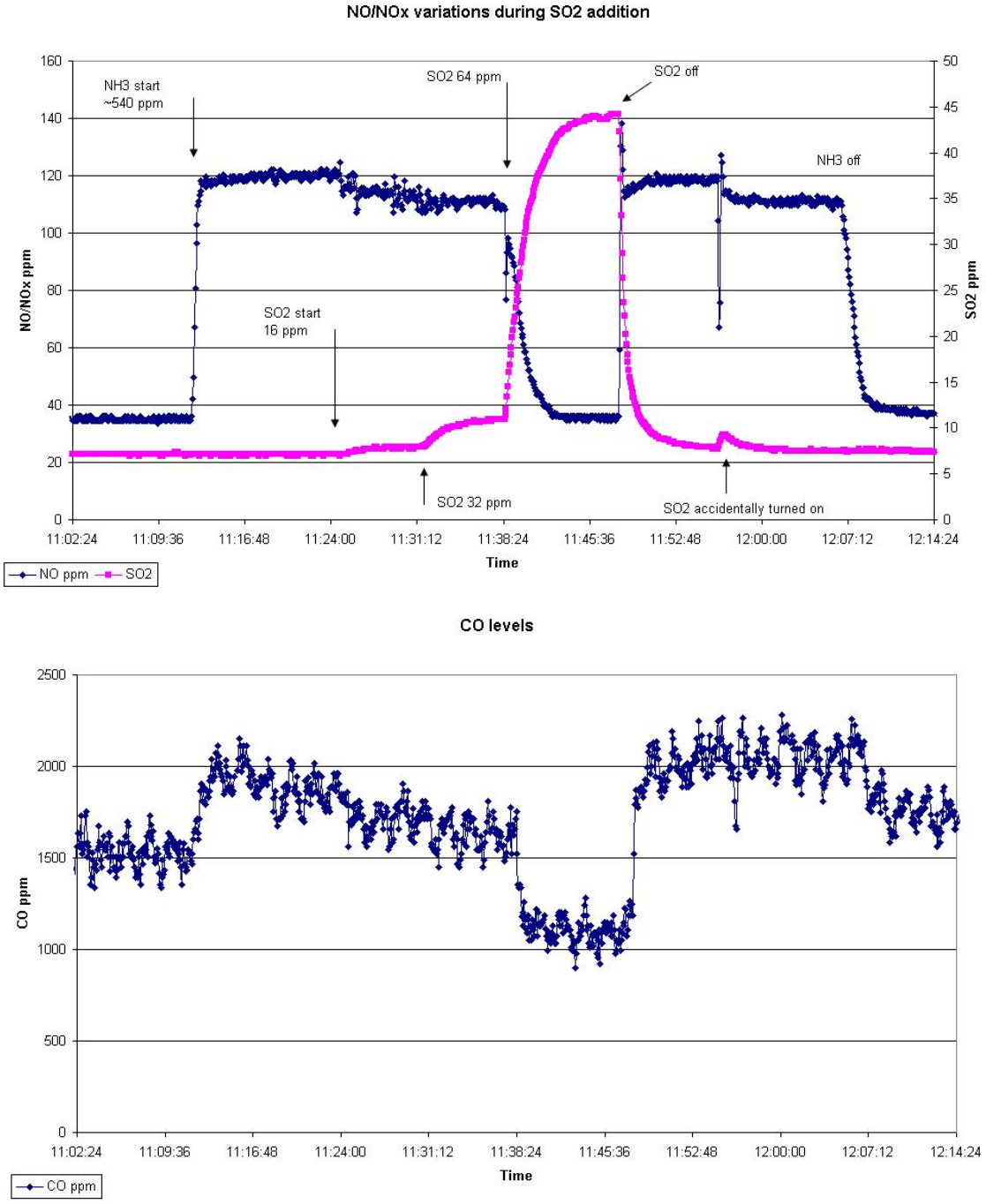

Figure 10.10: *SO_2, NO(top figure) and CO(bottom figure) emissions from a 23 kW experiment where SO_2 and NH_3 are added simultaneously. Note the identical x axis.*

Figure 10.10 shows the emissions of SO_2, NO (practically all NO_x was NO) and CO during this experiment. What is really interesting about this experiment is the effect of SO_2 on the NO levels – it seems that the presence of a critical amount of SO_2 succeeds in removing all of the ammonia caused NO. As discussed in section 3.5.1 the effect of sulfur on NO formation is assumed to be inhibiting because of the radical recombining effect of SO_2.[7]

(10.1) $SO + NH \rightleftharpoons NO + SH$ [20]

(10.2) $NS + OH \rightleftharpoons SH + NO$ [32]

Reactions 10.1 and 10.2, which are also discussed in section 3.5.1, point toward an increased NO formation due to SO_2 – so both inhibiting and promoting effects of SO_2 has been reported in the literature. It is however surprising that SO_2 is able to remove such a comparably large amount of NO. During all other experiments the NO emission (which was in the range 20-50 ppm) was not influenced significantly by the SO_2 addition.

As noted in appendix F a white salt was observed in the pipeline, where the NH_3 and SO_2 mix before entering the natural gas flow. This salt is presumably ammonium sulphate, and it could explain how some of the NO is removed (NH_3 never enters the reaction chamber). However NH_3 concentrations are almost 10 times higher than the SO_2 concentration and the SO_2 emissions does not seem to be significantly lower than what has been seen during other experimental series (approximately one third to half is not accounted for at the analyzer) – so a large amount of both NH_3 and SO_2 must enter the reactor.

Addition of ammonia causes the CO emissions to increase; this could be due to the overall increased competition for the available oxygen, the effect of adding approximately 500 ppm NH_3 causes an approximate increase in CO of about 500 ppm.

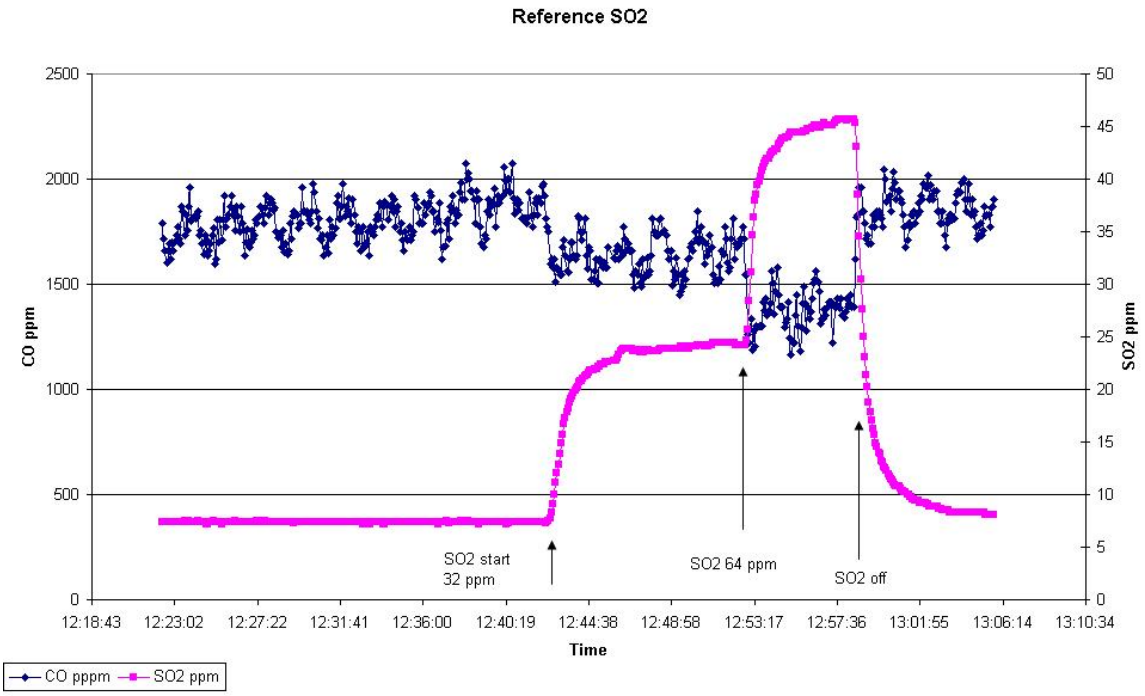

Figure 10.11: *SO_2, and CO emissions from a 23 kW experiment.*

Figure 10.11 illustrates the CO and SO_2 emissions from an experiment performed just after the NH_3-SO_2 experiment described with figure 10.10. This experiment was meant as a reference to the CO emissions observed in figure 10.10. Figure 10.11 show a 500 ppm reduction in CO emissions which is also what is observed in figure 10.10 (when measuring from before NH_3 is added) so there is no indication of any connection co-operation between N and S species in promoting the combustion. In other words the presence of ammonia does not affect the CO reduction by SO_2, but it is interesting that SO_2 seems to be capable of preventing the NH_3 to leave the reactor as NO.

10.1.5. Comparing SO_2 and O_2 addition

By observing the reduced emissions of CO when adding SO_2 it is clear that the effect of SO_2 is higher than the molar equivalence of the injected oxygen. The experiment displayed in figure 10.12 was made to quantify what the decrease in CO emissions would be, if O_2 was added to the natural gas flow instead of SO_2.

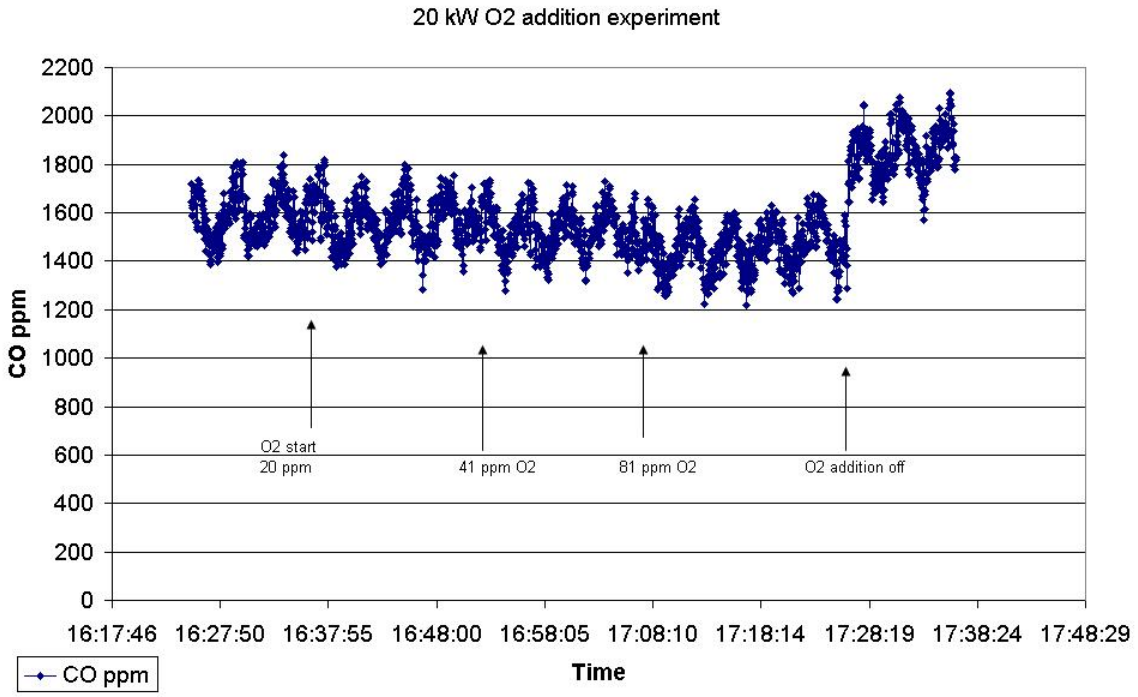

Figure 10.12: *CO emissions from a 20 kW experiment O_2 addition experiment.*

Figure 10.12 shows that a 80 ppm addition of O_2 causes an approximate CO decrease of 400 ppm – more than twice the equivalence ratio, however a small effect might also come from any temperature increases caused by the increased combustion.

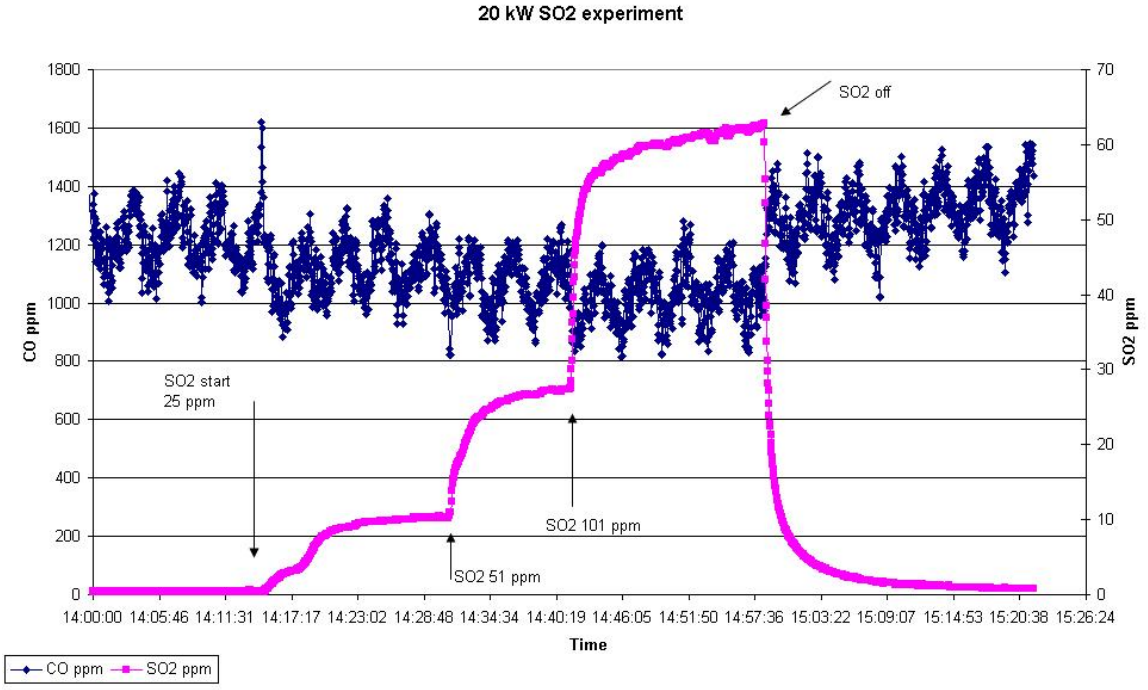

Figure 10.13: *SO_2 and CO emissions from a 20 kW experiment O_2 addition experiment.*

In comparison a SO_2 experiment conducted just before the O_2 addition is shown in figure 10.13. The effect of adding 100 ppm SO_2 also seems to be a 3-400 ppm reduction in CO emission. Even though the conditions in these experiments are very sensitive to changes it is interesting to notice that effects of adding SO_2 and O_2 to the natural gas seem quantitatively to be quite similar. This could point to the explanation that addition of SO_2 causes increased formation of radical chain carriers in the fuel rich part of the flame in a similar manner as it would be expected that addition of O_2 results in formation of O and OH radicals.

10.2. Summary and conclusions based on swirl burner experiments

It is quite obvious from the swirl burner experiments that the combustion promoting effect of SO_2 is occurring in the fuel rich flame zone. The experiments of adding SO_2 to different gas flows point to this conclusion and changing the sampling position to just below the flame confirm that the effect of SO_2 is present in top region of the reaction chamber. These results also seem to exclude surface reactions on reactor walls as a pathway to combustion promotion by SO_2, mainly because of the necessity of adding the SO_2 to the natural gas in order to see an effect. The experiment where SO_2 is sampled just below the flame, and the 26 kW fuel rich experiment (see appendix C) shows that at very rich conditions, as in the diffusion flame, SO_2 is not likely to be the dominant sulfur species – and other sulfur species (maybe S or SH radicals) are likely to play the dominant combustion promoting effect. Quantitatively the effect seems to increase with increasing natural gas flows, even though this results in lower sulfur concentrations. But higher natural gas flows also result in increased flame lengths and it is possible that this increased sulfur presence in reducing zone area stimulates the combustion promoting effect of SO_2. The effect of adding SO_2 is quantitatively quite similar to that of adding O_2 to the flame, and this observation adds to the suspicion of SO_2 being able to contribute to/ be converted to radical chain carriers.

It does however still remain an open question how it is possible for sulfur to contribute to the combustion process, and especially how it is possible to promote the combustion in a more than molar equivalent fashion (60 ppm SO_2 results in a 1000 ppm CO decrease). Recirculation zones in the top region of the reaction chamber can maybe account for an increased residence time for the sulfur species, making it possible for them to be reused in multiple reaction series.

10.2.1. Reduced PAH mechanism theory

Since the effect of SO_2 so distinctively is active in the flame zone it is obvious to assume that the sulfur species in some way can affect soot formation maybe by preventing the formation of PAH's (poly aromatic hydrocarbons) in the soot inception zone of the flame. By looking at the flame in the swirl burner there is no indication of actual smoke (soot particle escaping the flame) from the flame, but it is likely that minor PAH's are formed but are not growing large enough to reach the nucleating stage. Increasing the concentration of oxidizing radicals in the soot inception zone might be able to prevent or minimize PAH growth, and when the minor hydrocarbon molecules reach the oxidizing regions they are more easily fully oxidized to CO_2.

10.2.2. Non promoting effects

Another theory could be that adding sulfur actually does not promote the combustion but instead affect the water gas shift reaction favouring the right side products in reaction 10.3:

(10.3) $$CO + H_2O \rightleftharpoons CO_2 + H_2$$

Since it has not been possible to measure either H_2 or H_2O content in the flue gas it is difficult based on these experiments to discover if the effect of adding SO_2 is affecting the equilibrium in 10.3. Furthermore the changes in concentration for the more abundant combustion participants such as CO_2 and also O_2 are so small (CO_2 and O_2 are measured in % and the changes are expected to be in the ppm range) that it is difficult to account for the presumed changes caused by SO_2.

If addition of SO_2 actually increases/causes soot formation it could explain why CO is removed from the system, unfortunately is has not been possible to confirm this effect by quantifying any soot that might be formed. However, there was not anything in the experiments indicating that actual soot particles were formed. The flame usually had a clear blue color, indicating that hydrocarbons are oxidized (although it could be hard to see due to radiation from the wall material). Furthermore the gas filter did not seem to collect significant amounts of particles.

11. CFD modeling

The purpose of modeling the swirl burner using computational fluid dynamics (CFD) is to get an idea of flow streams and recirculation zones inside the reaction chamber. The approach taken is to model two experiments – the 26 kW high swirl experiment where the largest CO decrease was observed and the 8 kW high swirl experiment where no CO change was observed. Even though the CFD calculation also include chemical reactions, it is not possible by using the CFD modeling tool to get a detailed description of the chemical reactions taking place in the furnace. The detailed kinetics is instead modeled by using Chemkin.

The CFD program Fluent 6 is used for the CFD modeling.

11.1. Geometry creation and meshing

The CFD program Fluent uses a finite volume method to calculate flow features in a given domain; therefore this domain needs to be thoroughly divided into small computational cells. This is done using the Fluent pre-processing tool Gambit.

The most accurate way to describe the swirl burner is by using a 3D model. This approach was first taken, but the load of computational cells made the 3D description unfeasible.

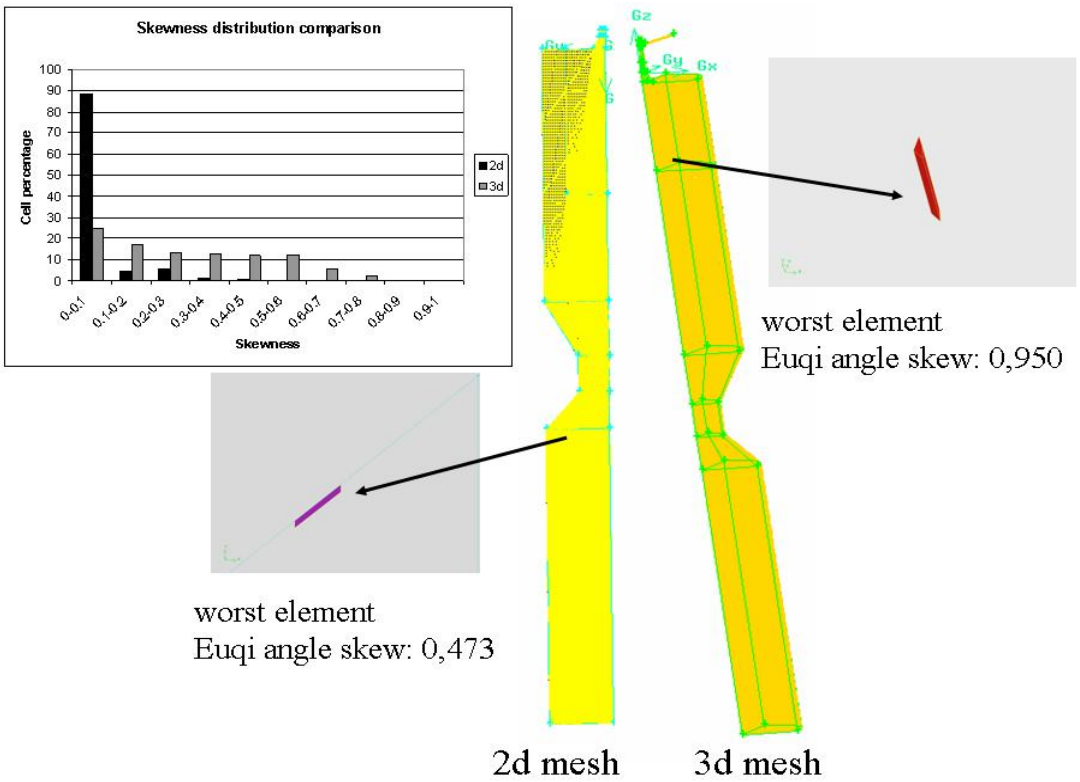

Figure 11.1: *Left: 2d meshed burner 19980 cells. Right 3d meshed burner 1013548 cells. Skewness distribution comparison in upper left corner.*

It is a commonly used trick when doing CFD modeling to use any symmetry in the computational domain to decrease the number of cells. Apart from the 4 tangential inlets in the top burner section the geometry is entirely axi-symmetric. This means that in a 3d model the burner can be split in quarts as displayed in figure 11.1. A 2d approach was then applied, where the boundary conditions for the inlet flow was moved to after the tangential inlets. The tangential and axial inlet velocities where then calculated as described in appendix B (with a modification for the temperature deviance from standard conditions – inlet gas temperature was assumed to be 300 K).

It was chosen to proceed to the numerical simulations with the 2d model. The 2d description of the burner is meshed entirely with quadrants, and the general skewness is quite low as displayed in figure 11.1 especially compared to the 3d mesh, where highly skewed cells where located at the flame zone.
For the 2d geometry a more dense mesh was applied for the inlets and upper burner region, where the combustion is expected to take place.
A full instruction on how to create the 2d geometry and mesh it can be found in appendix J.

11.2. Fluent simulations

The main purpose of the CFD modeling is to investigate flow features in the furnace. In order to simplify the analysis two experiments were chosen to be analysed using CFD: The 26 kW high swirl experiment where a 90 % reduction of CO emissions was obtained and the 8 kW high swirl experiment where no obvious reduction in CO emissions where observed.

11.2.1. Solver settings

In the CFD analysis of the swirl burner the Fluent 6 default segregated solver was chosen.
The Fluent software program includes many different submodels describing turbulence, radiation and also chemical reactions. The approach taken in this analysis was not to model the detailed chemistry with radical reactions and influence of minor species as N, S and soot – simply because it is not expected proving an accurate picture of what is going on in the furnace in such detail. Instead a one step global reaction mechanism for methane combustion was used to describe the chemistry:

(11.1) $CH_4 + 2\ O_2 \rightarrow CO_2 + 2\ H_2O$ $\quad r = 5{,}012e11 \cdot \exp(2e11 J/mol / RT) \cdot [CH_4]^{0,7} [O_2]^{0,8}$

The rate of reaction is computed in Fluent using the combined eddy dissipation/finite rate chemistry model. With this combined chemistry model Fluent evaluates the mixing rate of reaction and the kinetic rate of reaction in each cell, and uses the minimum of these two rates. Usually in diffusion flames the chemistry is mixing limited, however the Arrhenius rate can act as a kinetic "switch", preventing mixing induced reaction at lower temperatures. [52] The Arrhenius rate for reaction 11.1 is displayed to the right of the reaction. The mixing rate of reaction in the eddy dissipation model is evaluated using the measures for k (turbulence kinetic energy) and ε (turbulent dissipation rate) and combustion proceeds whenever turbulence is present. [52]

The eddy dissipation/finite rate combustion model in Fluent is located in the menu 'Species Transport' which means that along with combustion rates; transport properties (convective and diffusive) are calculated for all combustion participants and products.

In order to get a detailed description of the turbulent mixing in the reactor a more detailed turbulence model, the Reynold stress model (RSM), was chosen. In comparison with the standard k-ε turbulence model the RSM is expected to perform better for high swirling flows. [52] However the standard k-ε model is experienced to be more robust, so the approach taken was to find a temporary solution using the standard k-ε model, and then switch to the RSM to find the final solution.

Radiation is a major source of heat loss from the flame, and therefore needs to be accounted for. This has been done using the P1 radiation model, which is reported to describe combustion applications reasonably well. [52]

11.2.2. Boundary conditions

Although it is important to choose reasonable solver settings it is at least as important to set appropriate boundary conditions. Figure 11.2 show the upper furnace region, where initial gas mass flows are specified for the tangential and natural gas inlets.

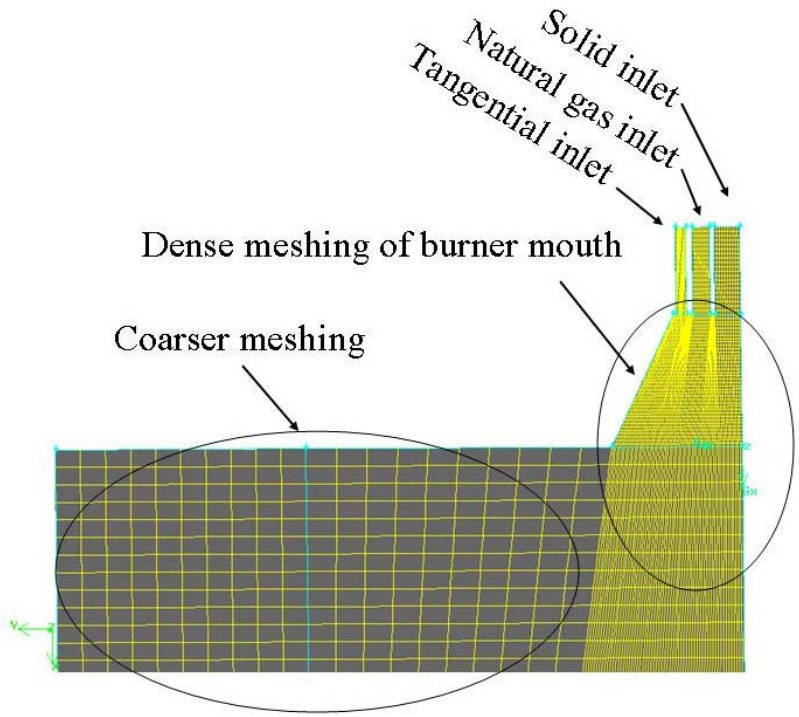

Figure 11.2: *Illustration of the mesh at the inlet.*

An example on how to calculate the inlet conditions is shown in appendix K.

Another boundary condition specified in Fluent is the outlet, which is defined as a pressure outlet zone. Since the burner is operating at sub pressure caused by ventilation through this outlet, a gauge pressure of 100 Pa (1 mbar) is attributed to the outlet zone, furthermore the backflow temperature is set to 1000 K (500 K for the 8 kW simulation) and in order to evaluate the effect of any backflow, the species composition is set to pure N_2.

Another boundary setting that needs to be applied is the wall temperatures. In Gambit the wall zones are split into five different areas. A constant temperature has been chosen for each of the specific wall surfaces. Table 6 shows the fixed wall temperatures in both experimental settings. The wall emissivity was chosen to be 0,9 for all walls, this was found to be in good agreement with values for refractory materials. [53]

Table 6: *Wall boundary conditions*

	Burner wall	Top furnace wall	Neck wall	Bottom furnace wall
26 kW simulation	400 K	1400 K	1150 K	1000 K
8 kW simulation	400 K	900 K	900 K	700 K

After applying solver settings and choosing boundary conditions, the discretization parameters need to be specified. The PRESTO scheme was used for pressure interpolation, and 2nd order upwind was used for all fluid species, swirl velocity and momentum, for the remaining parameters first order upwind scheme was used. The simple pressure velocity coupling was used. The relaxation factor for momentum was reduced to 0,5 and relaxation factors for the fluid species was reduced to 0,6 other relaxation factors was kept at default.
A thorough instruction of the Fluent setup is given in Appendix K along with residual plots.

11.3. Results from CFD simulations

When the residuals reached a steady level and grid adaption did not seem to influence the overall solution it was assumed that convergence was obtained. However the mass balance also needs to add up, which is also the case as shown in table 7.

Table 7: *Mass balances for 8 kW and 26 kW converged solutions*

	26 kW simulation	8 kW simulation
Natural gas inlet	4,4331e-4 kg/s	1,34848e-4 kg/s
Tangential inlet	8,1725e-3 kg/s	2,455e-3 kg/s
Outlet	-8,6005-3 kg/s	-2,7218726e-3 kg/s
Deviation	*1,523-5 kg/s*	*1,2568e-7 kg/s*
Deviation in %	**0,18 %**	**0,005%**

Since the mass balance disagreements displayed in table 7 is very small, the solutions are accepted.

This chapter contains several plots produced using the Fluent post-processing features. Common for all of them is that the reactor has rotated 90 degrees so that it is presented horizontally.

In the simulations full stoichiometric combustion is obtained even though the actual experiment was carried out at marginally fuel rich conditions; this is due to the model assumption of the fuel being pure methane. By modeling methane inlet velocities equal to the amount of natural gas in the actual experiments, all the higher alkanes in the natural gas is modeled as methane and the loss of this amount of fuel shifts the combustion condition to fuel lean. It was chosen to keep the actual gas velocities and hereby compromising the combustion stoichiometry in order to get a more accurate

flow field picture from the simulations. Table 8 displays the shift in λ value along with other relevant fuel and flow characteristics.

Table 8: *Estimates of flow and combustion characteristics*

Experiment	Natural gas inlet flow			Tangential air inlet flow			
	Nl/min	kg/s	m/s	Nl/min	Kg/s	Axial vel. m/s	Tang. Vel. m/s
8 kW	12,1	1,35e-4	0,9	120	2,45e-3	9,9	29,5
26 kW	39,8	4,43e-4	2,9	400	8,17e-3	33,0	98,22

Experiment	λ		Average velocities (m/s)	
	Experiment	Fluent simulation (CH_4 assumption)	Wide furnace area (diameter 31,5cm)	Neck (diameter 15cm)
8 kW	0,95	1,04	0,10	0,46
26 kW	0,962	1,055	0,34	1,52

Experiment	Reynold number		'Ideal' flue gas composition mole (mass) fractions, wet			
	Wide Furnace area	Neck	CO_2	H_2O	O_2	N_2
8 kW	267	562	0,143 (0,228)	0,286 (0,187)	0,012 (0,014)	0,560 (0,570)
26 kW	890	1870	0,141 (0,226)	0,282 (0,186)	0,016 (0,018)	0,561 (0,571)

11.3.1. CFD analysis of 8 kW experiment

The main reason for choosing to model the 8 and 26 kW experiment was to see if flow features inside the reactor could explain the difference in combustion promoting effect of SO_2. Figure 11.3 shows the temperature distribution for the 8 kW simulation.

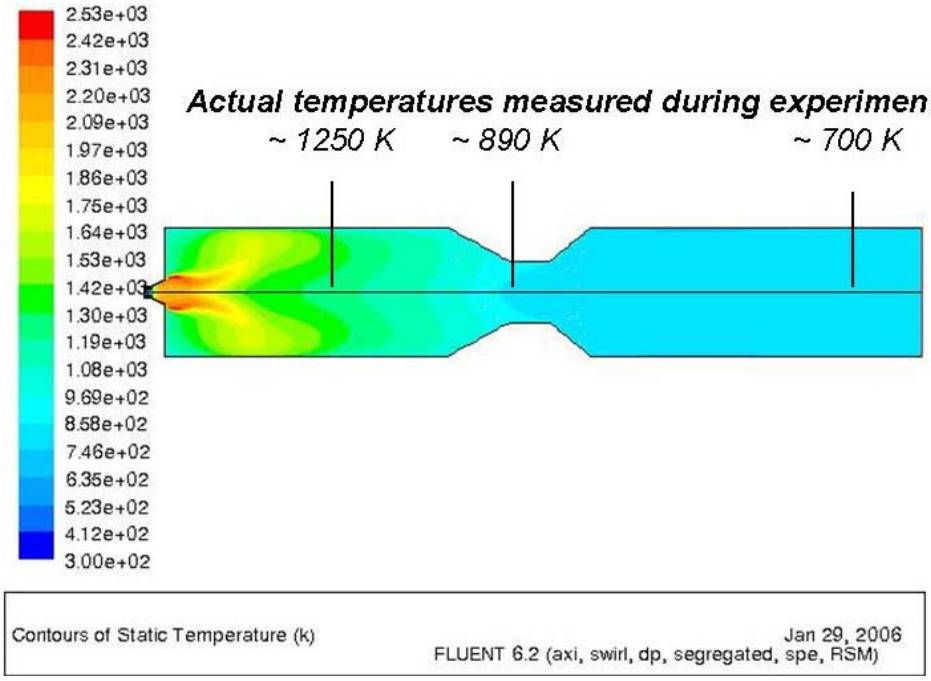

Figure 11.3: *Contour plot of temperature in the burner in the 8 kW experiment.*

The agreement between experimental and simulated temperatures seems quite good; however the wall temperature boundary condition has also been "fitted" in a way so a realistic temperature profile is observed. The flame structure also resembles the visual impression of the flame quite well, with a concavity in the centre.

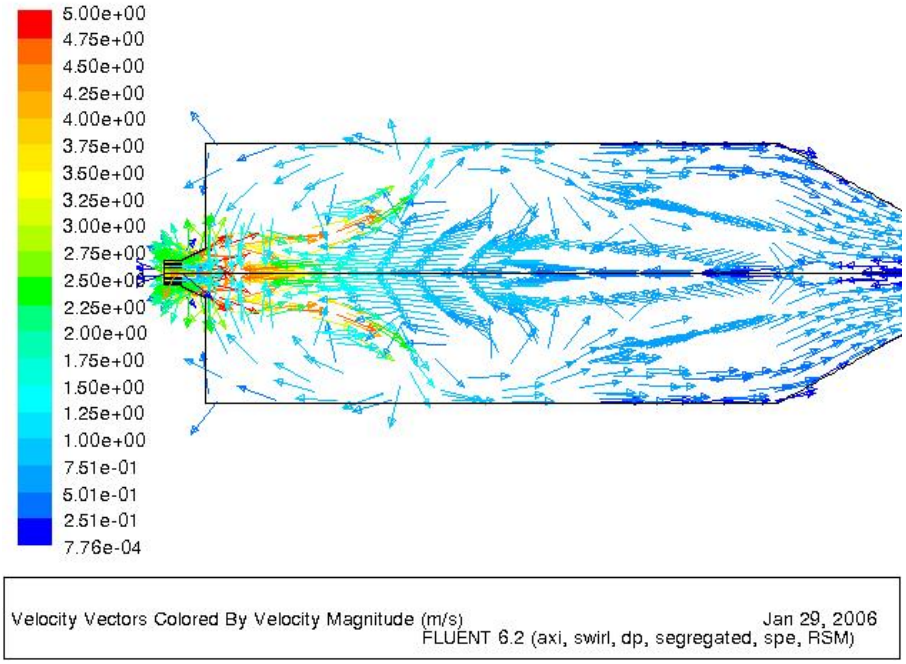

Figure 11.4: *Velocity vectors for the upper furnace area colored by velocity magnitude.*

Figure 11.4 shows that the temperature cavity arises from an inner recirculation zone, where products of the flame combustion are recirculated into the flame centre. The swirling motion of the flame causes this flow feature because of shear and mixing of the swirling flow with the surrounding fluids. [50] A low pressure area is then created in the center of the swirling flow much like in a cyclone and gases are recirculated towards the inlet.

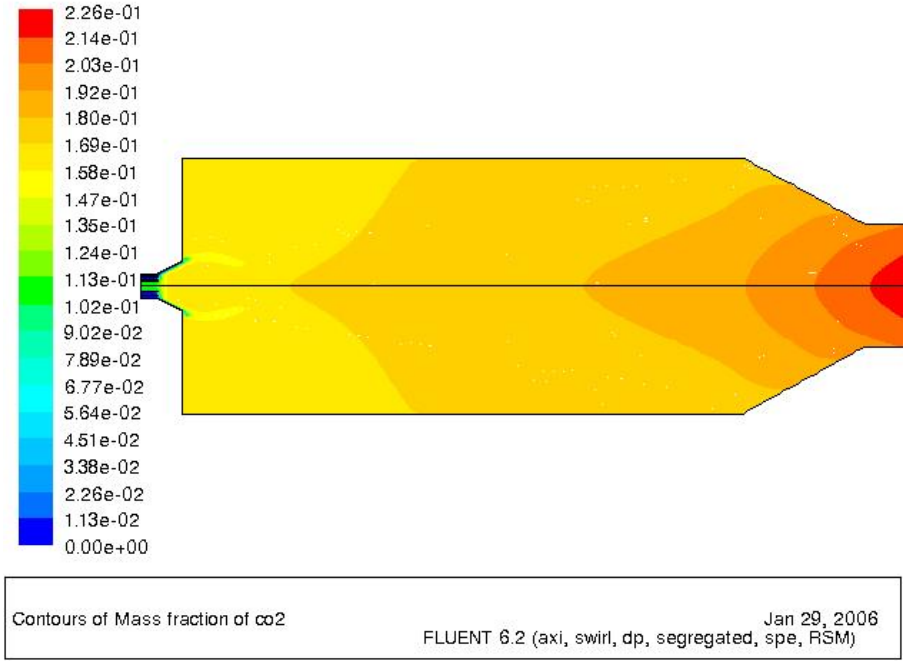

Figure 11.5: *Contour plot of the CO_2 mass fraction in the upper furnace region.*

Figure 11.5 displays mass fractions of CO_2 in the upper reactor area. Complete conversion of the fuel is obtained in the neck area, however most of the CO_2 is already formed in the near burner (flame) region. Figure 11.5 illustrates the limitations of applying a 1 step global mechanism; in reality the formation of CO_2 would probably to a greater extend occur in the post-flame region through oxidation of CO formed in the flame region.

11.3.2. CFD analysis of 26 kW experiment

The conditions in the 26 kW experiment is somewhat different compared to the 8 kW experiment. Because of the increase in overall gas flow the Reynold number increases (see table 8) and the increased conversion of fuel causes significantly higher temperatures.

The temperature contour plot displayed in figure 11.6 shows the temperature variations through the reactor for the simulation of the 26 kW experiment.

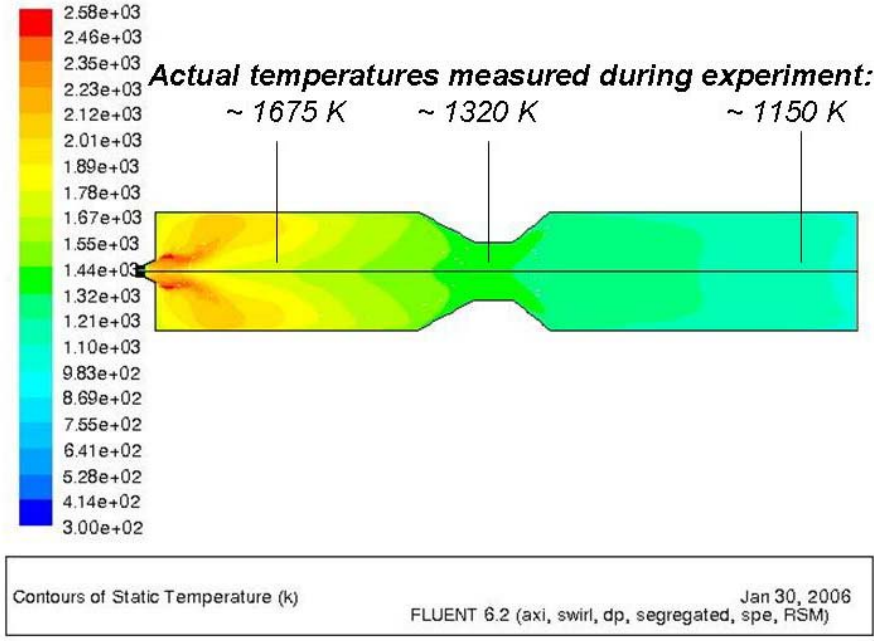

Figure 11.6: *Contour plot of temperature in the burner.*

Again the temperatures calculated by Fluent seem to fit the experimental measurements quite well. Apart from the generally higher temperatures through the reactor, the temperature profile for this 26 kW experiment actually resembles the 8 kW quite well regarding peak temperatures and the length of the peak temperature area. This is somewhat surprising, since the visual appearance of the flames where quite different regarding flame length for the two experiments. Another interesting observation is the peak temperature position, which is not in the centre of the reactor (where the thermocouples where positioned) but at the wall areas, so the top thermocouple is likely to not be able to capture any disturbances in the flame temperature due to SO_2 addition.

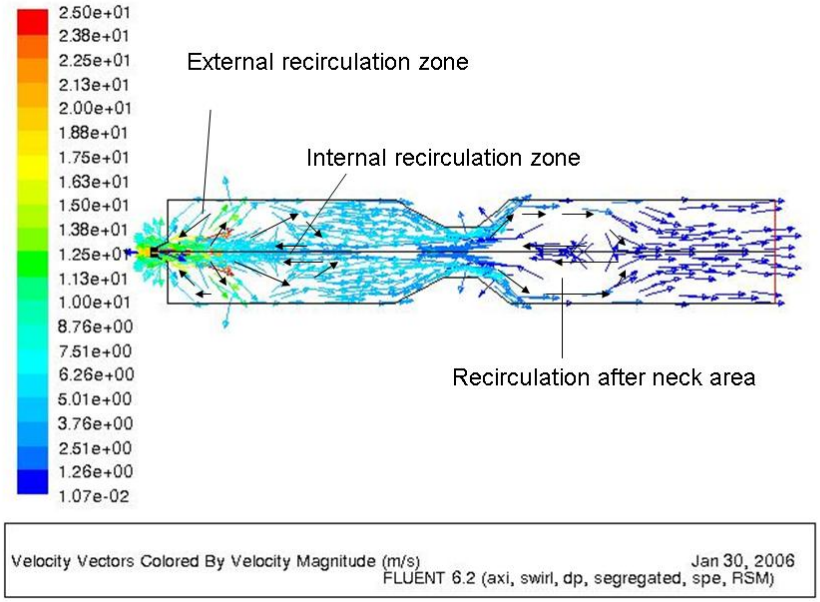

Figure 11.7: *Velocity vectors for the entire furnace colored by velocity magnitude – black arrows are inserted to magnify the important recirculation tendencies.*

From the velocity plot displayed in figure 11.7 it appears that a major internal recirculation zone is formed in the centre of the reactor. It seems that the recirculation zone stretches as far as beyond the neck area. Also an external recirculation zone is observed at the upper part of the furnace – this is more obvious in figure 11.8, which only shows velocity vectors for this upper furnace area.
Figure 11.8 shows a zoom of the upper part of the reactor, which is the more interesting regarding flow features in the flame region. Here the recirculation zones are more conspicuous.

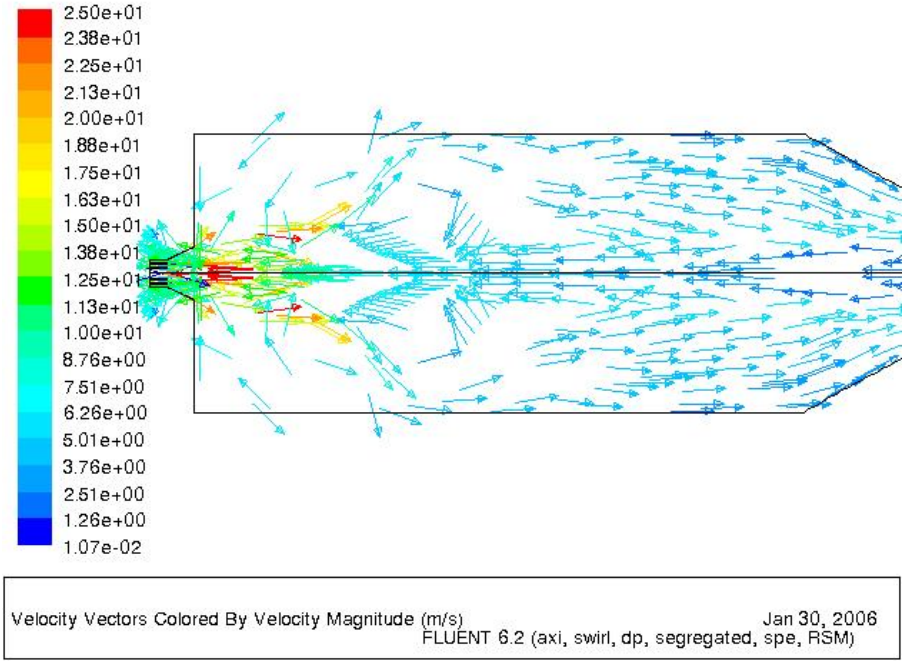

Figure 11.8: *Velocity vectors for the upper furnace colored by velocity magnitude.*

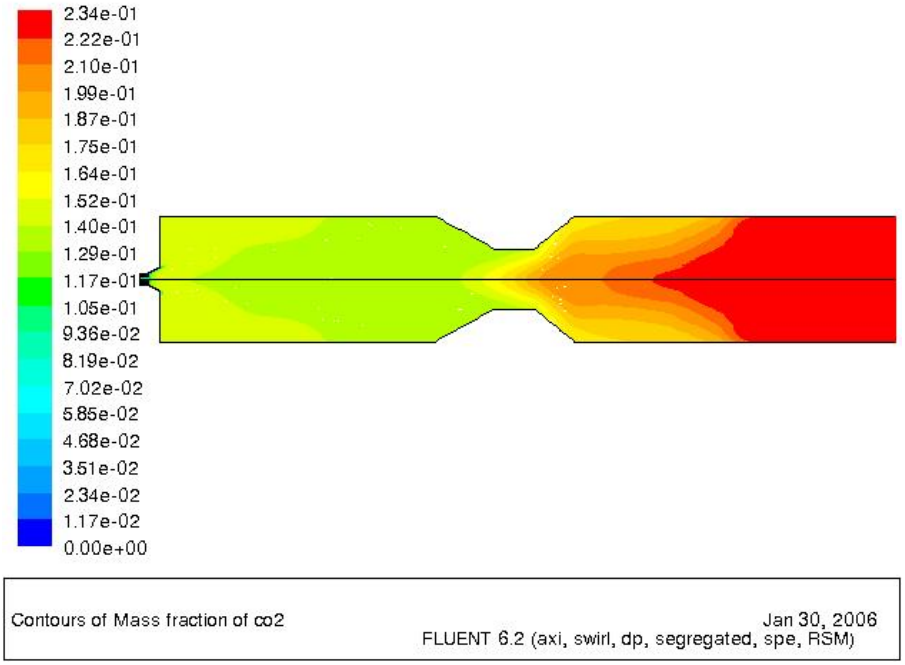

Figure 11.9: *Contour plot of CO_2 mass fraction, 26 kW simulation.*

The CO_2 mass fraction plot in figure 11.9 shows that a large part of the fuel conversion happens instantly – or at least that is what is predicted using this simple global one step model. It seems that in the initiation of the conversion of the remaining CO_2 takes place in the neck area, where better mixing is induced by the geometry.

11.4. Conclusions on CFD analysis

The CFD analysis did not show any distinct differences in the flow patterns for an 8 kW and a 26 kW experiment simulation. A matching temperature profile was observed in comparison with experimental measurements. The peak temperatures do however seem a bit high compared to adiabatic flame temperatures for methane (2226 K) or ethane (2229 K). [29]

In both cases recirculation zones appear, which make it possible for any sulfur to re-enter the flame area in some extent. The mixing conditions in the upper furnace area seem to be very good due to both internal and external recirculation zones.

It is also noticed that peak temperatures are not located in the centre of the reaction chamber, due to the internal recirculation. This means that it is possible that peak temperatures could have been somewhat higher than what was measured. This also means that the top thermocouple may not have given an accurate picture of the flame temperature, and any small temperature changes due to differences in the fuel conversion in the flame zone caused by SO_2 may not be observed by the thermocouple. Furthermore there is some uncertainties on the experimental temperature measurements, especially at high temperatures, because the thermocouple was not shielded against radiation.

12. Chemkin modeling

Since CFD modeling is not able to deal with detailed chemistry down to the elementary reaction steps, the kinetic modeling program Chemkin 3.7 [59] was introduced to get ideas about radical interactions, and dominant intermediate species during sulfur doped natural gas combustion.

In Chemkin the aurora transient model was used (performing an integration in time), with isothermal temperature conditions. A complete list of detailed elementary reactions along with their thermodynamic data was implemented – the sulfur chemistry kinetics can be seen in appendix L. The sulfur mechanism is similar to that used by Rasmussen et al. [54], and the part of the mechanism describing C-H-O interactions was the currently updated mechanism in the CHEC research group [56].

12.1. Initial sulfur species

The first question of interest is the state of sulfur, before it starts interacting with the oxidative combustion species. H_2S is presumably the thermodynamically favoured sulfur component at rich conditions, however SO_2 is the compound added to the natural gas which then can be converted to H_2S if the reaction kinetics are fast enough for such a conversion. Inlet conditions were specified according to the natural gas flow composition in the 26 kW high swirl experiment, where a 90 % (1000 ppm) reduction of CO was observed.

Table 9: *Inlet conditions during "sulfur inlet" simulation*

Reaction species	CH_4	SO_2	N_2
Flow (Nl/min)	40	0,02	0,98
Mole fractions	0,976	0,000488	0,0239

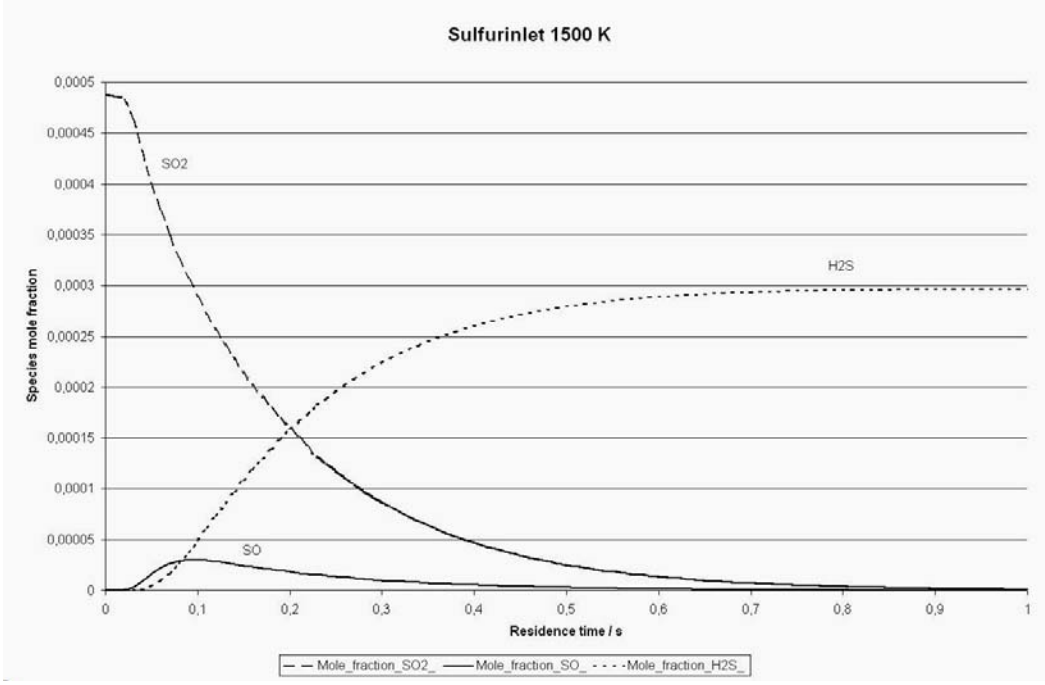

Figure 12.1: *Output data for a 1500 K isothermal simulation – focus on S components. Reactants: CH_4: 40; SO_2:0,02; N_2:0,98*

Figure 12.1 shows the dominant sulfur compounds at 1500 K as a function of residence time. For a total conversion of SO_2 to H_2S at this temperature a residence time of almost a second is needed, SO is formed as an intermediate, but also other radicals such as SH, HSO and HOSO appear during the conversion. The fuel/SO_2 is lead into the burner mouth in a pipe annulus where the outer radius is 11 mm and the inner radius is 7 mm. Assuming that a temperature of 1500 K is a good estimate for the temperature in the burner mouth region, and that the fuel flow can run for 10 cm before mixing with the combustion air, a residence time can be estimated:

Fuel flow cross section: $\pi \cdot (r_{outer}^2 - r_{inner}^2) = \pi \cdot (1{,}1cm^2 - 0{,}7cm^2) = 2{,}26\,cm^2$

Fuel volume flow: $40\,Nl/\min \frac{s \cdot m^3}{60\min \cdot 1000l} \cdot \frac{1500K}{273K} = 3{,}66e-3\,m^3/s$

Residence time: $\frac{2{,}26e-4\,m^2 \cdot 0{,}1\,m}{3{,}66e-3\,m^3/s} \approx 6\,ms$

From comparing the calculated residence time of the fuel flow with the time needed for converting SO_2 to H_2S from figure 12.1 it is clear that higher temperatures are required in order to convert SO_2 to H_2S in the fuel rich section.

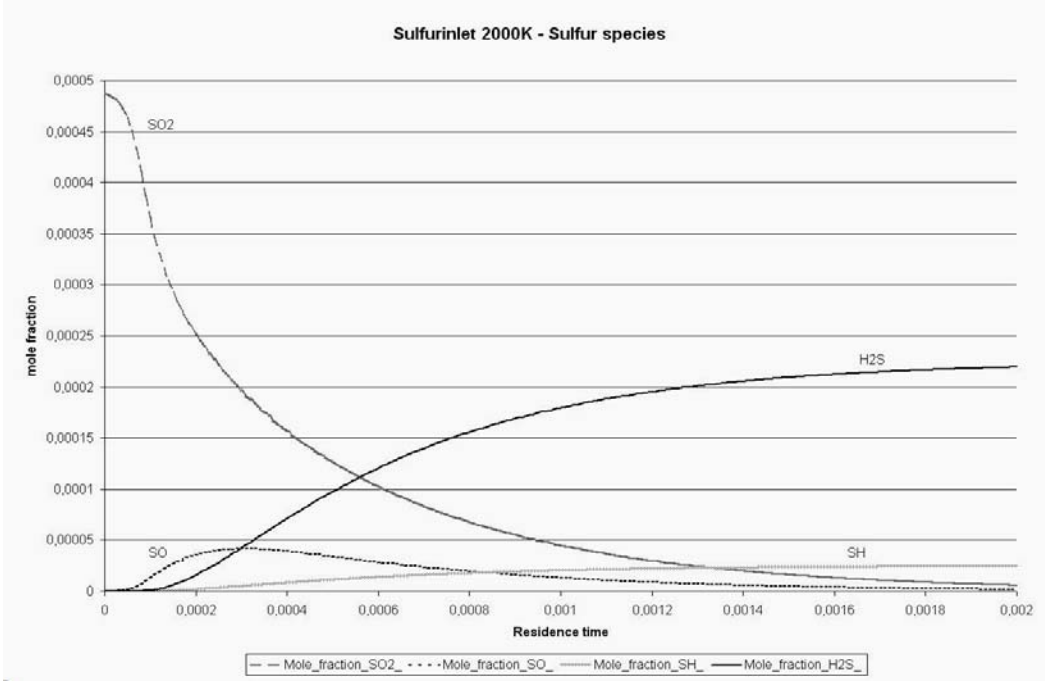

Figure 12.2: *Output data for a 2000 K isothermal simulation – focus on S components.*
Reactants: CH_4: 40; SO_2:0,02; N_2:0,98

Figure 12.2 show that at 2000 K the time for SO_2 converting to H_2S is down to 2 ms, and the actual residence time is estimated to 4,6 ms by adjusting for the increased temperature.

Table 10: *Residence time comparison at different temperatures*

Temperature / K	1000	1500	1600	1700	1800	1900	2000
Calculated residence time	9,3 ms	6,2 ms	5,8 ms	5,4 ms	5,1 ms	4,9 ms	4,6 ms
Time for H_2S conversion	>10 s	1 s	150 ms	40 ms	10 ms	4 ms	2 ms

Table 10 displays the calculated residence times in comparison with the estimated residence times for conversion of SO_2 to H_2S. Conclusions are, that if the inlet temperature is high enough H_2S is the abundant sulfur component. Temperatures as high as 1690 K are measured during experiments (with a thermocouple, which was not shielded for radiation), so it is possible, that temperatures up to 2000 K are obtainable in the burner mouth. The CFD modeling also predict temperatures around 2000 K at the burner mouth area. So it is not unlikely that most SO_2 has been converted to H_2S before reaching the flame front, this also means that oxygen is "activated" in the flame, and can start oxidation of the fuel, than if no SO_2 was introduced to the flame.

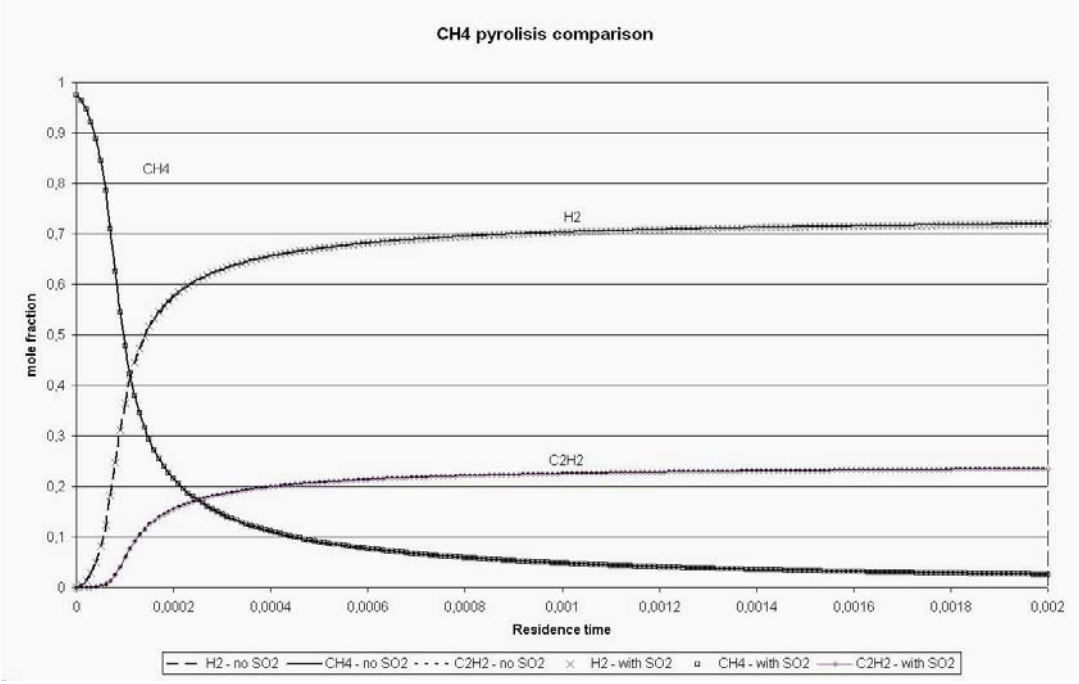

Figure 12.3: *Comparison of data from 2000 K isothermal simulations with and without SO_2 – focus on major components. Reactants: CH_4: 40; SO_2:0,02; N_2:0,98*

Figure 12.3 shows that the kinetic model does not find any difference in the major chemical compositions due to the small SO_2 addition – every major component from a simulation with SO_2 coincide with the result from the simulation without SO_2. It is noticed that the high temperature causes a thermal degradation of CH_4 into H_2 and C_2H_2 (which is believed to play an important role in soot formation) [37]. Compared to the sulfur conversion in figure 12.2 the break down of methane occurs significantly faster, and it is probably due to formation of H radicals or the product H_2 from the methane pyrolysis, that SO_2 is converted to H_2S. Nothing in these simulations indicate any major impact on pyrolisis rate or major pyrolisis product composition due to sulfur addition.

However SO_2 conversion to H_2S could happen through a reaction sequence like stated by Alzueta et al. [14]:

(12.1) $SO_2 + H \rightleftharpoons SO + OH$

(12.2) $SO + H \rightleftharpoons S + OH$

(12.3) $S + H_2 \rightleftharpoons SH + H$

(12.4) $SH + H_2 \rightleftharpoons H_2S + H$

Total: $SO_2 + 2\,H_2 \rightleftharpoons H_2S + 2\,OH$

The reaction sequence above results in a gain of 2 reactive OH radicals early in the flame, which could have a combustion promoting effect.

When entering the postflame zone O_2 is present in higher concentrations and H_2S will then react to some extent to form SO_2.

Frenklach et al [57] suggests several oxidation steps for H_2S oxidation, among them:

(12.6) $H_2S + O \rightleftharpoons SO + H_2$

(12.7) $SO + O_2 \rightleftharpoons SO_2 + O$

Total $H_2S + O_2 \rightleftharpoons SO_2 + H_2$

The sequence reaction 12.7 and 12.8 does not lead to any gain in reactive radicals, which could enhance the combustion rate due to sulfur presence, however it gives rise to formation of H_2 further down in the reactor, and this could cause a change in the combustion product composition forming more H_2 and less CO.

(12.8) $H_2S + O \rightleftharpoons HSO + H$

(12.9) $HSO + M \rightleftharpoons H + SO + M$

(12.10) $SO + O_2 \rightleftharpoons SO_2 + O$

Total: $H_2S + O_2 \rightleftharpoons SO_2 + 2\,H$

Reactions 12.8 to 12.10 represent an example of chain branching H_2S oxidation also presented by Frenklach et al. [57], where 2 H radicals are formed.

Montoya et al. [58] suggests that a key step to degradation of H_2S is via hydrogen abstraction by O_2:

(12.11) $H_2S + O_2 \rightleftharpoons HO_2 + SH$

Reaction 12.11 is an initiating reaction forming radicals from stable molecules, and if it contributes to the pathway of H_2S oxidation it could enhance the combustion rate as well.

Combining the reduction of SO_2 to H_2S (reactions 12.1-12.4) and back to SO_2 (12.8-12.10) yields 4 extra radicals to the radical pool for each SO_2 molecule that converts. The CFD modeling showed that recirculation back to the flame area appears in the reactor, and so it could be that SO_2 formed in the postflame area is recycled to the flame zone yet again to convert to H_2S each time contributing to the radical pool.

12.2. Modeling combustion process

In order to investigate how natural gas combustion occurs on an elementary reaction level, a Chemkin simulation was performed with an isothermal temperature of 1500 K taken as an estimate of the average temperature in the upper furnace region. The inlet species can be seen in table 11.

Table 11: *Inlet conditions during "sulfur inlet" simulation*

Reaction species	CH_4	SO_2	N_2	O_2
Fuel flow	42,2	0,02	400·0,79	400·0,21
Mole fractions	0,09522	4,51e-5	0,7152	0,1895

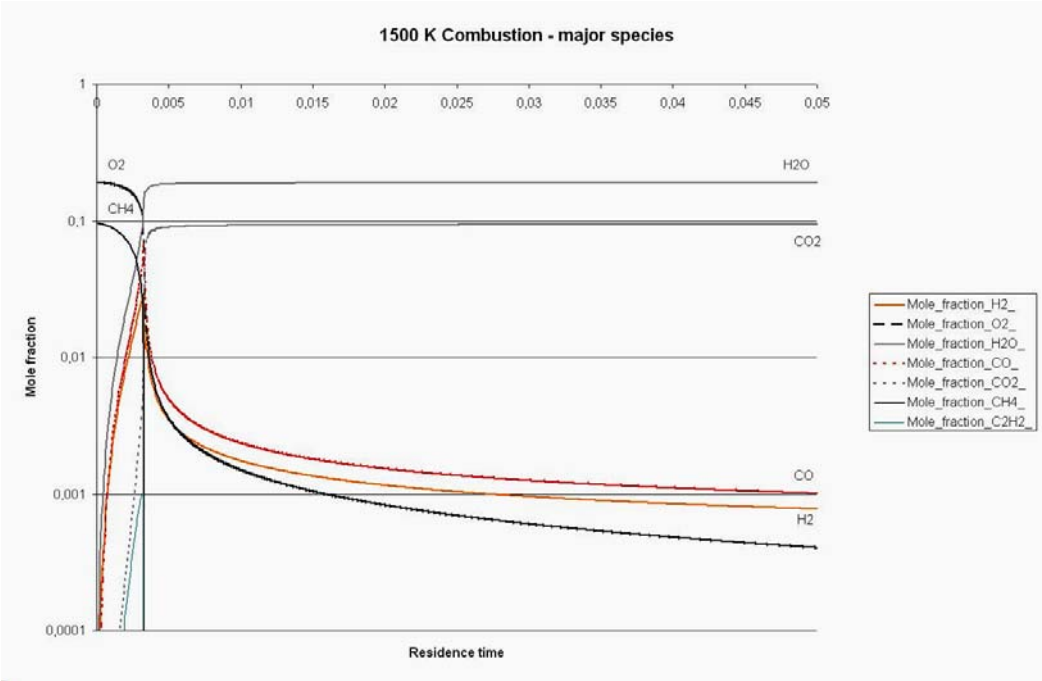

Figure 12.4: *1500 K isothermal simulation without SO_2 – focus on major components. Reactants: CH_4: 42,2; N_2:317;O_2:84 (λ=0,99)*

Figure 12.4 show that at 1500 K and ideal conditions, a fast conversion of fuel to products is obtained, with CO_2 and H_2O as the major products, but also emissions of around 1000 ppm (~mole fraction 0,001) of CO and H_2 is observed at these slightly fuel rich conditions.

The time for complete conversion of fuel to products is less than 10 ms, and a crude estimate of the gas residence time in the swirl burner is around 10 seconds, so there is no doubt that mixing of fuel and air is what limits the rate of combustion in the actual reactor at these nearly stoichometric conditions.

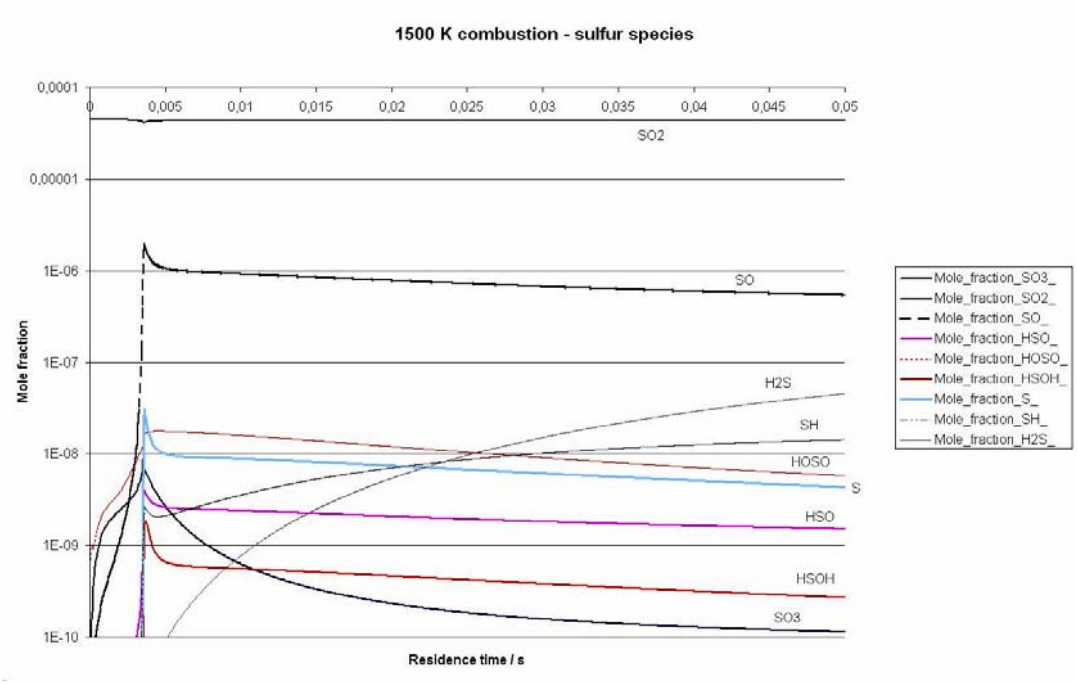

Figure 12.5: *1500 K isothermal simulation – focus on sulfur components.*

Reactants: CH_4: 42,2; SO_2:0,02; N_2:316,98;O_2:84 (λ=0,99) note logarithmic scale

Figure 12.5 shows that in a close to stoichiometric ideally mixed (premixed) combustion at 1500 K SO_2 stays as the dominant sulfur component throughout the process, and only trace amounts of primarily SO but also sulfur radicals such as SH and S are formed but in amounts 1000 times less than the combustion carrying radicals such as OH, O and H.

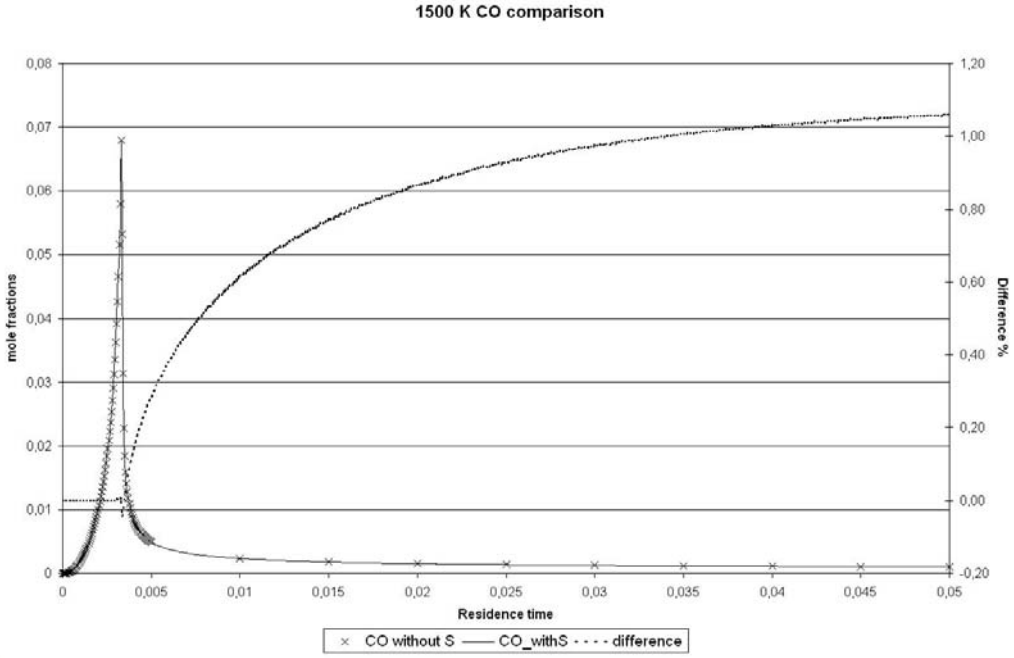

Figure 12.6: *Comparison between CO levels for 1500 K isothermal simulations with and without SO_2.*

Reactants: CH_4: 42,2; (SO_2:0,02); N_2:316,98;O_2:84 (λ=0,99)

In figure 12.6 the CO mole fraction for two simulations is compared, one with a 4,5e-5 initial mole fraction of SO_2, and one, where the SO_2 is replaced with N_2. It is difficult to see any difference in the CO levels from the two situations. The difference in percentage is also included in the plot and can be read on the secondary y axis – the difference in percentage is calculated as:

(12.12) $$difference\ \% = ([CO]_{without} - [CO]_{withS}) / [CO]_{without} * 100)$$

Figure 12.6 shows that the CO levels are a bit lower for the case where sulfur is added, but not in what appears to be any significant way.

Table 12: *Difference in percentage at steady (exit) level for CO*

	1000 K	1500 K	2000 K	2300 K
CO difference	-30	1,01	0,15	0,08
CO difference*	-41	-3,2	-0,07	-0,04

** Indicates that H_2S was simulated added instead of SO_2*

Note: (-) indicates more CO is formed in the sulfur experiment.

Table 12 show that CO levels does not differ significantly when very small fractions of SO_2 is added. The only exception is the 1000 K CO comparison, where 30 % higher CO emissions are predicted when adding SO_2 – the result is graphically displayed in figure 12.9.

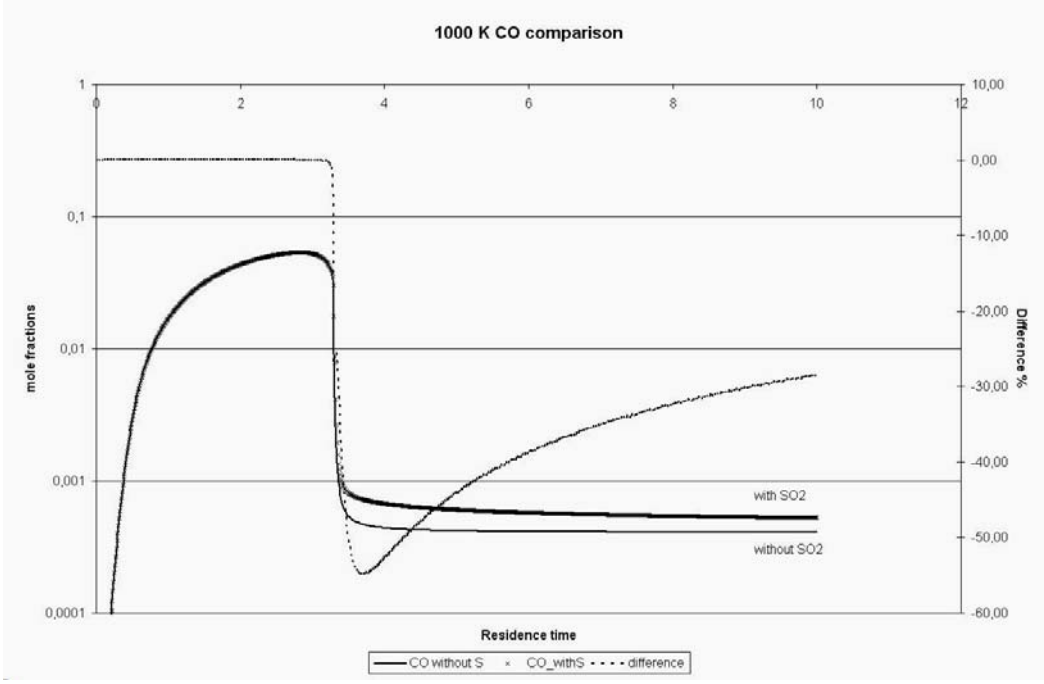

Figure 12.7: *Comparison between CO levels for 1000 K isothermal simulations with and without SO_2.*

Reactants: CH_4: 42,2; (SO_2:0,02); N_2:316,98;O_2:84 (λ=0,99)

The higher CO levels caused by SO_2 addition displayed in figure 12.7 representing a combustion inhibiting effect of SO_2 at low temperatures is in agreement with, what was stated in the chapter 3; that SO_2 has a radical recombining effect [7]. So with the current modeling data, which is similar to that used by Rasmussen et al. [54], it is possible to capture the low temperature combustion inhibiting effect of SO_2, but not any high temperature promoting effect.

In the simulations presented above SO_2 was used as the inlet sulfur component. It was also attempted to use H_2S as the initial sulfur species to see if oxidation of H_2S could contribute CO reduction as it was speculated in section 12.1. The results did however not differ in any significant way from the simulations without sulfur, and in general a small increase in CO levels was obtained as table 12 also shows.

12.2.1. Soot precursors

It was suggested in chapter 5 that sulfur might influence the soot formation rate, and hereby affect the overall carbon mass balance and thereby also the CO emissions.

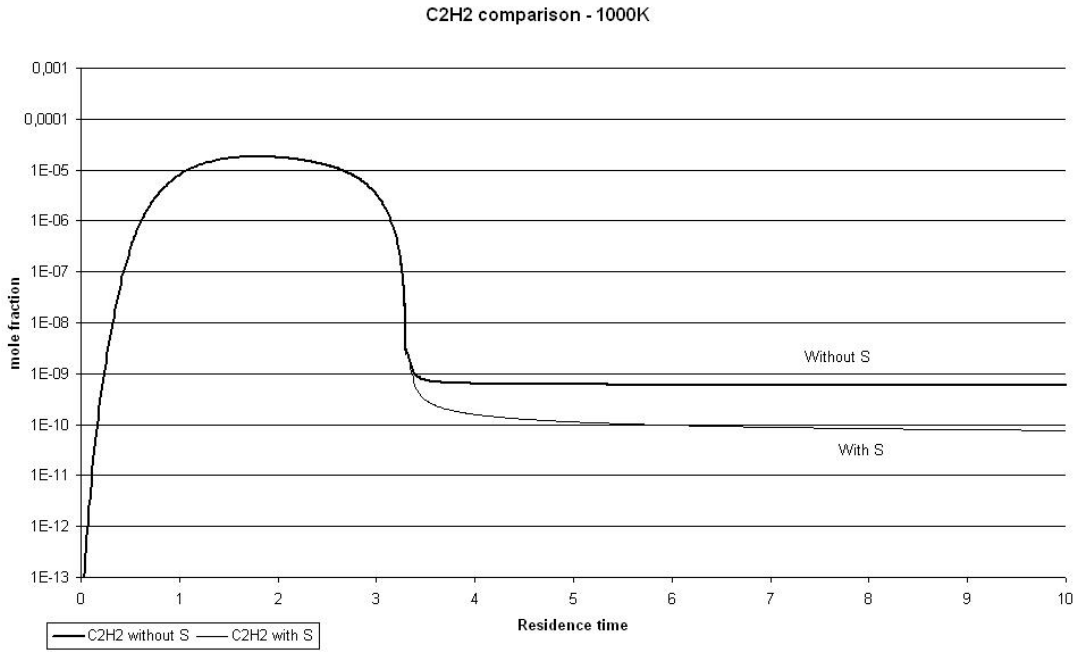

Figure 12.8: *Comparison between C_2H_2 levels for 1000 K isothermal simulations with and without SO_2. Reactants: CH_4: 42,2; (SO_2:0,02); N_2:316,98;O_2:84 (λ=0,99)*

Figure 12.8 shows the differences in C_2H_2 mole fraction. C_2H_2 peaks as fuel is converted products, and in this time the presence of sulfur does not seem to affect C_2H_2 levels, at increasing residence times a significant difference appear between the acetylene concentrations for the two cases with

and without sulfur. If acetylene is supposed to act as a soot precursor the main formation of soot is expected during fuel formation, where the sulfur presence has no effect. However further surface growth on soot particles through reactions with acetylene is expected to occur after the initial formation steps, so maybe this sulfur induced difference in acetylene concentration can result in decreased growth of sulfur particles.

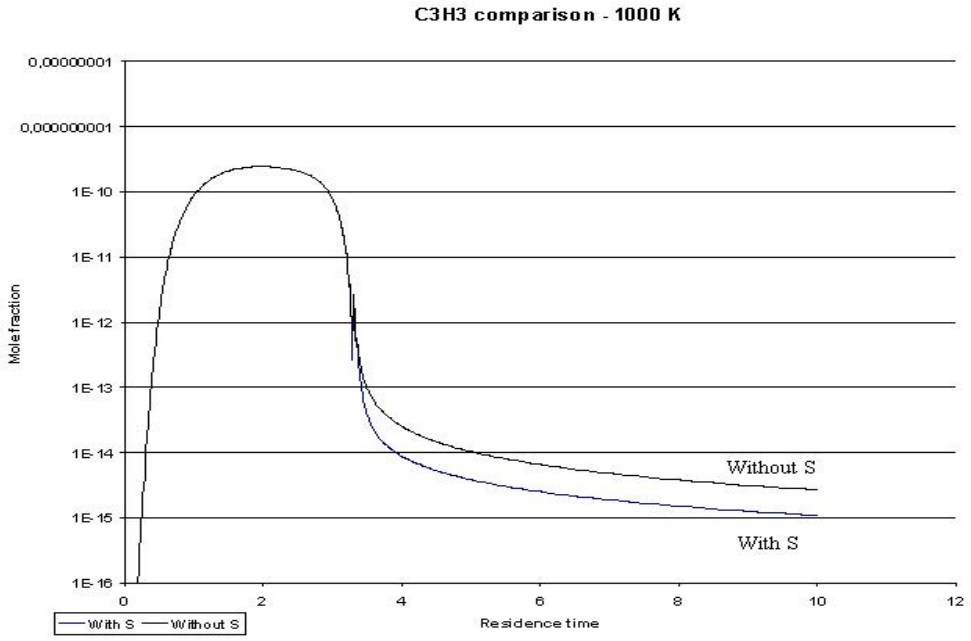

Figure 12.9: *Comparison between C_3H_3 levels for 1000 K isothermal simulations with and without SO_2. Reactants: CH_4: 42,2; (SO_2:0,02); N_2:316,98;O_2:84 (λ=0,99)*

Figure 12.9 shows differences in mole fraction for another believed soot precursor C_3H_3 [37] (propargyl). As for acetylene the there is no observable difference during the fuel conversion where propargyl concentrations peak, however in the time after peak concentrations simulations without S predict concentrations ~8 times higher than when sulfur is present.

This decreased concentration of proposed soot precursors acetylene and propargyl by sulfur addition was more pronounced at low temperatures, and it is quite obvious, when comparing figures 12.7 and 12.8 with figure 12.6 that it is the radical recombining effect of SO_2, that through the radical pool prevents formation of these alleged soot precursors. At higher temperatures (around 1300 K) this sulfur induced difference vanishes along with the radical recombining effect of SO_2 as the following chapter will reveal.

12.3. Mechanism comparison

In the literature quite a number of reaction rate constants and thermodynamical data have been discussed in order to optimize the ability of the current kinetic models to predict a wide variety of experimental results. It appears that the reaction 12.13 has major influence on the SO_2 interaction capability with the radical pool:

(12.13) $H + SO_2 \rightleftharpoons$ products

The products in reaction 12.13 are predicted by Murakami et al. [18] to be mainly OH and SO at temperatures above 1000 K. It was also the rate constant for reaction 12.13 that was modified in order to account for the differences in experimental result between the work by Dagaut et al.[13] and Alzueta et al.[14] as discussed in chapter 6. The general observation is that at high temperatures SO and OH radicals work as the product from reaction 12.5, whereas at lower temperatures the HOSO intermediate becomes more stable and can recombine radicals [54]:

(12.14) $HOSO + H \rightleftharpoons SO_2 + H_2$

(12.15) $HOSO + OH \rightleftharpoons SO_2 + H_2O$

The rate constant from the work of Murakami et al. and the sulfur reaction mechanism from Alzueta et al. were inserted into/ replaced the original sulfur mechanism from Rasmussen at al. [54]. Furthermore a subset describing C-S interactions was implemented to see if formation of products such as COS and CS_2 [55]. The S-subsets were implemented in a detailed mechanism describing C/H/O interactions (up to C_3 carbon species) [56].

All sulfur mechanisms can be found in appendix L.

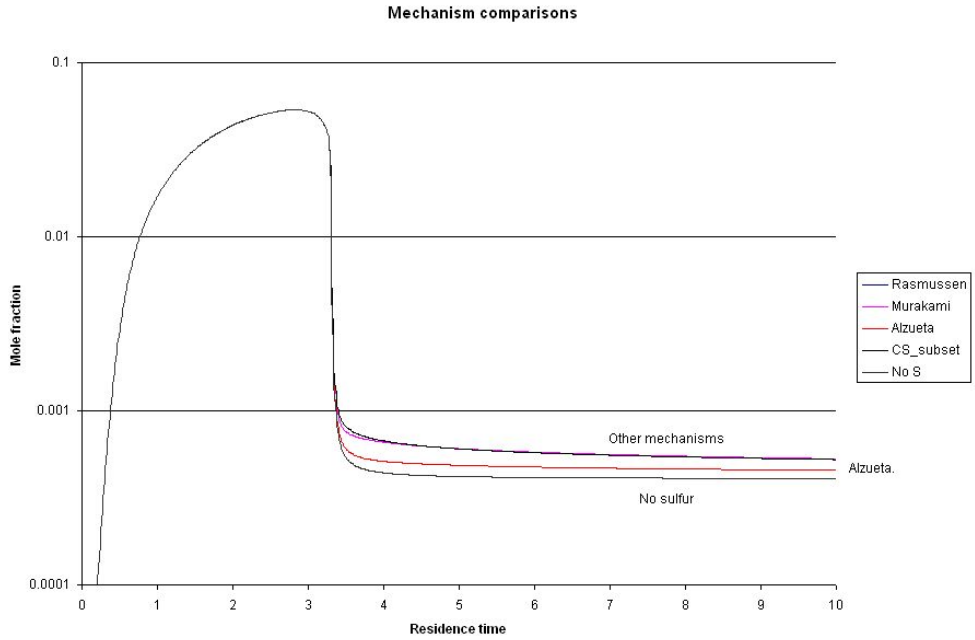

Figure 12.10: *Comparison between CO levels for 1000 K simulations using different sulfur sub-mechanisms*

Reactants: CH_4: 42,2; (SO_2:0,02); N_2:316,98;O_2:84 (λ=0,99)

Figure 12.10 shows how the sub mechanism by Alzueta et al. [14] predicts moderately lower CO emissions than the other mechanisms, which totally coincide, so there was not observed any impact on CO levels by the C-S interactions. However all mechanisms predict higher CO levels than the 'no sulfur case' due to the radical recombining efffect. Table 13 quantifies the product composition for the Alzueta and Rasmussen mechanisms.

Table 13: *Species mole fractions at 10 sec (exit level) for Alzueta and Rasmussen sulfur mechanisms.*

Mechanism	CO	O_2	CO_2	H_2	H_2O	N_2	Total
Alzueta [14]	4,56e-4	8,34e-6	9,46e-2	1,12e-3	0,189	0,715	0,9999
Rasmussen [54]	5,25e-4	2,41e-5	9,45e-2	1,09e-3	0,189	0,715	0,9999
Difference (ppm)	**69**	**16**	**-71**	**-38**	**35**	-11	

Table 13 shows that the mechanism proposed by Alzueta et al. predicts that CO levels are lowered 69 ppm - which is not even close to what was seen experimentally, but the trend itself is very interesting, and show the disagreement in the current kinetic gas phase models. The lower CO levels in the Alzueta mechanism are based on an oxidation to CO_2, but this requires more oxygen, and in this slightly fuel rich stoichiometry the oxygen is partly taken from O_2 and partly on expense of less H_2O and more H_2 compared to the other mechanisms.

Table 14: *Difference in percentage at steady (exit) level for CO for different mechanisms compared to a case without sulfur.*

	1000 K	1100 K	1200 K	1300 K	1500 K	2000 K
Alzueta	-11,5	-1,8	-0,23	0,5	0,4	0,12
Rasmussen	-28,5	-7,7	-1,5	1,2	1,1	0,08
C-S subset	-28,5	-7,7	-1,5	1,2	1,1	-

Table 14 shows the CO difference to a simulation without sulfur for three different sulfur mechanisms (remember it is only the sulfur mechanism that is difference, the C/H/O reactions and thermodynamics are identical). Although there are small difference the main trend is clear – a combustion inhibiting sulfur effect at low temperatures vanishes at higher temperatures, and the extra oxidator (SO_2) added has a very little but promoting effect on the CO emissions.

12.4. Conclusions on kinetic modeling

The kinetic modeling did not show any clear explanations on how gas phase reactions could cause a significant reduction in CO emissions due to addition of very small amounts of SO_2 (~60ppm). Even though different sulfur mechanisms were applied, none of them predicted significant decreases in CO concentrations. Only the radical recombining effect of SO_2 was observed and it seemed to have the most effect at lower temperatures (<1300K) increasing CO levels and also causing a decrease in C_2H_2 and C_3H_3 concentration.

It is considered that reduction of SO_2 to H_2S in a fuel rich area can contribute to formation of reactive radicals. Also the re-oxidation of H_2S to SO_2 in a later stage in the combustion process, where oxidizer is mixed with the fuel, could promote oxidation or change the product composition towards H_2 and CO_2 instead of CO and H_2O.

So in order to explain the experimental observations the effect of SO_2 must either not appear through a gas phase mechanism, or the reaction mechanisms used are insufficient in describing the promoting effect of SO_2.

13. Theories and discussion

It seems that no decisive and clear conclusion on how small amounts of sulfur influences natural gas combustion can be drawn from the experiments conducted during this project.

The major experimental results are that the ability of sulfur to reduce CO emissions is related to the presence of sulfur in the flame zone, and that the effect increases with increasing temperature. In (premixed) engine combustion sulfur did not have any impact on CO levels.

The literature study has shown that sulfur is able to influence combustion in different ways:

- Pilot and full scale measurements have shown that small amounts of sulfur can decrease CO emissions even when sulfur is added late in the combustion process – it has not been possible to reproduce that specific effect in this project. A catalytic radical producing effect is suggested. [1]
- A radical recombining effect of sulfur is well-known and well described in the literature. This effect causes an increase in CO emissions. [7,11-15]
- In many flame studies larger amounts of sulfur is reported to be able to reduce soot emissions [40-44]
- In diesel combustion fuel sulfur is expected to cause soot formation. [45]
- Sulfur has been reported to appear in soot remnants even from clean burning flames. [46]

These observations along with CFD and kinetic modeling have given rise to four different theories on how sulfur influences CO emissions. Presented here in an order so that the theory which this author beliefs is the most likely one is presented first.

13.1. Theory I: Sulfur increases soot formation

The first theory is that sulfur in some way is capable of influencing the soot formation process in a way so that more carbon is held in the solid particles. If more carbon is held in solid residue the gas phase stoichiometric conditions change (actual λ increases) and more CO will be oxidized.

Overall change: $CO \rightarrow soot (+ O_2)$

What can support this theory is the study on Diesel emissions [45] where more solid carbon is reported, with increasing fuel sulfur content.

Also the results that even from clean burning natural gas flames solid carbon particles containing 1-2% sulfur appear [46] indicate some relationship between sulfur and soot formation.

Another observation that supports this theory is the small increases in O_2 level that occurred during some of the swirl burner experiments. If oxidation of CO to CO_2 was responsible for the CO decrease O_2 emissions should decrease as well. In some experiments, as displayed for the 26 kW high swirl experiment where the highest CO decrease was observed a small increase in O_2 concentration was observed as figure 13.1 shows.

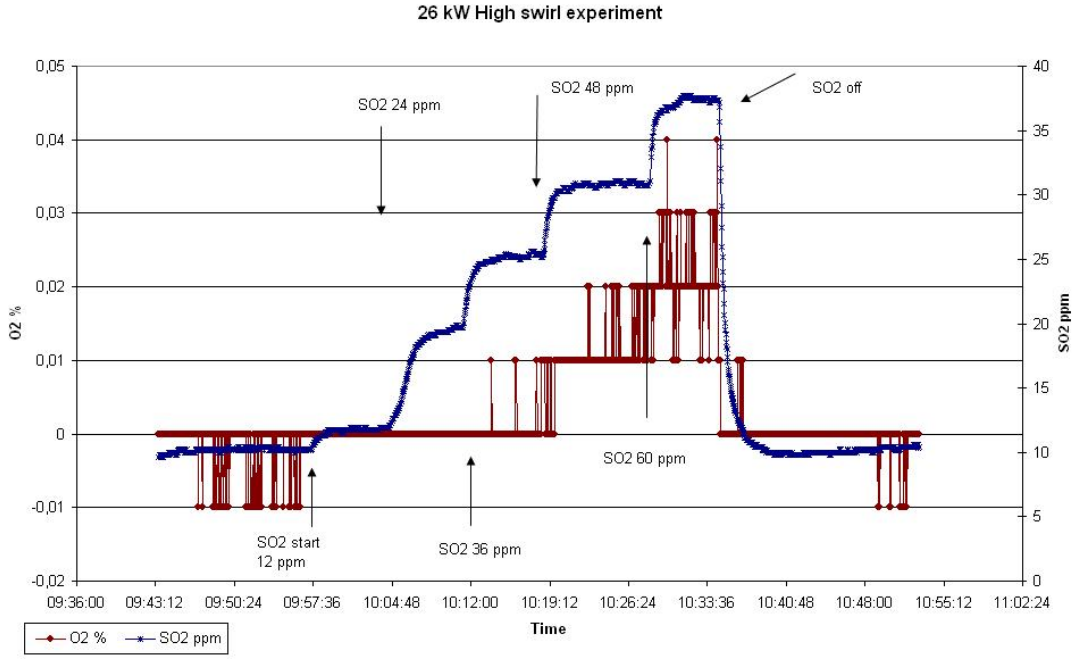

Figure 13.1: *O_2 and SO_2 emissions during 26 kW high swirl experiment.*

Other experiments also a tendency towards increasing O_2 concentrations during SO_2 addition but none as clear as the example in figure 13.1. Increasing O_2 concentrations indicate that less carbon is present in the gas phase – however these changes are not observed in every experiment and the concentration changes are well within experimental uncertainties.

What contradict this theory are the engine results. If soot particle formation is increased during diesel engine combustion and in gas flames then why not during gas combustion in an engine? Soot was actually observed from the fuel rich engine experiments – but no changes appeared when SO_2 was added. Also the many references reporting decreased soot formation due to sulfur addition contradicts this theory.[40-44]

Figure 13.2 displays the basic theory of soot formation (see also chapter 5) where aromatic carbon is formed from aliphatic compounds (presumably propargyl or acetylene). Eventually these

constantly growing PAH's reach a size where they can nucleate and form soot particles. These soot particles can then grow larger primarily through coagulation and aggregation.

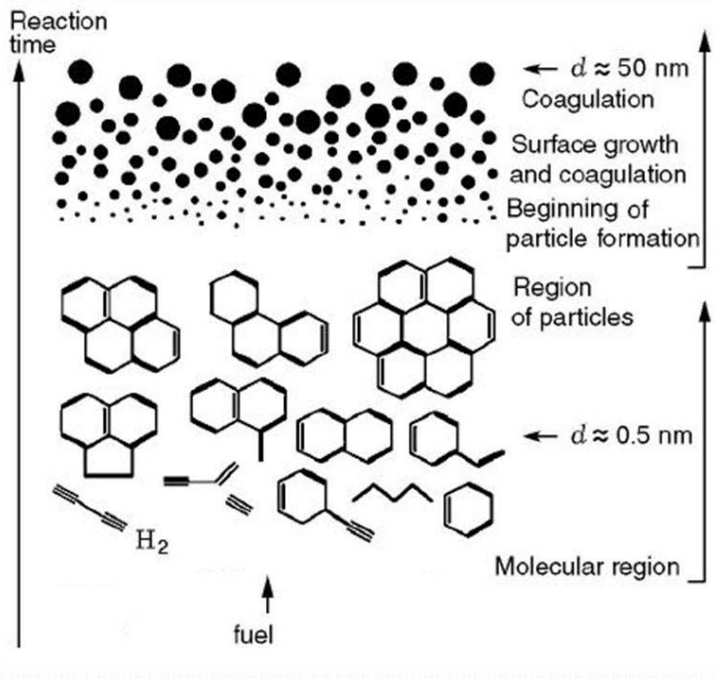

Figure 13.2: *Soot formation process. [60]*

Maybe sulfur compounds can adsorb to the soot particles and increase the stickyness so that larger particles are formed – or soot can contribute in the growth of the aromatic hydrocarbons for instance via attack by SH radicals. It is also suggested in the literature that sulfate particles can act as nuclei necessary for hydrocarbons to nucleate. [45]

13.2. Theory II: Sulfur prevents soot formation

This theory, that sulfur should be able to prevent or decrease soot formation, is the opposite of what was stated in theory I.

The introduction of an oxidant (SO_2) in the flame area tips a balance so that soot particles or PAH is not formed (or less is formed) increasing the oxidation in the post flame part.

Either through affecting the radical pool and maybe preventing soot precursors (propargyl, acetylene) from being formed or maybe by saturating the aromatic structures for instance by forming thiophenols (mercaptans).

Early in the combustion: soot → CO

Later on: CO (+½O_2)→ CO_2

Several flame studies [39-45] support that SO_2 or other sulfur compounds can decrease soot particle formation. And also the kinetic modeling results that show some decrease in acetylene and propargyl concentrations due to the presence of sulfur support this theory.

However the oxygen concentrations are very low and it is doubtful whether there it actually would be possible to oxidate any CO formed from the soot. Also the O_2 trends from figure 13.1 does not support an increased oxidation of CO – then O_2 emissions should decrease.

13.3. Theory III: Radical formation through gas phase mechanism

It was discussed in chapter 12 how conversion of SO_2->H_2S->SO_2 could create radicals and recirculation of the burned gases back to the flame area makes it possible for each SO_2 molecule to convert to H_2S several times, contributing in a more than stoichiometric fashion.

Possible pathway for SO_2 conversion to H_2S in fuel rich flame [14]:

$SO_2 + H \rightleftharpoons SO + OH$

$SO + H \rightleftharpoons S + OH$

$S + H_2 \rightleftharpoons SH + H$

$SH + H_2 \rightleftharpoons H_2S + H$

Total: $SO_2 + 2\,H_2 \rightleftharpoons H_2S + 2\,OH$

Possible pathway for H_2S oxidation [57] (which could appear postflame):

$H_2S + O \rightleftharpoons HSO + H$

$HSO + M \rightleftharpoons H + SO + M$

$SO + O_2 \rightleftharpoons SO_2 + O$

Total: $H_2S + O_2 \rightleftharpoons SO_2 + 2\,H$

Overall: $2\,H_2 + O_2 \rightleftharpoons 2\,OH + 2\,H$

CFD modeling and basic swirl burner theory have showed that recirculation of the burned gases to the flame area takes place, so it could be that SO_2 is converted several times. Experimental measurements does also show a decrease in hydrocarbon emissions as well as CO emissions, which could indicate a sulfur induced contribution to the radical pool. These findings support that this theory.

What contradicts this theory is the kinetic modeling, which does not give any impression of increased radical concentration due to sulfur addition – indicating that the pathways described above is not dominant when SO_2 is converted to H_2S and back.

Also the oxygen trend in figure 13.1 speaks against any increased conversion of CO to CO_2 (which evidently must be the overall consequence of increased radical activity).

13.4. Theory IV: Sulfur causes a shift in the product composition

This theory suggests that the addition of SO_2 causes a change in the product composition:

$$CH_4 + O_2 (+ SO_2) \rightarrow CO_2 (+CO) + H_2O + (H_2) (+ \text{soot})$$

So that less CO and more H_2 is formed, affecting the water gas shift equilibrium in some way:

$$CO_2 + H_2 \rightleftharpoons CO + H_2O$$

This could for instance be through oxidation of H_2S in the postflame releasing H_2 later on in the reactor [57]:

$$H_2S + O \rightleftharpoons SO + H_2$$

$$SO + O_2 \rightleftharpoons SO_2 + O$$

Total $H_2S + O_2 \rightleftharpoons SO_2 + H_2$

This theory could explain why CO levels decrease without any significant O_2 in the exit gas.

However the mechanism above can not account for any shift in CO-H_2 emissions more than equivalent to the SO_2 concentration. Furthermore a decrease in the THC emission was also observed, so in some way the radical pool must also be influenced by any change in the water gas shift equilibrium.

13.5. Wall effects

It was suggested in the literature study that catalytic sulfur reactions with deposits or active sites on wall surfaces could lead to increased oxidation of CO to CO_2. However the experimental results suggest the presence of sulfur in the flame is necessary in order to reduce CO emissions – this finding does not support the theory that surface reactions are responsible for the CO decrease. Furthermore the experiments in the swirl burner showed a CO decrease both in these experiments and the ones carried out by Lin [2] even though the surface material of the reactor was changed from steel to refractory cement. Pilot scale experiments of adding SO_2 to a combustion process in a quartz isolated reactor did also show CO decrease [1].

Since the effect of sulfur is occurring under all these different wall conditions it does not seem likely that wall effects are responsible for the CO decrease.

14. Commercial potential

One of the initial objectives with this study was to evaluate to commercial potential of adding sulfur compounds to combustion systems with the intention of promoting combustion. This project has shown that even though CO emissions can decrease due to sulfur addition it is probably because of increased formation of carbonaceous particles (soot).

Sulfur is already added to natural gas as an odorant, and even clean burning natural gas flames emit some soot particles [46], so maybe replacement of this sulfur odorant could reduce the amount of unwanted soot formed from natural gas flames. Synthesis of carbon nanotubes from flames [60] can perhaps benefit from sulfur addition but this is a quite different area.

15. Conclusion

The work carried out during this project has shown that addition of small amounts of SO_2 can significantly reduce CO emissions.

In a 20 kW swirl burner 1000 ppm (90 %) decrease in CO emission was obtained by adding 60 ppm of SO_2 to a slightly fuel rich natural gas combustion process. It was also found that the CO reducing effect of SO_2 was only obtained when SO_2 was added to the fuel flow. When SO_2 was added to the tertiary combustion air CO emissions increased instead, this can be attributed to the well-known radical recombining effect of SO_2. These observations point to a connection between sulfur in the flame zone and this CO decrease. Another observation was a connection between reactor effect and the quantity of CO reduced by SO_2. It appeared that increasing the fuel flow, which resulted in an increase in temperature, also increased the CO reducing effect of SO_2. A reduction in unburned hydrocarbons was also observed in fuel rich experiments when SO_2 was added. It was surprising to observe that O_2 emissions also seemed to increase slightly when adding SO_2, indicating reduction of CO instead of oxidation to CO_2.

Experiments in a 22 kW naturally aspirated spark ignition engine fired with natural gas did not show the same CO or unburned hydrocarbon reducing effect of SO_2. In fact the engine emissions were not affected at all by the addition of very small amounts of SO_2.

A CFD analysis of the swirl burner showed that recirculation of burned gases back to the flame zone was occurring and that the temperature inside the burner was not peaking in the center of the reactor, where thermocouples had been placed during experiments. This could indicate that temperatures in the reaction chamber were higher than measured and that any temperature increase in the flame that might occur would probably not be detected by the thermocouples.

Kinetic modeling of gas phase reactions could not explain any significant CO decrease due to addition of small amounts of sulfur. Only the radical recombining effect of SO_2 at low temperatures was observed to cause increasing CO emissions as it was expected from the literature study.

The kinetic modeling showed that conversion of SO_2 to H_2S in the flame is possible to occur, especially at higher temperatures. Reaction pathways were found in the literature that made it possible for SO_2 to form combustion reactive radicals (H and OH) during its conversion to H_2S and

re-conversion to SO_2 again in the post-flame zone. Increased formation of reactive radicals could lead to increased combustion rate and thereby increased oxidation of CO to CO_2.

Increased soot formation is mentioned as a more likely explanation for the CO decrease and references in the literature is found where sulfur is known to increase soot formation during diesel engine combustion. Sulfur was also found incorporated in soot remnants from clean burning natural gas combustion indicating a connection between sulfur and soot formation. This theory also matches the observations of increased O_2 concentrations with increasing SO_2 addition.

The results from this project do not advocate SO_2 addition as a method for promoting the combustion rate. It is suspected that even small amounts of sulfur can influence the soot formation process but further and more detailed studies are necessary in order to reveal the underlying mechanisms.

16. Future work

Since the presence of SO_2 in the flame area is essential for a CO decreasing effect to occur it would be obvious as a next step to perform flame studies where quantity of solid residue and its composition is measured. It could be interesting to investigate if even the low initial content of sulfur in natural gas can somehow affect soot formation.

Better defined reactor conditions would also be desirable, so that gas phase reactions can be modeled more accurately with idealized reactor models.

It could also be interesting to add other sulfur compounds than SO_2 to a combustion system, to see if any CO decreasing effect is obtainable

Finally an experiment was carried out in this project where ammonia and SO_2 was added to the flame through the same line. The result was a total removal of ammonia induced NO, but the result may have been corrupted by chemical reactions in the SO_2-NH_3 line. A reproduction of this experiment whit SO_2 and NH_3 added from different places or experiments with addition of SO_2 and NO to a flame could be very interesting to evaluate the effect of small amounts of sulfur on (fuel) NO emissions.

17. References

1. Kassman, H.; Andersson C.; Carlsson, J.; Björklund, U.; Strömberg, B.; *Minskade utsläpp av CO och NO_x genom dosering av ammoniumsulfat i förbränningsrummet*, VÄRMEFORSK Service AB, Sverige, **2005**.
2. Lin, W., *Effect of SO_2, on the emission of CO and NO in the combustion of natural gas and co-firing it with pulverized wood*, unpublished work from CHEC research group at the department of Chemical Engineering, DTU Denmark, **2005**.
3. Andersen, J.; Jakobsen, J. G., *Afgivelsen til gasfase af K, Cl og S i biomasse fyrede kedler*, midtvejsprojekt ved CHEC forskningsgruppen ved Institut for Kemiteknik, DTU Denmark, **2003**.
4. Noter "KURSUS 36001 Produkter og Processer – kraftværkskemi og kraftværksprocesser", Department of Chemical Engineering, DTU Denmark, **2000**.
5. http://www.gastra.dk/dk/index.asp
6. Cullins, C. F.; Mulcahy, M. F. R., *The Kinetics of Combustion of Gaseous Sulfur Compounds*, Combustion and Flame, 18, **1972**, 225.
7. Johnsson, J. E.; Glarborg, P. *Sulfur Chemistry in Combustion I*, Pollutants from Combustion, **2000**, 263
8. http://147.29.40.91/delfin/html/b2003/0080805.htm#b6 : Bekendtgørelse om begrænsning af visse luftforurenende emissioner fra store fyringsanlæg, **2003**.
9. Van Lith, S. C.; Jensen, P. A.; Frandsen, F. J.; Glarborg, P.;Alonso, V., *Release to the Gas Phase of Inorganic Elements during Wood Combustion. Part 1: Development and Evaluation of Quantification Methods*, work to be published from CHEC research center Department of Chemical Engineering, DTU Denmark, **2005**.
10. Jones, J. M.; Harding, A. W.; Brown, S. D.; Thomas, K. M. *Detection of Reactive Intermediate Nitrogen and Sulfur Species in the Combustion of Carbons that are Models for Char Coals*, Carbon, 33, **1995**, 833.
11. Schofield, K., *The kinetic nature of sulfur chemistry in flames*, Combustion and flame, 124, **2001**, 137.
12. Cerru, F. G.; Kronenburg, A.; Lindstedt, R. P., *A systematically reduced mechanism for sulfur oxidation*, Proceedings of the Combustion Institute, 30, **2005**, 1227.

13. Dagaut, P.; Lecomte, M.; Mieritz, J.; Glarborg, P. *Experimental and Kinetic Modeling Study of the Effect of NO and SO_2 on the Oxidation of CO-H_2 Mixtures*, Int. J. Chem. Kinet., 35, **2003**, 564.
14. Alzueta, M. U.; Bilbao, R.; Glarborg, P. *Inhibition and Sensitization of Fuel Oxidation by SO_2*, Combustion and Flame, 127, **2001**, 2234.
15. Glarborg, P.; Marshall, P., *Mechanisms of Radical Removal by SO_2*, journal, årstal.
16. Wang, B.; Hou, H., *Theoretical investigations on the SO_2 + HO_2 reaction and the SO_2-HO_2 radical complex*, chemical physical letters, 410, **2005**, 235.
17. Mueller, M. A.; Yetter, R.A.; Dryer, F.L., *Kinetic modeling of the $CO/H_2O/O_2/NO/SO_2$ System: Implications for high-pressure fall off in the SO_2+ O (+ M) = SO_3 (+ M) Reactio*n, International Journal of Chemical Kinetics, 32, **2000**, 317.
18. Murakami, Y.; Onishi, S.; Fujii, *Shock Tube Kinetic Study for the Reaction of H atoms with SO_2: Comparison between Experiments and Theory*, N., J. phys. chem., 108, **2004**.
19. Bendtsen, A. B.; Glarborg, P.; Dam-Johansen. K. *Low temperature oxidation of methane: the influence of nitrogen oxides*, Combustion science and technology, 151, **2000**, 31.
20. Hampartsoumian, E.; Nimmo, W.; Gibbs, B. M. *Nitrogen sulfur interactions in coal flames*, Fuel, 80, **2001**, 887.
21. Dagaut, P.; Nicolle, A., *Experimental and Kinetic modeling Study of the Effect of Sulfur Dioxide on Mutual Sensitization of the Oxidation of Nitric Oxide and Methane*, Published online in Wiley interscience (www.interscience.wiley.com), **2005**.
22. Bacskay, G. B.; Mackie, J. C., *Oxidation of CO by SO_2: A Theoretical Study*, Journal of Physical Chemistry, 109, **2005**, 2019.
23. Rodriguez, J. A; Hrbek, J, *Interaction of Sulfur with Well-Defined metal and Oxide Surfaces: Unraveling the mysteries behind Catalyst Poisoning and Desulfurization*, Accounts of Chemical research, vol 32, number 9, **1999**.
24. Sellers, H; Shustorovich, E, *Chemistry of sulfur oxides on transition metal surfaces: BOC-MP analysis*, Journal of molecular catalysis, 119, **1997**, 367.

25. Torrecilla, S. J., *Submicron particle formation in biomass combustion*, PhD thesis, University of Zaragoza, Spain, **2004**.
26. Li, X. M.; Henrich, V. E., *Reaction of SO_2 with Stoichiometric and defective NiO(100) surfaces*, Physical Review B, 48(23), **1993**, 17486.
27. Roslik, A. K.; Konev, V. N.; Maltsev, A. M., *Some Aspects of the Mechanism of High-Temperature Oxidation of Nickel in SO_2*, Oxidation of Metals, 43 (1-2), **1995**, 59.
28. Nielsen, H. P., *Deposition and High-Temperature Corrosion in Biomass-Fired Boilers*, Ph.D. thesis, DTU, **1998**.
29. Dunn, J. P.; Stenger, H. G.; Wachs, I. E.; *Molecular structure-reactivity relationships for the oxidation of sulfur dioxide over supported metal oxide catalysts*, Catalysis Today, 53 (4), **1999**, 543.
30. ChlorOut. Swedish patent SE 9903656-8, 2003. International patent application PCT/SE 02/00129 (2002) nr. 812 , **2003**.
31. Lindau, L.;Skog, E., *CO-reduktion I FB-panna via dosering av elementärt svavel*, VÄRMEFORSK Service AB, Sverige, **2003**.
32. Hughes, K. J.; Tomlin, A. S.; Dupont, V. A.; Pourkashanian, M., *Experimental and modeling study of sulfur and nitrogen doped premixed methane flames a low pressure*, Faraday discussions, 119, **2001**, 337.
33. Dagaut, P.; Lecomte, M., *Experimental and kinetic modeling study of the reduction of NO by hydrocarbons and interactions with SO_2 in a JSR at 1 atm*, Fuel, 82(9), **2003**, 1033.
34. Calcote, H. F.; *Mechanisms of Soot Nucleation in Flames*- A Critical Review*, Combustion and Flame, 42, **1981**, 215.
35. Cotton, D. H; Friswell, N. J.; Jenkins, D. R.; *The Suppression of Soot Emission from Flames by Metal Additives*, Combustion and Flame, 17, **1971**, 87.
36. Kennedy, I. M.; *Models of Soot Formation and Oxidation*, Energy and Combustion Science, 23, **1997**, 95.
37. Frenklach, M.; *Reaction mechanism of soot formation in flames*, Physical Chemistry Chemical Physics, 4, **1997**, 2028.
38. Skjøth-Rasmussen, M. S.; *Modelling of Soot Formation in Autothermal Reforming*, Ph.D. thesis, DTU, **2003**.

39. Puri, R.; Santoro, R. J.; Smith, K. C.; *The Oxidation of Soot and Carbon Monoxide in Hydrocarbon Diffusion Flames*, Combustion and Flame, 97, **1994**, 125.
40. Radi, P. P.; Mischler, B.; Schlegel, A.; Tzannis, A-P.; Beaud, P.; Gerber, T.; *Absolute Concentration Measurements Using DFWM and Modeling of OH and S_2 in a Fuel-Rich H_2/Air/SO_2 Flame*, Combustion and Flame, 118, **1999**, 118.
41. Lawton, S. A.; *The Effect of Sulfur Dioxide on Soot and Polycyclic Aromatic Hydrocarbon Formation in Premixed Ethylene Flames*, Combustion and Flame, 75, **1989**, 175.
42. Haynes, B. S.; Jander, H.; Mätzing, H.; Wagner, H. Gg.; *The influence of Gaseous Additives on the Formation of Soot in Premixed Flames*, Nineteenth Symbiosum (International) on Combustion/The Combustion Institute, **1982**, 1379.
43. Ni, T.; Gupta, B.; Santoro, R. J.; *Suppression of Soot Formation in Ethene Laminar Diffusion Flames by Chemical Additives*, Twenty-Fifth Symbiosum (International) on Combustion/The Combustion Institute, **1994**, 585.
44. Gülder, Ö. L.; *Influence of Sulfur Dioxide on Soot Formation in Diffusion Flames*, Combustion and Flame, 92, **1993**, 410.
45. J.H. Johnson, T.M. Baines, and J.C. Clerc, *Diesel Particulate Emissions: Measurement Techniques, Fuel Effects, Control Technology*, SAE, Inc., Warrendale, PA, **1992**.
46. Murr, L. E.; Bang, J. J.; Esquivel, E. V.; Guerrero, P. A.; Lopez, D. A., *Carbon nanotubes, nanocrystal forms, and complex nanoparticle aggregates in common fuel-gas combustion sources and the ambient air*, Journal of nanoparticle Research, 6, **2004**, 241.
47. Wolfe, T.; *Swirl burner setup (045-8)*, CHEC research group, Department of Chemical Engineering, Technical University of Denmark, **2005**.
48. Dabkowski, , M.; *Co-combustion of natural gas with pulverized wood in a 20 kW swirl burner*, bachelor thesis at Department of Chemical Engineering, CHEC research group, Technical University of Denmark, **2005**.
49. Turns, S. R.; *An introduction to Combustion – Concepts and Applications*, 2nd edition, McGraw Hill, **1996**.

50. Leuckel, W; Fricker, N., *The Characteristics of Swirl-stabilized Natural gas flames; Part I: Different Flame types and their Relation to Flow and Mixing Patterns*, Journal of the institute of energy, **1976**, 103.
51. Heywood, J. B., *Internal Combustion Engine Fundamentals*, McGraw Hill, **1989**.
52. Fluent 6.2 users guide, Fluent inc., **2005**.
53. R. B. Bird, W. E. Stewart and E. N. Lightfoot, *Transport Phenomena*, 2nd edition, John Wiley and Sons, **2002**.
54. Rasmussen, C. L,; Glarborg, P.; Marshall, P., *Mechanisms of radical removal by SO_2*, proceedings of the combustion institute, **2006** (submitted).
55. Personal communication with Christian Lund Rasmussen, PhD student at CHEC group, Department of Chemical Engineering, DTU, **2006**.
56. Personal communication with Peter Glarborg, Associate Professor at CHEC group, Department of Chemical Engineering, DTU, **2006**.
57. Frenklach, M.; Lee, J. H.; White, J. N.; Gardiner Jr., J.C., *Oxidation of Hydrogen Sulfide*, Combustion and Flame, 41, **1981**, 1.
58. Montoya, A,; Sendt, K.; Haynes, B.S., *Gas Phase Interaction of H_2S wit O_2: A Kinetic and Quantum Chemistry Study of the Potential Energy Surface*, J. Phys. Chem, 109, **2005**, 1057.
59. http://www.reactiondesign.com
60. Mansurow, Z. A.; *Soot formation in combustion processes*, Combustion, explosions and shock waves, 41, **2005**, 727.

Institut for Mekanik, Energi og Konstruktion
MEK
Danmarks Tekniske Universitet
DTU

APPENDIX 2

Emission Control by Sulphur Addition

Emiliano Bruni, Jesper Ahrenfeldt, Peter Glarborg, Ulrik Birk Henriksen
Biomass Gasification Group, Department of Mechanical Engineering
Technical University of Denmark

September 2005 - January 2006

Summary

The purpose of the project was to investigate the possibilities of reducing the emissions of CO, UHC and NO from natural gas fired spark ignition engines by injection of SO_2 to the air-fuel mixture.

Previous researches carried out on biomass fired boilers and on swirl-stabilized natural gas flames showed that addition of sulphur compounds helps to decrease the emissions of CO (20% - 60%) and has an effect on NO_X emissions.

The experiments have been carried out at the Biomass Gasification Group, Technical University of Denmark, as a collaboration between the Department of Mechanical Engineering and the Department of Chemical engineering.

The engine used for the tests was a 3,1 litre MWM spark ignition gas engine, rated to produce 20 kW power. SO_2 has been added in different amounts to the air-fuel mixture at different values of equivalence ratio.

The tests showed that in rich conditions a small increase of CO emission is observed. In lean conditions CO emission seems to decrease when SO_2 is being added. These effects are very small and the uncertainties due to the variance of the results are relevant.

Small effects on UHC emission are observed when adding SO_2 in lean conditions.

NO emission is slightly affected by SO_2 addition. When SO_2 is added in stoichiometric conditions, NO emission is lower compared to the baseline (no addition). When SO_2 is added in lean conditions, NO emission increases. Thus, in presence of SO_2 addition, NO emission has a lower dependence on the equivalence ratio with respect to the baseline case. Being NO emission from SI engines due mainly to the thermal mechanism, a lower dependence on the

equivalence ratio could allow to decrease the excess of air without increasing significantly NO levels. The effects observed for NO are coupled to the effects observed for CO.

Fluctuations of the emissions due to the engine's instability are observed and investigated. Relevant results related to SO_2 addition are not found.

The output power of the engine is not affected by SO_2 addition.

All the effects observed during the tests are very weak.

The results of the experiments carried out at the Biomass Gasification Group show that the injection of SO_2 has not any significant effect on CO, UHC and NO emissions from a natural gas fired spark ignition engine.

CONTENTS

Introduction and problem identification

The aim of the project was to investigate the potential for SO_2 addition as an emission control method in engines fuelled with natural gas (reduction of unburned hydrocarbons) or gasification gas (reduction of CO emissions).

Experience from swirl-stabilized natural gas flame experiments[1] at the Technical University of Denmark ("**Error! Reference source not found.**"), from a pilot-scale facility at TPS* and from the full-scale plant in Eskilstuna† indicate that addition of small amounts of sulphur compounds may have a relevant effect on the oxidation of unburned species in the combustion flue gas[2].

Unburned hydrocarbon emissions (UHC) are due to the fuel (hydrocarbons) that escapes the combustion and is found in the exhaust gas.

CO emissions from engines have two different origins: incomplete combustion (CO is an intermediate product of combustion, see "CO emission", page 13) and unburned fuel CO.

Unburned fuel CO

When burning fuels that contain relevant amounts of CO (producer gas: 20% CO, vol.) CO emissions are due to the fuel that passes through the combustion chamber without being oxidized, like UHC when hydrocarbon-based fuels are being burned. The same mechanisms that lead to hydrocarbon

---

* TPS Termiska Processer AB (located in Nyköping, Sweden) offers products and services, performs research and development on gasification and combustion. The developed processes are tested in pilot plants and exploited at commercial scale. The research and development performed by TPS is often funded by the Swedish National Energy Administration, the European Commission and by private companies.

† The CHP plant at Eskilstuna (Sweden) uses biomass fuels and produces 38 MWe and 71 MWth (plus 15 MW of heat from the flue gases).

emission in natural gas fired engines lead to CO emission when the fuel contains CO.

Unburned fuel CO is the source of CO emission when CO-containing fuels are being burned.

In most countries there is no distinction between the regulatory limit for engines operating on natural gas and for engines operating on CO-containing fuels. For this reason CO emission from engines fuelled by producer gas is a significant problem.

The strategy is to use sulphur dioxide as an additive when the fuel contains CO (producer gas) in order to decrease the emissions of carbon monoxide. Thus, attention is focused on the mechanisms that lead to UHC emission (“Background”, page 3) and on the effect that SO_2 addition has on CO emission (“Experiments”, page 29).

Background

1.1 Hydrocarbon emission

HC emissions result from several different mechanisms. Each mechanism is a process or path by which some of the fuel does not burn during the normal flame propagation process which starts with the spark discharge some 20 – 30 degrees before top centre (TC) crank position and ends about 30 degrees after TC when the flame extinguishes on the far combustion-chamber wall.

Typically spark-ignition engine-out HC levels are 1.5 – 2% of the fuel flow into the engine; about half of this amount is unburned and half is partially reacted fuel components. “Burned” means the fuel is oxidized to combustion products CO_2 and H_2O, perhaps with some CO and H_2. The remainder of the engine-out hydrocarbon emissions are the partial-reaction products of the fuel compound oxidation process (ethene, formaldehyde).

The process of hydrocarbon emissions from spark-ignition engines is divided into four sequential steps: (1) the formation of unburned hydrocarbon emissions; (2) the oxidation of a fraction of these HC emissions within the cylinder, following mixing with the bulk gases; (3) the flow of a fraction of the unoxidized HC from the cylinder into the exhaust; (4) the oxidation in the exhaust system of a fraction of the HC that exit the cylinder.

The rate of mixing of unburned HC with the hot bulk cylinder gases, the temperature and composition of the gases with which these HC mix and the subsequent temperature-time and composition-time histories of the mixture govern the amount of in-cylinder oxidation that occurs. The distribution of these HC around the combustion chamber is nonuniform and changes with time, they are concentrated close to the walls of the chamber. The fraction of these HC that will exit the chamber during the exhaust process will depend on the details of the in-cylinder flow patterns that take them through the exhaust valve. The residual gas is known to be much richer in HC than the average exhaust. In particular, the flow patterns in the cylinder toward the end of the exhaust stroke as the gas scraped off the cylinder wall by the piston moves

toward the exhaust valve will be important. Finally, a fraction of the unburned HC which leave the cylinder through the exhaust valve will burn up within the exhaust system. Gas-phase oxidation in the exhaust port and hotter parts of the exhaust manifold is significant. The amount depends on the gas temperature, composition and residence time[3].

Critical factors and engine variables in HC emissions mechanisms are summarized in Table 1:

Table 1 Critical factors and engine variables in HC emissions mechanisms

Formation of HC	Crevices	Crevice volume
		Crevice location (relative to spark plug)
		Load
		Crevice wall temperature
		Mixture composition (fuel/air equivalence ratio) and burned gas fraction (residual plus recycled exhaust gas)
	Oil layers	Oil consumption
		Wall temperature
		Speed
	Incomplete combustion	Burn rate and variability
		Mixture composition and burned gas fraction
		Load
		Spark timing
	Combustion chamber walls	Deposits
		Wall roughness
In-cylinder mixing and oxidation	Mixing rate with bulk gas	Speed
		Swirl ratio
		Combustion chamber shape
	Bulk gas temperature during expansion and exhaust	Speed
		Spark timing
		Mixture composition and burned gas fraction
		Compression ratio
		Heat losses to walls
	Bulk gas oxygen concentration	Equivalence ratio
	Wall temperature	Important if HC source near wall
		For crevices: importance depends on geometry
Fraction HC flowing out of cylinder	Residual fraction	Load
		Exhaust pressure
		Valve overlap
		Compression ratio
		Speed
	In-cylinder flow during exhaust flow	Valve overlap
		Exhaust valve size and location
		Combustion chamber shape
		Compression ratio
		Speed
Oxidation in exhaust system	Exhaust gas temperature	Speed
		Spark timing
		Mixture composition and burned gas fraction
		Compression ratio
		Secondary air flow
		Heat losses in cylinder and exhaust
	Oxygen concentration	Equivalence ratio
		Secondary air flow and addition point
	Residence time	Speed
		Load
		Volume of critical exhaust system component
	Exhaust reactors	Oxidation catalyst
		Three-way catalyst
		Thermal reactor[3]

Source of unburned hydrocarbons

Four possible HC emissions formation mechanisms for spar-ignition engines (where the fuel-air mixture is essentially premixed) have been proposed:

1) flame quenching at the combustion chamber walls, leaving a layer of unburned fuel-air mixture adjacent to the wall;
2) the filling of crevice volumes with unburned mixture which, since the flame quenches at the crevice entrance, escapes the primary combustion process;
3) absorption of fuel vapour into oil layers on the cylinder wall during intake and compression, followed by desorption of fuel vapour into the cylinder during expansion and exhaust;
4) incomplete combustion in a fraction of the engine's operating cycles (either partial burning or complete misfire), occurring when combustion quality is poor[3].

Unburned fuel has three subsequent effects:

1) the oxidation of unburned fuel in the chamber after flame propagation;
2) the preferential exhausting of the burned products from the chamber;
3) the oxidation of unburned fuel in the exhaust system[4].

The most extensive system of crevices in the usual combustion chamber is that formed by the piston, bore and compression rings (Figure 1).

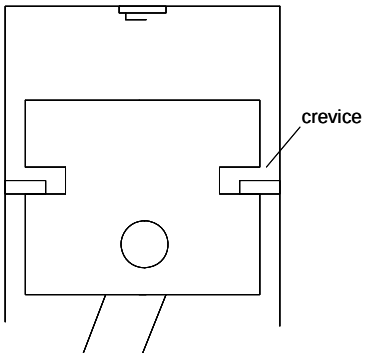

Figure 1 A scheme of the top ring crevice

A remote pocket of air-fuel mixture, such as that existing in the void behind the top compression ring, may escape combustion because the flame may be extinguished by close clearances in the approach path. Unburned fuel expands back into the chamber during the expansion stroke and some is passed out in the exhaust gas[5].

The amount of unburned fuel from crevices is determined by the volume and fuel density (see “Crevices”, page 8).

Oxidation of some of the unburned fuel occurs in the chamber after flame propagation. Gas motion due to combustion, piston motion and possibly inlet configuration mixes some of the unburned fuel with the burned gases, raising the unburned gas temperature and causing reaction to occur. The fraction of unburned fuel reacted in this manner depends on the amount of mixing, the temperature of the mixed gases, the hydrocarbon and oxygen concentrations in the mixed gases and the time available.

Gas motion, however, is insufficient to mix homogeneously all the unburned fuel with the burned gases. When the exhaust valve opens, burned gases from the centre of the chamber are preferentially exhausted. Proportionately more unburned fuel than burned products remains inside the chamber in the residual gases. The amount of unburned fuel exhausted from the chamber is determined by the degree of mixing, which determines the homogeneity of the gases in the chamber and by the fraction of the total cylinder contents exhausted.

The unburned fuel and burned gases exhausted from the chamber are mixed during the exhaust process and reaction continues in the exhaust system. The fraction reacted in the exhaust system is a function of the temperature, the hydrocarbon and oxygen concentrations and the time available[4].

The unburned HC are exhausted into two peaks of approximately equal mass: the first of these coincides with the exhaust blowdown mass flow pulse (which removes the majority of the mass from the cylinder); the second occurs

towards the end of the exhaust stroke where HC concentrations are very high and the mass flow rate is relatively low.

Approximately one-third of the hydrocarbons left unburned in an engine combustion event is retained in the cylinder and recycled.

Buildup of deposits on the combustion chamber surface also affect HC emission levels[3].

Chemical and physical phenomena like variations in the residual gas fraction, in the fuel-air ratio, in the fuel composition and fluid motion in the combustion chamber cause cyclic variations. Some combustion cycles are faster than the average (tendency to knocking), some are slower. For the slow combustion cycles there is a risk that the combustion is not completed when the exhaust valve opens. This results in higher UHC emissions and lower efficiency. High turbulence and an improved mixture quality are important factors for the flame initiation and help to decrease the total cyclic variations[6]. The cyclic variation is especially a problem for lean burn operating engines[7].

Crevices

Hydrocarbon emissions are dependent on the width and length of the top ring land[5] (Figure 1). Under most warmed-up operating conditions this top ring land contributes about 50% of the engine's total unburned hydrocarbon. The cause is the failure of the flame to penetrate the narrow gap between the cylinder and the piston.

There are three basic ways in which the top ring can act as a crevice for the storage of the fuel/air mixture:

1) the top land region between the piston crown, cylinder bore, piston and top ring can act directly as crevice;
2) the space between the top ring groove not occupied by the top ring can act as a subsidiary crevice;
3) the mixture can be squeezed through the ring gap and into the region between the top and second rings to re-emerge later when the cylinder pressure drops falls below the ring pack pressure.

This crevice has a very significant effect on the UHC levels.

As the cylinder pressure rises during compression, unburned mixture is forced into the crevice regions. Since these volumes are thin, they have a large surface/volume ratio; the gas flowing into each crevice cools by heat transfer to close to the wall temperature.

During combustion, while the pressure continues to rise, unburned mixture continues to flow into the crevice volumes. When the flame arrives at each crevice it can either propagate into the crevice or it can quench at the crevice entrance. Whether the flame quenches depends on crevice entrance geometry, the composition of the unburned mixture and its thermodynamic state. Quenching distance depends inversely on the laminar flame speed and pressure, neither of which is size dependent. The two-plate quench distance can be estimated to be 0.18 mm.

After flame arrival and quenching, burned gases will flow into each crevice until the cylinder pressure starts to decrease (after about 15° ATC). Once the crevice gas pressure is higher than the cylinder pressure, gas flows back from each crevice into the cylinder.

The fraction (5% to 10%) of the total cylinder charge trapped in crevices at the time of peak cylinder pressure escapes the primary combustion process.

The fate of these crevices HC when they flow back into the cylinder during expansion and exhaust has been described with different models. Both jet-like flows from the ring gap[8] and low-velocity creeping flows from the piston top-land crevice have been observed. The former could mix rapidly with the high-temperature bulk burned gases, but it seems to be a rough assumption to model the ring crevice as a free jet[7]. The latter will enter the cool gases in the cylinder wall boundary layer and mix and probably burn much more slowly[3].

A model that includes the effect of mixing of fuel from crevices and hot bulk gas in a relatively simple way has been developed. The outflow from the crevices is treated as a free jet, the mixing of gas in the jet and the entrained bulk gas causes a temperature raise in the jet. This approach is based on the

assumption that the crevice mechanism can be described mathematically as one crevice[7].

Two other crevices are the spark plug thread and the gap between the centre electrode and the plug body. Neither has any detectable effect on UHC. In the first case it is probably because the volume involved is very small. In the second case the gap is close in size to that indicated in the literature as the limit into which a flame can penetrate. The flame is able to penetrate the gap and consume the mixture inside[9].

Absorption and desorption in engine oil

Vapour transfer between the bulk gas and the oil/gas interface is governed by convection and diffusion.

The fuel vapour concentration within the cylinder is close to the inlet manifold concentration during intake and compression. Thus, for about one crankshaft revolution, any oil film on the walls will absorb fuel vapour. During the latter part of compression the fuel vapour pressure is increasing, so by Henry's law, absorption will continue even if the oil was saturated during intake. At the interface, it is usually assumed that Henry's law, which relates the partial pressure of each vapour component p_f to the dissolved mole fraction of that component in the oil $\tilde{x}_f$, is valid:

$$\tilde{x}_f = p_f / H$$

Henry's constant H varies strongly with temperature, so the amount of vapour absorbed into the oil is significantly higher at lower oil temperatures and at higher gas pressures[10]. During combustion the fuel vapour concentration in the bulk gases goes to zero so the absorbed fuel vapour will desorb from the liquid oil film into the gaseous combustion products. Desorption could continue throughout the expansion and exhaust strokes. Some of the desorbed fuel vapour will mix with the high-temperature combustion products and oxidize. Desorbed vapour that remains in the cool boundary layer or mixes with the cooler bulk gases late in the cycle may escape full oxidation and contribute to unburned HC emissions.

The increase in exhaust HC is primarily unreacted fuel and not oil or oil-derived compounds.

The increase in the exhaust HC is proportional to the solubility of the fuel in the oil. At high coolant temperatures the increase in HC on oil addition is less, as indicated by Henry's law, because it changes the solubility and diffusion rate of the fuel in the oil. Increasing oil temperature, also decreases viscosity, as it increases the rate of drainage into the sump.

Oil film thicknesses on the cylinder wall vary during the operating cycle between about 1 and 10 μm. Therefore diffusion times for engine conditions are 10^{-1} to 10^{-3} s; for the thinnest oil layers approximate equilibration would be achieved[3].

Engine tests run with and without oil layers present indicate that no measurable change in HC emissions occurs when propane is used as the fuel. In contrast, HC emissions increase substantially (in the order of 35%) for gasoline when oil layers are present. Since the solubility of methane in oil is about ten times smaller than for propane in oil, the amount of methane that can be stored in oil layers in gas engines is almost certainly negligible. The solubility of ethane in oil is somewhat greater than that of methane but still less than that of propane, so none of the major components of natural gas should be absorbed to any significant extent in engine oil layers[11].

Flame quenching

With a well designed fast-burn combustion system, under normal steady-state engine operating conditions, flame quenching phenomena are not expected to contribute significantly to HC emissions[10].

The importance of wall quench has been shown to increase at lower temperatures.

One of the first theories about the sources of UHC was that the flame was quenched as it approached the cool wall of the chamber and the unburned boundary layer was subsequently exhausted. The advent of detailed models describing the mixing and oxidation processes showed that the combustion

boundary layer is almost completely oxidized by the rapid mixing and post-flame reactions in the cylinder[9]. For reference, in typical automotive gasoline engines the amount of fuel that is protected from combustion by wall quenching is small, estimated as being on the order of 0.5%. About 2/3 of this is eventually burned completely before leaving the engine[11].

Poor combustion quality

Flame extinction in the bulk gas, before all of the flame front reaches the wall, is a source of HC emissions under certain engine operating conditions.

As the cylinder pressure falls during the expansion stroke, the temperature of the unburned mixture ahead of the flame decreases. This slows the burning rate (the laminar speed decreases). If the pressure and temperature fall too rapidly, the flame can be extinguished.

Burning the mixture faster, so that combustion is completed before conditions conductive to slow and partial burning exist in the cylinder (two spark plugs instead of one, fuel with a fast burning rate) does reduce engine exhaust HC emissions[3].

Blowby

Blowby is the gas that flows form the combustion chamber, past the piston and into the crankcase. It is forced through any leakage paths afforded by the piston-bore-ring assembly in response to combustion chamber pressure.

Blowby at a given speed and load is controlled primarily by the greatest flow resistance in the flow path between the cylinder and the crankcase.

Blowby of gases from the cylinder to the crankcase removes gas from this crevice region and thereby prevents some of the crevice gases from returning to the cylinder.

Crankcase blowby gases used to be vented directly to the atmosphere and constituted a significant source of HC emissions. The crankcase is now vented to the engine intake system, the blowby gases are recycled, and this source of HC emissions is now controlled.

Crankcase blowby gases represent a direct performance loss. They are a smaller efficiency loss because crankcase gases are now recycled to the engine intake system[3].

Valve leakage is not a significant contributor to UHC emissions in a new engine, but could be a significant cause of the increase in UHC emissions with engine age[9].

Hydrocarbon oxidation

Engine operating conditions that give highest exhaust temperatures (stoichiometric operation, higher speeds, retarded spark timing, lower compression ratio) and longest residence times (lighter load) give higher UHC reductions.

To oxidize the hydrocarbons in the gas phase, a residence time of order 50 ms or longer at temperatures in excess of 600 °C are required. Average exhaust gas temperatures at the cylinder exit (at the exhaust valve plane) are about 800 °C; average gas temperatures at the exhaust port exit are about 600 °C (there is a significant variation in the temperature of the exhaust gases throughout the exhaust process; the gas exhausted first is about 100 °C hotter than the gas exhausted at the end of the process). Thus a large fraction of the HC leaving crevice regions or oil layers during the exhaust process can be expected to survive with little further oxidation.

Reduction in exhaust port heat losses through the use of larger port cross-sectional areas (to reduce flow velocity and surface area per unit volume), insertion of port liners to provide higher port wall temperatures and attention to port design details to minimize hot exhaust gas impingement on the walls are known to increase the degree of reaction occurring in the port[3].

1.2 CO emission

When burning a hydrocarbon-based fuel, combustion can be thought as a two-step process: the first step involves the breakdown of the fuel to carbon

monoxide, the second step is the final oxidation of the carbon monoxide to carbon dioxide.

CO emissions are controlled mainly by the air/fuel ratio. For fuel-rich mixtures, CO concentrations in the exhaust increase proportionally with increasing excess fuel. For fuel-lean mixtures, CO concentrations in the exhaust vary little with air/fuel ratio.

To oxidize carbon monoxide temperatures in excess of 700 °C are required.

1.3 Formaldehyde emission

The trapped fuel-air mixture is both compressed and heated during the compression stroke. Depending on such factors as the compression ratio, initial temperature and mixture ratio, it is possible for some fraction of the fuel to be partially oxidized to formaldehyde. After ignition and during flame propagation, the end gases in front of the flame are further heated and compressed. Partial oxidation reactions can continue and additional CH_2O may be formed.

The presence of CH_2O and CH_3CHO in significant quantities indicate that low-temperature oxidation processes are occurring[3].

Most of the fuel and formaldehyde are subsequently burned to products of combustion such as CO_2 and H_2O in the propagating flame and in the high-temperature, oxygen-rich gases behind the flame. None of the formaldehyde formed as an intermediate specie inside the flame structure survives.

Some finite fraction of the fuel and possibly some of the formaldehyde already formed is protected by crevices and in quench zones or poorly mixed regions into which the flame does not propagate. If this protected fuel and formaldehyde is subsequently mixed with the high temperature products it will oxidize rapidly and be consumed. Some of the protected mixture will survive until the bulk gas temperature has been reduced by piston motion during the expansion stroke. At this point the temperature can be low enough that only a part of the protected fuel and formaldehyde are oxidized completely to

products as they leave the cylinder. This may occur, even if the bulk temperature is high, if mixing is incomplete. Also, during the flow to the exhaust port, a fraction of the surviving fuel may be partially oxidized to form additional formaldehyde. After entering the exhaust port formaldehyde formation reactions may continue into the exhaust manifold and ducting, depending on engine operating conditions and design. Eventually, the temperature will decrease to the point that the gas composition is effectively frozen. It is also possible, especially for high flame temperature engine designs, for the temperature to remain high enough downstream of the exhaust port that some additional complete combustion of fuel and formaldehyde occurs in the exhaust flow[11].

Wall quenching

The flame does not propagate to the wall but reaches a standoff distance that depends on the fuel and operating conditions. Subsequently, the fuel-air mixture between the flame and the wall diffuses into the flame and is converted to products in times that are on the order of a few milliseconds. Thus, even if formaldehyde is created in the region between the wall and the flame, most of it will be destroyed in the hot products in times that are short compared with the residence time of the gas in the engine. Turbulent flows near the wall may exhibit multiple extinctions and ignitions and result in the production of locally high levels of formaldehyde[11].

Crevices

The crevice volumes into which flames do not propagate may serve as sources of formaldehyde. If the outflow from these crevices is exposed to the correct range of temperature, it could be a major source or formaldehyde for large gas engines. If the outflow temperature is too low, no formaldehyde will be formed and only unburned fuel will show up in the exhaust from this source. If the outflow temperature is too high, on the other hand, most of the formaldehyde formed will be consumed by subsequent reactions[11].

Experiments

The influence of SO_2 addition on the emissions from a natural gas spark-ignition engine has been investigated.

The engine experiments have been carried out at the Biomass Gasification Group as a collaboration between the Department of Mechanical Engineering and the Department of Chemical Engineering.

2.1 Test equipment

The following equipment has been used (Figure 2):

- natural gas engine (Biomass Gasification Group)
- additive injection (Biomass Gasification Group)
- sample line and exhaust gas analyzers (CHEC)
- data acquisition devices (Biomass Gasification Group)

The experimental setup has been planned, organized and realized by the Biomass Gasification Group.

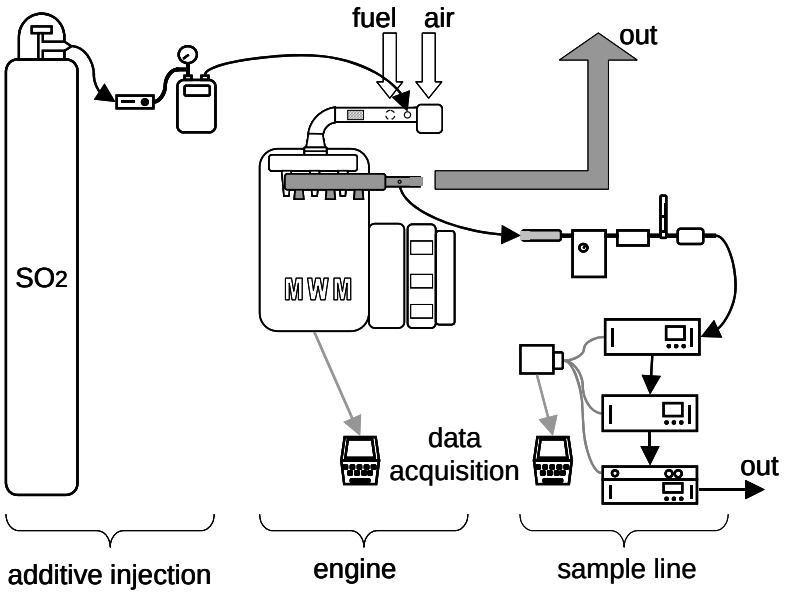

Figure 2 A schematic view of the experimental setup

The components of the experimental setup are described below.

Natural gas test engine

The test engine is a MWM diesel engine converted for natural gas operation. It is a naturally aspirated, 3-cylinder, 3.12 litre, four-stroke spark ignition engine (Picture 1).

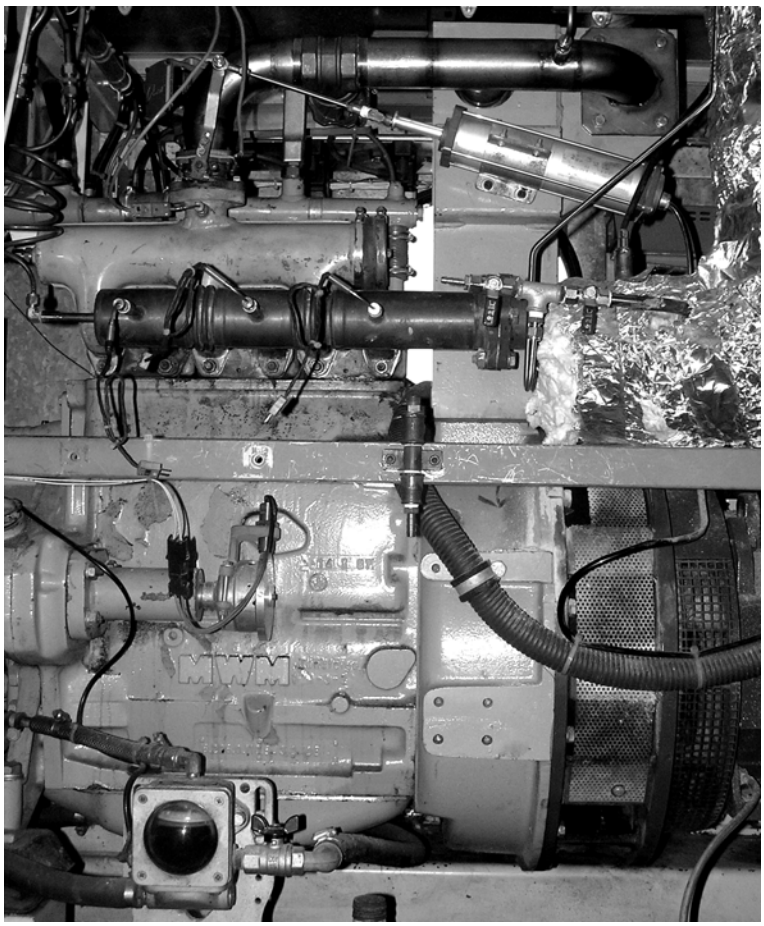

Picture 1 The MWM engine used for the tests

Table 2 Technical specifications of the test engine

Engine type	MWM D226-3
Number of cylinders	3
Arrangement of cylinders	In line
Working process	Four-stroke
Swept volume	3,12 dm^3
Cooling	Water
Number of valves	2
Bore	105 mm
Stroke	120 mm
Compression ratio	10.5:1

Natural gas supplied by the municipal line is fed to the engine.

The air-fuel mixture is naturally aspirated by the engine and a mixing device is located in the supply pipe prior to the intake manifold (Picture 2).

The engine is coupled to an asynchronous generator and the produced electricity is supplied to the main electric net. In order to produce alternate current at 50 Hz, the engine runs constantly at 1540 rpm.

The engine can run at different λ values, lean and rich conditions. The equivalence ratio is regulated by the fuel flow, which can be adjusted by means of a valve placed on the natural gas pipe.

The electrical output changes depending on λ. When the output is below 22 kW, the engine operates at full open throttle. When the output exceeds 22kW, the throttle is partially closed by an automatic mechanism and the output reduced to 22kW.

The produced heat from cooling water is supplied to a heating system.

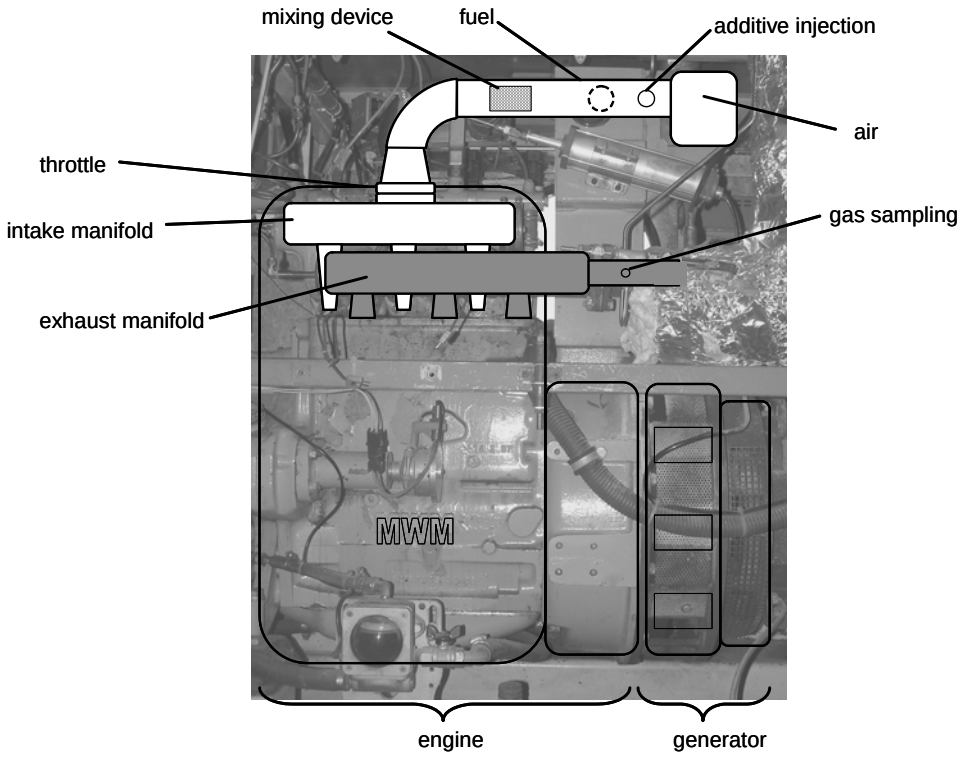

Picture 2 The MWM engine used for the tests

The engine is equipped with data acquisition and the following data are logged on a computer:

- temperature of the air-fuel mixture prior to the throttle
- pressure of air-fuel mixture in the intake manifold
- temperature of air in the intake
- pressure of exhaust gas in the exhaust manifold
- temperature of the exhaust gas after manifold
- temperature of cooling water entering the engine
- temperature of cooling water leaving the engine
- output of the electricity generator

Additive injection

A blend of 5% SO_2 in nitrogen (vol.) is used for the experiments. The blend is added to the air-fuel line prior to the mixing device (Picture 2).

SO_2 is a colourless, poisonous, toxic, corrosive, non-flammable gas, with a sharp, pungent odour (choking odour above 3-5 ppm).

Table 3 Materials compatibility of SO_2

Metals	Stainless steel Carbon steel Monel
Plastics	Kel-F PTFE FEP PFA fluoropolimers resins Tefzel Kynar PVC
Elastomers	Kalrez Viton Polyurethane

Incompatibility (materials to avoid): chlorine trifluoride, chlorates, sodium carbide, powdered aluminium, moisture, zinc and its alloys, manganese, alkali metals, metal nitrates, rubidium carbide, sodium, ferrous oxide at 300 °C, fluorine, stannous oxide, metal acetylides, metal oxides, metal hydrides, acrolein.

A mass flow controller is used to regulate the flow of the additive. A flow meter gives an additional check of the flow (Figure 3).

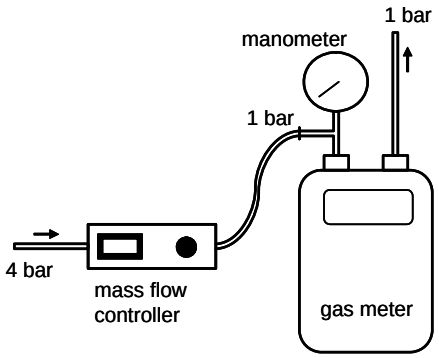

Figure 3 A schematic view for the dosage unit for the sulphur dioxide

The pressure at the inlet of the mass flow controller is set to 4 bar (absolute pressure) by means of a stainless steel regulator, the pressure drop due to the mass flow controller is 3 bar. Atmospheric pressure at the exit of the mass flow controller is enough to ensure a flow to the engine, being the

pressure in the air-fuel line prior to the throttle below atmospheric pressure (between 0.90 and 0.95 bar depending on the opening of the throttle).

The principle of operation of the mass flow controller is based on the heat transfer along a section of a capillary tube. The instrument consists of a metal block with a straight hole. Two stainless steel probes (a heater probe and a temperature probe) are inside the bore. A temperature difference between the probes is maintained constant adjusting the power to the heater probe. The energy required to maintain the ΔT is dependent on the mass flow rate

$$\Delta T = K \cdot C_p \cdot \Phi_m$$

C_p = specific heat
K = constant
Φ_m = mass flow

The control valve is a solenoid valve which is closed when the mass flow controller is turned off or the flow set to zero. The plunger is lifted by the magnetic field of the coil.

The output signals from the mass flow controller are the value displayed by the instrument itself and a current. Both outputs have been taken into account during the experiments.

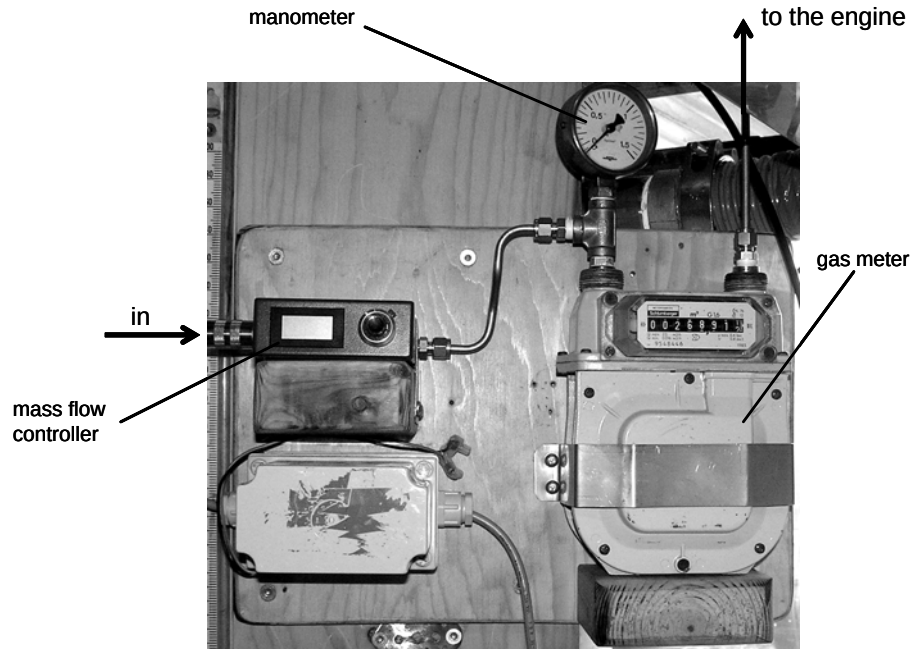

Picture 3 The dosage unity for the sulphur dioxide

The flow meter is placed in series after the mass flow controller (Picture 3). The pressure at the inlet of the flow meter is measured by a manometer (the flow meter can not stand pressures that are 0.4 bar higher than atmospheric pressure). The pressure drop across the flow meter is negligible. Pressure pulsations due to the engine will not affect the flow meter.

The mass flow controller and the flow meter connected by the pipe and the manometer have been calibrated together as a unity. The display of the mass flow controller or the output current can be used as the setpoint, the calibration curve gives the flow.

Exhaust gas sampling and analysis

Gas sampling takes place after the exhaust manifold.

A small fraction of the engine exhaust gas stream is drawn off into a sample line, which is heated up to 130 °C to prevent condensation.

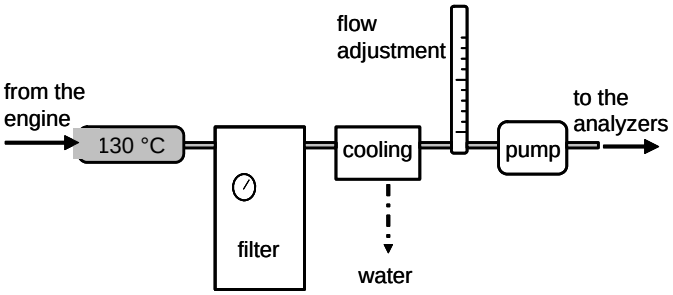

Figure 4 A scheme of the sample line

Before the sample gas is fed to the instruments, it is filtered to remove particles and cooled to remove water (Figure 4). The dry gas flow is adjusted and sent to three analysers.

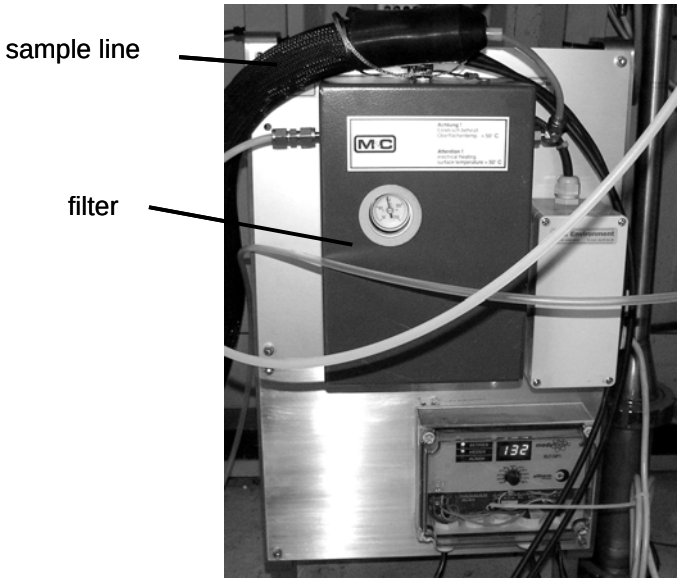

Picture 4 Heated sample line and filter

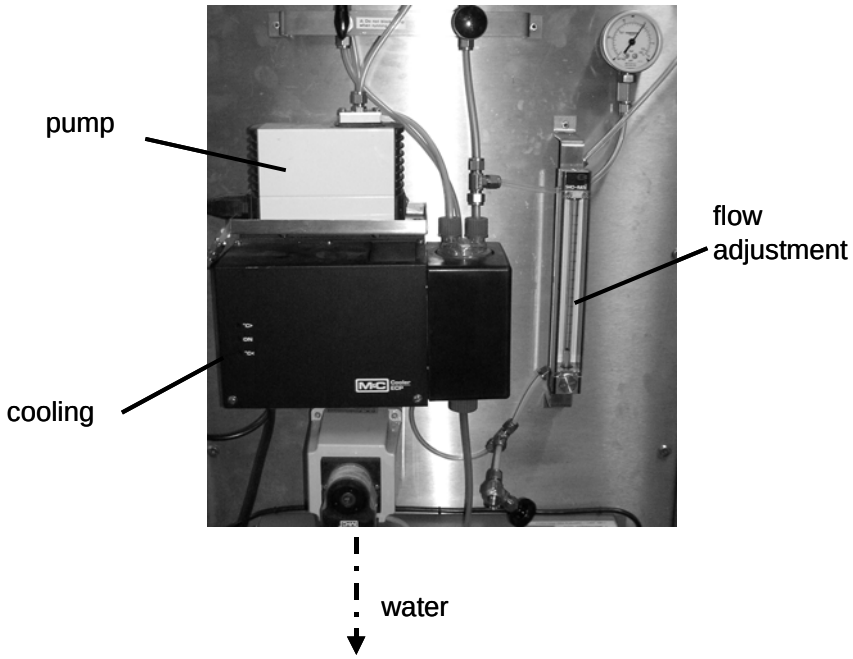

Picture 5 Sample line: cooling, flow adjustment, pump

The concentrations of NO, SO_2, CO, CO_2, O_2 and UHC are measured (dry) by means of the three analysers.

The NDIR analyser is used for CO and CO_2 concentrations. Infrared absorption in a cell containing exhaust gas is compared to absorption in a reference cell.

Oxygen concentrations are measured with a paramagnetic analyser.

NO is measured with a chemiluminescent analyser.

The instrument used for unburned hydrocarbon analysis is a flame ionisation detector (FID). The hydrocarbons present in the exhaust gas sample are burned in a small hydrogen-air flame, producing ions in an amount proportional to the number of carbon atoms burned.

The three analysers are displaced in series, the FID analyser (UHC) being the last. The position of the two other analysers (NO + SO_2 and CO + CO_2 + O_2) does not affect the measurements. The FID has to be at the end of the series, because its hydrogen-air flame modifies the composition of the sample

gas. The hydrogen needed to ignite the flame inside the FID is contained in a small cylinder placed on the side of the FID (Figure 5, Picture 7).

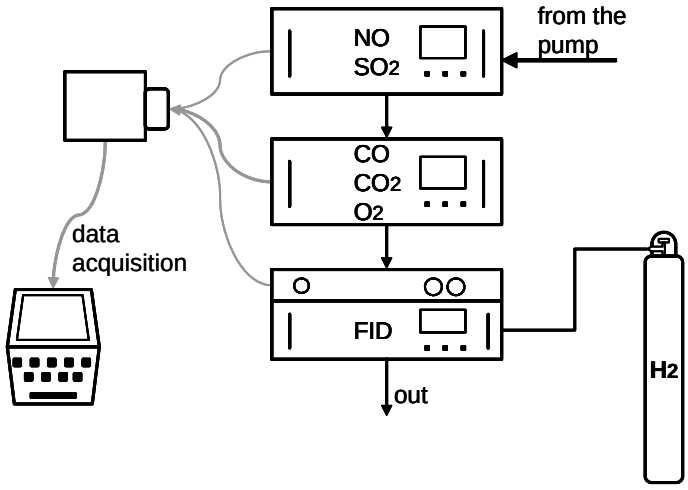

Figure 5 A scheme of the analysers and the data acquisition devices

The concentration of each analysed specie is transmitted as a voltage through its own channel, then it is converted into a digital signal (Picture 6) and sent to the data acquisition device. The data acquisition device is connected to a pc (Picture 7).

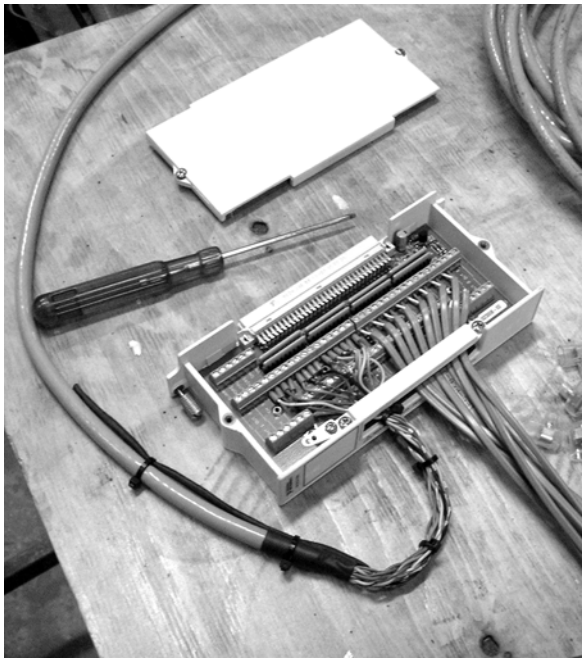

Picture 6 The card used to convert the output from the analysers (voltage) into a digital signal (input to the data acquisition device)

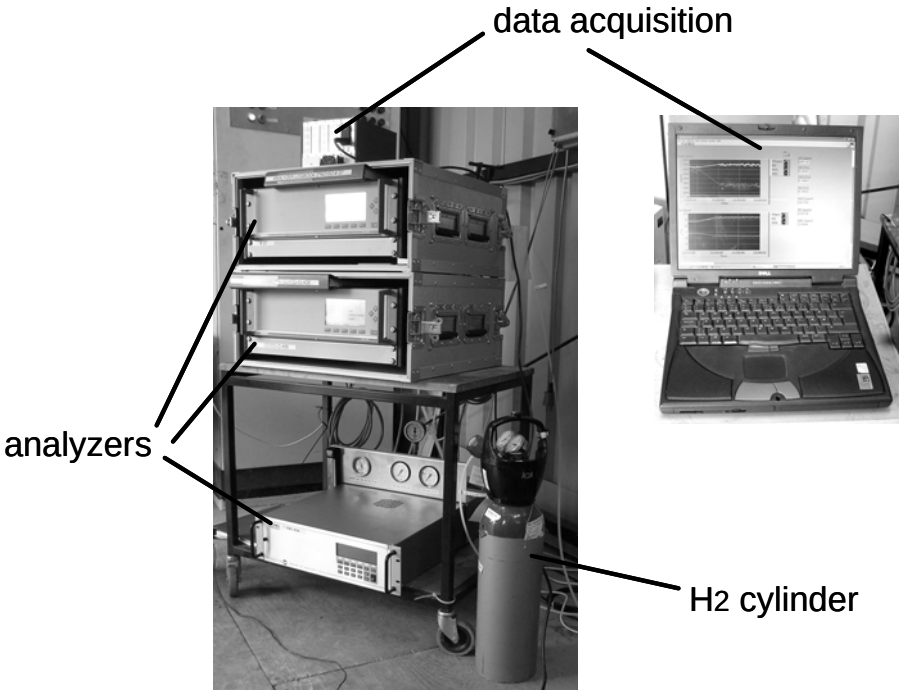

Picture 7 The analysers and the data acquisition devices

Calibration

The analysers are calibrated with sample gases of known composition.

Each analyser needs two calibration points for each channel, i.e. two calibration points for each specie to analyse. The first point is needed to zero-calibrate, the second point to span-calibrate the instrument.

Three different blends are used for the calibration:

Table 4 Calibration gases, composition and use

Blend	Composition	Use
Blend 1	4850 ppm CO 14.5% CO_2 9.7% O_2 nitrogen	zero-calibration NO and SO_2 span-calibration CO, CO_2, O_2
Blend 2	848 ppm NO nitrogen	span-calibrate NO
Blend 3	918 ppm SO_2 nitrogen	zero-calibrate NO and CO, CO_2, O_2 span-calibrate SO_2

The SO_2 analyser can not be calibrated with Blend 2, because that instrument is cross-sensitive to NO. It can be assumed that the concentration of SO_2 detected by the analyser is the sum of the real SO_2 concentration and another concentration that depends on the concentration of NO. A typical vale for this "additional" concentration of SO_2 is 10 ppm when a gas containing 848 ppm of NO and no SO_2 is analysed.

SO_2 has the characteristic to stick on surfaces for a long time, therefore after calibrating with Blend 3 it is important to flush the SO_2 out from pipes, valves and analysers.

Data acquisition and procedure

The whole system is monitored during operation. The engine is equipped with two separate data acquisition systems to monitor the exhaust gas composition and the engine operating conditions. The data is logged on pc.

Other measurements including fuel flow and SO_2 flow have been conducted during the tests.

All the measurements have been carried out at the same conditions (temperature of air and fuel, composition of fuel, ignition timing). The only variables are λ and the amount of SO_2 added.

λ is adjusted by tuning the flow of the fuel and its value is calculated from the composition of the exhaust gas. The methods used to calculate λ are described in "**Error! Reference source not found.**". It is important to observe that the value computed for λ is dependent on the performance of the engine, because it is calculated from the composition of the combustion products.

The following procedure has been developed:

1. the engine is started and warmed up for 10 minutes to ensure stable conditions;
2. the additive (blend of 5% SO_2 in N_2) is added with a constant flow for 10 minutes to ensure stable conditions ($flow_1$ = 1.1 l/min);
3. the flow of the additive is increased and maintained constant for 10 minutes ($flow_2$ = 2.1 l/min);
4. a third and higher flow is added ($flow_3$ = 3.2 l/min);
5. the valve of SO_2 is closed and the engine is run for 10 minutes to reach stable conditions;
6. the equivalence ratio is changed and the procedure is repeated.

2.2 Results

Different amounts of SO_2 have been added to the air-fuel mixture of a natural gas fired spark-ignition engine. The influence of SO_2 addition on CO, UHC and NO emissions has been investigated. The tests have been repeated at different λ values and constant boundary conditions. Data have been collected from the exhaust gas analysers, from the engine, from the fuel and SO_2 meters. The data collected during the experiments (concentrations versus time without additional calculations) are in "**Error! Reference source not found.**". An investigation of the influence of SO_2 addition on the emissions' fluctuations is in "Fluctuations of the emissions", page 39. A partial statistical analysis is in "**Error! Reference source not found.**".

In the following charts, the measurements of the emissions of CO and NO are expressed as mg/normal m^3 at a reference oxygen content of 5% vol. in the exhaust gas, dry (mg//Nm^3 @ 5% O_2, dry). The concentration of UHC is expressed in ppm[‡].

CO emissions

In Figure 6 the emission of carbon monoxide is depicted versus the excess of air at different amounts of SO_2 addition:

---

‡ To convert ppm into mg/Nm^3 at a given (reference) oxygen concentration, the following expression has been used:

$$\text{mg/Nm}^3[\text{X}] = \text{ppm}[\text{X}]_{\text{measured}} \cdot \rho_{\text{X standard}} \cdot \frac{(21 - [\text{O}_2]_{\text{reference}})}{(21 - [\text{O}_2]_{\text{measured}})}$$

$\text{ppm}[\text{X}]_{\text{measured}}$ = measured concentration of the specie X, as ppm
$\rho_{\text{X standard}}$ = mass density of specie X at standard conditions (0 °C, 101325Pa), as g/Nm^3
$[\text{O}_2]_{\text{reference}}$ = reference oxygen concentration, as vol.%
$[\text{O}_2]_{\text{measured}}$ = measured concentration of oxygen, as vol.%

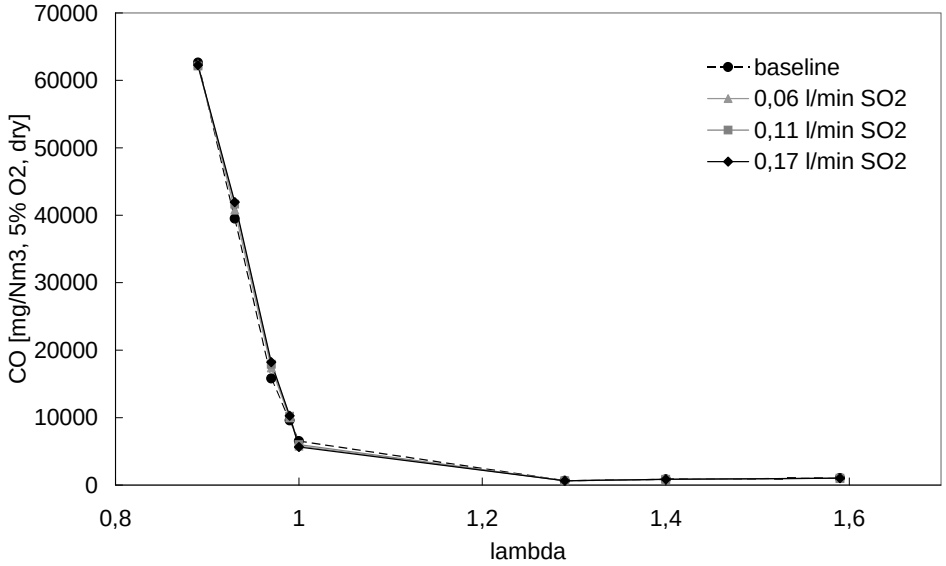

Figure 6 CO emission versus λ at different degrees of SO_2 addition

In the baseline case (no addition of SO_2), CO emissions are high at rich conditions (available oxygen is not enough to complete the combustion) and decrease with increasing lambda. A minimum for CO emissions is reached around λ = 1,3 and then CO emissions increase. The trend observed for the baseline is observed also for the cases with addition of SO_2.

Even though the general trend for CO emission does not change in presence of the additive, small effects related to SO_2 addition are found. Figure 7, Figure 8, Figure 9 and Figure 10 depict CO emission at four different lambda values. CO concentration is expressed as CO / CO_{ref}[§].

[§] CO / CO_{ref} = measured CO during injection of SO_2 / measured CO without injection of SO_2

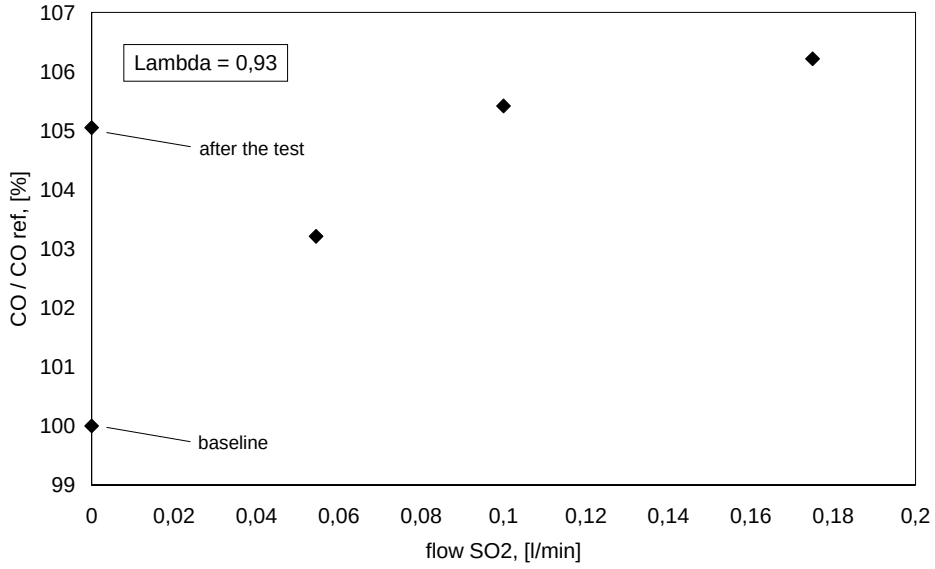

Figure 7 CO emissions vs additive flow at λ = 0,93

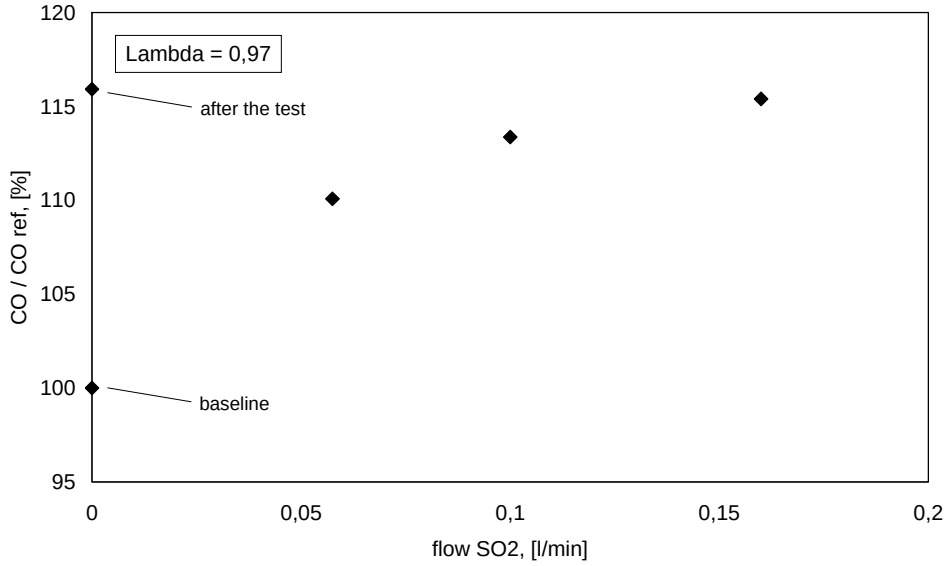

Figure 8 CO emissions vs additive flow at λ = 0,97

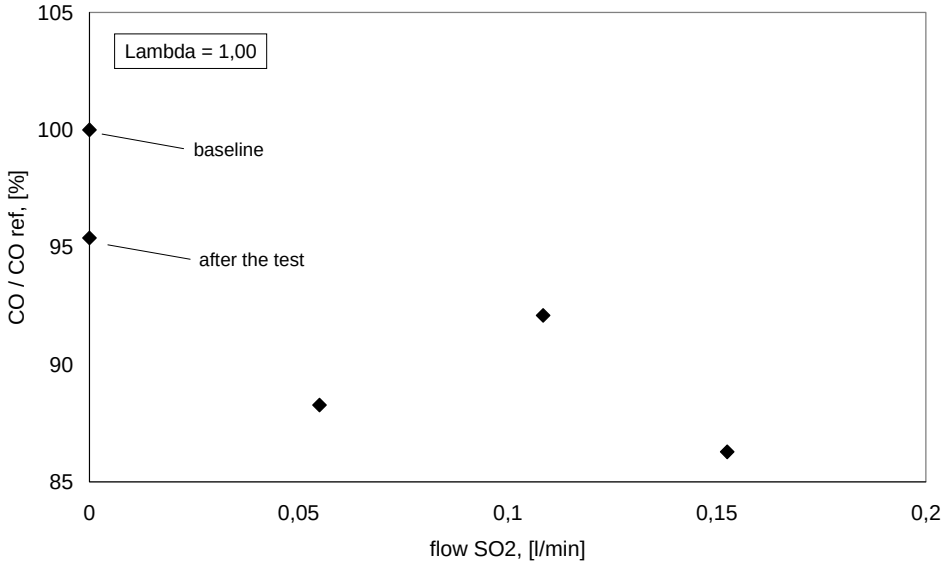

Figure 9 CO emissions vs additive flow at λ = 1,00

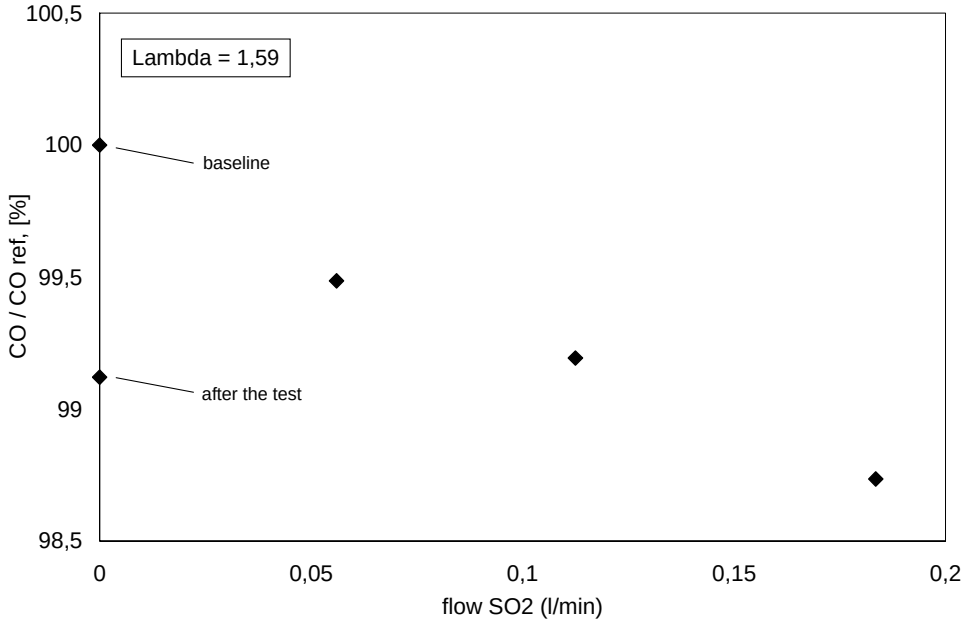

Figure 10 CO emissions vs additive flow at λ = 1,59

Addition of SO_2 seems to make CO emissions increase at rich conditions and decrease at lean conditions. These effects, which are very small, increase in proportion to the amount of SO_2 added.

Difficulties are found when trying to reproduce the results, as depicted by the different values of the two points at 0 l/min of SO_2 (the label "after the test" corresponds to step number 5 in the procedure described in "Data acquisition and procedure", page 27). The value obtained "after the test" is on the side of the values obtained with addition of SO_2. This effect could be due to residual SO_2 in the additive injection line (sulphur dioxide has the characteristic to stick on surfaces for a long time) which is released slowly and enters the combustion chamber even when the additive flow is set to zero. If the difference observed between "baseline" and "after the test" is effectively due to residual SO_2, the results from the case called "after the test" are still affected by SO_2 addition. In order to avoid this influence, the pipelines should have been flushed for a longer time. A statistical analysis of the cases "baseline" and "after the test" is in "**Error! Reference source not found.**". The result of it is that the mean CO emissions in the two cases can not be considered equal. Because of the cross-sensitivity of the SO_2 analyser to NO, the SO_2 concentrations detected by the analysers in the cases "baseline" and "after the test" can not be used to decide whether residual SO_2 is injected into the system or not.

The differences observed between "after the test" and "baseline" do not affect the conclusions (page 43), because all the effects due to SO_2 addition are not relevant.

UHC emissions

Figure 11 depicts the emission of unburned hydrocarbons versus lambda.

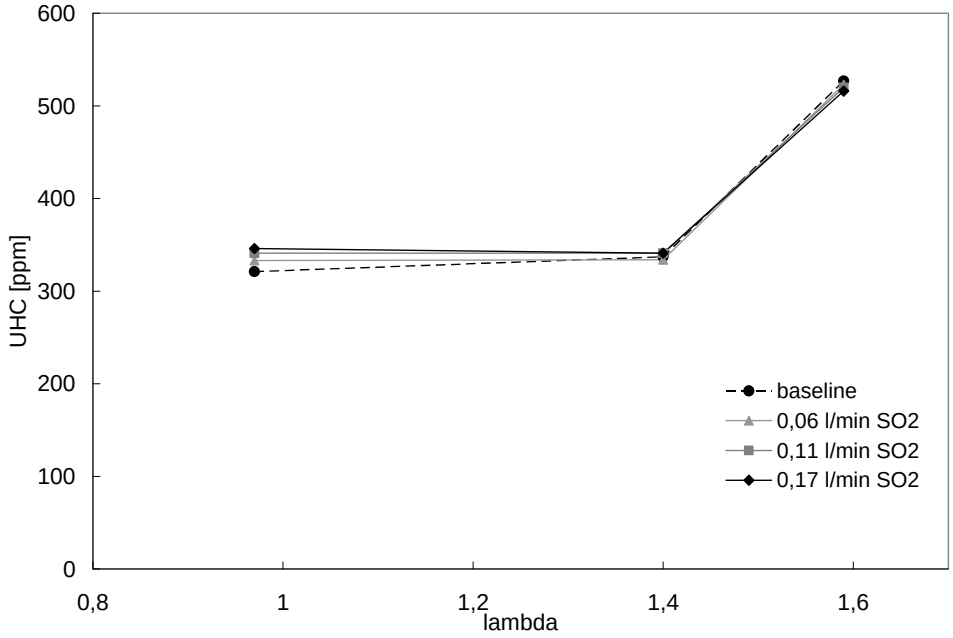

Figure 11 The UHC emission vs λ at different degrees of SO_2 addition

Because of technical reasons, the emission of UHC has been measured only at three lambda values.

SO_2 addition makes UHC emissions increase at rich-stoichiometric conditions and decrease at lean conditions. The positive effect observed at lean conditions is smaller than the negative effect at $\lambda = 0{,}97$ (Figure 12, Figure 13, Figure 14) and it can be considered negligible when compared to the error due to the instruments and to the fluctuations of the emissions.

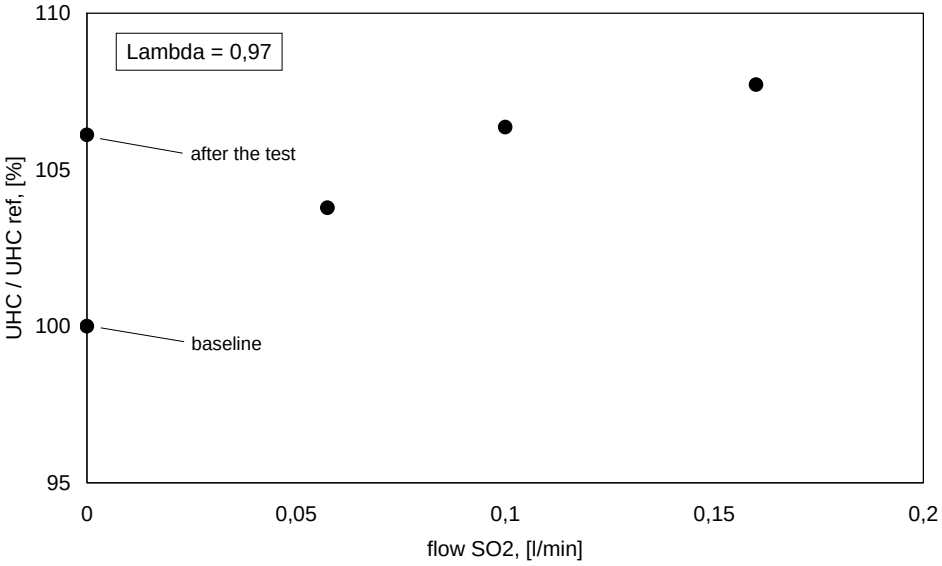

Figure 12 UHC emissions vs additive flow at λ = 0,97

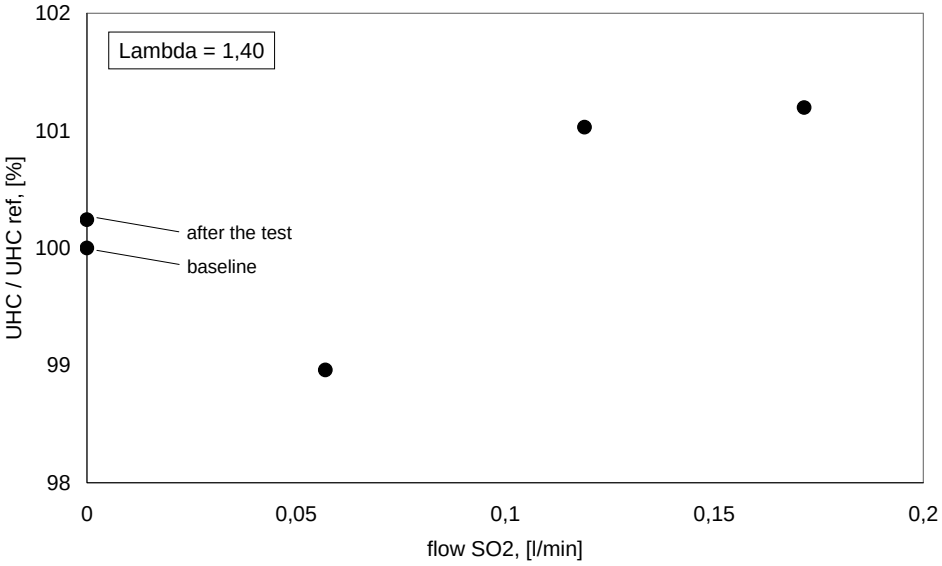

Figure 13 UHC emissions vs additive flow at λ = 1,40

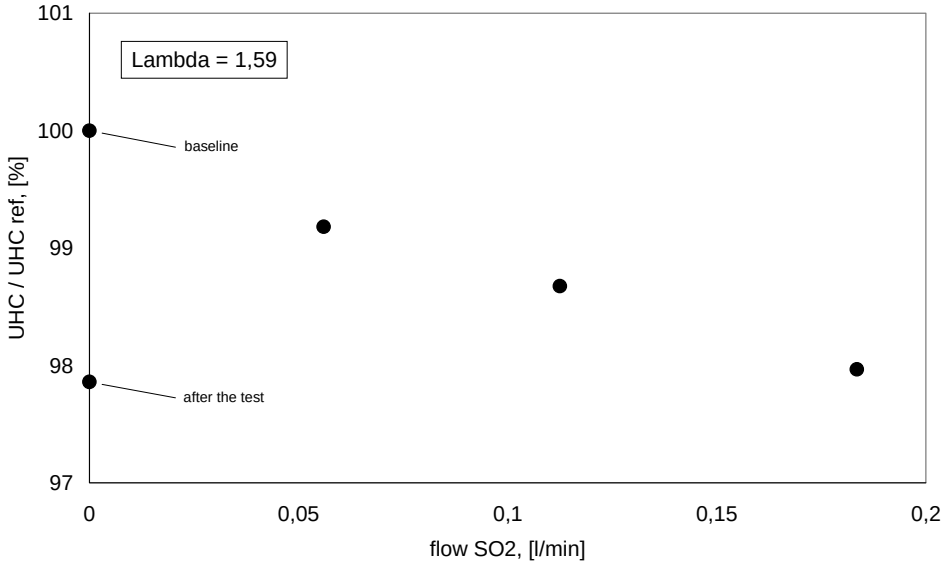

Figure 14 UHC emissions vs additive flow at λ = 1,59

NO emissions

Figure 15 depicts the emission of NO versus lambda at different additions of SO_2.

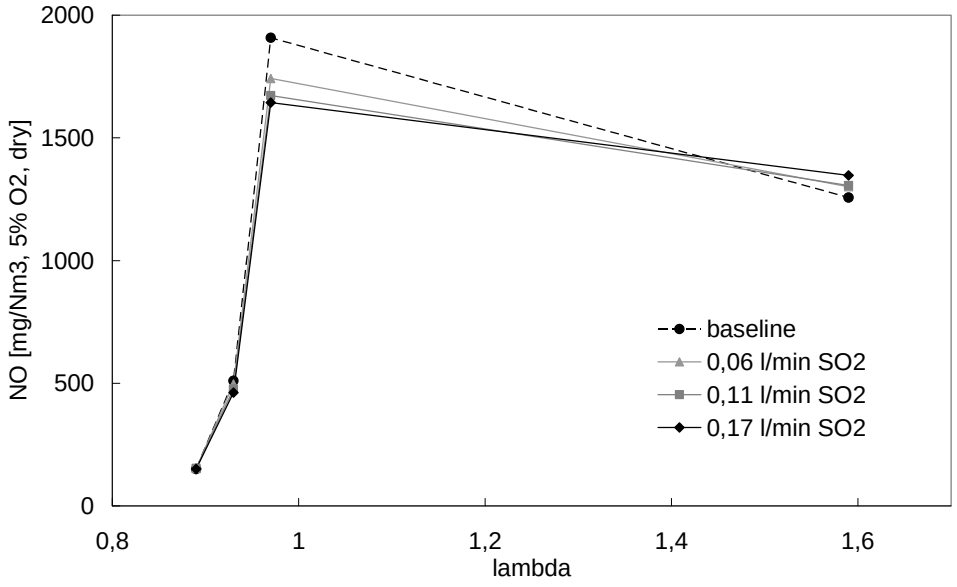

Figure 15 The NO emission vs λ at different degrees of SO_2 addition

Because of technical reasons, the emission of NO has been measured only at four lambda values.

Considering the baseline case, in rich conditions NO emission increases with increasing lambda and reaches a maximum around stoichiometric conditions (high temperature, thermal NO). In lean conditions, NO emission decreases as the excess of air increases.

When adding SO_2, small effects are found around the stoichiometric region and at lean conditions. The maximum positive effect is observed at high temperature ($\lambda = 1$). The importance of this effect decreases as λ increases and an intersection point with the baseline case is found around $\lambda = 1,4$. At $\lambda = 1,6$ NO emissions with SO_2 addition are higher than NO emissions without SO_2 addition. These effects are proportional to the amount of SO_2 added.

SO_2 addition results in a lower dependence of NO on the equivalence ratio. A lower dependence on the equivalence ratio could allow to decrease the excess of air (i.e. increase temperature) maintaining low NO levels.

Figure 16 and Figure 17 depict NO emission versus SO_2 addition at $\lambda = 0,97$ and $\lambda = 1,59$.

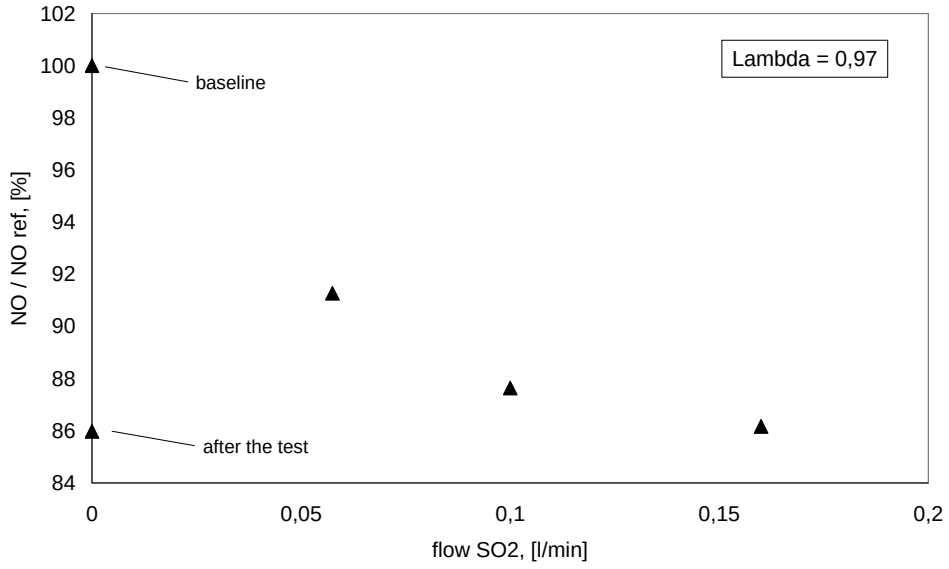

Figure 16 NO emissions vs additive flow at $\lambda = 0,97$

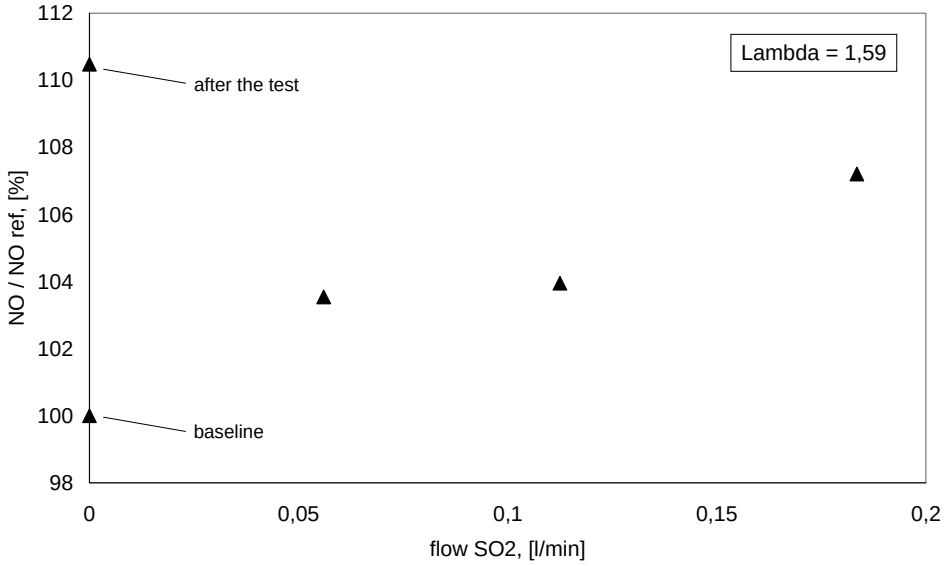

Figure 17 NO emissions vs additive flow at λ = 1,59

The lower dependence of NO on the equivalence ratio depicted in Figure 15 is coupled to the effect on CO emission, as depicted by Figure 18.

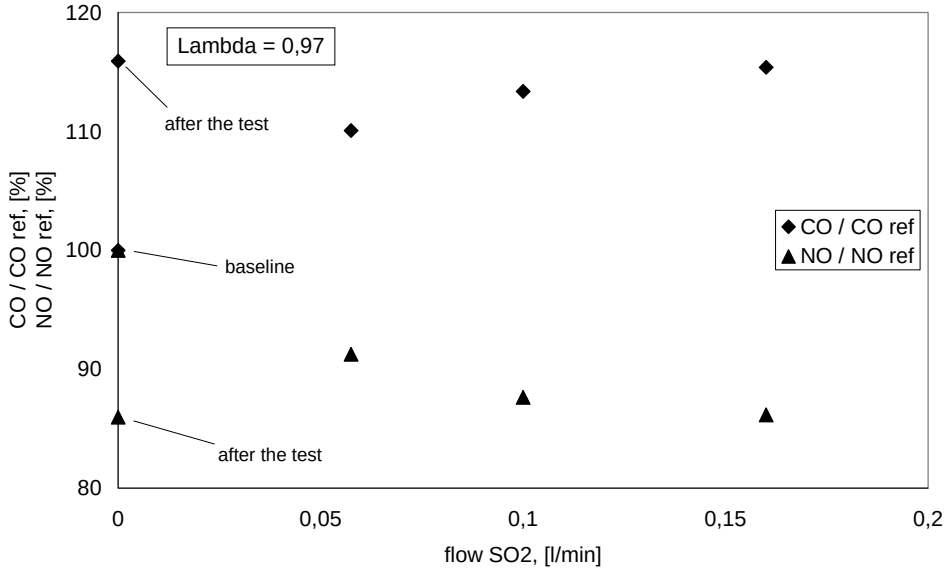

Figure 18 CO and NO emission vs additive flow at λ = 0,97

NO emission decreases as addition of SO_2 increases, whilst CO emission increases. The reduction of NO emission corresponds to a proportional increase

of CO emission. This is probably due to the instability of the emissions when the engine runs close to stoichiometric conditions.

Fluctuations of the emissions

As showed in "**Error! Reference source not found.**", the emissions are very unstable. Effects on the emissions' fluctuations related to SO_2 addition are investigated in this paragraph. The present investigation does not include any statistical tool, aside from the mean and the variance. A more correct analysis of the variance of the results is in "**Error! Reference source not found.**".

Relevant fluctuations of the emissions are due to engine's instabilities, whilst the noise of the instruments is a minor contributor.

Assuming that the emissions have a distribution $N(\mu, \sigma^2)$, additional observations can be made[**]. Because of the fluctuations, high values of standard deviation (σ) are found. If SO_2 addition has an effect on the fluctuations of the emissions, it is possible to use the standard deviation as a tool for detecting this effect. The following tables show μ and σ of CO, NO and UHC at different λ values and SO_2 additions:

Table 5 Mean value and standard deviation of CO, NO, UHC at different SO_2 additions (λ = 0,89)

λ = 0,89						
Flow SO_2 (l/min)	**CO**		**NO**		**UHC**	
	(mg/Nm^3, @5% O_2, dry)				**(ppm)**	
	μ	**σ**	**μ**	**σ**	**μ**	**σ**
Baseline	62641	306	150	3	-	-
0,06	62407	96	152	1	-	-
0,11	62120	223	153	2	-	-
0,17	62257	121	150	2	-	-
After the test	62076	142	152	1	-	-

[**] When the emissions of specie X (at a fixed λ value and SO_2 addition) have a distribution $N(\mu , \sigma^2)$, the expression $\mu \pm \sigma$ indicates that with a probability equal to 0,68 the "real" value is between $\mu - \sigma$ and $\mu + \sigma$.

Table 6 Mean value and standard deviation of CO, NO, UHC at different SO_2 additions (λ = 0,93)

λ = 0,93						
Flow SO_2 (l/min)	**CO (mg/Nm³, @5% O_2, dry)**		**NO**		**UHC (ppm)**	
	μ	**σ**	**μ**	**σ**	**μ**	**σ**
Baseline	39496	296	510	8	-	-
0,06	40763	310	498	8	-	-
0,11	41636	480	477	11	-	-
0,17	41950	256	462	6	-	-
After the test	41489	578	479	14	-	-

Table 7 Mean value and standard deviation of CO, NO, UHC at different SO_2 additions (λ = 0,97)

λ = 0,97						
Flow SO_2 (l/min)	**CO (mg/Nm³, @5% O_2, dry)**		**NO**		**UHC (ppm)**	
	μ	**σ**	**μ**	**σ**	**μ**	**σ**
Baseline	15782	585	1908	60	321	4
0,06	17372	549	1742	56	333	5
0,11	17892	471	1673	45	341	4
0,17	18212	461	1644	41	346	4
After the test	18294	537	1641	48	341	5

Table 8 Mean value and standard deviation of CO, NO, UHC at different SO_2 additions (λ = 0,99)

λ = 0,99						
Flow SO_2 (l/min)	**CO (mg/Nm³, @5% O_2, dry)**		**NO**		**UHC (ppm)**	
	μ	**σ**	**μ**	**σ**	**μ**	**σ**
Baseline	9573	193	-	-	-	-
0,06	9971	404	-	-	-	-
0,11	10195	329	-	-	-	-
0,17	10272	570	-	-	-	-
After the test	10772	653	-	-	-	-

Table 9 Mean value and standard deviation of CO, NO, UHC at different SO_2 additions (λ = 1,00)

λ = 1,00						
Flow SO_2 (l/min)	**CO (mg/Nm³, @5% O_2, dry)**		**NO**		**UHC (ppm)**	
	μ	σ	μ	σ	μ	σ
Baseline	6531	628	-	-	-	-
0,06	5765	412	-	-	-	-
0,11	6015	668	-	-	-	-
0,17	5635	635	-	-	-	-
After the test	6230	535	-	-	-	-

Table 10 Mean value and standard deviation of CO, NO, UHC at different SO_2 additions (λ = 1,29)

λ = 1,29						
Flow SO_2 (l/min)	**CO (mg/Nm³, @5% O_2, dry)**		**NO**		**UHC (ppm)**	
	μ	σ	μ	σ	μ	σ
Baseline	634	7	-	-	-	-
0,06	642	6	-	-	-	-
0,11	643	6	-	-	-	-
0,17	645	5	-	-	-	-
After the test	635	1	-	-	-	-

Table 11 Mean value and standard deviation of CO, NO, UHC at different SO_2 additions (λ = 1,40)

λ = 1,40						
Flow SO_2 (l/min)	**CO (mg/Nm³, @5% O_2, dry)**		**NO**		**UHC (ppm)**	
	μ	σ	μ	σ	μ	σ
Baseline	850	7	-	-	337	4
0,06	848	7	-	-	334	3
0,11	857	7	-	-	341	2
0,17	854	8	-	-	341	3
After the test	852	9	-	-	338	1

Table 12 Mean value and standard deviation of CO, NO, UHC at different SO_2 additions (λ = 1,59)

λ = 1,59						
Flow SO_2 (l/min)	**CO (mg/Nm^3, @5% O_2, dry)**		**NO**		**UHC (ppm)**	
	μ	σ	μ	σ	μ	σ
Baseline	1020	8	1257	57	527	6
0,06	1014	8	1301	53	523	7
0,11	1011	8	1306	54	520	6
0,17	1007	7	1347	75	516	7
After the test	1011	8	1388	52	516	7

From the previous tables it is evident that the standard deviation of the emissions, which is an index of the fluctuations of the emissions, does not change as an effect of SO_2 addition.

Measurements of the power output of the engine and of the exhaust gas temperature after the manifold have been carried out and no effect related to SO_2 addition has been found.

No detectable effect on soot is seen.

Conclusions

A blend of 5% SO_2 in nitrogen has been added to the air-fuel mixture of a natural gas spark-ignition engine in order to investigate the effects on CO, UHC and NO emissions.

Analysis of the results gives the following conclusions:

- relevant effects on CO emission due to SO_2 addition are observed neither at rich conditions nor at lean conditions. A small increase of CO emission with respect to the baseline case is observed when adding SO_2 at $\lambda = 0,97$ and a decrease is observed when adding at lean conditions;
- UHC emission is not significantly affected by SO_2 addition. Small effects are seen at $\lambda = 0,97$ (increase of UHC with respect to the baseline case) and at $\lambda = 1,6$ (decrease of UHC emission);
- NO emission is slightly affected by SO_2 addition at $\lambda = 0,97$ and at $\lambda = 1,6$. Compared to the baseline case, the flame established with SO_2 addition at $\lambda = 0,97$ produces lower NO emissions. At $\lambda = 1,6$ NO emission increases with additive injection. The result is a lower dependence of NO on the equivalence ratio. The decrease of NO emissions at $\lambda = 0,97$ is coupled to the increase of CO emissions;
- no relevant effect on the amplitude of the emissions' fluctuations has been observed;
- no detectable effect on soot, output power of the engine, exhaust gas temperature;

The small measured effects, the reproducibility difficulties together with the instability of the emissions indicate that SO_2 addition has not relevant effects on CO, NO and UHC emissions from a natural gas SI engine.

REFERENCES

[1] Andersen, J., "The influence of sulphur addition on CO oxidation during combustion", M. Sc. thesis, CHEC Department of Chemical Engineering DTU, 2005

[2] Kassman, H., et al., "Decreased emissions of CO and NO_X by injection of ammonium sulphate into the combustion chamber", VÄRMEFORSK Service AB, ISSN 0282-3772, Feb. 2005

[3] Heywood, J. B., "Internal combustion engine fundamentals", Mc Graw-Hill, 1988

[4] Wayne, A. D., "Exhaust hydrocarbon emission", SAE Papers 700108, 1970, Society of Automotive Engineers, Warrendale, Pa

[5] Wentworth, J. T., "Piston and ring variables affect exhaust hydrocarbon emissions", SAE Paper 680109, 1968, Society of Automotive Engineers, Warrendale, Pa

[6] Ishizawa, S., "An experimental study of quenching crevice widths in the combustion chamber of a spark-ignition engine", Twenty-sixth symposium (international) on combustion, The Combustion Institute, Pittsburgh, PA, pp. 2605-2611, 1996

[7] Jensen, T., K., "Hydrocarbon emissions from lean burn natural gas SI engines", MEK-ET-Ph.D.-2001-01

[8] Saika, T., Korematsu, K., "Effects of a ring crevice on hydrocarbon emission from spark ignition engines", Combust. Sci. and Tech. Vol. 108, pp. 279 – 295, 1995

[9] Boam, D. J. et al., "Sources of unburned hydrocarbon emissions from spark ignition engines during cold starts and warm-up". Proc. Inst. Mech. Eng., Vol. 208, 1994

[10] Cheng, W. K. et al., "An overview of hydrocarbon emissions mechanisms in spark – ignition engines" SAE Papers 932708, 1993, Society of Automotive Engineers, Warrendale, Pa

[11] Mitchell, C. E., Olsen, D. B. "Formaldehyde formation mechanisms in large bore natural gas engines". ASME Paper 98-ICE-80 ICE-Vol. 30-1, 1998

[12] Alzueta, M. U., Glarborg, P., "Formation and destruction of CH_2O in the exhaust system of a gas engine", 4512 Environmental Science & Technology / vol. 37 n. 19, 2003

[13] Brendtsen, A. B., Glarborg, P., Dam-Johansen, K., "Low temperature oxidation of methane: the influence of nitrogen oxides", Combust. Sci. and Tech., 2000, vol. 151, pp. 31-71

[14] Kristensen, P. G., Karll, B., Brendtsen, A. B., Glarborg, P., Dam-Johansen, K., "Exhaust oxidation of unburned hydrocarbons from lean-burn natural gas engines", Combust. Sci. and Tech., 2000, vol. 157, pp. 263-292

[15] Naber, J. D., Siebers, D. L., Di Julio, S. S., Westbrook, C. K., "Effects of natural gas composition on ignition delay under diesel conditions", Combustion and Flame 1994, 99 : 102 - 200

[16] Gerk, T. J., Karagozian, A. R., "Ignition delay associated with a strained fuel strip", The Twenty-sixth symposium (international) on combustion, The Combustion Institute, Pittsburgh, PA, pp. 1095 – 1102, 1996

[17] Ozdor, M. N., Dulger, M., Sherk, E., "Cyclic variability in spark ignition engines: a literature survey", SAE paper 940987, 1994, Society of Automotive Engineers, Warrendale, Pa

[18] Fraser, R. A., Siebers, D. L., Edwards, C. F., Trans. SAE 100, Sec. 4 : 33 – 45 (1991) (SAE Paper 910227)

[19] Schramm, J. and Sorenson, S. C., "A model for hydrocarbon emissions from SI engines", Combust. Sci. and Tech., vol. 108, pp. 279 – 295, 1995

[20] Richards, G. A., Mc Millan, M. N., Gemmen, R. S., Rogers, W. A., Cully, S. R., "Issues for low emission, fuel-flexible, power systems", Progr. In. En. and Comb. Sci. 27, pp. 141 – 169 (2001)

[21] Ahrenfeldt, J., Jensen, T. K., Schramm, J., "Experiments with wood gas engines", SAE 2001 – 01 – 3681

[22] Ahrenfeldt, J. et al. "Investigation of continuous gas engine CHP operation on biomass producer gas", SAE 2005 – 01 – 3778

[23] Turns, S. R., "An introduction to combustion", Mc. Graw – Hill, 2000

[24] Miller, J. A., Bowman, C. T., "Mechanism and modelling of nitrogen chemistry in combustion", Pogr. Energy Combust. Sci., vol. 15 pp. 287 – 338, Pergamon Press, 1989

[25] Montgomery, D. C., "Design and analysis of experiments", John Wiley & Sons, 2001

[26] www.tps.se

[27] Spadaccini, L. J., Colket, M. B., "Ignition delay characteristics of methane fuels", Progress in energy and combustion science 1994, 20 : 431 – 60

[28] www.power-technology.com

[29] Zabetakis, M. G., "Flammability characteristics of combustibles gases and vapours", bulletin 627, Bureau of Mines, USA, 1965

[30] Chomiak, J., Longwell, J. P. and Sarofim, A. F., "Combustion of low calorific value gases, problems and prospects", Progress in Energy Combustion Science, 15, 109 – 129

[31] Dapporto, P., Spinicci, R., "Chimica", Edizioni Cusl Firenze, 1993

APPENDIX 3

Available online at www.sciencedirect.com
ScienceDirect
Proceedings of the Combustion Institute 31 (2007) 77–98
Proceedings of the Combustion Institute
www.elsevier.com/locate/proci

Hidden interactions—Trace species governing combustion and emissions

Peter Glarborg *

Department of Chemical Engineering, Technical University of Denmark, DK-2800 Kgs. Lyngby, Denmark

Available online at www.sciencedirect.com
ScienceDirect
Proceedings of the Combustion Institute 31 (2007) 77–98
Proceedings of the Combustion Institute
www.elsevier.com/locate/proci

Hidden interactions—Trace species governing combustion and emissions

Peter Glarborg *

Department of Chemical Engineering, Technical University of Denmark, DK-2800 Kgs. Lyngby, Denmark

Abstract

Concern about pollutant formation and emissions continues to be a driving force for research in combustion chemistry. Important pollutants include nitrogen oxides (NO_x), sulfur oxides (SO_x), chlorine species, unburned or partly burned fuel components (e.g., UHC, aldehydes, CO), aromatic and polycyclic aromatic compounds, and aerosols (soot, alkaline aerosols). In this review, it is discussed how N, S, Cl, and K/Na species, typically present in small quantities, may affect the overall combustion process, as well as the formation or transformation of each other. Of special interest is their ability to sensitize or inhibit oxidation of fuel and CO, depending on the reaction conditions; the impact of S, Cl and K/Na on formation of NO_x, PAH, and soot; and the interaction of sulfur, chlorine and alkali species, which may have significant implications for emissions of SO_2, HCl, and aerosols.

Keywords: Pollutants; Nitrogen oxides; Sulfur oxides; Chlorine; Alkali metals; PAH; Soot; Inhibition; Sensitization; Kinetics

1. Introduction

More than 20 years ago, Arthur Levy concluded in his plenary at the 19th International Symposium on Combustion [1] that "Combustion–pollutant technology is probably on its firmest grounds in the area of SO_x, on slightly less firm ground in the area of NO_x control, and has furthest to go on soot control". In the years passed since then our understanding of combustion and pollutant formation has increased considerably and some combustion technologies may now be considered mature. However, despite the progress made, the situation regarding pollutant control is pretty much the same as that outlined by Levy. Concern about pollutant formation and emissions continues to be a driving force for research in combustion chemistry [2]. There are still unresolved issues in nitrogen and sulfur chemistry, and the chemistry of PAH and soot has evolved as the major research area in pollutant formation [3,4].

Pollutant species from combustion may be formed from fuel/oxidizer interactions or they may derive from fuel impurities. Gaseous fuels are typically quite clean. Natural gas from most fields consists almost entirely of hydrocarbons, with very low levels of sulfur, alkali metals, and heavy metals (Hg and As). In gas combustion, emissions may be a result of incomplete combustion. Pollutants belonging to this category include carbon monoxide (CO), aldehydes, unburned hydrocarbons (UHC), polycyclic aromatic hydrocarbons (PAH), and soot. Nitrogen oxides (NO,

* Fax: +45 4588 2258.
E-mail address: pgl@kt.dtu.dk

1540-7489/$ - see front matter © 2006 The Combustion Institute. Published by Elsevier Inc. All rights reserved.
doi:10.1016/j.proci.2006.08.119

NO_2) may be formed by oxidation of molecular nitrogen (N_2) from the combustion air. It is common to these pollutants that they may be abated by modifying the combustion process. Unfortunately, conditions favorable to complete combustion, that is rapid mixing between fuel and oxidizer, excess oxygen, and high temperatures, tend to promote the formation of nitrogen oxides, while attempts to control NO_x through delayed mixing and lower temperatures often result in problems with incomplete fuel oxidation.

Solid and liquid fuels typically contain impurities that may give rise to pollutant emissions. Table 1 shows typical levels of N, S, Cl and K/Na for selected fuels. The fuel N may be oxidized to NO or to N_2, depending on combustion conditions. Sulfur oxides, formed from fuel-bound sulfur during oxidation, are typically unaffected by combustion conditions and need to be controlled by secondary measures. Also chlorine is difficult to control by primary measures; during combustion it will largely be oxidized and emitted as hydrogen chloride (HCl). However, chlorine may also participate in the formation of polychlorinated dibenzo-*p*-dioxins and dibenzofurans (PCDD/Fs). Volatile trace metals include alkali metals, which may react with chlorine or sulfur and give rise to aerosol formation and/or cause operational problems, such as deposit formation.

Since the pollutant species are typically present in fairly small concentrations compared to the major reactants, it is often assumed in combustion modeling and analysis that they do not affect the overall combustion process—or the formation or transformation of each other. One exception to this rule is soot. Since this aerosol strongly emits radiation it is known to be important to the heat transfer from many flames and thus the overall combustion process.

In this review, it is discussed how these trace species may affect the overall combustion process as well as the fate of each other. This topic has a number of practical implications. In some cases, pollutant interactions are responsible for phenomena which are otherwise difficult to explain. Examples include the importance of the nitric oxide concentration to emissions of UHC from natural gas fired engines [14] and the interaction between sulfur, chlorine and potassium in biomass combustion [15]. It is also of interest to what extent control of one pollutant species, e.g., by fuel pretreatment, affects emissions of other pollutants. For instance, both the content of sulfur [16] and chlorine [17] in a fuel may have an impact on NO_x-emissions, and the formation of PAH and soot may be influenced by a range of trace species and additives [18,19]. In addition, sulfur and/or chlorine may affect the partitioning of trace metals such as Cd, Cu, Mn, Zn, Cr, As, Hg, and lead salts [20,21].

With the increased emphasis on fuel flexibility and fuel mixing, new combinations of trace species and pollutants may become relevant. This opens up novel possibilities of pollution control, taking advantage of the way pollutants interact. It is of interest to what extent the presence of a specific pollutant species can be used actively for control of other pollutants in a combustion process. A recent example is the use of sulfur additives to improve the operation and control the emissions in biomass-fired combustion units [22]. These examples, as well as others, will be discussed in the present paper, with the emphasis on the effect of trace species on fuel burnout, NO formation, and aerosol formation.

2. Pollutant formation mechanisms

In order to understand how the various pollutant species affect the fuel oxidation and each other, it is instructive to discuss briefly their formation mechanisms. In the following, the mechanisms of formation and transformation of selected pollutants are outlined. More thorough treatments have been published on the combustion chemistry of nitrogen [2,13,23,24], sulfur [5,25–27], chlorine [28–32], alkali metals [33–36], and PAH/soot [4,37–47].

Table 1
Fuel impurities (% weight from the ultimate analysis) in selected liquid and solid fuels [5–13]

Fuel	N	S	Cl	K + Na
Fuel oil	0.2–0.9	0.1–4.5	<0.1	⩽0.1
Straw	0.3–1.5	0.10–0.24	0.1–1.7	0.2–1.9
Other annual biomass	0.1–3.5	0.03–0.6	0.01–0.6	0.05–3.0
Wood	0.03–1.0	<0.10	<0.10	0.05–0.4
Coal	0.5–2.5	0.3–4.3	0.01–0.10	0.05–0.20
Plastics	0.00–0.01	0.0	0.0; 50	0.0–0.1
Paper	0.1–0.2	0.05–0.3	0.03–0.40	0.0–0.1
Residential solid waste	0.2–1.0	0.1–0.4	0.1–0.9	0.02–0.08

Plastics such as HDPE and LDPE contain no chlorine while PVC typically contains about 50%.

2.1. Formation of nitrogen oxides

Several separate mechanisms have been identified that can lead to formation of nitrogen oxides in significant quantities. These mechanisms involve either fixation of the molecular nitrogen contained in the combustion air or oxidation of organic nitrogen chemically bound in the fuel.

Fixation of N_2 in the combustion air involves the attack of very reactive radicals on the triple bond in molecular nitrogen. In the thermal NO mechanism, N_2 reacts with atomic oxygen [23,48],

$$O + N_2 \rightleftharpoons NO + N \quad (N1)$$

This reaction is followed by oxidation of the atomic nitrogen,

$$N + O_2 \rightleftharpoons NO + O \quad (N2)$$

$$N + OH \rightleftharpoons NO + H \quad (N3)$$

The thermal mechanism requires temperatures above 1800 K and excess oxygen to be efficient, and it occurs primarily in the post-flame zone where the residence time at high temperatures may be considerable. Prompt NO formation is initiated by attack of CH_i-radicals on N_2 forming cyanide species [49,50]. The most important initiation step is [4,23,51,52]

$$CH + N_2 \rightleftharpoons NCN + H \quad (N4)$$

This reaction takes place in the flame zone where CH may be formed in significant quantities from hydrocarbon fuels. The probable product of the $CH + N_2$ reaction, NCN, is subsequently converted mostly to atomic nitrogen through a sequence of steps involving cyanide, oxicyanide and amine radicals (Fig. 1). The nitrogen atoms may be oxidized to NO by reaction with OH (N3) or converted back to N_2 by reaction with NO (N1b). Here, (N1b) is the reverse reaction of (N1). Prompt NO is less sensitive to temperature and reaction time than thermal NO; it is most important under stoichiometric or slightly fuel-rich conditions.

Less important reaction paths to NO from atmospheric nitrogen are initiated by recombination of N_2 with atomic oxygen, $O + N_2(+M) \rightleftharpoons N_2O(+M)$ (N5) [53], or hydrogen, $H + N_2(+M) \rightleftharpoons NNH(+M)$ (N6) [54], followed by oxidation of the nitrogen intermediate to NO. The N_2O scheme may be important at high pressure and moderate temperatures, such as in gas turbines, while the NNH mechanism seems to be most important in diffusion flames where NNH may form on the fuel-rich side of the flame sheet and then react with O inside the flame sheet [55].

Oxidation of fuel-bound nitrogen is the principal source of NO_x in combustion of most solid fuels. The mechanism of fuel NO formation is more complex than the other NO formation pathways and it is still under investigation [13]. For solid fuels, the fuel N is distributed between the volatiles and the solid char matrix with the apportionment determined in part by the thermal exposure. The volatile N may be released as tarry compounds, which at high temperatures decay rapidly to hydrogen cyanide, or as amines [13]. Cyanides and amines are then oxidized to NO or N_2 through pathways that are presumably similar to that of prompt NO formation (Fig. 1). The remaining char N undergoes heterogeneous oxidation to NO or it may at high temperatures evolve as light components such as HCN. Nitric oxide, once formed, may be recycled by hydrocarbon radicals to cyanide or reduced to N_2 by surface reactions on char or soot.

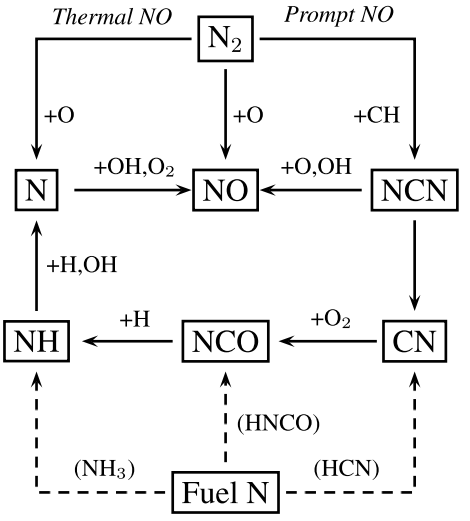

Fig. 1. Simplified reaction path diagram illustrating the major steps in the formation of thermal NO, prompt NO, and fuel NO. Recycling of NO to N_2 through reaction with atomic nitrogen or to cyanides through reaction with hydrocarbon radicals is not shown.

At high temperatures the NO yield depends strongly on the fuel N concentration and the stoichiometry, while the speciation of the gas phase nitrogen compounds has no significant effect [13]. Under these conditions, the fuel N is rapidly converted to NH or N, and the subsequent reactions of these radicals determine the selectivity for forming NO or N_2. At lower temperatures or under very fuel-rich conditions a number of alternative reaction pathways for the reactive nitrogen species open up, and both the overall reaction rate and product N speciation may vary between HCN, NH_3 and HNCO [23,56–61]. Fuel NO formation is most efficiently abated by staging the combustion process, securing a fuel-rich region that promotes conversion of reactive nitrogen species to N_2.

2.2. Sulfur transformations

Most fossil fuels, as well as biofuels and household waste, contain sulfur. The sulfur is largely released to the gas phase during combustion, either as simple species such as H_2S or complex organic compounds. Following release, the gaseous sulfur is oxidized rapidly to sulfur oxides, mainly sulfur dioxide (SO_2) [5,25,26]. Reduced sulfur species such as H_2S and S_2 are stable only under very oxygen deficient conditions. Sulfur oxides are thermodynamically favored and even under reducing conditions most of the gas phase sulfur may be present as SO_2.

A minor part of the SO_2 may be oxidized further to SO_3 [5,25,26]. This is undesirable in the combustion process, since the presence of SO_3 enhances corrosion problems and increases the probability of aerosol emissions [62]. While the gas phase chemistry important to the SO_3/SO_2 ratio is fairly well understood, heterogeneous reactions that may contribute to SO_2 oxidation in solid fuel combustion systems are not fully established [25,63]. Sulfur trioxide is thermodynamically favored at lower temperatures, but kinetic limitations and/or high gas cooling rates often prevent an SO_3/SO_2 partial equilibrium from being attained. Under oxidizing conditions, O and OH are the main chain carriers. Sulfur trioxide may be formed directly from recombination of SO_2 with O,

$$SO_2 + O(+M) \rightleftharpoons SO_3(+M) \quad (S1)$$

or from the reaction sequence

$$SO_2 + OH(+M) \rightleftharpoons HOSO_2(+M) \quad (S2)$$

$$HOSO_2 + O_2 \rightleftharpoons SO_3 + HO_2 \quad (S3)$$

Reaction (S1) is the main source of SO_3 at higher temperatures [64,65]. The (S2), (S3) reaction sequence is believed to contribute to formation of SO_3 only during cooling of the flue gas from combustion. $HOSO_2$ is thermally unstable above 1000 K [66].

In most combustion systems the fuel S will largely be emitted as sulfur oxides, but recent results show that under favorable conditions the sulfur may be recaptured by reaction with the char, forming strong bonds to inorganic elements [67]. Part of the sulfur may also react with trace metals from the fuel, forming metal sulfates. Depending on the nature of the metal, these sulfates may form part of the ash structure, form deposits, or be emitted as aerosols.

2.3. Chlorine transformations

Different types of waste, as well as coal and biomass, may contain chlorine in significant quantities. Chlorine is typically released during pyrolysis as chlorinated hydrocarbons (e.g., chloromethane, CH_3Cl), hydrogen chloride (HCl) or alkali chloride (mainly KCl). During combustion the chlorine will largely be oxidized and emitted as HCl. Hydrogen chloride is typically the desired chlorine containing product in combustion, because it can easily be removed from the flue gas by a scrubbing process. However, chlorine may also participate in dioxin/furan formation through mechanisms that may involve high-temperature gas phase reactions as well as low-temperature reactions catalyzed by fly ash [68], or it may react with alkali metals and form aerosols and/or deposits [15].

2.4. Alkali metal transformations

Most solid fuels contain alkali metals in minor quantities (Table 1). During combustion, a portion of the alkali metals is released to the vapor phase, where it remains until condensing in the cooler convective regions of the boiler. Sodium is the most important alkali metal released from coal [69] while biomasses such as wood and annual crops mainly release potassium [70,71]. Chlorine in the fuel has been shown to facilitate alkali release as alkali chlorides during combustion [8,70,72]. Once released, the alkali chlorides may be partially converted to alkali hydroxide or alkali sulfates [36]. During cooling the alkali components will condense, contributing to aerosol formation and/or cause operational problems, such as deposit formation [15,73]. The fate of the alkali will depend on interactions with the sulfur and chlorine species of the gas. These are described in more detail below.

2.5. Formation of aromatic compounds and soot

The chemistry of aromatic compounds and soot, which are formed to some extent in most combustion processes, has been studied extensively [4,37–47,74–82]. Soot formation is a complicated multi-step process. The important steps in soot formation from gas phase hydrocarbons involve formation of the first ring, formation of polycyclic aromatic hydrocarbons (PAH), soot inception, and subsequently soot growth. The formation of the first aromatic ring is believed to be the rate controlling step in the PAH formation. This ring must be formed by combination of smaller hydrocarbon fragments. For fuels already containing a five or six membered ring structure, the formation of the second ring is rate limiting, and so on. In combustion of liquid and solid fuels, soot may be formed directly from cracking of the fuel itself or from fuel derivatives such as tar.

The mechanism of formation of the initial benzene molecule in combustion of hydrocarbons depends on both the fuel and the reaction conditions. Two classes of ring-forming reactions have been proposed. The first class [40] involves

addition of acetylene to a C_4 vinyl radical, with subsequent cyclization. This may take place by the reactions

$$HCCHCCH + C_2H_2 \rightleftharpoons C_6H_5 \quad (P1)$$

$$CH_2CHCHCH + C_2H_2 \rightleftharpoons C_6H_6 + H \quad (P2)$$

In these reactions, one reactant (C_2H_2) is a major product of fuel-rich combustion, and the adduct does not require intramolecular rearrangements prior to cyclization. However, both HCCHCCH and $CH_2CHCHCH$ have more stable isomers (H_2CCCCH and CH_2CHCCH_2, respectively) into which they can readily be converted [45]. For this reason, the availability of the C_4 radicals in reactions (P1) and (P2) is limited and under most conditions these reactions are thought to be of secondary importance.

The second class of ring-forming reactions [39,45] is a combination of resonantly stabilized free radicals, with subsequent rearrangement and ring formation. The most important steps are believed to be recombination of two propargyl radicals,

$$C_3H_3 + C_3H_3 \rightleftharpoons C_6H_5 + H \quad (P3)$$

or of a propargyl and an allyl radical,

$$C_3H_3 + C_3H_5 \rightleftharpoons \text{fulvene} + H + H \quad (P4)$$

followed by conversion of fulvene to benzene. The relative importance of these two reactions depends strongly on the fuel. Other pathways may be important to specific fuels. An example is the sequence $C_3H_3 + H \rightarrow C_3H_2 + H_2$ (P5), $C_3H_2 + C_2H_2 \rightarrow C_5H_3 + H$ (P6), $C_5H_3 + CH_3 \rightarrow$ fulvene (P7). This reaction pathway is promoted by high CH_3 concentrations and will be most important in methane flames.

Formation of the second aromatic ring in naphtalene has been thought to involve two subsequent additions of acetylene to a phenyl radical (C_6H_5) or occur directly by recombination of two cyclopentadienyl (C_5H_5) radicals, in both cases followed by hydrogen elimination. However, these pathways have been questioned [78,83], and the mechanism is still in discussion.

3. A kinetic model for pollutant interactions

The gas phase chemistry of combustion, in particular that of pollutant formation and destruction, is quite complex and in general it can only be understood from detailed chemical kinetic modeling. The kinetic models developed and refined over the years represent to a large extent the accumulated knowledge of combustion chemistry. After proper validation the models can be used to analyze and perhaps optimize high-temperature processes, and predictions may even be extrapolated into unknown territory with more confidence than for most other combustion modeling tools.

To elucidate aspects of pollutant interactions, a reaction mechanism was assembled that covers the oxidation of light hydrocarbons, as well as formation and destruction of nitrogen oxides, sulfur oxides, hydrogen chloride and potassium species. The subsets were largely drawn from literature, i.e., C_1–C_3 hydrocarbons [79,81,84,85], nitrogen [60,61,84,86] and fuel/N interactions [84,85,87], sulfur [64,88,89], chlorine and Cl/N interactions [32,36,90,91], and potassium/sodium and their interaction with S and Cl [36]. A preliminary subset for sulfur/nitrogen interactions at high temperatures was established as a part of this work. This subset is discussed in some detail in Appendix A.

4. Effect of trace species on combustion and emissions

The chemistry of hydrocarbon, nitrogen, sulfur, chlorine and alkali species is highly interrelated. The interactions may take place indirectly through effects of N, S, Cl and K/Na on the radical pool or through direct reaction. To understand how species present only in parts per million concentrations can affect the overall fuel oxidation rate, it is instructive to look at the generation of chain carriers. In order for a flame to propagate, a net increase in radicals is required. This comes about through chain branching reactions such as $H + O_2 \rightarrow O + OH$. Under some conditions a small shift in importance between the chain branching and the chain terminating steps may cause a dramatic change in the oxidation rate of the fuel. Glassman [92] shows how, in an idealized system, an increase in the net radical formation from 0 to 1 radical in 100 reactions reduces the reactant consumption time from 30 years to 10 ms! If a reaction system is close to an explosion limit, species present in trace amounts may cause a shift the system between the slow and the fast reaction regime.

Trace species may enhance oxidation by the simple sequence A:

$$T + XY \rightarrow TX + Y \quad (A1)$$

$$TX(+M) \rightarrow T + X(+M) \quad (A2)$$

Here, T is the trace species, and X and Y may be H, O, or OH. We note that two radicals are gained ($XY \rightarrow X + Y$) in each cycle, i.e., the sequence is chain-branching. Furthermore, since T is regenerated, the sequence is catalytic. Obviously, if trace species participate in catalytic cycles, their impact on the overall reaction may be strongly enhanced.

If the reactions in cycle A are reversed,

$$T + X(+M) \rightarrow TX(+M) \quad (A2b)$$

$$TX + Y \rightarrow T + XY \quad \text{(A1b)}$$

the result is an efficient terminating cycle (A′), since there is a net loss of two radicals. The relative importance of sequences A and A′ depends on the reactivity of the trace species and the reaction conditions.

An alternative catalytic cycle involves a chain-propagating sequence. A propagating sequence may have a significant impact on the fuel oxidation rate if it converts less reactive radicals, such as peroxides, to more active chain carriers. Presence of trace species such as NO offers a fast pathway for the peroxide radical (RO_2) to a more reactive radical (RO),

$$T + RO_2 \rightarrow TO + RO \quad \text{(B1)}$$

Subsequently TO may be recycled to T, completing the cycle,

$$TO + R \rightarrow T + RO \quad \text{(B2)}$$

This sequence, B, corresponds to the net reaction $RO_2 + R \rightarrow RO + RO$. Even though it preserves the number of chain carriers, it may strongly sensitize fuel consumption, as shown below. With nitric oxide as the trace species, reaction (B1) is fast and in effect selective; peroxide radicals typically have a low reactivity towards other stable species than NO.

Selective reactions are also pivotal in trace species interactions. To be competitive, direct reactions between trace species have to be considerably faster than reactions of the trace species with components in larger concentrations. A well-known example of a selective reaction between trace species is the thermal $DeNO_x$ process [60,93] where amine radicals, upon injection of NH_3 into the flue gas, react selectively with nitric oxide in a certain temperature range. Trace species interactions in combustion, for instance N/S or K/S/Cl, are generally important only to the extent they are selective.

4.1. Sensitization and inhibition of fuel oxidation

All the pollutants addressed in this review are known to affect fuel oxidation under certain conditions. It seems that both nitrogen oxides, sulfur oxides, chlorine species, and alkali metals have the ability to either promote or inhibit reaction, depending on the reaction conditions. In this section these interactions are discussed in some detail, emphasizing burnout of CO. The impact of soot on the combustion process is addressed elsewhere [37,41].

4.1.1. Effect of nitrogen oxides on fuel oxidation

The presence of even small amounts of nitrogen oxides can have a significant impact on fuel oxidation characteristics [94]. This interaction has been investigated for a wide range of fuels, including H_2 [95,96], CO [87,91,96,97], CH_2O [95,98], CH_4 [85,95,96,99–102], C_2 hydrocarbons [96,100,103–105], higher hydrocarbons [96,100, 106–109], and oxygenated hydrocarbons like CH_3OH [110–113] and DME [114,115]. The sensitization takes place through a type B mechanism. Oxidation of moist CO is promoted mainly through the reaction [87,91]

$$NO + HO_2 \rightleftharpoons NO_2 + OH \quad \text{(N5)}$$

This reaction corresponds to the first step in the B cycle; it converts the relatively unreactive HO_2 radical to OH. By oxidizing NO to NO_2, (N5) is also important to the NO/NO_2 ratio in the flue gas [96,100].

In larger concentrations or under reducing conditions NO may act to inhibit the oxidation process through a type A′ sequence,

$$X + NO + M \rightarrow XNO + M$$

$$Y + XNO \rightarrow XY + NO$$

This cycle is responsible for the catalytic effect of NO on the recombination of hydrogen atoms in flames [116,117] as well as the delay in the oxidation of CO under reactor conditions [87,91,97,118].

Figure 2 (top) shows the predicted influence of nitric oxide on CO oxidation under conditions typical of the burnout region in stationary combustion systems. The CO oxidation rate is here characterized by the half-life $t_{1/2}$ of CO, i.e., the time it takes to consume 50% of the CO. The lower the value of $t_{1/2}$, the more rapid is the CO oxidation. The results indicate that moist CO oxidation in a flue gas with 5% O_2 shifts from a rapid to a slow reaction as the temperature drops below 1050 K. The presence of NO in concentrations from 50 to 1000 ppm strongly enhances the CO oxidation rate below this temperature and extends the fast oxidation regime by about 100 K to lower temperatures. At high NO concentrations (1000 ppm) the sensitization becomes slightly less efficient due to type A′ cycles involving NO_2 and HONO.

In the presence of hydrocarbons, sensitization involving nitrogen oxides may be even more pronounced. Contrary to other trace species, even fairly small amounts of NO_x can dramatically enhance the oxidation rate for hydrocarbons [94]. Figure 3 shows results from flow reactor experiments on NO sensitized oxidation of methane [85]. In the absence of NO_x, temperatures of about 1100 K are required to initiate rapid oxidation of CH_4 [85], but in the presence of NO, reaction occurs at temperatures as low as 850 K. The results indicate a low temperature region (900–1000 K) with partial oxidation of methane, an intermediate temperature regime with little reaction (1000–1150 K), and a high temperature regime (>1150 K) with complete oxidation.

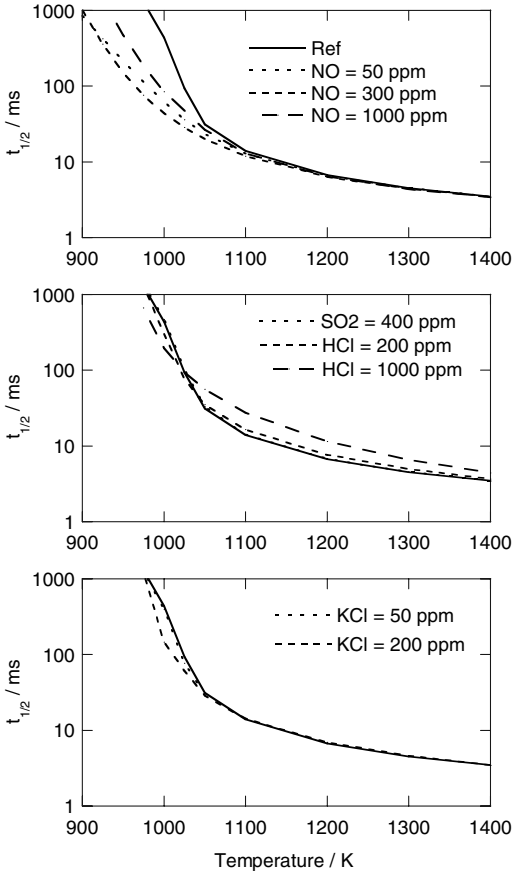

Fig. 2. Predicted times for 50% CO oxidation ($t_{1/2}$) at atmospheric pressure as a function of temperature and flue gas composition. Inlet composition: CO = 1000 ppm, $O_2 = 5\%$, $CO_2 = 15\%$, $H_2O = 8\%$; varying amounts of NO (0, 50, 300, 1000 ppm), SO_2 (0, 400 ppm), HCl (0, 200, 1000 ppm) and KCl (0, 50, 200 ppm) (balance N_2).

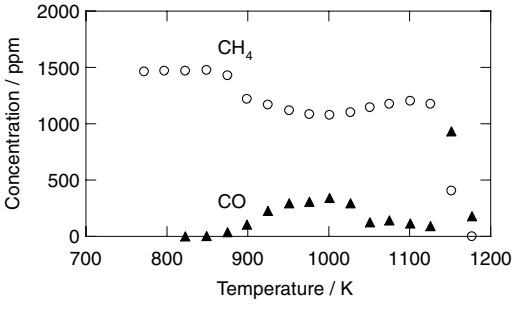

Fig. 3. Flow reactor results for lean oxidation of methane in the presence of nitric oxide [85]. Inlet composition: 1480 ppm CH_4, 2.7% O_2, 6.1% H_2O, 186 ppm NO, balance N_2. The residence time is about 170 ms at 1000 K.

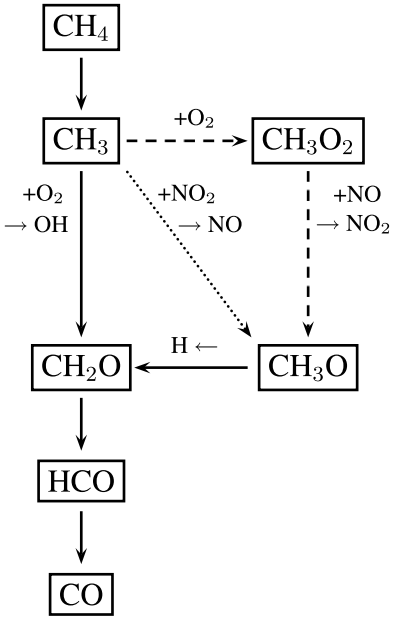

Fig. 4. Reaction paths in the sensitization of methane oxidation by NO and NO_2 [85,99].

The sensitizing mechanism involves hydrocarbon peroxides [85,99], for methane the methyl peroxide radical CH_3O_2 (Fig. 4),

$$CH_3O_2 + NO \rightleftharpoons CH_3O + NO_2 \quad (N6)$$

$$CH_3 + NO_2 \rightleftharpoons CH_3O + NO \quad (N7)$$

These reactions correspond to reactions (B1) and (B2) in sequence B. Similar mechanisms are active for higher hydrocarbons [94]. Reaction (N8) competes favorably with other CH_3O_2 consumption reactions and offers a fast pathway to the methoxy radical, which subsequently dissociates to yield atomic hydrogen. As the temperature increases the propagating reaction $CH_3 + O_2 \rightleftharpoons CH_2O + OH$ competes with formation of CH_3O_2, resulting in a negative temperature coefficient region similar to that often observed in practical systems [119]. At high temperatures CH_3O_2 is no longer thermally stable, but chain branching steps such as $H + O_2 \rightleftharpoons O + OH$ secure sufficient generation of radicals for oxidation.

Figure 5 shows results for the UHC emission (mainly CH_4) from a natural gas lean–burn test engine [14]. Levels of NO_x above 100 ppm are seen to promote strongly the extent of UHC oxidation. The extent of UHC oxidation in the exhaust system of a practical engine would be expected to be smaller due to a higher cooling rate. However, reactions promoted by NO_x could conceivably enhance the emission of other harmful components such as CO and aldehydes [120].

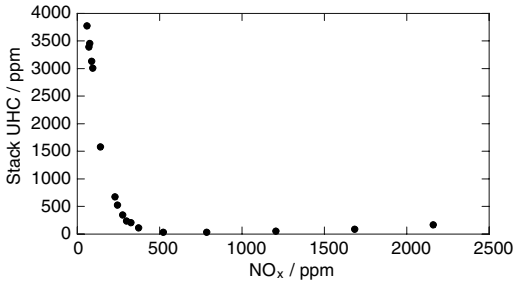

Fig. 5. Stack concentrations of UHC as a function of NO_x in the exhaust of a lean-burn natural gas fired engine equipped with an insulated exhaust reactor to enhance the post-cylinder residence time and temperature [14]. The NO_x level was increased by adding NO to the natural gas. The O_2 level was about 8% and the reactor residence time about 0.2 s.

4.1.2. Effect of sulfur oxides on fuel oxidation

In combustion, fuel sulfur is rapidly oxidized to sulfur oxides, mainly SO_2. Sulfur dioxide may subsequently affect the combustion and fuel burnout by interacting with the O/H radical. The presence of SO_2 may have a significant impact on flame behavior and explosion limits [25,121–128] and is known to inhibit CO burnout under fluidized bed combustion conditions [129–132]. Under fuel lean conditions, SO_2 catalyzes the recombination of the main chain carriers by a simple A′ cycle involving SO_3,

$$SO_2 + O(+M) \rightleftharpoons SO_3(+M) \quad (S1)$$

$$SO_3 + O \rightleftharpoons SO_2 + O_2 \quad (S4)$$

This sequence is active during CO oxidation in the burnout zone. According to the modeling predictions in Fig. 2 (middle part) the influence of 400 ppm SO_2 on CO oxidation is small, however. Under stoichiometric and reducing conditions the impact of SO_2 on the radical pool is more pronounced. Recent results [89] indicate that this interaction is more complex than a simple A′ cycle with HOSO. Rather, the inhibiting mechanism appears to involve a number of interrelated, extended A′ cycles (Fig. 6). The rate limiting step is still a type (A2b) reaction,

$$SO_2 + H(+M) \rightleftharpoons HOSO(+M) \quad (S5)$$

but since the reaction $HOSO + H \rightarrow SO_2 + H_2$ (type (A1b)) is probably insignificant [89], the recycling back to SO_2 involves two steps rather than a single reaction, e.g.,

$$HOSO + H \rightleftharpoons SO + H_2O \quad (S6)$$

$$SO + O_2 \rightleftharpoons SO_2 + O \quad (S7)$$

This sequence is propagating rather than terminating and thus the removal of chain carriers becomes less efficient. At high temperatures, such as in flames, also cycles based on SO may be important, e.g.,

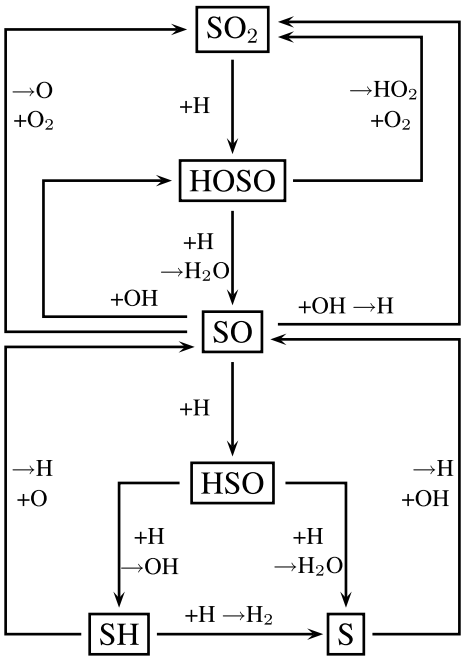

Fig. 6. Interaction of SO_2 with the radical pool under stoichiometric to fuel-rich conditions [89].

$$SO + H(+M) \rightleftharpoons HSO(+M) \quad (S8)$$

$$HSO + H \rightleftharpoons S + H_2O \quad (S9)$$

$$S + OH \rightleftharpoons SO + H \quad (S10)$$

Even though the effect of SO_2 on oxidation of H_2 and moist CO can be predicted quite well over a wide range of conditions [89], the interaction of sulfur with the fuel oxidation is not completely understood. Recent results from natural gas combustion in turbulent diffusion flames [133] and from wood combustion on a grate and in FBC [22] indicate that for low-sulfur fuels addition of sulfur in small amounts may enhance the CO burnout. Figure 7 shows the effect of addition of 0–100 ppm SO_2 on the exit CO concentration in natural gas oxidation in a bench-scale swirl-stabilized burner under slightly substoichiometric conditions [133]. Small amounts of SO_2 are seen to cause a dramatic decrease in the CO emission. These results are not consistent with the model predictions discussed above. The sensitizing mechanism apparently occurs on the fuel side of the flame sheet and may involve sulfur/soot interactions, but it is not known at this point. The results from wood combustion obtained under excess air burnout conditions [22] seem to involve another sensitizing mechanism, which is also yet to be explained. It has been reported that sulfur, present

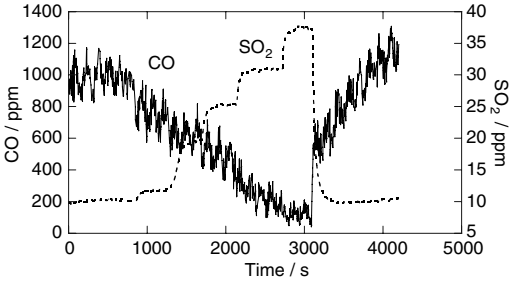

Fig. 7. Effect of addition of small amounts of SO_2 on emissions of CO from slightly substoichiometric combustion of natural gas in a 26 kW bench-scale swirl-stabilized diffusion flame [133].

in petroleum-derived fuels, promotes engine knock and decreases the antiknock effectiveness of lead alkyls [134]. The influence of sulfur compounds depends markedly on the nature of the hydrocarbon fuel and in particular its pre-flame reactions. The mechanism is not known in detail, but it may involve attack of sulfur-containing radicals on the hydrocarbon fuel [134].

4.1.3. Effect of chlorine species on fuel oxidation

A high chlorine content in a fuel may act to inhibit ignition [135], lower flame speeds [30], and facilitate flame quenching [136]. The presence of HCl or chlorinated hydrocarbons is also known to inhibit oxidation of CO to CO_2 under reactor conditions [31,90,91,137–139] and in fuel lean pulverized coal flames [140].

The interaction of HCl with the O/H radical pool is quite complex, and even though the overall mechanism of inhibition is known [90], details are still under investigation. Presumably, the inhibition takes place through simple A′ cycles, initiated by type (A2b) reactions such as

$$HCl + H \rightleftharpoons Cl + H_2 \quad (Cl1)$$

$$HCl + OH \rightleftharpoons Cl + H_2O \quad (Cl2)$$

and completed by a type (A1b) step such as

$$Cl + H + M \rightleftharpoons HCl + M \quad (Cl3)$$

or the terminating reaction

$$Cl + HO_2 \rightleftharpoons HCl + O_2 \quad (Cl4)$$

As the Cl atom concentration builds up in the post-flame region, reactions (Cl1) and (Cl2) may become partially equilibrated and even driven in the reverse direction. Under these conditions inhibition is significantly reduced [90]. The inhibiting cycles compete with a type B chain propagating cycle [141],

$$Cl + HO_2 \rightleftharpoons ClO + OH \quad (Cl5)$$

$$ClO + CO \rightleftharpoons Cl + CO_2 \quad (Cl6)$$

which corresponds to the overall reaction $CO + HO_2 \rightarrow CO_2 + OH$. The competition between the A′ and B cycles determines whether the chlorine has an overall promoting or inhibiting effect on the fuel oxidation. It is very sensitive to the branching ratio of the $Cl + HO_2$ reaction, which is well established only at low temperatures [142].

Figure 2 (middle part) shows the predicted impact of HCl (200 and 1000 ppm) on CO oxidation under burnout conditions. The results indicate a small inhibiting effect of HCl, increasing with [HCl], in the fast oxidation regime above 1050 K. However, in the transition to the slow oxidation regime around 1000 K, the presence of HCl slightly enhances the oxidation rate. Under these conditions the impact of HCl on the CO oxidation rate is determined mainly by the competition between the chain terminating step (Cl4) and the chain propagating sequence (Cl5) and (Cl6).

4.1.4. Effect of alkali metals on fuel oxidation

Similar to the other trace species, alkali metals may act as sensitizers or inhibitors, depending on the reaction conditions. Alkali-containing additives have been known for a long time as inhibitors for flame propagation [143], and the ability of alkali metals to catalyze radical removal is well documented by data from laminar premixed flames [33,144–156], laminar diffusion flames [157,158], turbulent diffusion flames [159], and flow reactor experiments [160]. However, under other conditions addition of alkali metals may serve to promote reaction [34,35,161–164].

Even though also heterogeneous effects have been proposed, the inhibiting effect of alkali metals is attributed mostly to gas phase radical removal reactions. The mechanism of inhibition is still in discussion, but it is most likely a simple type A′ cycle. Results from flames [148,149,153] and from flow reactors [160] are consistent with the cycle (here for K),

$$K + OH + M \rightleftharpoons KOH + M \quad (K1)$$

$$KOH + H \rightleftharpoons K + H_2O \quad (K2)$$

$$KCl + H \rightleftharpoons K + HCl \quad (K3)$$

In combustion systems alkali chlorides and alkali hydroxides are rapidly equilibrated through the extremely fast reaction [36]

$$KCl + H_2O \rightleftharpoons KOH + HCl \quad (K4)$$

A high rate constant for (K1) is needed in order to explain the observed inhibition; such a value is not confirmed experimentally. A lower rate constant for (K1) would require an additional chain-terminating reaction, perhaps involving KO_2 (or NaO_2) [150],

$$K + O_2 + M \rightleftharpoons KO_2 + M \quad (K5)$$

However, according to the presently accepted thermodynamic properties for KO_2 and NaO_2, it is doubtful if they play an important role under flame conditions [160].

Promotion of reaction by alkali metals occurs through the same reaction sequence as inhibition, but the low radical levels cause the reactions to proceed in the reverse direction, creating a type A cycle

$$KOH + M \rightleftharpoons K + OH + M \quad (K1b)$$

$$K + H_2O \rightleftharpoons KOH + H \quad (K2b)$$

Studies of alkali metal addition to the reburn process [163,164] have shown that atomic Na inhibits the combustion process by reducing H and OH under conditions with high radical concentrations, while it serves to regenerate chain carriers if radical concentrations are low. Alkali metals would be expected to be most efficient in removing radicals under reducing conditions. However, they have been shown to inhibit CO burnout also under excess air conditions [164]. This observation is not explained by the predictions of the present model (Fig. 2, lower part). Here, the impact of KCl (50, 200 ppm) on the CO oxidation rate is seen to be small in the fast reaction regime, while below 1050 K the model predicts that KCl enhances the reaction rate. More work is desirable to clarify the interaction of alkali metals with the radical pool.

4.1.5. Combination effects

Depending on the fuel composition and reaction conditions, combustion processes yield varying amounts of nitrogen and sulfur oxides, hydrogen chlorides and alkali metals. Figure 8 shows how different combinations of these trace species are predicted to affect the half-life of CO at 1000 K in a flue gas corresponding to that of Fig. 2. Under these conditions the half-life of CO in the absence of any trace species (the reference conditions) is more than 0.4 s. Most of the tested gas compositions yield CO oxidation rates that are within a factor of two of the reference value, indicating a minor impact only of the trace species. The presence of HCl with SO_2 and/or KCl causes a modest increase in the CO oxidation rate, while $SO_2 + KCl$, similar to SO_2 alone, slightly inhibits oxidation. The reaction rate increases considerably if NO is present in the flue gas. The presence of NO largely eliminates any effect of SO_2 or KCl under these conditions. The trend that NO off-sets the inhibiting effect of SO_2 is in agreement with reactor experiments on CO and CH_4 oxidation with NO and SO_2 [87,165]. In the absence of chlorine, nitric oxide increases the oxidation rate of CO by an order of magnitude. The presence of both NO and HCl results in an oxidation rate which is faster than that of CO + HCl, but significantly slower than CO + NO. The coupling between NO and HCl in moist CO oxidation is quite complex. At high chlorine levels this coupling may generate a considerable synergistic inhibition of the CO oxidation [91]. The promoting effect of NO is partly off-set in the presence of HCl, because HCl interferes with the type B NO cycle. As discussed previously, oxidation of moist CO is promoted mainly through the reaction $NO + HO_2 \rightleftharpoons NO_2 + OH$ (N7). The competing step $Cl + HO_2 \rightleftharpoons HCl + O_2$ (Cl4) is terminating and thus reduces the sensitizing effect of NO.

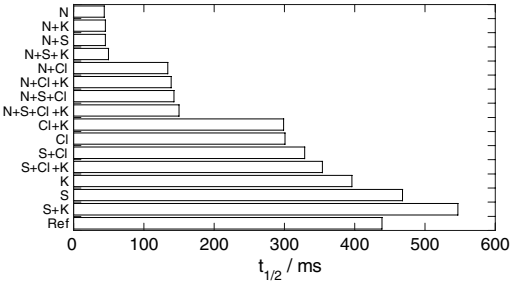

Fig. 8. Predicted half-life of CO at atmospheric pressure and 1000 K as a function of flue gas composition. Inlet composition: CO = 1000 ppm, O_2 = 5%, CO_2 = 15%, H_2O = 8%; varying amounts of NO (0/300 ppm), SO_2 (0/400 ppm), HCl (0/200 ppm) and KCl (0/50 ppm) (balance N_2).

4.2. Effect of trace species on NO_x-formation

4.2.1. S/N interactions

Nitrogen/sulfur chemistry interactions in combustion is a field of major uncertainty [27], as it was twenty years ago [1]. In this section we will use chemical kinetic modeling to assess trends in the sulfur/nitrogen interactions and to identify possible key reactions. Since the S/N subset of the reaction mechanism is quite uncertain (see Appendix A), the calculations are qualitative at best and modeling predictions will be discussed in the context of experimental observations, mainly from flames.

Studies on the effect of sulfur on NO formation from fixation of N_2 in the combustion air have been conducted in hydrocarbon flames [16,166–168]. Results from these flames indicate that addition of sulfur species reduces the exit NO concentration over a range of equivalence ratios from lean to fuel-rich. This observation is in agreement with modeling predictions for NO formation in adiabatic combustion of CH_4/air in a stirred reactor (Fig. 9). According to the model, the effect of the sulfur is mainly to catalyze radical recombination, rather than to react directly with nitrogen species. Both the O/H radical pool and the CH concentration are repressed in the presence of

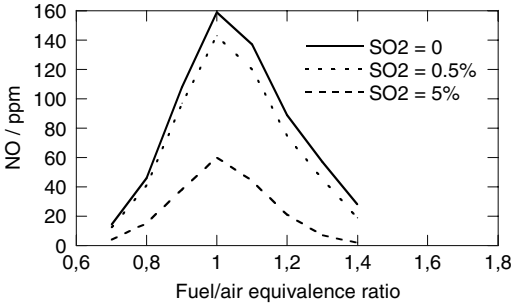

Fig. 9. Predicted effect of SO_2 addition on emissions of NO from combustion of CH_4 in an adiabatic, stirred reactor with a nominal residence time of 5 ms.

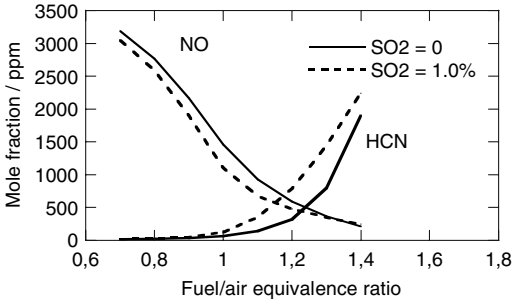

Fig. 10. Predicted effect of SO_2 addition on emissions of NO and HCN from combustion of C_2H_6 doped with 0.6% CH_3CN in a stirred reactor at 1800 K with a nominal residence time of 7 ms.

SO_2, causing a decrease in thermal NO as well as in prompt NO. However, unless large quantities of sulfur are present, the effect is fairly small.

Observations from a very fuel-rich methane flame show that addition of SO_2 causes an increase in the NO formation in the reaction zone, but accelerates the decay of NO in the post-flame zone [16]. Modeling predictions indicate that the promotion of NO in the reaction zone, as well as the enhanced NO consumption downstream, may be caused by the same set of reactions. Under very reducing conditions, the presence of sulfur oxides may promote NO formation by oxidizing atomic nitrogen,

$$N + SO \rightleftharpoons NO + S \quad (S11)$$

$$N + SO_2 \rightleftharpoons NO + SO \quad (S12)$$

Downstream of the reaction zone in the flame, reactions (S10) and (S11) may proceed in the reverse direction and remove NO,

$$NO + S \rightleftharpoons N + SO \quad (S11b)$$

$$NO + SO \rightleftharpoons N + SO_2 \quad (S12b)$$

While reaction (S11) is fairly well established, the importance of reaction (S12) is only a hypothesis at this point. To the author's knowledge there are no measurements of the reaction and it may conceivably have a higher energy barrier than assumed in the present study.

The effect of sulfur on fuel NO formation in premixed flames has been investigated mostly under reducing conditions, both in hydrogen [169,170], moist CO [171] and hydrocarbon [16,169,170,172,173] flames. Exit concentration measurements in combustion of hydrocarbons doped with fuel N indicate that sulfur may result in a decrease [167,168] or a slight increase [174] in NO, while HCN (the main reactive nitrogen component next to NO) is generally increased [174]. The results indicate that the NO yield is the result of a competition between mechanisms that promote NO formation, inhibit NO formation, and reduce NO already formed.

Figure 10 shows modeling predictions for conversion of CH_3CN to NO and HCN in C_2H_4 combustion in a stirred reactor, with and without doping with SO_2. The calculations indicate that, except for very reducing conditions, the presence of sulfur under these conditions causes a slight decrease in [NO], while [HCN] is increased. For HCN the results agree with observations from jet-stirred reactor experiments [174], while for NO the experiments showed a slight promotion by sulfur, contrary to the slight inhibition indicated by the modeling. However, the NO yield results from a delicate balance between competing mechanisms, as discussed below.

The flame results [16,169,170] indicate that, independent of the speciation of the fuel, fuel N, and fuel S, the presence of sulfur acts to increase the formation of NO in the reaction zone of fuel-rich flames. This is in line with the results from fuel-rich flames without fuel N [16], and the modeling predictions indicate that the mechanism is the same, i.e., oxidation of atomic nitrogen by reaction with SO (S11) and SO_2 (S12).

In the post-flame region of the fuel-rich flames, the remaining combustibles largely consist of a CO/H_2 mixture and, apart from temperature effects, the chemistry should be more or less independent of the fuel type. Here, the effect of fuel S is more complex. Modeling predictions indicate that the ability of sulfur to catalyze radical removal under reducing conditions is important in this region. Sulfur dioxide is particularly effective in removing H atoms, primarily through the sequence $SO_2 + H(+M) \rightarrow HOSO(+M)$ (S5), $HOSO + H \rightarrow SO + H_2O$ (S6), $SO + H + M \rightarrow HSO + M$ (S8). By repressing the O/H radical pool, conversion of HCN and NH_3 to N_2 in the post-flame zone is inhibited, as observed experimentally [170,172,174]. Thus, the total emission of fixed nitrogen from these fuel-rich flames increases with the sulfur concentration.

There are indications that the presence of sulfur may enhance the NO consumption rate in

the post-flame zone. This is most pronounced in high-temperature flames [16,171,172]; at lower temperatures this effect was not observed [170]. The flame results were explained in terms of a direct interaction between N, NO, S and SO, resulting in an increase in the steady-state N-atom concentration [171]. This interpretation is supported by the modeling predictions. At high temperatures, radicals like SO, SH and S may be present in significant concentrations and serve to remove NO. According to the present model this takes place mainly through reaction of SO and S with NO, $NO + S \rightarrow N + SO$ (S11b), $NO + SO \rightarrow N + SO_2$ (S12b), while the SH + NO reaction is less important. However, in particular the reactions of SH and SO with NO need to be characterized better before the mechanism of NO removal can be identified.

The work on premixed gas flames has served to increase our understanding of sulfur–nitrogen chemistry, but since gaseous fuels contain little or no sulfur, the S/N interactions in combustion of liquid and solid fuels are of more practical concern. Sulfur–nitrogen interactions have been studied in oil flames [175–177], pulverized coal flames [141,178] and in fluidized bed combustion [129,132,179–181]. Results from these systems indicate that the S–N interactions take place mostly in the gas phase subsequent to the release of volatile sulfur and nitrogen species from the parent fuel. In fluidized bed combustion, the presence of SO_2 has been reported to inhibit the oxidation of HCN and NH_3 to NO [130,132,179–181]. This can partly be explained by the fact that sulfated limestone is less active than limestone in catalyzing oxidation of NH_3 to NO in FBC combustion [132,179]. However, flow reactor experiments [129,131,132] show that also the catalyzed radical recombination by SO_2 serves to inhibit HCN consumption and increase the selectivity of HCN oxidation to N_2O rather than NO.

4.2.2. Cl/N interactions

Studies of the interaction between chlorine and fuel N oxidation are limited. Results from combustion of a C_2H_4/CH_3NH_2 mixture in a jet-stirred reactor [182] and from combustion of coal in CFBC [183] and in fuel lean pulverized fuel flames [140,141] indicate that chlorine causes a decrease in NO formation, while it does not affect NO formation in a staged pulverized coal flame [141]. Kinetic analysis of the pulverized coal data [141] indicates that it is an effect of radical removal by the chlorine species, rather than a direct interaction with nitrogen compounds. Oxidation of HCN to NO in the post-flame region is inhibited, similarly to what has been observed in sulfur-doped flames. An observed increase in the CO emission [140] supports this interpretation.

4.2.3. Alkali/N interactions

Information on the effect of alkali metals on NO formation is scarce. However, it has been reported [164] that addition of K or Na compounds serves to reduce NO formation when burning natural gas in a pilot-scale burner. The effect is attributed to radical removal by the alkali metals, resulting in inhibition of the NO formation mechanisms, rather than a direct interaction between K/Na and N-species.

Alkali metals have been proposed as additives in in-furnace NO_x control techniques such as selective non-catalytic reduction (SNCR) with isocyanuric acid [34] and reburning [35,161–164,184]. The observation that alkali metals enhance reaction under conditions with low radical levels indicates that they may be useful as additives for reburning and advanced reburning processes [163,164], and it is possible that they enhance the efficiency of staged combustion for alkali-containing fuels such as biomass.

4.3. Effect of trace species on sulfur and chlorine transformations

Sulfur and chlorine transformations in combustion are of interest to the extent that they alter the ratio of SO_3/SO_2 or Cl_2/HCl in the flue gas, lead to aerosol formation, or contribute to operational problems such as deposition and corrosion. For chlorine, the participation in dioxin/furan formation is a further issue. Nitrogen oxides and chlorine species are believed to promote SO_3 formation under some conditions while alkali metals may react with sulfur oxides and chloride to form alkali aerosols.

4.3.1. The SO_3/SO_2 ratio

The effect of NO_x on the SO_3/SO_2 ratio in the flue gas has attracted some interest, since NO-catalyzed oxidation of SO_2 has been reported to take place even at fairly low temperatures [185]. Nitrogen oxides can affect the sulfur oxides either through a direct reaction or through their effect on the radical pool composition. At low temperatures the oxidation of SO_2 may proceed by a direct reaction with NO_2 [186,187],

$$SO_2 + NO_2 \rightleftharpoons SO_3 + NO \quad \text{(S13)}$$

During cooling NO may indirectly promote SO_3 formation by converting HO_2 back to OH,

$$SO_2 + OH(+M) \rightleftharpoons HOSO_2(+M) \quad \text{(S2)}$$

$$HOSO_2 + O_2 \rightleftharpoons SO_3 + HO_2 \quad \text{(S3)}$$

$$NO + HO_2 \rightleftharpoons NO_2 + OH \quad \text{(N5)}$$

This sequence corresponds to the overall chain reaction $SO_2 + NO + O_2 \rightarrow SO_3 + NO_2$. Downstream injection of a combustible such as methanol that promotes HO_2 formation has been

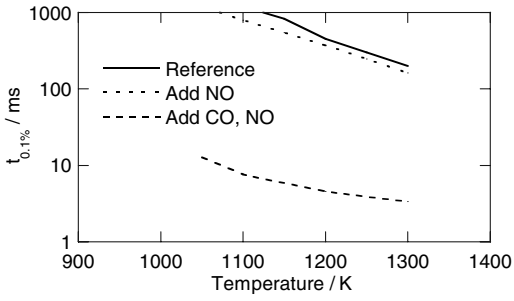

Fig. 11. Predicted times for 0.1% SO_2 oxidation ($t_{0.1\%}$) at atmospheric pressure as a function of temperature and flue gas composition. Inlet composition: $O_2 = 5\%$, $CO_2 = 15\%$, $H_2O = 8\%$, $SO_2 = 400$ ppm; varying amounts of NO (0, 300 ppm) and CO (0, 1000 ppm).

proposed as a means of controlling both the NO/NO_2 and the SO_3/SO_2 ratios [111]. The presence of HO_2 promotes oxidation of NO to NO_2 through reaction (N7) simultaneously with a reduction of SO_3 to SO_2 by reaction (S3b) followed by (S2b).

Despite these interactions, the impact of nitrogen oxides on SO_2 oxidation during cooling is believed to be small [188]. This is confirmed by modeling predictions. Figure 11 shows the predicted influence of NO and CO on oxidation of SO_2 to SO_3 under conditions typical of the burnout region in stationary combustion systems. The SO_2 oxidation rate is characterized by the time for conversion of 0.1% of the SO_2 to SO_3 ($t_{0.1\%}$). The calculations indicate that in the absence of combustibles, the SO_2 oxidation rate is very low, whether or not NO is present. Addition of chlorine or alkali species (not shown) has also only a small impact on the reaction rate. However, the presence of a combustible (here, 1000 ppm CO) leads to generation of chain carriers and enhances the SO_2 oxidation rate by two orders of magnitude. These results imply that trace species affect the SO_3/SO_2 ratio in a flue gas through promotion or inhibition of fuel burnout, rather than through direct interactions with sulfur species.

4.3.2. The Cl_2/HCl ratio

There has been some interest in the Cl_2/HCl ratio in combustion flue gases due to its potential impact on the formation of furans and dioxins. Molecular chlorine (Cl_2) is believed to be a key intermediate in the formation of chlorophenols, which have been proposed as precursors for dioxins and furans [189]. Hydrogen chloride is less likely than molecular chlorine to undergo aromatic substitution reactions to form PCDD and PCDF precursors [190]. The Cl_2/HCl ratio may also be important to the transformation of mercury species (elemental or oxidized forms) in combustion [191–193].

A number of experimental studies indicate that addition of sulfur or fuels with a high sulfur content causes a decrease in the formation of organic chlorides and PCDD/F both on laboratory scale [189,194–197] and on a full scale [198]. It has been proposed that a high sulfur content suppresses Cl_2 formation and consequently PCDD/F formation [189,199] through the overall reaction

$$SO_2 + Cl_2 + H_2O \rightarrow SO_3 + 2HCl$$

The details of this mechanism is not known. If active it acts to convert Cl_2 to HCl, while SO_2 is oxidized to SO_3. However, the reaction is barely measurable below 1073 K [200,201], and it is doubtful if it has any significance in combustion processes. The effect of SO_2 on the Cl_2/HCl ratio is probably mostly related to the ability of sulfur to form $CuSO_4$ and thus prevent Cu from catalyzing the conversion of HCl to Cl_2 [68,196,200].

Either way, under conditions of large-scale thermal processes the precursor mechanism is not likely to contribute significantly to PCDD/F formation compared to the so-called de novo synthesis mechanism [68,202]. The de novo synthesis involves oxidation and chlorination of unburned carbon in particulates, and the importance of the Cl_2/HCl ratio to dioxin formation via this mechanism is not yet clarified.

4.3.3. S/Cl/K interactions

It is commonly believed that sulfur and chlorine bound in fuels are largely emitted as sulfur oxides and hydrogen chloride, independent of combustion conditions. However, recent results indicate that the fate of these elements in some combustion systems is more complex than that. Measurements of the SO_2-emission from combustion of annual biomass (straw) in a full-scale grate-fired boiler [203] show variations of two orders of magnitude in daily mean values of SO_2 and HCl. Also short-term fluctuations for these components are evident. Figure 12 shows results for SO_2. The fluctuations do not correlate with changes in combustion conditions, and they cannot be explained easily by variations in the sulfur or chlorine content of the fuel or by variations in release/recapture of the elements by char.

Annual biomass crops such as straw often contain considerable amounts of chlorine and potassium [205]. During pyrolysis and combustion a large fraction of the Cl and K is released to the gas phase and may subsequently cause problems with aerosol formation and with deposition and corrosion. Analysis of full-scale measurements [203] indicates that the SO_2 and HCl emissions are correlated mainly with the potassium release from the biomass. In grate combustion K, Cl and S may remain in the bottom ash or be

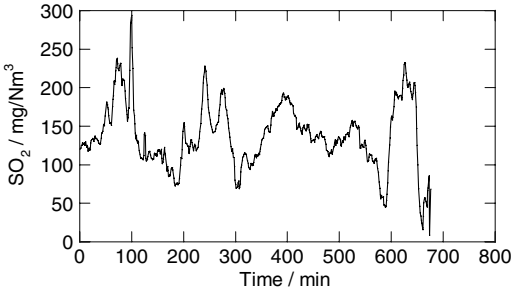

Fig. 12. Emissions of SO_2 from combustion of straw on a grate at the Ensted boiler [204]. The data are 5 min mean values on a dry basis, normalized to 6% O_2.

transported to the freeboard by particle entrainment or evaporation of volatile species. In the presence of potassium, sulfur and chlorine released to the gas phase are partly bound as KCl and K_2SO_4 that condensate as aerosols. Large amounts of aerosols (100–1900 mg/N m^3) have been detected upstream of the flue gas filter in these units [15,73], and data show a correlation between particle concentrations and the stack emissions of SO_2 and HCl. A large potassium release from the fuel, and hence a large molar ratio K/(Cl + 2S), results in low emissions of SO_2 and HCl [203]. The fluctuations in emissions can be explained in terms of variations in the potassium release. The content of potassium in annual biomass may vary significantly since it is very sensitive to leaching.

The sulfation of KCl is important to the HCl/SO_2 ratio in the flue gas. The overall sulfation reaction is

$$KCl + SO_2 + H_2O + \frac{1}{2}O_2 \rightarrow K_2SO_4 + HCl$$

This reaction replaces SO_2 in the exhaust with HCl. If formed in the gas phase, potassium sulfate may condense by homogeneous nucleation and then act as condensation nuclei for the subsequent condensation of KCl. However, the mechanism of formation of alkali sulfates found in deposits has long been in dispute. Both heterogeneous [33,69, 154,206–208] and homogeneous [15,36,73,209–216] mechanisms have been advocated in the literature. In the heterogeneous mechanism, a gas phase alkali-containing precursor is transported to the surface where it is sulfated by reactions in condensed or solid phase. The homogeneous mechanism involves formation of alkali sulfate in the gas phase, followed by condensation onto the deposition surfaces. It has been questioned whether gaseous alkali sulfates are formed in combustion systems [33,154,207], but recently a plausible mechanism was proposed [36]. According to this mechanism, the sulfation is initiated by oxidation of SO_2 to SO_3, which is also claimed to be the rate limiting step. Alkali transformations then proceed by a number of fast molecule–molecule reactions, which bear similarity to ionic reactions. For potassium,

$$SO_3 + KOH(+M) \rightleftharpoons KHSO_4(+M) \quad (K6)$$

$$SO_3 + KCl(+M) \rightleftharpoons KClSO_3(+M) \quad (K7)$$

$$KClSO_3 + H_2O \rightleftharpoons KHSO_4(+M) \quad (K8)$$

$$KHSO_4 + KCl \rightleftharpoons K_2SO_4 + HCl \quad (K9)$$

According to theoretical estimates [36], both the alkali hydrogen sulfate and alkali oxysulfur chloride complexes are sufficiently stable in the gas phase to act as precursors for alkali sulfate. Modeling predictions with this mechanism [36] compare favorably with experimental results on gas phase sulfation of potassium chloride at 1373 K [212], but due to the slow oxidation of SO_2 to SO_3 in the absence of combustibles it underestimates the degree of sulfation (L. Hindiyarti, F. Frandsen, H. Livbjerg, P. Glarborg, unpublished results) observed experimentally at lower temperatures [212,214,215]. More work on the S/Cl/K interactions is desirable.

4.4. Effect of trace species on PAH and soot

It has been known for a long time [217] that additives may suppress soot formation in hydrocarbon flames. A wide range of additives has been tested [18,19,218–224], with metal compounds containing iron and manganese considered most efficient. The mode of additive influence depends on flame type, additive concentration, point of additive introduction, and degree of flame sooting. Data from practical systems indicate that the additives are most efficient in reducing soot under heavily sooting conditions, while systems with a relatively clean exhaust may exhibit an increase in particulate emission due to metal oxides from the additive [18]. There are several ways in which an additive or a trace species can reduce soot emissions [222]. Firstly, it can inhibit the formation of soot, e.g., by removing the precursor species, the nuclei, or the growth species, or by decelerating the rates of coalescence and coagulation of soot particles. Alternatively, an additive can remove soot after it has been formed by accelerating its subsequent oxidation, either by stimulating the generation of oxidizing species such as O or OH, or by a direct reaction with the soot. Finally, any effect of the additive on the ignition behavior, the flame temperature, or the fuel oxidation rate may have an impact on soot emissions.

As in the preceding sections, we focus on the trace elements that occur naturally in combustion, i.e., N, S, Cl, and alkaline species. The way these species interact with the PAH and soot chemistry appears to be specific to the different elements. In general, the trace species appear to have little impact on the C_1–C_4 concentrations in sooting

flames [223,225], presumably because radical scavenging effects diminish under very fuel-rich conditions [224]. Instead, the interaction occurs mainly through reaction with the PAH species or with the soot particles, as discussed below.

4.4.1. N and S interactions with PAH and soot

The impact of nitrogen and sulfur species on PAH and soot chemistry in flames appears to be comparatively low. Addition of reactive nitrogen species such as NH_3 and NO to premixed flames results in a minor decrease in soot formation [19]. The results are consistent with formation of HCN, which ties up one carbon atom and can be considered inert in terms of soot formation [19]. Nitric oxide may also enhance soot oxidation. Soot formed from gas phase precursors reacts rapidly with NO at high temperatures [226,227].

Results from premixed hydrocarbon flames [228] show that the presence of SO_2 causes a decrease in the soot volume fraction and particle diameter, while the number density and the coagulation rate are unaffected. The data indicate that SO_2 enhances the oxidation of soot once formed, presumably by a direct reaction with the particle. In diffusion flames [218,229–231], adding SO_2 on the fuel or oxidizer side causes a reduction in the soot yield, but the effect is small and may be attributed to dilution and thermal effects. However, addition of CS_2 to the fuel stream reduces the soot volume fraction by what appears to be a chemical effect [232]. Sulfur bound in the fuel (0–2%) does not appear to affect soot formation in diffusion flames [233]. In diesel engines presence of sulfur in the fuel may lead to a large increase in the particle number density of the exhaust [234,235], but rather than a sulfur/soot interaction during combustion this observation may be attributed mainly to sulfate aerosols and sampling artifacts [236]. Neither nitrogen or sulfur species seem to affect the coagulation rate of the soot particles [19,228].

4.4.2. Cl interactions with PAH and soot

The addition of chlorine yields an increase in soot in hydrocarbon pyrolysis [237] and flames, both premixed [238,239] and non-premixed [230,240,241]. In diffusion flames and pyrolysis systems, the presence of chlorine increases the fractional conversion of carbon to soot, while in premixed combustion it lowers the critical equivalence ratio for onset of soot formation [242]. The main effect of chlorine can be attributed to the ability of chlorine atoms to abstract readily hydrogen atoms from other organic hydrocarbons. This phenomena is well-known for smaller hydrocarbons, e.g.,

$$Cl + CH_4 \rightleftharpoons HCl + CH_3 \qquad (Cl7)$$

Such reactions serve to extend the radical chain and through steps like

$$CH_2Cl + CH_3 \rightleftharpoons C_2H_4 + HCl \qquad (Cl8)$$

the production of heavier hydrocarbons is accelerated with the possible formation of aromatic compounds and soot [243]. Of even larger importance, the chlorine atoms may abstract atomic H from stable PAH molecules [239,242,244]. By activating the PAH, the chlorine accelerates the soot formation and growth, while it reduces the PAH level.

4.4.3. K/Na interactions with PAH and soot

Addition of alkali metals to premixed hydrocarbon flames [221,222,225,245] causes a decrease in soot particle size, while the number density is increased significantly. The C_1–C_3 species concentrations are unaffected. In diffusion flames alkali metals may promote or suppress soot emissions depending on the overall flame stoichiometry, dopant level and the point of introduction [218,220,246–248]. In-flame measurements [249–251] show that alkali metals serve to reduce the soot particle size. However, in some flames [249] the number density increases considerably, similarly to observations from premixed flames, while in other flames [250,251] the soot volume fraction is reduced without affecting the number density. Under oxidizing conditions alkali metals have been reported to reduce the PAH yield from toluene and benzene [252,253].

The impact of ionic reactions on soot nucleation, coagulation and growth is still in debate [37,43,222,254–256]. However, there are strong indications that the interaction of alkali metals with soot formation takes place through an ionic mechanism. The efficiency of a given metal has been shown to depend almost exclusively on the temperature and the ionization potential of the metal [219,221,225]; the higher the temperature and the lower the ionization potential, the greater is the soot removal. For instance, potassium has a much stronger impact than sodium on the soot characteristics in both premixed [221] and diffusion flames [218,248,250,251]. It has been suggested that the effect comes from ionization and thereby charging of incipient soot particles, causing them to resist further collisional growth and inhibit coagulation [37,221,245]. However, there are some indications [247,257,258] that the alkali metal may neutralize the charge on the soot particle,

$$M + soot^+ \rightleftharpoons M^+ + soot$$

and thereby inhibit the coagulation process. Due to dipole effects, the rate of coagulation between two soot particles is larger between a charged particle and a neutral particle, than between two neutral particles [257,259]. However, if both particles are charged, the rate drops significantly. Thus, the overall coagulation rate may have a maximum for a certain fraction of the soot particles being charged. Either way, a lower coagulation rate

leads to smaller particles, which are more easily destroyed by an oxidative attack. Conceivably, incorporation of the metals in the soot may even act to catalyze gasification of the carbon [220,251].

5. Conclusions

Based on the present review, some major points can be made about the interaction of trace components with fuel oxidation and with emissions.

- Fuel oxidation and burnout may, depending on the reaction conditions, be promoted or inhibited by trace concentrations of N, S, Cl or K/Na. Nitrogen oxides are the most efficient sensitizing agents but also sulfur species in low quantities seem to have a promoting effect, which is yet to be explained. Under reducing conditions all of these elements may catalyze radical recombination.
- In flames the presence of S, Cl or K/Na limits the conversion of fuel N to NO and N_2 by catalyzing radical removal. Under reducing conditions, the presence of sulfur oxides may enhance NO formation in the flame zone, but sulfur radicals may subsequently remove NO downstream. These interactions may involve reactions such as $N + SO \rightleftharpoons NO + S$ and $N + SO_2 \rightleftharpoons NO + SO$.
- Interactions of sulfur, chlorine and alkali metals may have a significant impact on emissions of SO_2, HCl, and aerosols, through formation of alkali chlorides and alkali sulfates that condense during cooling. These interactions, which may depend on the SO_3 formation rate, are not yet completely understood.
- Formation of PAH and soot may be affected by the presence of N, S, Cl and K/Na, but the impact and mechanism vary between the different trace species. By abstracting H atoms, chlorine may promote the formation of higher hydrocarbons as well as activate PAH to enhance its conversion to soot. Alkaline species are thought to participate in ion exchange reactions with the soot particles. This interaction, which serves to reduce the soot particle size by inhibiting coagulation, may facilitate soot burnout. Direct interactions of N and S species with PAH and soot are probably limited, but NO and SO_2 may contribute to soot oxidation under reducing conditions.

Acknowledgments

I would like to thank Marcus Alden and Steve Pope for inviting me to write this paper and to give the accompanying lecture. I would also like to acknowledge the fruitful collaboration that I have had over the years with my mentor Jim Miller, my colleagues Anker Jensen, Jan Johnsson and Kim Dam-Johansen, and with Bob Kee, Per Kristensen, Maria Alzueta, Martin Skjøth-Rasmussen and Paul Marshall. Finally, I would like to thank Christian Rasmussen, Jimmy Andersen, Peter Arendt Jensen, Flemming Frandsen, Bo Sander and Jacob Knudsen for their help in preparing the paper. The work was supported by the CHEC (Combustion and Harmful Emission Control) Research Program.

Appendix A. Development of an S/N Subset

Despite years of research, the direct interaction of nitrogen and sulfur species in flames is still controversial. Reliable thermodynamic properties for S/N species are scarce and several potential key reactions have not been characterized experimentally. To assist in the present analysis, a preliminary subset for sulfur/nitrogen interactions at high temperatures was established. Table 2 lists thermodynamic data for selected N/S species and in Table 3 rate constants for a number of reactions in the N/S reaction subset are found. Similar to previous modeling efforts [168,171,173,176,264], the present S/N subset contains many rate constants that are no more than rough guesses. A number of four-centered reactions proposed in the literature [168,173,176,264], such as $SH + NH \rightleftharpoons NS + H_2$, $NS + OH \rightleftharpoons SH + NO$ and $NS + NO \rightleftharpoons SO + N_2$, were omitted. Many of these reactions can be reconstituted as a sequence of atom/molecule reactions [27].

Key reactions include attack of N and NH radicals on SO_2 and of S and SH on NO. In the absence of reported data on the reactions,

$$N + SO_2 \rightleftharpoons NO + SO \quad \text{(S12)}$$

$$NH + SO_2 \rightleftharpoons HNO + SO \quad \text{(S14)}$$

the rate coefficients were estimated from *iso*-electronic analogies with $N + O_2$ and $O + SO_2$, respectively. The rate constant for (S12) is probably an upper limit; the reaction may have a significantly higher barrier to reaction than the $N + O_2$ reaction. At low temperatures both the $S + NO$ [262] and $SH + NO$ [268] are association reactions forming SNO (S15) and HSNO (S16), respectively, while at high temperatures other product channels may open up. In addition to recombination, the $S + NO$ reaction has two potential product channels,

$$S + NO \rightleftharpoons SO + N \quad \text{(S11b)}$$

$$S + NO \rightleftharpoons NS + O \quad \text{(S17b)}$$

Table 2
Thermodynamic data for selected sulfur species

Species	$\Delta_f H_{298}$	S_{298}	C_{p300}	C_{p400}	C_{p500}	C_{p600}	C_{p800}	C_{p1000}	C_{p1500}	Ref.
NS	278.0	222.2	31.78	32.45	33.29	33.81	34.08	35.34	36.97	[260,261]
SNO	176.0	257.9	41.43	44.83	47.42	49.44	52.27	54.00	56.12	[262] (P. Marshall, Unpublished)
NSO	168.0	262.6	42.70	46.11	48.85	50.92	53.56	55.04	56.70	[262] (P. Marshall, Unpublished)
HSNO	94.0	267.8	53.72	58.53	62.04	64.89	69.32	72.55	77.28	[263] (P. Marshall, Unpublished)

Units are J-mol-K.

Table 3
Reactions from the N/S subset

		A	β	E_a	Ref.
S11	$SO + N \rightleftharpoons S + NO$	7.0E12	0.00	0	[265,266], rv
S12	$SO_2 + N \rightleftharpoons SO + NO$	6.4E09	1.00	6280	Est. as $O_2 + N$
S13	$SO_2 + NO_2 \rightleftharpoons NO + SO_3$	6.3E12	0.00	27,000	[267]
S14	$SO_2 + NH \rightleftharpoons SO + HNO$	5.0E12	0.00	20,000	Est. as $SO_2 + O$
S15	$S + NO(+M) \rightleftharpoons SNO(+M)$	3.4E13	0.24	0	[262]
	Low pressure limit	2.2E15	0.00	−1870	
	Troe fall-off: 0.78 exp($-T$/7445)				
S16	$SH + NO(+M) \rightleftharpoons HSNO(+M)$	1.6E13	0.00	0	[263,268]
	Low pressure limit	1.4E23	−2.50	0	
	Troe parameters: 0.5, 1E30, 1E−30				
S17	$NS + O \rightleftharpoons S + NO$	3.0E12	0.00	0	[265], rv
S18	$SNO + H \rightleftharpoons SH + NO$	1.0E13	0.00	0	Est.
S19	$S + HNO \rightleftharpoons SH + NO$	1.0E13	0.00	0	Est.
S20	$SO + NH \rightleftharpoons NS + OH$	3.0E13	0.00	0	See text

Units are mol, cm, s, cal.

Both reactions (S11b) and (S17b) are endothermic and they become important in the forward direction only at high temperatures. Shock tube results [265,266] indicate that the SO + N channel dominates at high temperatures, with a branching ratio $k_{S11b}/(k_{S11b} + k_{S17b}) = 0.80$–$0.95$ [265]. These results are consistent with rate constants for the reverse (exothermic) reactions of $k_{S11} \approx 7 \times 10^{12}$ cm^3 mol^{-1} s^{-1} and $k_{S17} \approx 3 \times 10^{12}$ cm^3 mol^{-1} s^{-1}. The SH + NO reaction has been proposed as a four-centered step forming NH + SO or SN + OH [168,173,176], but currently there is no evidence for these channels. Here, the products have been assumed to be SNO + H (S18b) and S + HNO (S19b). The rate constant for NH + SO has been measured to be 3×10^{13} cm^3 mol^{-1} s^{-1} over the temperature range 298–703 K (see [173]). If recombination to HNSO or its isomers is disregarded, the only exothermic product channels appear to be SH + NO and NS + OH. In the present work, the products of this reaction are tentatively assumed to be NS + OH (S20), but the SH + NO product channel cannot be ruled out [173]. Little is known about subsequent reactions of NS, NSO and HSNO. However, the potentially important reactions of NS with O_2 and with NO have been shown to be slow [269].

References

[1] A. Levy, *Proc. Combust. Inst.* 19 (1982) 1223–1242.
[2] C.T. Bowman, *Proc. Combust. Inst.* 24 (1992) 859–878.
[3] J.A. Miller, *Proc. Combust. Inst.* 26 (1996) 461–480.
[4] J.A. Miller, M.J. Pilling, J. Troe, *Proc. Combust. Inst.* 30 (2005) 43–88.
[5] C.T. Bowman, in: W. Bartok, A.F. Sarofim (Eds.), *Fossil Fuel Combustion, Chemistry of Gaseous Pollutant Formation and Destruction*, John Wiley & Sons, Inc., 1991 (Chapter 4).
[6] J.G. Singer (Ed.), *Combustion Fossil Power*, fourth ed., Combustion Engineering, Inc., 1991.
[7] B. Sander, *Biomass Bioenergy* 12 (1997) 177–183.
[8] L.L. Baxter, T. R Miles, T.R. Miles Jr., B. M Jenkins, T. Milne, D. Dayton, R.W. Bryers, L.L. Oden, *Fuel Proc. Technol.* 54 (1998) 47–78.
[9] B.M. Jenkins, L.L. Baxter, T.R. Miles Jr., T.R. Miles, *Fuel Process Technol.* 54 (1998) 17–46.
[10] J. Werther, M. Saenger, E.-U. Hartge, T. Ogada, Z. Siagi, *Prog. Energy Combust. Sci.* 26 (2000) 1–27.
[11] H. Belevi, H. Moench, *Environ. Sci. Technol.* 34 (2000) 2501–2506.
[12] I. Delay, J. Swithenbank, B.B. Argent, *J. Alloys Compds.* 320 (2001) 282–295.
[13] P. Glarborg, A.D. Jensen, J.E. Johnsson, *Prog. Energy Combust. Sci.* 29 (2003) 89–113.

[14] P.G. Kristensen, B. Karll, A.B. Bendtsen, P. Glarborg, K. Dam-Johansen, *Combust. Sci. Technol.* 157 (2000) 263–292.
[15] K.A. Christensen, M. Stenholm, H. Livbjerg, *J. Aerosol Sci.* 29 (1998) 421–444.
[16] J.O.L. Wendt, J.T. Morcomb, T.L. Corley, *Proc. Combust. Inst.* 17 (1979) 671–678.
[17] W.P. Linak, J.O.L. Wendt, *Combust. Sci. Technol.* 115 (1996) 69–82.
[18] J.B. Howard, W.J. Kausch Jr., *Prog. Energy Combust. Sci.* 6 (1980) 263–276.
[19] B.S. Haynes, H. Jander, H. Mätzing, H.Gg. Wagner, *Proc. Combust. Inst.* 19 (1982) 1379–1385.
[20] W.P. Linak, J.O.L. Wendt, *Fuel Process. Technol.* 39 (1994) 173–198.
[21] B. Miller, D.R. Dugwell, R. Kandiyoti, *Energy Fuels* 17 (2003) 1382–1391.
[22] H. Kassman, C. Andersson, J. Carlson, U. Björklund, B. Strömberg, *Decreased Emissions of CO and NO_x by Injection of Ammonium Sulphate into the Combustion Chamber (in Swedish)*, Technical Report F4-313, ISSN 0282-3772, VÄRMEFORSK Service AB, 2005.
[23] J.A. Miller, C.T. Bowman, *Prog. Energy Combust. Sci.* 15 (1989) 287–338.
[24] W.C. Gardiner (Ed.), *Gas-Phase Combustion Chemistry*, second ed., Springer-Verlag, 2000.
[25] C.F. Cullis, M.R.F. Mulcahy, *Combust. Flame* 18 (1972) 225.
[26] J.E. Johnsson, P. Glarborg, in: C. Vovelle (Ed.), *Pollutants from Combustion, Sulfur Chemistry in Combustion I – Sulfur in Fuels and Combustion Chemistry*, Kluwer Academic Publishers, 2000 (Chapter).
[27] K. Schofield, *Combust. Flame* 124 (2001) 137–155.
[28] S.B. Karra, D. Gutman, S.M. Senkan, *Combust. Sci. Technol.* 60 (1988) 45–62.
[29] W.-P. Ho, R.B. Barat, J.W. Bozzelli, *Combust. Flame* 88 (1992) 265–295.
[30] H. Wang, T.O. Hahn, C.J. Sung, C.K. Law, *Combust. Flame* 105 (1996) 291–307.
[31] J.F. Roesler, R.A. Yetter, F.L. Dryer, *Combust. Sci. Technol.* 120 (1996) 11–37.
[32] S. Senkan, in: W.C. Gardiner (Ed.), *Gas-Phase Combustion Chemistry*, second ed., *Survey of Rate Coefficients in the C/H/Cl/O System*, Springer-Verlag, 2000 (Chapter 4).
[33] M. Steinberg, K. Schofield, *Prog. Energy Combust. Sci.* 16 (1990) 311–317.
[34] R.A. Perry, J.A. Miller, *Int. J. Chem. Kinet.* 28 (1996) 217–234.
[35] V.M. Zamansky, V.V. Lissianski, P.M. Maly, L. Ho, D. Rusli, W.C. Gardiner Jr., *Combust. Flame* 117 (1999) 821–831.
[36] P. Glarborg, P. Marshall, *Combust. Flame* 141 (2005) 22–39.
[37] B.S. Haynes, H.Gg. Wagner, *Proc. Combust. Inst.* 17 (1979) 1365–1374.
[38] M. Frenklach, J. Warnatz, *Combust. Sci. Technol.* 51 (1987) 265–283.
[39] J.A. Miller, C.F. Melius, *Combust. Flame* 91 (1992) 21–39.
[40] H. Wang, M. Frenklach, *Combust. Flame* 110 (1997) 173–221.
[41] I.M. Kennedy, *Prog. Energy Combust. Sci.* 23 (1997) 95–132.
[42] J. Appel, H. Bockhorn, M. Frenklach, *Combust. Flame* 121 (2000) 122–136.
[43] H. Richter, J.B. Howard, *Prog. Energy Combust. Sci.* 26 (2000) 565–608.
[44] A. D'Anna, A. Violi, A. D'Alessio, *Combust. Flame* 121 (2000) 418–429.
[45] C.J. Pope, J.A. Miller, *Proc. Combust. Inst.* 28 (2000) 1519–1527.
[46] H. Richter, J.B. Howard, *Phys. Chem. Chem. Phys.* 4 (2002) 2038–2055.
[47] M. Frenklach, *Phys. Chem. Chem. Phys.* 4 (2002) 2028–2037.
[48] Y.B. Zeldovich, *Acta Physicochem. USSR* 21 (1946) 577–628.
[49] C.P. Fenimore, *Proc. Combust. Inst.* 13 (1971) 373–379.
[50] A.N. Hayhurst, I.M. Vince, *Prog. Energy Combust. Sci.* 6 (1980) 35–51.
[51] P. Glarborg, J.A. Miller, R.J. Kee, *Combust. Flame* 65 (1986) 177–202.
[52] L.V. Moskaleva, M.C. Lin, *Proc. Combust. Inst.* 28 (2000) 2401–2893.
[53] P. C Malte, D.T. Pratt, *Proc. Combust. Inst.* 15 (1975) 1061–1070.
[54] J.W. Bozzelli, A.M. Dean, *Int. J. Chem. Kinet.* 27 (1995) 1097–1109.
[55] J.B. Bell, M.S. Day, J.F. Grcar, W.G. Bessler, C. Schulz, P. Glarborg, A.D. Jensen, *Proc. Combust. Inst.* 29 (2002) 2195–2202.
[56] J.A. Miller, C.T. Bowman, *Int. J. Chem. Kinet.* 23 (1991) 289–313.
[57] P. Glarborg, J.A. Miller, *Combust. Flame* 99 (1994) 475–483.
[58] P. Glarborg, K. Dam-Johansen, J.A. Miller, R.J. Kee, M.E. Coltrin, *Int. J. Chem. Kinet.* 26 (1994) 421–436.
[59] P. Glarborg, P.G. Kristensen, S.H. Jensen, K. Dam-Johansen, *Combust. Flame* 98 (1994) 241–258.
[60] J.A. Miller, P. Glarborg, *Int. J. Chem. Kin.* 31 (1999) 757–765.
[61] Ø. Skreiberg, P. Kilpinen, P. Glarborg, *Combust. Flame* 136 (2004) 501–508.
[62] R.K. Srivastava, C.A. Miller, C. Erickson, R. Jambhekar, *J. Air Waste Manage. Assoc.* 54 (2004) 750–762.
[63] J.S. Dennis, A.N. Hayhurst, *Combust. Flame* 72 (1988) 241–258.
[64] P. Glarborg, D. Kubel, K. Dam-Johansen, H.-M. Chiang, J.W. Bozzelli, *Int. J. Chem. Kinet.* 28 (1996) 773–790.
[65] M.A. Mueller, R.A. Yetter, F.L. Dryer, *Int. J. Chem. Kin.* 32 (2000) 317–339.
[66] M.A. Blitz, K.J. Hughes, M.J. Pilling, *J. Phys. Chem. A* 107 (2003) 1971–1978.
[67] J.N. Knudsen, P.A. Jensen, W.G. Lin, K. Dam-Johansen, *Energy Fuels* 19 (2005) 606–617.
[68] B.R. Stanmore, *Combust. Flame* 136 (2004) 398–427.
[69] S. Srinivasachar, J.J. Helble, D.O. Ham, G. Domazetis, *Prog. Energy Combust. Sci.* 16 (1990) 303–309.
[70] S.C. van Lith, P.A. Jensen, F.J. Frandsen, P. Glarborg, V.A. Ramirez, *Energy Fuels* 20 (2006) 964–978.
[71] J.N. Knudsen, P.A. Jensen, K. Dam-Johansen, *Energy Fuels* 18 (2004) 1385–1399.

[72] D.C. Dayton, T.A. Milne, *Energy Fuels* 9 (1996) 855–865.
[73] K.A. Christensen, H. Livbjerg, *J. Aerosol Sci.* 25 (1996) 185–199.
[74] J.A. Miller, J.V. Volponi, J.-F. Pauwels, *Combust. Flame* 105 (1996) 451–461.
[75] N.M. Marinov, W.J. Pitz, C.K. Westbrook, M.J. Castaldi, S.M. Senkan, *Combust. Sci. Technol.* 116 (1996) 211–287.
[76] N.M. Marinov, M.J. Castaldi, C.F. Melius, W. Tsang, *Combust. Sci. Technol.* 128 (1996) 295–342.
[77] R.P. Lindstedt, G. Skevis, *Combust. Sci. Technol.* 125 (1997) 73–137.
[78] R.P. Lindstedt, L. Maurice, M. Meyer, *Faraday Discuss.* 119 (2001) 409–432.
[79] M.S. Skjøth-Rasmussen, P. Glarborg, M. Østberg, M.B. Larsen, S.W. Sørensen, J.E. Johnsson, A.D. Jensen, T.S. Christensen, *Proc. Combust. Inst.* 29 (2002) 1329–1336.
[80] A. Violi, *Combust. Flame* 139 (2004) 279–287.
[81] M.S. Skjøth-Rasmussen, P. Glarborg, M. Østberg, J.T. Johannesen, H. Livbjerg, A.D. Jensen, T.S. Christensen, *Combust. Flame* 136 (2004) 91–128.
[82] A. D'Anna, A. Violi, *Energy Fuels* 19 (2005) 79–86.
[83] N.W. Moriarty, M. Frenklach, *Proc. Combust. Inst.* 28 (2000) 2563–2568.
[84] P. Glarborg, M.U. Alzueta, K. Dam-Johansen, J.A. Miller, *Combust. Flame* 115 (1998) 1–27.
[85] A.B. Bendtsen, P. Glarborg, K. Dam-Johansen, *Combust. Sci. Technol.* 151 (2000) 31–72.
[86] J.A. Miller, S.J. Klippenstein, P. Glarborg, *Combust. Flame* 135 (2003) 357–362.
[87] P. Glarborg, P.G. Kristensen, D. Kubel, J. Hansen, K. Dam-Johansen, *Combust. Sci. Technol.* 110-111 (1995) 461–485.
[88] M.U. Alzueta, R. Bilbao, P. Glarborg, *Combust. Flame* 127 (2001) 2234–2251.
[89] C.L. Rasmussen, P. Glarborg, P. Marshall, *Proc. Combust. Inst.*, in press.
[90] J.F. Roesler, R.A. Yetter, F.L. Dryer, *Combust. Sci. Technol.* 85 (1992) 1–22.
[91] J.F. Roesler, R.A. Yetter, F.L. Dryer, *Combust. Flame* 100 (1995) 495.
[92] I. Glassman, *Combustion*, Academic Press, Inc., 1987.
[93] R.K. Lyon, J.E. Hardy, *Ind. Eng. Chem. Fundam.* 25 (1986) 19–24.
[94] T. Faravelli, A. Frassoldati, E. Ranzi, *Combust. Flame* 132 (2003) 188–207.
[95] N. Murakami, J. Izumi, S. Shirakawa, *Nenryo Kyokaishi* 61 (1982) 329.
[96] M. Hori, N. Matsugana, P.C. Malte, N.M. Marinov, *Proc. Combust. Inst.* 24 (1992) 909.
[97] P. Dagaut, F. Lecomte, J. Mieritz, P. Glarborg, *Int. J. Chem. Kinet.* 35 (2003) 564–575.
[98] P. Glarborg, M.U. Alzueta, K. Kjærgaard, K. Dam-Johansen, *Combust. Flame* 132 (2003) 629–638.
[99] J.H. Bromly, F.J. Barnes, S. Muris, X. You, B.S. Haynes, *Combust. Sci. Technol.* 115 (1996) 259–296.
[100] M. Hori, N. Matsugana, N.M. Marinov, J.W. Pitz, C.K. Westbrook, *Proc. Combust. Inst.* 27 (1998) 389–396.
[101] A.A. Konnov, J.N. Zhu, J.H. Bromly, D.-K. Zhang, *Proc. Combust. Inst.* 30 (2005) 1093–1100.
[102] P. Dagaut, A. Nicolle, *Combust. Flame* 140 (2005) 161–171.
[103] A. Doughty, F.J. Barnes, J.H. Bromly, B.S. Haynes, *Proc. Combust. Inst.* 26 (1996) 589–596.
[104] P. Dagaut, O. Mathieu, A. Nicolle, *Combust: Sci. Technol.* 177 (2005) 1767–1791.
[105] A.A. Konnov, F.J. Barnes, J.H. Bromly, J.N. Zhub, D.-K. Zhang, *Combust. Flame* 141 (2005) 191–199.
[106] J.H. Bromly, F.J. Barnes, R. Mandyczewsky, T.J. Edwards, B.S. Haynes, *Proc. Combust. Inst.* 24 (1992) 899.
[107] P.F. Nelson, B.S. Haynes, *Proc. Combust. Inst.* 25 (1994) 1003–1010.
[108] M. Hori, Y. Koshiishi, N. Matsugana, P. Glaude, N.M. Marinov, *Proc. Combust. Inst.* 29 (2002) 2219–2226.
[109] P.A. Glaude, N. Marinov, Y. Koshiishi, N. Matsunaga, M. Hori, *Energy Fuels* 19 (2005) 1839–1849.
[110] N. Murakami, N. Kojima, M. Hashiguchi, *Nenryo Kyokaishi* 61 (1982) 276.
[111] R.K. Lyon, J.A. Cole, J.C. Kramlich, S.L. Chen, *Combust. Flame* 81 (1990) 30.
[112] K. Hjuler, P. Glarborg, K. Dam-Johansen, *Ind. Eng. Chem. Res.* 34 (1995) 1882–1888.
[113] M.U. Alzueta, R. Bilbao, M. Finestra, *Energy Fuels* 15 (2001) 724–729.
[114] M.U. Alzueta, J. Muro, R. Bilbao, P. Glarborg, *Israel J. Chem.* 39 (1999) 73–86.
[115] P. Dagaut, J. Luche, M. Cathonnet, *Combust. Sci. Technol.* 165 (2001) 61–84.
[116] E.M. Bulewicz, T.M. Sugden, *Proc. Roy. Soc. A* 277 (1964) 143.
[117] C.J. Halstead, D.R. Jenkins, *Chem. Phys. Lett.* 2 (1968) 281.
[118] P. Glarborg, M. Østberg, M.U. Alzueta, K. Dam-Johansen, J.A. Miller, *Proc. Combust. Inst.* 27 (1998) 219–226.
[119] C.K. Westbrook, *Proc. Combust. Inst.* 28 (2000) 1563–1577.
[120] M.U. Alzueta, P. Glarborg, *Environ. Sci. Technol.* 37 (2003) 4512–4516.
[121] P. Webster, A.D. Walsh, *Proc. Combust. Inst.* 10 (1965) 463–472.
[122] C.P. Fenimore, G.W. Jones, *J. Phys. Chem.* 69 (1965) 3593–3597.
[123] C.J. Halstead, D.R. Jenkins, *Trans. Faraday Soc.* 65 (1969) 3013–3022.
[124] A.S. Kallend, *Combust. Flame* 13 (1969) 324.
[125] R.A. Durie, G.M. Johnson, M.Y. Smith, *Combust. Flame* 17 (1971) 197–203.
[126] A.S. Kallend, *Combust. Flame* 19 (1972) 227–236.
[127] O.I. Smith, S.-N. Wang, S. Tseregounis, C.K. Westbrook, *Combust. Sci. Technol.* 30 (1983) 241.
[128] M.R. Zachariah, O.I. Smith, *Combust. Flame* 69 (1987) 125.
[129] K. Dam-Johansen, L.-E. Åmand, B. Leckner, *Fuel* 72 (2005) 565–571.
[130] E.J. Anthony, Y. Lu, *Prog. Energy Combust. Sci.* 27 (1998) 3093–3101.
[131] S. Schäfer, B. Bonn, *Fuel* 79 (2000) 1239–1246.
[132] F. Miccio, G. Löffler, V.J. Wargadalem, F. Winther, *Fuel* 80 (2001) 1555–1566.
[133] J. Andersen, *Emission Control Through Sulfur Addition*. M.Sc. thesis, Department of Chemical

Engineering, Technical University of Denmark, 2006.
[134] C.F. Cullis, M.M. Hirschler, S.W. Wall, *Proc. Combust. Inst.* 21 (1986) 1223–1230.
[135] J.A. Mulholland, A. F Sarofim, J.M. Beer, *Combust. Sci. Technol.* 85 (1992) 405–417.
[136] C.R. Casias, J.T. McKinnon, *Combust. Sci. Technol.* 116 (1996) 289–315.
[137] J.F. Roesler, R.A. Yetter, F.L. Dryer, *Combust. Sci. Technol.* 82 (1992) 87–100.
[138] J. Brouwer, J.P. Longwell, A.F. Sarofim, R.B. Barat, J.W. Bozzelli, *Combust. Sci. Technol.* 85 (1992) 87–100.
[139] J.F. Roesler, R.A. Yetter, F.L. Dryer, *Combust. Sci. Technol.* 101 (1994) 199–229.
[140] X. Wei, U. Schnell, X. Han, K.R.G. Hein, *Fuel* 83 (2004) 1227–1233.
[141] X. Wei, X. Han, U. Schnell, J. Maier, H. Wörner, K.R.G. Hein, *Energy Fuels* 17 (2003) 1392–1398.
[142] K.M. Hickson, L.F. Keyser, *J. Phys. Chem. A* 109 (2005) 6887–6900.
[143] C.R. Dautriche, *Seances Acad. Sci.* 146 (1908) 535.
[144] W.A. Rosser, S.H. Inami, H. Wise, *Combust. Flame* 7 (1963) 107.
[145] A. van Tiggelen, M. Dewitte, J. Vrebosch, *Combust. Flame* 8 (1964) 257.
[146] W. Hoffmann, *Chemie Ing. Tech.* 43 (1971) 556–560.
[147] K. Iya, S. Wollowitz, W. Kaskan, *Proc. Combust. Inst.* 15 (1975) 329–336.
[148] D.E. Jensen, G.A. Jones, A.C.H. Mace, *J. Chem. Soc. Faraday Trans. I* 75 (1979) 2377–2385.
[149] D.E. Jensen, G.A. Jones, *J. Chem. Soc. Faraday Trans. I* 78 (1982) 2843–2850.
[150] A.J. Hynes, M. Steinberg, K. Schofield, *J. Chem. Phys.* 80 (1984) 2585–2597.
[151] H.T. Kim, J.J. Reuther, *Combust. Flame* 57 (1984) 313–317.
[152] E.M. Bulewicz, B.J. Kucnerowicz-Polak, *Combust. Flame* 70 (1987) 127–135.
[153] M. Slack, J.W. Cox, A. Grillo, R. Ryan, O. Smith, *Combust. Flame* 77 (1989) 311–320.
[154] K. Schofield, M. Steinberg, *J. Chem. Phys.* 96 (1992) 715–726.
[155] V. Babushok, W. Tsang, G.T. Linteris, D. Reineldt, *Combust. Flame* 115 (1998) 551.
[156] B.A. Williams, J.W. Fleming, *Proc. Combust. Inst.* 29 (2002) 345–351.
[157] R. Friedman, H. Levy, *Combust. Flame* 7 (1963) 195.
[158] R.A. Dodding, R.F. Simmons, A. Stephens, *Combust. Flame* 15 (1970) 313–315.
[159] J.D. Birchall, *Combust. Flame* 14 (1970) 85.
[160] L. Hindiyarti, F. Frandsen, H. Livbjerg, P. Glarborg, *Fuel* 85 (2006) 978–988.
[161] V.M. Zamansky, L. Ho, P.M. Maly, W.R. Seeker, *Proc. Combust. Inst.* 26 (1996) 2075–2082.
[162] V.M. Zamansky, P.M. Maly, L. Ho, V.V. Lissianski, D. Rusli, W.C. Gardiner Jr., *Proc. Combust. Inst.* 27 (1998) 1443–1449.
[163] V.M. Zamansky, M.S. Sheldon, P.M. Maly, *Proc. Combust. Inst.* 27 (1998) 3001–3008.
[164] V.V. Lissianski, V.M. Zamansky, P.M. Maly, *Combust. Flame* 125 (2001) 1118–1127.
[165] P. Dagaut, A. Nicolle, *Int. J. Chem. Kinet.* 37 (2005) 406–413.
[166] J.O.L. Wendt, J.M. Ekmann, *Combust. Flame* 25 (1975) 355–360.
[167] S.-K. Tang, S.W. Churchill, N. Lior, *AIChE Symp. Ser. 77* 211 (1981) 77–86.
[168] L.D. Pfefferle, S.W. Churchill, *Ind. Eng. Chem. Res.* 28 (1989) 1004–1010.
[169] S.I. Tseregounis, O.I. Smith, *Combust. Sci. Technol.* 30 (1983) 231–239.
[170] S.I. Tseregounis, O.I. Smith, *Proc. Combust. Inst.* 20 (1984) 761–768.
[171] J.O.L. Wendt, E.C. Wootan, T.L. Corley, *Combust. Flame* 49 (1983) 261–274.
[172] T.L. Corley, J.O.L. Wendt, *Combust. Flame* 58 (1984) 141–152.
[173] K.J. Hughes, A.S. Tomlin, V.A. Dupont, M. Pourkashanian, *Faraday Discuss.* 119 (2001) 337–352.
[174] A.T. Chen, P.C. Malte, M.M. Thornton, *Proc. Combust. Inst.* 20 (1984) 769–777.
[175] D.W. Pershing, J.E. Cichanowicz, G.C. England, M.P. Heap, G.B. Martin, *Proc. Combust. Inst.* 17 (1978) 715–726.
[176] E. Hampartsoumian, W. Nimmo, A.S. Tomlin, K.J. Hughes, T. Mahmud, *J. Inst. Energy* 71 (1998) 137–144.
[177] W. Nimmo, E. Hampartsoumian, K.J. Hughes, A.A. Tomlin, *Proc. Combust. Inst.* 27 (1998) 1419–1426.
[178] E. Hampartsoumian, W. Nimmo, B.M. Gibbs, *Fuel* 80 (2001) 887–897.
[179] W. Lin, J. Bu, R. Korbee, K. Svoboda, C.M. van den Bleek, *Fuel* 72 (1993) 299–304.
[180] W. Lin, J.E. Johnsson, K. Dam-Johansen, C.M. van den Bleek, *Fuel* 73 (1994) 1202–1208.
[181] C.J. Tullin, A.F. Sarofim, J.M. Beer, J.D. Teare, *Combust. Sci. Technol.* 106 (1995) 153–166.
[182] F.H. Mao, R.B. Barat, *Combust. Sci. Technol.* 116 (1996) 357–399.
[183] S. Julien, C.M.H. Brereton, C.J. Lim, J.R. Grace, E.J. Anthony, *Fuel* 75 (1996) 1655–1663.
[184] V. Lissianski, V. Zamansky, G. Rizeq, *Proc. Combust. Inst.* 29 (2002) 2251–2258.
[185] S. Jaffe, F.S. Klein, *Trans. Faraday Soc.* 62 (1966) 2150.
[186] C.F. Cullis, R.M. Henson, D.L. Trimm, *Proc. R. Soc. (London), Ser. A* 295 (1966) 72.
[187] J.W. Armitage, C.F. Cullis, *Combust. Flame* 16 (1971) 125–130.
[188] J.O.L. Wendt, C.V. Sternling, *Combust. Flame* 21 (1973) 387–390.
[189] Y. Xie, W. Xie, K. Liu, L. Dicken, W.-P. Pan, J.T. Riley, *Energy Fuels* 14 (2000) 597–602.
[190] B.K. Gullett, A.F. Sarofim, K.A. Smith, C. Procaccini, *Process Saf. Environ. Prot.* 78 (2000) 47–52.
[191] R.N. Sliger, J.C. Kramlich, N.M. Marinov, *Fuel Process. Technol.* 65–66 (2000) 423–438.
[192] M. Xu, Y. Qiao, C. Zheng, L. Li, J. Liu, *Combust. Flame* 132 (2003) 208–218.
[193] S.B. Ghorishi, C.W. Lee, W.S. Jozewicz, J.D. Kilgroe, *Environ. Eng. Sci.* 22 (2005) 221–231.
[194] P.H. Ruokojärvi, I. Halonen, K.A. Tuppurainen, J. Tarhanen, J. Ruuskanen, *Environ. Sci. Technol.* 32 (1998) 3099–3103.
[195] P. Samaras, M. Blumenstock, D. Lenoir, K.-W. Schramm, A. Kettrup, *Environ. Sci. Technol.* 34 (2000) 5092–5096.

[196] P.H. Ruokojärvi, A.H. Asikainen, K.A. Tuppurainen, J. Ruuskanen, *Sci. Total Environ.* 325 (2004) 83–94.
[197] M.E. Pandelova, D. Lenoir, A. Kettrup, K.-W. Schramm, *Environ. Sci. Technol.* 39 (2005) 3345–3350.
[198] B.K. Gullett, J.E. Dunn, K. Raghunathan, *Environ. Sci. Technol.* 34 (2000) 282–290.
[199] R.D. Griffin, *Chemosphere* 15 (1986) 1987.
[200] B.K. Gullett, K.R. Bruce, L.O. Beach, *Environ. Sci. Technol.* 26 (1992) 1938–1943.
[201] K. Raghunathan, B.K. Gullett, *Environ. Sci. Technol.* 30 (1996) 1827–1834.
[202] K. Everaert, J. Baeyens, *Chemosphere* 46 (2002) 439–448.
[203] P.A. Jensen, F.J. Frandsen, K. Dam-Johansen, HCl and SO_2 emissions from full-scale biomass-fired boilers, in: *Proceedings of the UEF Conference on Power Production in 21st Century: Impacts of Fuel Quality and Operations, Snowbird, Utah*, 2001.
[204] J.N. Knudsen, B. Sander, *Improved Operation of Full Scale Straw-fired CHP Plants with Low SO_2-emissions*, Technical Report Deliverable D-15, HIAL-biofuels for CHP plants, Elsam Engineering, 2004.
[205] P.A. Jensen, F.J. Frandsen, K. Dam-Johansen, B. Sander, *Energy Fuels* 14 (2000) 1280–1285.
[206] R.A. Durie, J.W. Milne, M.Y. Smith, *Combust. Flame* 30 (1977) 221–230.
[207] M. Steinberg, K. Schofield, *Proc. Combust. Inst.* 26 (1996) 1835–1843.
[208] M. Steinberg, K. Schofield, *Combust. Flame* 129 (2000) 453–470.
[209] V.I. Hanby, *J. Engn. Power* 96 (1974) 129–133.
[210] F.J. Kohl, G.J. Santoro, C.A. Stearns, D.E. Rosner, *J. Electrochem. Soc.* 126 (1979) 1054–1061.
[211] W.L. Fielder, C.A. Stearns, F.J. Kohl, *J. Electrochem. Soc.* 131 (1984) 2414–2417.
[212] K. Iisa, Y. Lu, K. Salmenoja, *Energy Fuels* 13 (1999) 1184–1190.
[213] K.A. Christensen, H. Livbjerg, *Aerosol Sci. Technol.* 33 (2000) 470–489.
[214] J.R. Jensen, L.B. Nielsen, C. Schultz-Møller, S. Wedel, H. Livbjerg, *Aerosol Sci. Technol.* 33 (2000) 490–509.
[215] S. Jimenez, J. Ballester, *Proc. Combust. Inst.* 30 (2005) 2965–2972.
[216] S. Jimenez, J. Ballester, *Combust. Flame* 140 (2005) 346–358.
[217] E. Bartholome, H. Sachse, *Z. Elektrochem.* 53 (1949) 326.
[218] D.H. Cotton, N.J. Friswell, D.R. Jenkins, *Combust. Flame* 17 (1971) 87–98.
[219] K.C. Saluja, *J. Inst. Fuel* (1972) 37–42, January.
[220] E.M. Bulewicz, D.G. Evans, P.J. Padley, *Proc. Combust. Inst.* 15 (1974) 1461–1470.
[221] B.S. Haynes, H. Jander, H.Gg. Wagner, *Proc. Combust. Inst.* 17 (1979) 1365–1374.
[222] A.N. Hayhurst, H.R.N. Jones, *Combust. Flame* 78 (1989) 339–356.
[223] A.S. Feitelberg, J.P. Longwell, A.F. Sarofim, *Combust. Flame* 92 (1993) 241–253.
[224] V. Babushok, W. Tsang, K.L. McNesby, *Proc. Combust. Inst.* 29 (2002) 2315–2323.
[225] P.A. Bonczyk, *Fuel* 70 (1991) 1403–1411.
[226] M.T. Cheng, M.J. Kirsch, T.W. Lester, *Combust. Flame* 77 (1989) 213–217.
[227] S. von Gersum, P. Roth, *Proc. Combust. Inst.* 24 (1992) 999–1006.
[228] S.A. Lawton, *Combust. Flame* 75 (1989) 175–181.
[229] H.G. Wolfhard, W.G. Parker, *Fuel* 29 (1950) 235–240.
[230] K.P. Schug, Y. Manheimer-Timnat, P. Yaccarino, I. Glassman, *Combust. Sci. Technol.* 22 (1980) 235–250.
[231] Ö.L. Gülder, *Combust. Flame* 92 (1993) 410–418.
[232] T. Ni, S.B. Gupta, R.J. Santoro, *Proc. Combust. Inst.* 25 (1994) 585–592.
[233] Ö.L. Gülder, B. Glavincevski, *Combust. Sci. Technol.* 77 (1991) 337–343.
[234] J.C. Wall, S.K. Hoekman, Fuel composition effects on heavy-duty diesel particulate emissions. *SAE Paper*, 841364, 1984.
[235] K.J. Baumgard, J.H. Johnson, The effect of low sulfur fuel and a ceramic particle filter on diesel exhaust particle size distributions. *SAE Paper*, 920566, 1992.
[236] E. Vouitsis, L. Ntziachristos, Z. Samaras, *Atmos. Environ.* 39 (2005) 1335–1345.
[237] M. Frenklach, J.P. Hsu, D.L. Miller, R.A. Matula, *Combust. Flame* 64 (1986) 141–155.
[238] J.A. Marr, D.M. Allison, L.M. Giovane, L.A. Yerkey, P. Monchamp, J.P. Longwell, J.B. Howard, *Combust. Sci. Technol.* 85 (1992) 65–76.
[239] J. Huang, S.M. Senkan, *Proc. Combust. Inst.* 26 (1996) 2335–2341.
[240] R.L. Scalla, G.E. McDonald, *Ind. Eng. Chem.* 45 (1953) 1497.
[241] R.L. Scalla, G.E. McDonald, *Proc. Combust. Inst.* 5 (1955) 316–324.
[242] J.T. McKinnon, J.B. Howard, *Combust. Sci. Technol.* 74 (1990) 175–197.
[243] T.J. Mitchell, S.W. Benson, S.B. Karra, *Combust. Sci. Technol.* 107 (1995) 223–260.
[244] A. Violi, A. D'Anna, A. D'Alessio, *Chemosphere* 42 (2001) 462–471.
[245] U. Wieschnowsky, H. Bockhorn, F. Fetting, *Proc. Combust. Inst.* 22 (1988) 343–352.
[246] K.C. Saluja, *Nature* 240 (1972) 350–351.
[247] J.B.A. Mitchell, J.M. Miller, *Combust. Flame* 75 (1989) 45–55.
[248] S.-L. Chung, N.-L. Lai, *J. Air Waste Manage. Assoc.* 42 (1992) 1082–1088.
[249] P.A. Bonczyk, *Combust. Flame* 51 (1983) 219.
[250] P.A. Bonczyk, *Combust. Sci. Technol.* 59 (1988) 143.
[251] M. Tappe, B.S. Haynes, J.H. Kent, *Combust. Flame* 92 (1993) 266–273.
[252] Y.-L. Wei, *Chemosphere* 37 (1998) 509–521.
[253] S.Y. Cheng, Y.L. Wei, C.J. Wu, *Bull. Environ. Contam. Toxicol.* 7 (2003) 675–681.
[254] V.J. Hall-Roberts, A.N. Hayhurst, D.E. Knight, S.G. Taylor, *Combust. Flame* 120 (2000) 578–584.
[255] H.F. Calcote, *Combust. Flame* 126 (2001) 1607–1610.
[256] M.W. Doherty, A.N. Hayhurst, S.F.S. Hunt, S.G. Taylor, *Combust. Flame* 126 (2001) 1611–1615.
[257] R.J. Bowser, F.J. Weinberg, *Nature* 249 (1974) 339.
[258] J.B.A. Mitchell, J.M. Miller, M. Sharpe, *Combust. Sci. Technol.* 74 (1990) 63–66.

[259] B.L. Wersborg, A.C. Yeung, J.B. Howard, *Proc. Combust. Inst.* 15 (1974) 1439.
[260] L.R. Peebles, P. Marshall, *Chem. Phys. Lett.* 366 (2002) 520–524.
[261] A. Burcat, B. Ruscic, *Third Millenium Ideal Gas and Condensed Phase Thermochemical Database for Combustion with Updates from Active Thermochemical Tables*, Technical Report TAE 960, Aerospace Engineering, Institute of Technology, Israel, 2005.
[262] A. Goumri, D.D. Shao, P. Marshall, *J. Chem. Phys.* 121 (2004) 9999–10005.
[263] R. Atkinson, D.L. Baulch, R.A. Cox, J.N. Crowley, R.F. Hampson, R. G Hynes, M.E. Jenkins, M.J. Rossi, J. Troe, *Atm. Chem. Phys.* 4 (2004) 1461–1738.
[264] H.K. Chagger, P.R. Goddard, P.L. Murdoch, A. Williams, *Fuel* 70 (1991) 1137–1142.
[265] D. Woiki, P. Roth, *Proc. Combust. Inst.* 26 (1996) 583–588.
[266] M. Oya, K. Tsuchiya, T. Asaba, Reduction of nitric oxide by hydrogen sulfide at high temperatures, in: *Proceedings of the First International Conference on Combustion Technologies for a Clean Environment, Vilamoura, Portugal*, 1991, pp. 26–31.
[267] H. Freund, H.B. Palmer, *Int. J. Chem. Kinet.* 9 (1977) 887.
[268] G. Black, L.E. Patrick, L.E. Jusinski, T.G. Slanger, *J. Chem. Phys.* 80 (1984) 4065–4070.
[269] M.A. Blitz, K.W. McKee, M.J. Pilling, M.A. Vincent, I.H. Hillier, *J. Phys. Chem. A* 106 (2002) 8406–8410.

Comments

Merdith Colket, United Technologies Research Center, USA. In your presentation, you proposed a mechanism involving SO_3 reaction with potassium. It is well established that a rate limiting process for the conversion of SO_2 to sulfuric acid and then drop formation within combustion exhaust streams is the oxidation of SO_2 to SO_3. Addition of SO_3 to water to form sulfuric acid is a subsequent and rapid process. Given that water is ubiquitous and in high concentration for most combustion systems, this process can expect to compete strongly with your proposed reaction sequence. Is this a valid concern?

Reply. The formation of sulfuric acid from SO_3 and H_2O proceeds readily at low temperatures (below 600 K) where it may involve more than one H_2O molecule [1]. However, at the temperatures for sulfate formation and nucleation (above 1000 K), H_2SO_4 is not thermally stable.

Reference

[1] T. Loerting, K.R. Liedling, *PNAS* 97 (2000) 8874–8878.

•

Katharina Kohse-Höinghaus, Universität Bielefeld, Germany. I would like to ask you about the influence of the fuel structure on these interactions you have outlined. Where there is detailed knowledge about the interactions of further elements than C, H, O (such as N, S, K, Na, etc.) with the hydrocarbon chemistry, this has been mostly derived from studies using structurally simple fuels, including methane, ethylene, etc. With regard to increasing interest in bio-derived fuels, chemical functionalities such as branched chains and unsaturated bonds may open up new pathways for interaction and add to the complexity. Some guidance with respect to prototypical fuel structure elements that you would find relevant (in particular regarding biomass burning) to study these interactions would be much appreciated.

Reply. This is an important point, which is not easily addressed, unfortunately. It is true that as you move towards more complex fuels, new pathways for interactions open up. However, the kind of interactions you may encounter depends on the combustion unit, as well as the fuel. In combustion of biomass or biomass-derived fuels in larger stationary facilities, the complex compounds, such as tars and oils, typically decompose rapidly into small hydrocarbons and other light gases. In small combustion units, such as stoves, they may have a larger lifetime and interactions with trace species may be a larger concern. Direct interactions between complex fuel structures and trace species would be important in the flame zone of stationary units and in systems with very short residence times, such as engines. Here the trace species could affect ignition/extinction, fuel oxidation rate, and PAH/soot formation. Information on these interactions for 'practical' fuels, such as engine reference fuels, as well as selected alcohols and ethers, are scarce and would be valuable.

APPENDIX 4

Available online at www.sciencedirect.com
ScienceDirect
Proceedings of the Combustion Institute 31 (2007) 339–347
Proceedings of the Combustion Institute
www.elsevier.com/locate/proci

Mechanisms of radical removal by SO_2

Christian Lund Rasmussen [a], Peter Glarborg [a,*], Paul Marshall [b]

[a] *Department of Chemical Engineering, Technical University of Denmark, DK-2800 Kgs. Lyngby, Denmark*
[b] *Department of Chemistry, University of North Texas, Denton, TX 76203-5070, USA*

Available online at www.sciencedirect.com
ScienceDirect
Proceedings of the Combustion Institute 31 (2007) 339–347
Proceedings of the Combustion Institute
www.elsevier.com/locate/proci

Mechanisms of radical removal by SO_2

Christian Lund Rasmussen [a], Peter Glarborg [a,*], Paul Marshall [b]

[a] Department of Chemical Engineering, Technical University of Denmark, DK-2800 Kgs. Lyngby, Denmark
[b] Department of Chemistry, University of North Texas, Denton, TX 76203-5070, USA

Abstract

It is well established from experiments in premixed, laminar flames, jet-stirred reactors, flow reactors, and batch reactors that SO_2 acts to catalyze hydrogen atom removal at stoichiometric and reducing conditions. However, the commonly accepted mechanism for radical removal, $SO_2 + H(+M) \rightleftharpoons HOSO(+M)$, $HOSO + H/OH \rightleftharpoons SO_2 + H_2/H_2O$, has been challenged by recent theoretical and experimental results. Based on *ab initio* calculations for key reactions, we update the kinetic model for this chemistry and re-examine the mechanism of fuel/SO_2 interactions. We find that the interaction of SO_2 with the radical pool is more complex than previously assumed, involving HOSO and SO, as well as, at high temperatures also HSO, SH, and S. The revised mechanism with a high rate constant for $H + SO_2$ recombination and with $SO + H_2O$, rather than $SO_2 + H_2$, as major products of the $HOSO + H$ reaction is in agreement with a range of experimental results from batch and flow reactors, as well as laminar flames.

Keywords: Sulfur chemistry; Inhibition; Kinetics

1. Introduction

The presence of SO_2 has been reported to catalyze H atom removal at medium to high temperatures in rich, premixed laminar flames [1–7] and laboratory reactors [8,9]. The mechanism for radical removal is commonly recognized to be of the type, $X + SO_2 + M \rightarrow XSO_2 + M$, $Y + XSO_2 \rightarrow XY + SO_2$, where X and Y may be H, O, or OH. The most important radical removal cycle under stoichiometric and reducing conditions is believed to be initiated by recombination of SO_2 with H to form an H/SO_2 adduct

$$SO_2 + H + M \rightleftharpoons H/SO_2 + M$$

followed by recycling of this adduct to SO_2 by reaction with H or OH. The H/SO_2 adduct is most likely HOSO, which is thermally more stable than the HSO_2 isomer,

$$SO_2 + H(+M) \rightleftharpoons HOSO(+M) \quad (R9)$$
$$HOSO + H \rightleftharpoons SO_2 + H_2 \quad (R27)$$
$$HOSO + OH \rightleftharpoons SO_2 + H_2O \quad (R29)$$

The reaction numbers refer to the listing in Table 1. This sequence of reactions has been proposed to be the principal radical sink in fuel-rich flames doped with SO_2 [2,5,7]. However, due to uncertainty in the H+SO_2 reaction rate and in the fate of the HOSO intermediate, the mechanism of inhibition is still in question. There are no direct measurements of the $H + SO_2$ recombination rate at high temperatures. Theoretical work [10–12] as well as values deduced from flames [13], batch reactor [8], and flow reactor experiments [9] imply that the reaction is comparatively fast, while other experimental results indicate a much slower reaction [14]. Regarding HOSO, recent theoretical

* Corresponding author. Fax: +45 4588 2258.
E-mail address: pgl@kt.dtu.dk (P. Glarborg).

1540-7489/$ - see front matter © 2006 Published by Elsevier Inc. on behalf of The Combustion Institute.
doi:10.1016/j.proci.2006.07.249

Table 1
Selected reactions from the H/S/O subset

	Reaction	A	β	E_a	Reference
1.	$^3SO + H + M \rightleftharpoons HSO + M^a$	1.9×10^{20}	−1.31	662	est, Troe formalism
2.	$^3SO + O(+M) \rightleftharpoons SO_2(+M^a)$	3.2×10^{13}	0.0	0	[14]
	Low pressure limit:	1.2×10^{21}	−1.54	0	
	Troe parameters: 0.55 10^{-30} 10^{30}				
3.	$^3SO + OH \rightleftharpoons SO_2 + H$	1.1×10^{17}	−1.35	0	[20]
4.	$^3SO + OH(+M) \rightleftharpoons HOSO(+M^a)$	1.6×10^{12}	0.50	−400	[10]
	Low pressure limit:	9.5×10^{27}	−3.48	970	
5.	$^3SO + O_2 \rightleftharpoons SO_2 + O$	7.6×10^{3}	2.37	2970	[21]
6.	$^3SO + HO_2 \rightleftharpoons SO_2 + OH$	3.7×10^{3}	2.42	7660	est, *ab initio*/TST
7.	$^1SO + M \rightleftharpoons {}^3SO + M$	1.0×10^{13}	0.0	0	est
8.	$^1SO + O_2 \rightleftharpoons SO_2 + O$	1.0×10^{13}	0.0	0	est
9.	$SO_2 + H(+M) \rightleftharpoons HOSO(+M^a)$	2.4×10^{8}	1.63	7340	[12]
	Low pressure limit:	1.8×10^{37}	−6.14	11070	
	Troe parameters: 0.283 272 3995				
10.	$SO_2 + H(+M) \rightleftharpoons HSO_2(+M^a)$	5.3×10^{8}	1.59	2470	[12]
	Low pressure limit:	1.4×10^{31}	−5.19	4510	
	Troe parameters: 0.390 167 2191				
11.	$SO_2 + O(+M) \rightleftharpoons SO_3(+M^a)$	3.7×10^{11}	0.0	1689	[22]
	Low pressure limit:	2.4×10^{27}	−3.60	5186	
	Troe parameters: 0.442 316 7442				
	$SO_2 + O(+N_2) \rightleftharpoons SO_3(+N_2)$	3.7×10^{11}	0.0	1689	[22,23]
	Low pressure limit:	2.9×10^{27}	−3.58	5206	
	Troe parameters: 0.43 371 7442				
12.	$SO_2 + OH(+M) \rightleftharpoons HOSO_2(+M^a)$	5.7×10^{12}	−0.27	0	[17]
	Low pressure limit:	1.7×10^{27}	−4.09	0	
	Troe parameters: 0.10 10^{-30} 10^{30}				
13.	$SO_2 + CO \rightleftharpoons {}^3SO + CO_2$	1.9×10^{13}	0.0	65900	[24]
14.	$SO_2 + S \rightleftharpoons {}^3SO + {}^3SO$	6.0×10^{-16}	8.21	9600	[25]
15.	$SO_3 + H \rightleftharpoons SO_2 + OH$	5.5×10^{10}	0.99	3740	est, *ab initio*/TST
16.	$SO_3 + O \rightleftharpoons SO_2 + O_2$	7.8×10^{11}	0.0	6100	[23,26]
17.	$SO_3 + {}^3SO \rightleftharpoons SO_2 + SO_2$	7.6×10^{3}	2.37	2980	[27]
18.	$HSO + H \rightleftharpoons {}^3SO + H_2$	1.0×10^{13}	0.0	0	est
19.	$HSO + H \rightleftharpoons SH + OH$	4.9×10^{19}	−1.86	1560	[16]
20.	$HSO + H \rightleftharpoons S + H_2O$	1.6×10^{9}	1.37	−340	[16]
21.	$HSO + O \rightleftharpoons SO_2 + H$	4.5×10^{14}	−0.40	0	[16]
22.	$HSO + O \rightleftharpoons {}^3SO + OH$	1.4×10^{13}	0.15	300	[16]
23.	$HSO + O_2 \rightleftharpoons HSO_2 + O$	8.4×10^{-7}	5.10	11312	est, *ab initio*/TST
24.	$HSO + OH \rightleftharpoons {}^3SO + H_2O$	1.7×10^{9}	1.03	470	[16]
25.	$HOSO(+M) \rightleftharpoons HSO_2(+M^a)$	1.0×10^{9}	1.03	50000	[10]
	Low pressure limit:	1.7×10^{35}	−5.64	55400	
	Troe parameters: 0.40 10^{-30} 10^{30}				
26.	$HOSO + H \rightleftharpoons {}^1SO + H_2O$	2.4×10^{14}	0.0	0	[15]
27.	$HOSO + H \rightleftharpoons SO_2 + H_2$	1.8×10^{7}	1.72	−1286	[15]
28.	$HOSO + O_2 \rightleftharpoons SO_2 + HO_2$	9.6×10^{1}	2.36	−10130	est, *ab initio*/TST ($T > 800$ K)
29.	$HOSO + OH \rightleftharpoons SO_2 + H_2O$	6.0×10^{12}	0.0	0	est, see text
30.	$HSO_2 + H \rightleftharpoons SO_2 + H_2$	5.0×10^{12}	0.46	−262	[15]
31.	$HSO_2 + O_2 \rightleftharpoons SO_2 + HO_2$	1.1×10^{3}	3.20	−235	est, *ab initio*/TST
32.	$HSO_2 + OH \rightleftharpoons SO_2 + H_2O$	1.0×10^{13}	0.0	0	est
33.	$HOSO_2 + O_2 \rightleftharpoons SO_3 + HO_2$	7.8×10^{11}	0.0	656	[28]
34.	$SH + O \rightleftharpoons {}^3SO + H$	1.0×10^{14}	0.0	0	[14]
35.	$S + OH \rightleftharpoons {}^3SO + H$	4.0×10^{13}	0.0	0	[29]
36.	$S + H_2 \rightleftharpoons SH + H$	1.4×10^{14}	0.0	19300	[30]

Units are mol, cm, s, and cal.
[a] Enhanced third-body efficiencies: $N_2 = 1.5$, $SO_2 = 10$, $H_2O = 10$, except for reactions (R9), (R10) where $N_2 = 1.0$; (R11), where $N_2 = 0.0$, and (R12), where $N_2 = 1.0$, $SO_2 = 5$, $H_2O = 5$.

investigations of the HOSO + H reaction [15] indicate that $SO + H_2O$, and not $SO_2 + H_2$, is the major product channel. Hence,

$$HOSO + H \rightleftharpoons {}^1SO + H_2O \quad (R26)$$

In the ground state SO is a triplet (^3SO), but in reaction (R26) it is formed in the singlet state. Both ^1SO and ^3SO are reactive towards O_2 to make $SO_2 + O$ in which case, the HOSO + H reaction becomes chain propagating rather than

terminating and the efficiency of the radical removal cycle decreases.

The objective of the present work is to re-examine the interaction of SO_2 with the radical pool at atmospheric pressure under stoichiometric and fuel-rich combustion conditions. The H/S/O reaction mechanism is updated and a number of key reactions are analyzed. Modeling predictions are compared with experimental results from a batch reactor [8], flow reactors [9,14] and laminar flames [5] for oxidation of H_2 and/or CO doped with SO_2, and the mechanisms of inhibition are discussed.

2. Reaction mechanism

The proposed reaction mechanism consists of a description of the CO/H_2 oxidation system and a subset describing sulfur reactions. The thermochemistry was mostly adopted from previous modeling studies [14,16], except for HOSO/HSO_2 [10], and $HOSO_2$ [17]. For the singlet SO species introduced in the present mechanism, we have estimated a heat of formation of $\Delta_f H_{298} = 23.90$ kcal/mol and an entropy of $S_{298} = 50.89$ cal/mol K. From *ab initio* CBS-QB3 calculations the excitation energy for the first singlet state was estimated to be 22.4 kcal/mol. This value is somewhat higher than the estimate from Huber and Herzberg [18] of 18.1 kcal/mol, but it is in agreement with the corresponding value for O_2 (22.7 kcal/mol).

The sulfur reaction chemistry was mainly adopted from Alzueta et al. [14]. However, a number of rate constants were modified according to *ab initio* CBS-QB3 calculations combined with transition state theory (TST), and the S_2H_x subset was updated with data from Sendt et al. [19]. Data for some important reactions in the sulfur subset are found in Table 1.

Interactions between SO_2 and the radical pool are primarily facilitated by recombination with H (R9, R10) and to a lesser extent O (R11). Recombination of SO_2 with OH is not important under the conditions of interest in this study due to the low thermal stability of $HOSO_2$ [17]. There are no direct measurements of the $SO_2 + H(+M)$ recombination reaction at high temperatures, but theoretical estimates are in fairly good agreement [10–12]. We have adopted the rate constants for formation of HOSO (R9) and HSO_2 (R10) from the recent work of Blitz et al. [12]. The recombination of H and SO_2 competes with the reaction $SO_2 + H \rightleftharpoons SO + OH$ (−R3), which is now well characterized over a wide temperature range [20,31]. The rate coefficients for the recombination of SO_2 with O to form SO_3 were drawn from recent work by the authors [22,23].

The key reactions of HOSO are those with H (R26, R27), OH (R29) and O_2 (R28). A recent *ab initio* study [15] of the HOSO + H reaction indicates a very fast reaction yielding >95% $^1SO+H_2O$ (R26) following an addition/elimination mechanism. Formation of SO in the singlet state conserves spin; however it is possible that intersystem crossing occurs during the course of reaction (R26) and that the triplet state occurs directly. The alternative abstraction channel to $SO_2 + H_2$ (R27) is significantly slower due to a bottleneck along the reaction coordinate. The HOSO + OH reaction (R29) could be abstraction or addition/elimination that either way leads to $SO_2 + H_2O$. We expect this reaction to proceed without a barrier.

In previous modeling work [9,14] the rate constant for the $HOSO + O_2$ reaction (R28) was adopted from the work of Lovejoy et al. [32]. However, in their work the H/SO_2 isomer was formed from the reaction of HSO with NO_2. This reaction is likely to form HSO_2 rather than HOSO and for this reason their measurements are expected to apply to the $HSO_2 + O_2$ reaction rather than $HOSO + O_2$. The $HOSO + O_2$ reaction is a system where both reactants and products can hydrogen bond (by about 5–6 kcal/mol) and we estimate the H-transfer barrier between the two complexes to be modest. Consequently, we expect no overall energy barrier for this exothermic process, which is in agreement with the recent theoretical study by Wang and Hou [33]. Wang and Hou estimate the reaction to be very fast due to an "outer" transition state that leads into an initial adduct. However, the formation of this transition state is only rate limiting at low temperatures. At elevated temperatures an "inner" transition state containing a tight entropy bottleneck comes into play. From our *ab initio* calculations, we estimate the 1000–1500 K rate constant to be of the order of 10^{11} cm^3/mol s and decreasing with temperature. These values were obtained from a simple transition state theory approach and are expected to represent an upper limit.

The SO formed in reaction (R26) is in the singlet state if spin is conserved [15]. It would be expected that ^1SO is more reactive than the ground triplet state ^3SO. However, under the dilute conditions of interest here (see below), ^1SO is mostly quenched to the ground state, even though a fraction may react with O_2. We have estimated a rate for the collisional intersystem crossing (R7) of 10^{13} cm^3/mol s. Modeling results are not sensitive to this value. Reactions with H_2 and H_2O were included in the mechanism, but they are too endothermic to gain importance. The reaction of ^3SO with O_2 (R5) is well characterized experimentally [14]. This is not the case for the reaction of ^3SO with HO_2 (R6), but our *ab initio* calculations indicate that this reaction is relatively fast and proceeds without barriers. Recombination of SO with H atoms is a potential radical sink [14], but according to our analysis via

the Troe formalism the reaction is slow. The present estimate is in good agreement with estimates previously used in modeling [14].

3. Results and discussion

For validation of the kinetic model, calculations were compared with experimental data on the effect of SO_2 addition on oxidation of H_2 and/or CO in a batch reactor [8], flow reactors [9,14] and laminar premixed flames [5]. The flow reactor data were obtained in laminar flow reactors designed to approximate plug flow and the data were modeled with SENKIN [34] from the CHEMKIN library [35]. SENKIN performs an integration in time. The results from the SENKIN calculations were compared to experimental data using the nominal residence time in the reactor. The batch reactor and flame data were also simulated with SENKIN, as discussed below.

3.1. Batch reactor results

We first consider a series of batch reactor experiments [8] where the inhibiting effect of SO_2 addition on the H_2/O_2 reaction at the second pressure limit of explosion is investigated at 784 K. Pure H_2, O_2, and SO_2 were premixed in specific ratios at a pressure greater than the second explosion limit. Gases were then withdrawn from the vessel until explosion occurred [8]. These conditions are modeled as an adiabatic batch reactor (SENKIN) where a temperature increase >100 K within a reactor residence time of 0.1 s constitutes the criterion for explosion. The second pressure limit of explosion is governed by the OH formation reactions: $H + O_2 \rightleftharpoons O + OH$ and $O + H_2 \rightleftharpoons H + OH$. Termination occurs via $H + O_2(+M) \rightleftharpoons HO_2(+M)$ and subsequent loss of HO_2 at the surface. The latter has been accounted for in the mechanism by the reaction $HO_2 \rightarrow wall$ with a fitted rate constant of $10^7\ s^{-1}$. It has been necessary to extend the loss of H atoms at the surface by enhancing the third-body efficiencies of the main components H_2 and O_2 in the reaction $H + O_2(+M) \rightleftharpoons HO_2(+M)$ until experimental and numerical predictions match each other at zero SO_2 addition. The resulting third-body efficiencies are 3.3 and 1.29 for H_2 and O_2, respectively, which is a 65% increase from the original values [36].

Figure 1 shows a satisfactory agreement between model predictions and measurements of the second pressure limit as a function of SO_2 concentration at four different H_2/O_2 mixing ratios. Webster and Walsh [8] attributed the observed reduction of the pressure limit to H atom removal by the $SO_2 + H(+M)$ recombination reaction (R9). This is confirmed by a sensitivity analysis

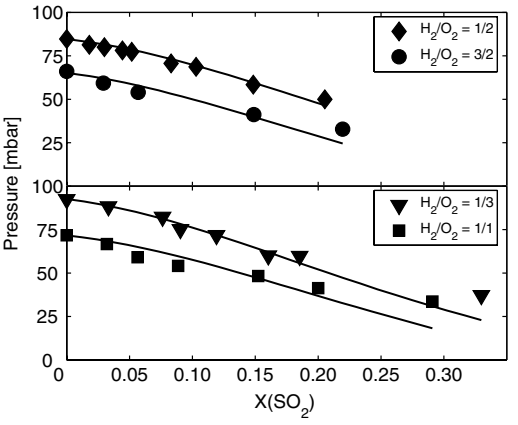

Fig. 1. Comparison between experimental data [8] and modeling predictions for the effect of SO_2 on the second pressure limit of explosion of H_2/O_2 mixtures in a batch reactor at 784 K. Initial conditions: Premixed $H_2/O_2/SO_2$ in specific ratios at a pressure greater than the second limit. Withdrawal of gases until explosion occurs. For modeling purpose, explosion must occur within 0.1 s to count.

that identifies (R9) as the single most important bottleneck in the sulfur conversion network at all four mixing ratios. Hence, at the pressure limit of explosion and a mixing ratio of $H_2/O_2 = 1/3$, the first order sensitivity coefficient of (R9) yields a magnitude of about 15–20% of the sensitivity coefficient of the most important reaction in the system; $H + O_2 \rightleftharpoons O + OH$. This value increases to about 25–30% when $H_2/O_2 = 3/2$.

Webster and Walsh estimated that the rate constant of (R9) at 784 K had to be 2.0 times the rate constant of reaction $H + O_2(+M) \rightleftharpoons HO_2(+M)$ to match the observed reduction of the pressure limit. In the proposed mechanism k_9 is only ~0.4 times this value. However, the satisfactory agreement between experimental and numerical data supports the present rate constant.

3.2. Flow reactor results

Laboratory reactor experiments show apparently conflicting results on the effect of SO_2 on CO or CO/H_2 oxidation at intermediate temperatures. Results from jet-stirred reactors and flow reactors under stoichiometric and fuel-rich conditions [9] support the observation from flames that SO_2 has a strong potential for removing radicals. However, other flow reactor experiments [14] conducted at similar stoichiometries and similar SO_2 levels, but with much lower fuel/oxidizer concentrations, show no evidence for the H removal cycle. As a result, the two studies provide recommendations for the value of k_9 that differ by more than an order of magnitude [9,14]. In the present study, we compare modeling

predictions to flow reactor data from both these studies.

Flow reactor results [9] from CO/H_2 oxidation in the presence and absence of SO_2 are compared with model predictions in Figs. 2 and 3 under stoichiometric and fuel-rich conditions, respectively. In the model, loss of radicals on the quartz surface was taken into account through a first-order hydrogen loss reaction [9]. In both cases, the presence of SO_2 causes a considerable inhibition of the fuel oxidation. The fact that the experimental results can be modeled satisfactory with a lower rate constant for the $SO_2 + H(+M)$ reaction (R9) than advocated by Dagaut et al. [9] and with the $HOSO + H$ reaction now being chain propagating rather than chain terminating is partly due to the lower present rate constant for $HOSO + O_2$. The interaction of SO_2 with the radical pool is discussed later.

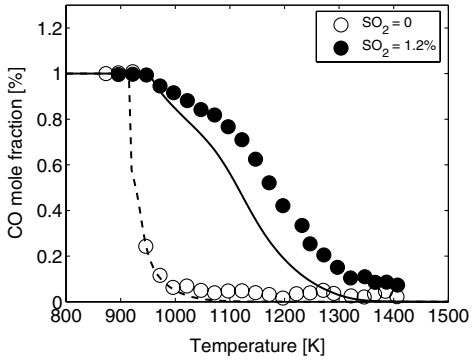

Fig. 2. Comparison between experimental data [9] and modeling predictions for the effect of SO_2 on the oxidation of CO/H_2 mixture under stoichiometric conditions in a flow reactor. Initial conditions: 1.0% CO, 1.0% H_2, 1.0% O_2, 2.0% H_2O, balance N_2, without and with 1.2% SO_2. The residence time is 192/T.

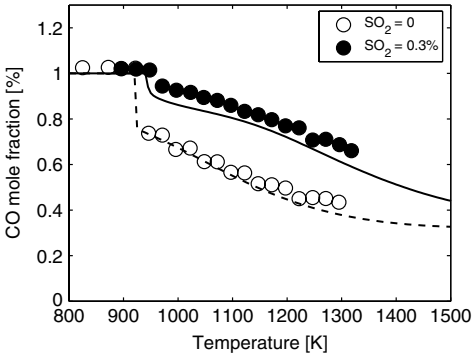

Fig. 3. Comparison between experimental data [9] and modeling predictions for the effect of SO_2 on the oxidation of CO/H_2 mixture under fuel-rich conditions in a flow reactor. Initial conditions: 1.0% CO, 1.0% H_2, 0.5% O_2, 2.0% H_2O, balance N_2, without and with 0.3% SO_2. The residence time is 192/T.

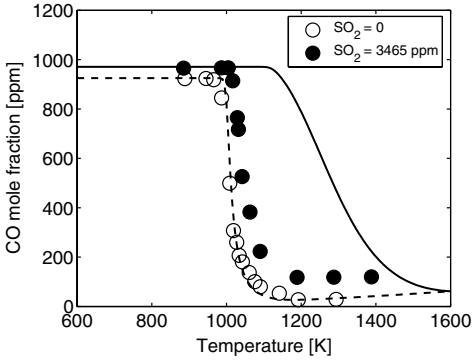

Fig. 4. Comparison between experimental data [14] and modeling predictions for the effect of SO_2 on the oxidation of CO in a flow reactor. Initial conditions without SO_2: 925 ppm CO, 260 ppm O_2, 2.0% H_2O, balance N_2. The residence time is 200/T. Initial conditions with 3465 ppm SO_2: 971 ppm CO, 253 ppm O_2, 2.0% H_2O, balance N_2. The residence time is 192/T.

Figure 4 compares modeling predictions with flow reactor data from Alzueta et al. [14]. These data were obtained under fuel-rich conditions, with SO_2 levels similar to those of Fig. 3, but with CO as fuel, and fuel and oxygen concentrations about two orders of magnitude lower. While the experimental data indicate little inhibiting effect of SO_2 under these conditions, the modeling predictions show a considerable effect and overestimate the onset temperature for rapid oxidation of CO by more than 100 K after which, it underpredicts the fuel conversion rate. We have currently no explanation for this discrepancy. Apparently, there is a chain branching mechanism active for the conditions of Fig. 4, which is less important at high fuel/oxidizer concentrations. Perhaps the high SO_2 level combined with low fuel and oxidizer levels enhance the impact of surface reactions in the reactor; sulfur species are known to be very active on surfaces [37].

3.3. Flame results

Following Alzueta et al. [14], we take a closer look at the flame data from Kallend [5]. Measured H atom concentration profiles in the post-flame zone of SO_2-doped premixed $H_2/O_2/N_2$ flames have been used to estimate rate constants for both the $SO_2 + H(+M)$ recombination reaction (R9) and the subsequent conversion of HOSO by H and OH [13]. It was found that at lower temperatures (<1720 K) removal of H atoms was first order, consistent with reaction (R9) being rate determining, while it was second order at high temperatures (>2000 K).

This was interpreted in terms of partial equilibration of reaction (R9), causing the HOSO

consumption steps to determine the rate of the reaction cycle [5]. However, rate constant derivation requires well-defined conditions as well as negligible interference from side-reactions that are not characterized with considerable accuracy. The latter is rarely satisfied in complex high temperature reaction systems like flames and the present data are no exception.

Figure 5 shows comparisons between calculated and measured downstream H atom concentration profiles from three SO_2 doped and one undoped flame with temperatures of 1695, 1980, and 2115 K [5]. Following Alzueta et al. [14], we have modeled these flames assuming plug flow, which is reasonable since temperature and concentration gradients are small in the post-flame region. Despite the changes made in the present model, such as making HOSO + H chain-propagating rather than terminating, all flames show satisfactory agreement between experiments and numerical predictions. Consistent with the previous discussion [14], we find that the sensitivity of sulfur reactions decrease with increasing temperature as recombination reactions in the O/H radical pool, such as H + H(+M) and H + OH, with H_2O as the predominant third-body collision partner, provide an increasingly dominant H atom sink with the temperature.

3.4. Sulfur catalyzed radical decay

According to the present calculations, the interaction of SO_2 with the radical pool is quite complex and involves several chain sequences where characteristic sulfur compounds are recirculated in ways that facilitate a net termination of chain carrying radicals. These cyclic mechanisms are shown together in Fig. 6. However, their fractional contributions to the sulfur flux are very dependent on the reaction conditions.

SO_2 is largely consumed by recombination with H atoms (R9) forming HOSO, which also reacts mainly with H (R26). The competing H atom addition/elimination reaction (−R3) yielding $^3SO + OH$, mainly operates as a ^3SO sink via (R3); as indicated in Fig. 6. However, at high temperatures (>1700 K) the sulfur flux is initially reversed and (−R3) becomes the dominating SO_2 consumption channel. The recombination reaction (R9) eventually takes over as the main SO_2 sink after which, the sulfur flux through

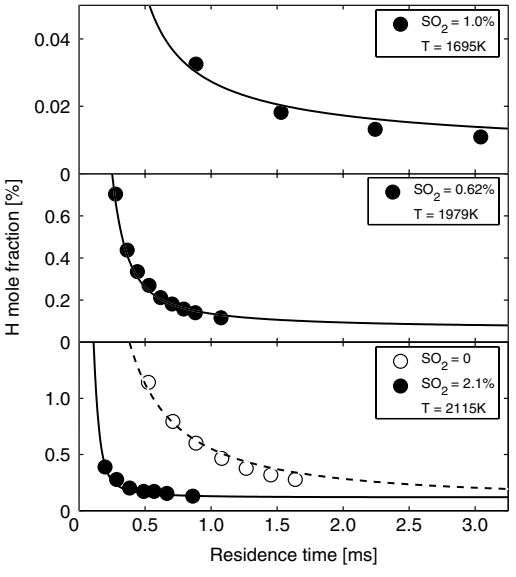

Fig. 5. Comparison between experimental data [5] and (plug flow) model predictions for the downstream H atom concentration in atmospheric pressure $H_2/O_2/N_2$ flames doped with SO_2. The calculated H atom profiles are shifted in time to match the experimental data at the largest gradient. (Top) Feed composition $H_2/O_2/N_2 = 4/1/6$ with 1.0% SO_2. (Middle) Feed composition $H_2/O_2/N_2 = 4/1/4$ with 0.62% SO_2. (Bottom) Feed composition $H_2/O_2/N_2 = 3/1/4$ with no and 2.1% SO_2, respectively. The listed temperature is the mean value of 2107 and 2123 K for the undoped and doped flame, respectively.

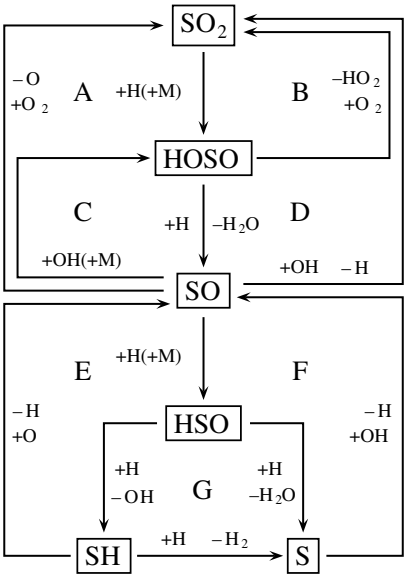

Fig. 6. Cyclic chain terminating sulfur sequences. Cycles are denoted by capital letters. The alphabetic order roughly reflects the important sequences at atmospheric pressure and increasing temperature from 1000 to 2000 K. The sum of each individual sequence yields (A) $H + H + O_2 \rightleftharpoons H_2O + O$; (B) $H + O_2 \rightleftharpoons HO_2$, (C, D, and F) $H + OH \rightleftharpoons H_2O$, (E) $H + O \rightleftharpoons OH$, (G): $H + H \rightleftharpoons H_2$. In the diagram we have implicitly included a rapid intersystem crossing from singlet to triplet SO. Mechanism (G) differs from (F) by the intermediate conversion of HSO to SH before yielding S. Mechanism (B) is not truly chain terminating, but replaces a H atom with the less reactive HO_2 radical.

(R3) becomes the main SO_2 formation channel. This behavior is not strongly affected by the reaction stoichiometry, whereas increasing temperature promotes the flux through (−R3) and at temperatures roughly above 1900 K, this SO_2 drain predominates throughout most of the fuel conversion.

The $^3SO + OH$ addition/elimination reaction (R3) in sequence (D) competes with the corresponding addition reaction $^3SO + OH(+M)$ (R4) from sequence (C). At lower temperatures (<1500 K) and atmospheric pressure, (D)/(C) ≈ 3–4, but this ratio decreases with increasing temperature until (C) > (D) around 1900 K. This competition between (C) and (D) is very sensitive to the pressure whereas the reaction stoichiometry has little influence.

Sequence (A) and (B) involve conversion of ^3SO and HOSO, respectively, by molecular oxygen. These two reactions are most important under fuel-rich conditions, low temperatures and high SO_2 concentrations. These conditions serve to suppress the main OH formation reactions ($H + O_2 \rightleftharpoons O + OH$ and $O + H_2 \rightleftharpoons H + OH$). They are partly obtained in the lower temperature range of the flow reactor experiments in Figs. 2 and 3, where mechanism (A) and (B) govern the main sulfur conversion. However, calculations indicate that mechanism (B) quickly vanishes from the reaction network as the temperature rises above 1000 K.

Sequence (A) also plays a minor role in the batch reactor experiments in Fig. 1. The substantial heat release at the time of the explosion combined with the high availability of oxygen promote the OH formation reactions and make sequence (D) the dominating sulfur conversion mechanism. However, flux analysis reveals that the SO pool is also subjected to a minor drain via mechanism (A), which is facilitated by the high absolute concentration of molecular oxygen. It is noteworthy that a significant part of this drain is facilitated by reaction (R8) where ^1SO is the reactant. A rough determination of the ratio between the two mechanisms indicates a decrease from (D)/(A) ≈ 4.5 to 2.5 when the mixing ratio in the explosion experiments changes from $H_2/O_2 = 3/2$ to 1/3.

H atom addition to ^3SO (R1), forming HSO, is only important at high temperatures (>1500 K). Consequently, sequence (E)–(G) only plays a significant role in the flame experiments. The ratio (C + D)/(E + F + G) is roughly 1/1 in all the doped flames. The reaction SH + O (E) only contributes significantly in the 1979 and 2115 K flames, whereas (F) and (G) predominate in the 1695 K flame. High temperatures favor formation of S over SH from HSO, which makes (F) > (E + G) in the 2115 K flame. However, since the increasing flame temperature also favors the pure O/H radical recombination reactions, the effect of the sulfur catalyzed H atom decay gradually diminishes in this temperature range.

Alzueta et al. [14] proposed that S_2 sulfur species might play a role for radical removal in these flames. However, according to our present understanding of the S_2 chemistry [19] and the H/S/O interactions discussed in this work, the S_2 species have only little impact on the radical pool.

4. Conclusions

Based on recent theoretical results for key reactions, the kinetic model for the H/S/O chemistry has been revised and the mechanism of fuel/SO_2 interaction has been re-examined. It is shown that the interaction of SO_2 with the radical pool is more complex than previously assumed, involving HOSO and SO, as well as, at high temperatures also HSO, SH, and S. The revised mechanism with a high rate constant for $H + SO_2$ recombination to HOSO, and with $SO + H_2O$, rather than $SO_2 + H_2$, as major products of the HOSO + H reaction, is in agreement with a range of experimental results from batch and flow reactors to laminar flames.

Acknowledgments

C.L.R. and P.G. acknowledge support from the CHEC (Combustion and Harmful Emission Control) Research Program and from PSO-Elkraft (Grant FU-2207). P.M. thanks the National Science Foundation (Grant CTS-0113605), the Robert A. Welch Foundation (Grant B-1174) and the UNT Faculty Research Fund.

References

[1] C.P. Fenimore, G.W. Jones, *J. Phys. Chem.* 69 (1965) 3593–3597.
[2] C.J. Halstead, D.R. Jenkins, *Trans. Faraday Soc.* 65 (1969) 3013–3022.
[3] A.S. Kallend, *Combust. Flame* 13 (1969) 324–327.
[4] R.A. Durie, G.M. Johnson, M.Y. Smith, *Combust. Flame* 17 (1971) 197–203.
[5] A.S. Kallend, *Combust. Flame* 19 (1972) 227–236.
[6] O.I. Smith, S.-N. Wang, S. Tseregounis, C.K. Westbrook, *Combust. Sci. Technol.* 30 (1983) 241–271.
[7] M.R. Zachariah, O.I. Smith, *Combust. Flame* 69 (1987) 125–139.
[8] P. Webster, A.D. Walsh, *Proc. Combust. Inst.* 10 (1965) 463–472.
[9] P. Dagaut, F. Lecomte, J. Mieritz, P. Glarborg, *Int. J. Chem. Kinet.* 35 (2003) 564–575.
[10] A. Goumri, J.-D.R. Rocha, D. Laakso, C.E. Smith, P. Marshall, *J. Phys. Chem. A* 103 (1999) 11328–11335.
[11] K.J. Hughes, M.A. Blitz, M.J. Pilling, S.H. Robertson, *Proc. Combust. Inst.* 29 (2002) 2431–2437.

[12] M.A. Blitz, K.J. Hughes, M. Pillling, S.H. Robertson, *J. Phys. Chem. A* 110 (2006) 2996–3009.
[13] D.L. Baulch, D.D. Drysdale, J. Duxbury, S.J. Grant, *Evaluated Data for High Temperature Reactions*, vol. 3, Butterworth, London, 1976.
[14] M.U. Alzueta, R. Bilbao, P. Glarborg, *Combust. Flame* 127 (2001) 2234–2251.
[15] X. Hu, P. Marshall, Reactions of H/SO_2 Adducts with Atomic Hydrogen, poster presented at the 18th International Symposium on Gas Kinetics, Bristol, UK, August, 7–12, 2004.
[16] P. Glarborg, D. Kubel, K. Dam-Johansen, H.M. Chiang, J.W. Bozzelli, *Int. J. Chem. Kinet.* 28 (1996) 773–790.
[17] M.A. Blitz, K.J. Hughes, M.J. Pilling, *J. Phys. Chem. A* 107 (2003) 1971–1978.
[18] K.P. Huber, G. Herzberg, *Molecular spectra and molecular structure IV. Constants of diatomic molecules*, Van Nostrand Reinhold, New York, 1979.
[19] K. Sendt, M. Jazbec, B.S. Haynes, *Proc. Combust. Inst.* 29 (2002) 2439–2446.
[20] M.A. Blitz, K.W. McKee, M. Pillling, *Proc. Combust. Inst.* 28 (2000) 2491–2497.
[21] K. Tsuchiya, K. Kamiya, H. Matsui, *Int. J. Chem. Kinet.* 29 (1997) 57–66.
[22] J. Naidoo, A. Goumri, P. Marshall, *Proc. Combust. Inst.* 30 (2005) 1219–1225.
[23] A. Yilmaz, L. Hindiyarti, A.D. Jensen, P. Glarborg, P. Marshall, *J. Phys. Chem. A* 110 (2006) 6654–6659.
[24] G.B. Bacskay, J.C. Mackie, *J. Phys. Chem. A* 109 (2005) 2019–2025.
[25] Y. Murakami, S. Onishi, T. Kobayashi, N. Fujii, N. Isshiki, K. Tsuchiya, A. Tezaki, H. Matsui, *J. Phys. Chem. A* 107 (2003) 10996–11000.
[26] O.I. Smith, S. Tseregounis, S.-N. Wang, *Int. J. Chem. Kinet.* 14 (1982) 679–697.
[27] P. Glarborg, P. Marshall, *Combust. Flame* 141 (2004) 22–38.
[28] R. Atkinson, D.L. Baulch, R.A. Cox, R.F. Hampson, J.A. Kerr, J. Troe, *J. Phys. Chem. Ref. Data* 21 (1992) 1125–1568.
[29] W.B. DeMore, S.P. Sander, D.M. Golden, R.F. Hampson, M.J. Kurylo, C.J. Howard, A.R. Ravishankara, C.E. Kolb, M.J. Molina, Chemical Kinetics and Photochemical Data for Use in Stratospheric Modeling. Evaluation Number 12, JPL Publication 97–4 (1997).
[30] H. Shiina, A. Miyoshi, H. Matsui, *J. Phys. Chem. A* 102 (1998) 3556–3559.
[31] Y. Murakumi, S. Onishi, N. Fujii, *J. Phys. Chem. A* 108 (2004) 8141–8144.
[32] E.R. Lovejoy, N.S. Wang, C.J. Howard, *J. Phys. Chem.* 91 (1987) 5749–5755.
[33] B. Wang, H. Hou, *Chem. Phys. Lett.* 410 (2005) 235–241.
[34] A. Lutz, R.J. Kee, J.A. Miller, SENKIN: a fortran program for predicting homogenous gas phase chemical kinetics with sensitivity analysis, Sandia Report SAND87–8248, Sandia National Laboratories, Livermore, CA (1987).
[35] R.J. Kee, F.M. Rupley, J.A. Miller, CHEMKIN–II: a fortran chemical kinetics package for the analysis of gas-phase chemical kinetics, Sandia Report SAND89-8009, Sandia National Laboratories, Livermore, CA (1989).
[36] M.A. Mueller, R.A. Yetter, F.L. Dryer, *Proc. Combust. Inst.* 27 (1998) 177–184.
[37] C.F. Cullis, M.R.F. Mulcahy, *Combust. Flame* 18 (1972) 225–292.

Comments

M.C. Lin, Emory University, USA. The potential energy profile of the H + HOSO reaction looks quite similar to the H + HONO reaction which we studied with C.F. Melius [1]. In the latter reaction the H-for-OH substitution process, in addition to H_2O and H_2 production, was found to be dominant. Is the H-for-OH replacement process also important in the H + HOSO reaction?

Reference

[1] C.-C. Hsu, M.C. Lin, A.M. Mebel, C.F. Melius, *J. Phys. Chem. A* 101 (1997) 60.

Reply. There is a difference from the nitrogen analog, in that the HSO + OH channel is endothermic with respect to H + HOSO. This means that even if there is a large A factor, this channel is minor compared to the fast exothermic channels that lead to $H_2O + SO$ and $H_2 + SO_2$.

•

John Kiefer, University Illinois at Chicago, USA. Is there no direct abstraction $H + HOSO \rightarrow H_2 + SO_2$? Even at high temperature?

Reply. There certainly is direct abstraction. Our CASPT2 calculations and variational transition state theory suggest a negligible barrier but tight TS, which leads to rate constants around 6×10^{12} cm^3 mol^{-1} s^{-1}. While fairly fast, this process is considerably slower than the addition/elimination process which we estimate to occur at the collision rate of around 2×10^{14} cm^3 mol^{-1} s^{-1}.

•

Michael Pilling, University of Leeds, UK. I am surprised that you find that $OH + SO + M \rightarrow HOSO + M$ is important under the flame conditions shown in your final comparison. It is a very minor channel compared with $OH + SO \rightarrow H + SO_2$ except at very high pressures. Is it important because the $OH + SO \rightarrow / \leftarrow H + SO_2$is cycling very quickly so that even this minor channel becomes significant?

Reply. Yes. We were also interested to see that both $OH + SO$ (+M) $\rightarrow$ HOSO (+M) and $SO + H + M \rightarrow HSO + M$ play important roles under the flame conditions (Fig. 5). Flux analyses indicate that $OH + SO \rightarrow /$

$\leftarrow H + SO_2$ becomes partially equilibrated under these conditions; most predominantly at the highest flame temperatures. This is combined with a high formation rate of SO through $SO_2 + H + M \rightarrow HOSO + M$, $HOSO + H \rightarrow SO + H_2O$ to promote a considerable sulfur flux through the minor SO consumption channels.

●

Keith Schofield, University of California at Santa Barbara, USA. I would like to clarify that this has been a long unanswered question concerning the effect of sulfur on the hydrogen–oxygen radicals in flames. However, other than this role, the sulfur species even as HOSO or HSO are extremely minor and have negligible steady state concentrations. As a result, they are of no importance in modeling the distribution of sulfur species in combustion but rather are relevant to modeling hydrogen/oxygen distributions where they do provide the mechanism for the well established catalytic recombination effects on H, OH and O. Because of the linear relation HP between H and OH in most flames these two radicals can become indistinguishable as in the present case. As a result, studies of these sulfur reactions are needed in flow tubes or by other systems that are unrelated to combustion to resolve once and for all time whether it is H or OH that is involved in this catalytic cycling.

Reply. We agree that it is important to consider the widest possible range of experimental conditions and also to rely on elementary rate constant measurements and *ab initio* results, to help constrain sulfur mechanisms.